Scuola Internazionale Superiore di Studi Avanzati – Trieste

INTERNATIONAL SCHOOL FOR ADVANCED STUDIES

PHARMACOLOGICAL NEUROPROTECTION OF RAT SPINAL LOCOMOTOR NETWORKS AGAINST EXPERIMENTAL SPINAL CORD INJURY IN VITRO

Thesis submitted for the degree of
"Doctor Philosophiae"

CANDIDATE
JASPREET KAUR

SUPERVISOR
PROF. ANDREA NISTRI

SISSA – Via Bonomea 265 – 34136 TRIESTE – ITALY

Affectionately dedicated to

"my loving family"

"Waheguru ji"

ACKNOWLEDGEMENTS

First and foremost, I bow the almighty for blessing me with strength and ability to accomplish my Ph D project. I am greatly indebted and thankful to my supervisor, Professor Andrea Nistri for giving me an opportunity to work in his lab for the Ph D thesis and for his sound support, valuable guidance and encouragement. He has always been a great inspiration for me and it has been a quality learning experience under his guidance. His constant supervision has helped me to persistently polish me as a researcher.

I sincerely thank Professor Vincent Torre for selecting me as a researcher and providing me with a chance to come to Trieste. I would like to express my gratitude to Professor Laura Ballerini, Professor Anna Menini and again to Professor Vincent Torre for their careful evaluation, critical remarks and suggestions during the yearly progress reports of Ph D.

My sincere thanks and due regards to Professor Laura Ballerini who has always been a great support with her little comments which motivated me to do better. She has also provided me with an opportunity to work in her lab to learn and perform calcium imaging experiments.

I am very grateful to my Professor Fateh Singh Nandel, Professor Ashwani Koul and Professor M.L Garg for their valuable guidance and suggestions during my Master course in the department

of Biophysics Panjab University, Chandigarh, India and during my Ph D course as well. They have always been a perpetual source of inspiration and blessing for me.

I am also thankful to Dr. Cynthia Sámano, Javier Flores Gutiérrez, Dr. Rossana Rauti, Dr Miranda and Antonela Petrović for their wonderful collaboration. It has been a great time working with fantabulous people.

My heartiest thank to my wonderful friend, Dr. Priyadharishini Veeraraghavan who immensely helped me in academic development during my time in SISSA. I am very grateful to my friends Dr. Aditya Mojumdar and Dr. Sadaf Usmani who were always there for me in all thick and thin during the four years journey of Trieste. They will be an integral part of my Trieste life. I am also thankful to Dr. Jennifer, Dr. Jashmini Deka, Kartik Gupta, Dr. Sonal Kulkarni, Dr. Nejada Dingu, Dr. Riffat Mehboob, Dzejla Bajrektarvic, Kevin Yarib Gonzalez, Zahra, Liana, Diksha, Sabyasanchi, Dr. Ramit, Dr. Arnab, Rossandra, Maja, Abraham, Dr. Merlyn, Dr. Sheetal, Mangesh, Xuân for being good friends. I would also say thanks to Dr. Wasim, Dr. Saurav, Dr. Niccolò Pampaloni ,Dr.Francesco PU Severino, Francesca, Dr. Silvia Corsini, Dr. Anna, Dr. Gosia, Dr. Sandra Vilotti, Tullio, Valeria, Cristina and all other SISSA people. I would also like to thank Sheela and Dionisio for organising Indian get-together and being so kind.

My special thanks to SISSA secretariat Riccardo, Federica and Luisella for their great help. Very special thanks to all SISSA Neuroscience staff, technicians and animal house staff Angel Camerota, Elettra and Morte for being always so kind and helpful to

provide animals. I am very grateful to all the animals that have been sacrificed during my stay in SISSA.

My deep sense of gratitude to my beloved parents for their crucial support and advice. I would like to dedicate all my work to my Father who is a role model for me.

Declaration

During my course tenure from November 2013 to October 2017 at the International school for advanced studies, Trieste, Italy, I have carried out the following list of studies as a part of my Ph D thesis:

The isolated spinal cord preparation, electrophysiological data collection, analysis and manuscript writing reported in the following manuscripts and unpublished studies were performed by me. Moreover, the immuno-histochemistry experiments including cord isolation, slice preparation, immune-histology and data analysis were performed by me in the nicotine neuroprotection manuscript and nicotine toxicity (unpublished). Calcium imaging data analysis was performed in collaboration with Dr. Rossana Rauti.

- Sámano C, Kaur J, Nistri A (2016) A study of methylprednisolone neuroprotection against acute injury to the rat spinal cord in vitro. Neuroscience 315, 136-149.

- Kaur J, Flores Gutiérrez J, Nistri A (2016) Neuroprotective effect of propofol against excitotoxic injury to locomotor networks of the rat spinal cord in vitro. Eur J Neurosci 44, 2418-2430.

- Kaur J, Rauti R, Nistri A (2017) Nicotine-mediated neuroprotection of rat spinal networks against excitotoxicity. Eur J Neurosci (Submitted manuscript)

- Kaur J, Nistri A; Unpublished work – Nicotine neurotoxicity.

- Unpublished work – Neuroprotective effect of celastrol

Immuno-histochemistry experiments in the first and second manuscript were carried out by Dr. Cynthia Sámano and Javier Flores Gutiérrez, respectively. Dr. Beatrice Pastore has helped me in preparing organotypic spinal slice cultures. Dr. Rossana Rauti has helped me in acquiring calcium imaging data and taught data analysis. Molecular biology experiments concerning celastrol neuroprotection will be performed by Antonela Petrović.

Table of Contents

1. LIST OF ABBREVIATIONS 3

2 ABSTRACT 6

3 INTRODUCTION 8

3.1 Central pattern generators for mammalian locomotion 8

3.1.1 Anatomy of spinal cord 10

3.1.2 Selection and initiation of locomotion 14

3.1.3 Generation of rhythm and pattern of locomotor behaviour 18

3.1.4 Dis-inhibited activity in an isolated spinal cord 23

3.1.5 Reflex pathways in the spinal cord 24

3.2 Spinal cord injury 27

3.2.1 Epidemiology 28

3.2.2 Pathophysiology 32

3.3 Glucocorticoid system 35

3.4 General anesthetics 41

3.5 Nicotinic Acetylcholine Receptors 45

3.5.1 Receptor types and distribution 45

3.5.2 Structure and topology of nAChR 48

3.5.3 Ligands –Agonists of nAChRs 49

3.5.4 Desensitization of nAChR 51

3.5.5 Role in Neuroprotection 53

3.6 Neuroprotection by a natural compound: Celastrol 55

4 AIMS 57

5 MATERIALS, METHODS AND RESULTS 59

Paper I: A study of Methylprednisolone neuroprotection against acute injury to the rat spinal cord in vitro

Paper II: Neuroprotective effect of propofol against excitotoxic injury to locomotor networks of the rat spinal cord in vitro

Paper III: Nicotine-mediated neuroprotection of rat spinal networks against excitotoxicity

6 DISCUSSION 144

7 CONCLUSIONS AND FUTURE PERSPECTIVES 154

8 REFERENCES 155

9 SUPPLEMENTARY DATA 181

9.1 Appendix I: Neurotoxicity of nicotine 181

9.2 Appendix II: Effects of celastrol 189

1. LIST OF ABBREVIATIONS

- 5-hydroxytryptamine 5-HT
- Acetylcholine ACh
- Adrenocorticotropic hormone ACTH
- Calcitonin gene related peptide CGRP
- Central Nervous System CNS
- Central Pattern Generator CPG
- Commissural interneurons CNs
- Corticotropin-releasing factor CRF
- Corticotropin-releasing hormone CRH
- Diacylglycerol DAG
- Dopaminergic neurons DA
- Electroencephalogram EEG
- Flexion reflex afferent FRA
- Food and Drug Administration FDA
- Glucocorticoid Receptor GR

- Glucocorticoid response elements — GREs
- Glucocorticoids — GC
- Heat shock protein — HSP
- Hypothalamic–pituitary–adrenal axis — HPA axis
- Inositol-trisphosphate — IP_3
- Intracerebroventricular — i.c.v
- Intravenous — i.v
- Mesencephalic locomotor region — MLR
- Methylprednisolone — MP
- Muscarinic acetylcholine receptor — mAChR
- Nicotinic acetylcholine Receptor — nAChR
- Nitric oxide — NO
- Nitrous oxide — N_2O
- N-Methyl-D-aspartic acid — NMDA
- Pathological medium — PM
- Pedunculopontine nucleus — PPN
- Progenitor domain — p
- Pro-opiomelanocortin — POMC

- Reciprocal Ia inhibitory neurons — rIa-INs
- Rhythm generating neurons — R
- Short stature homeobox protein 2 — SHOX2
- Spinal cord injury — SCI
- γ-aminobutyric acid — GABA

2 ABSTRACT

Background: Mammalian locomotor behaviour called fictive locomotion can be elicited in an isolated spinal cord in the absence of higher brain center or sensory input. This relatively simple behaviour is produced by the motoneuronal rhythmic activity which is under the control of spinal neuronal networks called central pattern generators (CPGs). Disturbance of this rhythmic motor output can occur following spinal cord injury (SCI). This elementary isolated spinal cord model gives us an opportunity to study the basic physiology of locomotion during control conditions, the pathological processes following lesion (which can be induced chemically), and eventually the application of therapeutic approaches curbing injury.

Objectives: Multiple aspects of spinal functions can be demonstrated by stimulating or/and blocking specific inputs and measuring the outputs using electrophysiological, immunohistochemical and calcium imaging tools. Using isolated neonatal rat spinal cords and organotypic spinal slices as SCI models, the basic mechanisms (such as dysmetabolic state or excitotoxicity) which can develop during the early phase of the lesion were addressed and studied. The injury was evoked chemically by applying either pathological medium (to mimic dysmetabolic/hypoxic conditions) or kainate (to produce excitotoxicity that completely abolishes fictive locomotion and network synaptic transmission) for 1 h. Fictive locomotion was examined stimulating the lumbar dorsal root and recording from the ipsilateral and ipsi-segmental ventral roots. Other network parameters were also studied such as synaptic transmission and rhythmicity. Various therapeutic drugs such as methylprednisolone sodium succinate (MPSS), propofol, nicotine and celastrol were used during or after the injury (to produce neuroprotection) and network properties were characterized during the treatment and after 24 h as well. Subsequently, the structural properties were monitored using different biomarkers (isolated spinal cord sectioned slices) and calcium imaging (here organotypic spinal slices were used).

Results and conclusions: We found that dose-dependent application of MPSS produced modest recovery of white matter damage evoked by pathological medium resulting in the

emergence of sluggish chemically induced fictive locomotor patterns. However, it could not prevent damage (to gray matter) evoked by the excitotoxic agent kainate. Therefore, to provide better neuroprotection to gray matter, we tested the widely used intravenous anaesthetic propofol. This drug has shown comparatively good protection to spinal neurons and motoneurons in the gray matter. As it is an anesthetic it acted by depressing the functional network characteristics by lowering the N-methyl-D-aspartate (NMDA) and potentiating the γ aminobutyric acid ($GABA_A$) mediated receptor responses.

The next issue we addressed was to study the neuroprotective roles of nicotinic acetylcholine receptors (nAChRs) by using the receptor agonist nicotine. Recent studies have shown that nicotine could provide good neuroprotection to the rat brainstem. To further investigate its effect on the spinal cord, we applied nicotine at the same concentration used in previous studies in the brainstem: such a concentration was toxic to spinal ventral motoneurons. Therefore the correct dose of nicotine was optimized and was found to be ten times lower. Thus, satisfactory protective effects to spinal neurons and motoneurons and the fictive locomotor patterns were observed. These neuroprotective effects were replicated with calcium imaging by using organotypic spinal slice cultures. The mechanism of protection predominantly involved α4β2 and less α7 nAChRs.

In addition, the subsequent goal of our study was to explore whether the motoneuron survival after excitotoxicity relies on cell expression of heat shock protein 70 (HSP70) or some other mechanisms. To test this hypothesis we used a bioactive drug, celastrol which induces the expression of HSP70. Prior application of the drug followed by kainate preserved network polysynaptic transmission and fictive locomotion, however, it could not reverse the depression of monosynaptic reflex responses. In vivo studies are necessary in the future to further investigate the long-term neuroprotective role of these drugs.

3 INTRODUCTION

3.1 Central pattern generators for mammalian locomotion

"Thus, from the war of nature, from famine and death, the most exalted object which we are capable of conceiving, namely, the production of the higher animals, directly follows. There is grandeur in this view of life, with its several powers, having been originally breathed into a few forms or into one; and that, whilst this planet has gone cycling on according to the fixed law of gravity,

***from so simple a beginning endless forms most beautiful and most wonderful have been, and are being, evolved**."*

❖ Charles Darwin

When speculating about the beginning of life on earth, one can get fascinated by tremendous animal behaviour. All kind of movements in animals, vertebrate or invertebrate are controlled by specific neural circuits that generate precise phasing and timing of muscle activation and thus locomotor behaviour (Grillner, 2003; Selverston, 2005). These networks are called Central Pattern Generators (CPGs). All animals have a stock of CPGs distributed in different parts of the Central Nervous System (CNS) and thus allow animals to perform distinct behaviour and movement (Grillner, 2006).

Considering locomotor activity, which is an innate rhythmic motor act, different from simple reflex, provide animals and humans to move. There are diverse locomotor forms such as walking, swimming, running, hopping and feeding (Delcomyn, 1980; Roberts & Roberts, 1983). Locomotion does not require sensory input and is generated by CPG

(Grillner, 2006), although sensory input is important for the refinement of CPG to respond to external events (Grillner 1985). CPGs do not produce fixed action patterns; otherwise, animals have behaved like stereotype robots. Rather they provide a malleable template which can be easily modified according to changes in the environment (Grillner, 2006).

Locomotion was first precisely characterized when Étienne-Jules Marey and Eadweard James Muybridge (in the 1880s), known for their pioneering work on animal locomotion, developed the photographic techniques which allowed users to capture motion in stop-motion photographs as shown in Fig. 1.

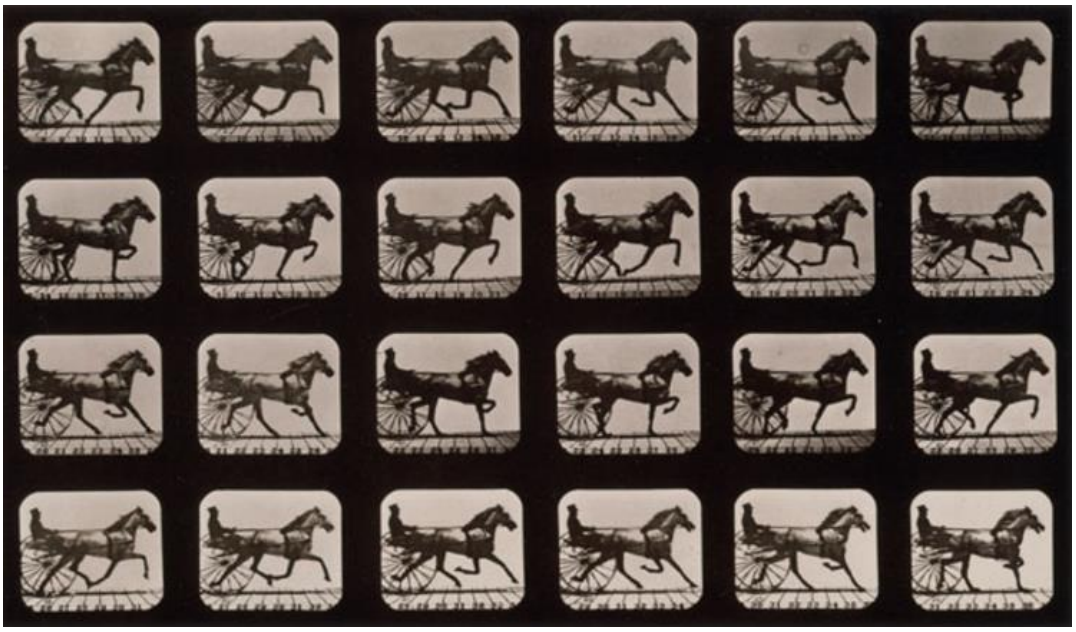

Fig. 1 An example of multiple locomotion pictures showing the consecutive motions of different locomotor acts by animals (http://www.imaging resource.com/news/2012/11/27/eadweard-muybridge-the-photographic-pioneer-who-froze-time-and-nature)

A major improvement in understanding the neural substrate for producing mammalian locomotion came into limelight in the 20th century when a Scottish neurophysiologist Thomas Graham Brown showed that the basic stepping pattern can be induced in the transected spinal cord of cats, rabbits and guinea pigs without sensory

inputs (Graham Brown, 1911, 1914). Thus, Graham Brown has concluded that spinal cord neuronal networks are able to produce flexor-extensor movements in the absence of sensory stimuli. To better understand the mechanism of action of CPG in the generation of movement in spinal cord, it is necessary to know the anatomy of the spinal cord.

3.1.1 Anatomy of spinal cord

The spinal cord is a part of CNS, extends caudally from the brainstem. It is enclosed in a protective bony structure, vertebral column. It is encircled by three meninges, i.e., dura mater (outer layer), arachnoid and pia mater as shown in Fig. 2. Unlike the brain, the cross-section of the peripheral region of the spinal cord is composed of white matter, comprising bundles of myelinated axons of neurons. Internal to the peripheral region of the cord is the butterfly-shaped gray matter region, which resembles the letter H, consisting of cell bodies of neurons, unmyelinated axons and neuroglia. At the centre of the gray commissure, which forms the crossbar H, is the central canal containing cerebrospinal fluid (CSF) circulating to and from the ventricles in the brain (Kandel et al., 2000).

.

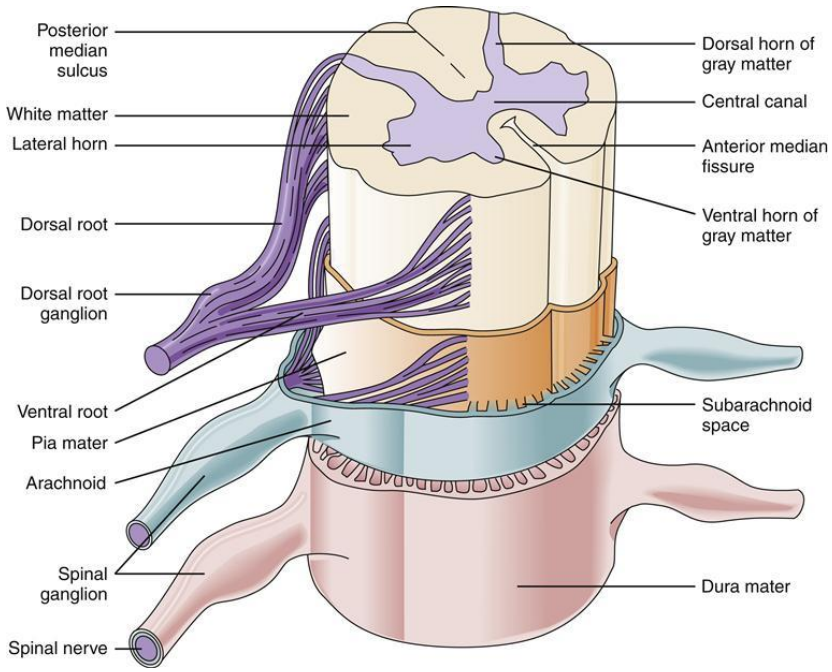

Fig. 2 A cross-section of spinal cord representing distinct layers and the butterfly pattern of white and gray matter of spinal cord (Jacquelyn L. Banasik, Structure and Function of the Nervous System, Chapter 43)

The spinal cord is about 17–18 inches (43–48 cm) long in humans and according to rostrocaudal location the 31 segments (varies from specie to specie) are divided into five parts, i.e., 8 cervical, 12 thoracic, 5 lumbar, 5 sacral and 1 coccygeal segments (Netter, 2006) (Fig. 2). In rats, 34 segments are grouped into; 8 cervical, 13 thoracic, 6 lumbar, 4 sacral and 3 coccygeal (Molander et al., 1984; Molander et al., 1989). Besides the medial sagittal plane, anterior and posterior median fissures divide the spinal cord into two portions which are further associated with transverse anterior and posterior commissure as shown in Fig. 3. The anterior and posterior lateral fissures depict the locus where the sensory and motor nerve rootlets emerge from the spinal cord to spinal nerves.

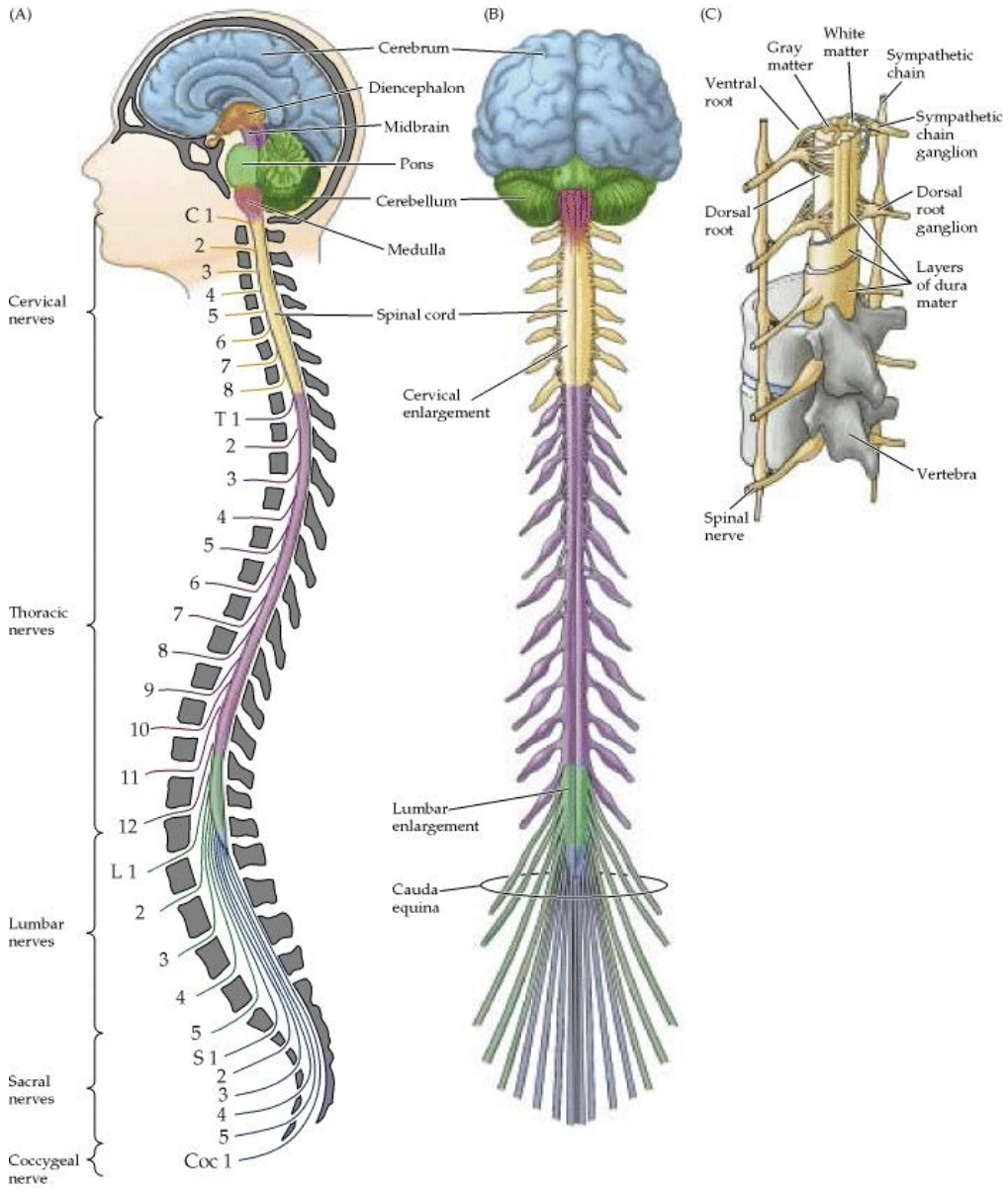

Fig. 3 Diagram of longitudinal section of spinal cord showing division of segments

At each side, the spinal cord is further divided into the dorsal, central and ventral horn (Fig. 2). From the dorsal horn, the dorsal roots emerge, integrate into bundles and enter into dorsal root ganglia (DRG), which contain cell bodies of sensory neurons, are afferent (Ham & Cormack, 1987). Away from the ganglia, the dorsal and ventral roots unite to form spinal nerves. These spinal nerves emerging from vertebrae form plexus which have both sensory and motor functions like muscle contraction, sensations (of cold, heat, pain) etc.

Cytoarchitecture of spinal cord

The first cytoarchitecture of the spinal cord was identified by Bror Rexed in the 1950s (Rexed, 1952; 1954) who labelled the portions of gray columns as 10 rexed laminae in cats. Each lamina carries several distinct characteristics in terms of physiological, histochemical and cytoarchitectonics (Heise and Kayalioglu, 2009). Molander and his colleagues examined the organization of these rexed laminae in neonatal and adult rat spinal cord at lower thoracic and lumbosacral segments and found similar architecture as in cats (Molander et al., 1984, 1989). Other scientists also confirmed the presence of these lamination patterns in the rats (Watson et al., 2009), mice (Sidman et al., 1971; Watson et al., 2009) and humans (Schoenen and Faull, 2004) at different time periods. Furthermore, there is not much difference in neonatal and adult rat spinal laminae except that there are less distinct borderlines between laminar regions.

- Laminae I cover the tip of the dorsal horn (See Fig. 4).

- Laminae II correspond to substantia gelatinosa where the first order neurons of spinothalamic tract synapse exist. There are two main subtypes of cells present in laminae II: Islets cells and stalked cells. Islets cells are considered as inhibitory cells of these laminae as they consist of GABA, which is an inhibitory neurotransmitter.

- Laminae III can be easily recognized because of less density of neurons. It is mainly composed of GABA and glycine neurotransmitters (Todd & Sullivan,

1990).

- Laminae IV neurons send projections to midbrain and brainstem and re-send the processes back to itself.

- Laminae V and VI complement to reticular formation in brainstem.

- Laminae VII consist of the intermediolateral nucleus (T1-L1) and dorsal nucleus of Clarke (T1-L2). Intermediolateral nucleus performs an important role in autonomic and sensory motor functions. On the other side, axons from dorsal nucleus of Clarke make ascending fibres of the dorsal spinocerebellar tract.

- Laminae VIII–IX make the ventral horn of spinal cord mainly consists of motoneurons.

- Laminae X form substantia grisea centralis, surround the central canal and consist of preganglionic neurons and neuroglia (Dafny, 1999).

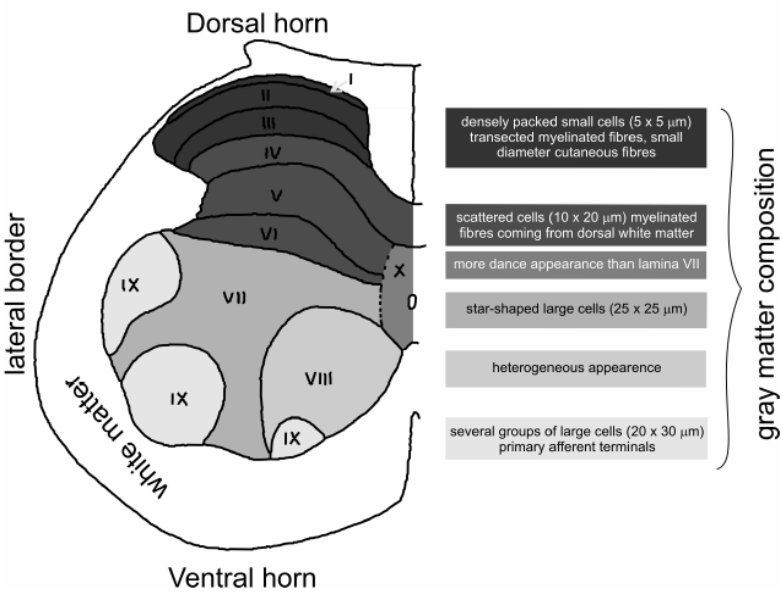

Fig. 4 Transverse section of lumbar 5 segment of spinal cord comprising different laminar regions (Ostroumov, 2006)

3.1.2 Selection and initiation of locomotion

The first question to answer in locomotion is how are these central motor programs selected and generated after selection?

Particular CPGs for a specific action (at a given moment) are selected by neuronal mechanisms in the brain. Experiments on different animal models, like vertebrates have shown that basal ganglia are the dominating selection system, select locomotor behaviour (Grillner et al., 2005a; Hikosaka et al., 2006).

Striatum (input layer of basal ganglia) receives excitatory sensory input from the cortex in mammals (known as pallium in lower vertebrates) or directly from thalamus (Fig. 5). It comprises the inhibitory neurotransmitter, γ-aminobutyric acid (GABA), activated at high threshold. Striatal neurons project onto pallidum (output layer of basal ganglia) and substantia nigra. The pallidum is also composed of inhibitory GABAergic neurons with even higher threshold which maintain CPGs at tonic inhibition at rest. For a locomotor behaviour to be elicited, striatum needs to be activated which further inhibits pallidum resulting in activation of particular CPGs providing an input to induce dis-inhibition, important for locomotion. The dopaminergic neurons play a crucial role in facilitating the response of striatal neurons to activation. Deficiencies or hyperactivation of dopaminergic system eventually leads to Parkinson-like hypokinetic or hyperkinesias symptoms, respectively in all vertebrates—from lamprey to man (see Grillner et al., 2005c).

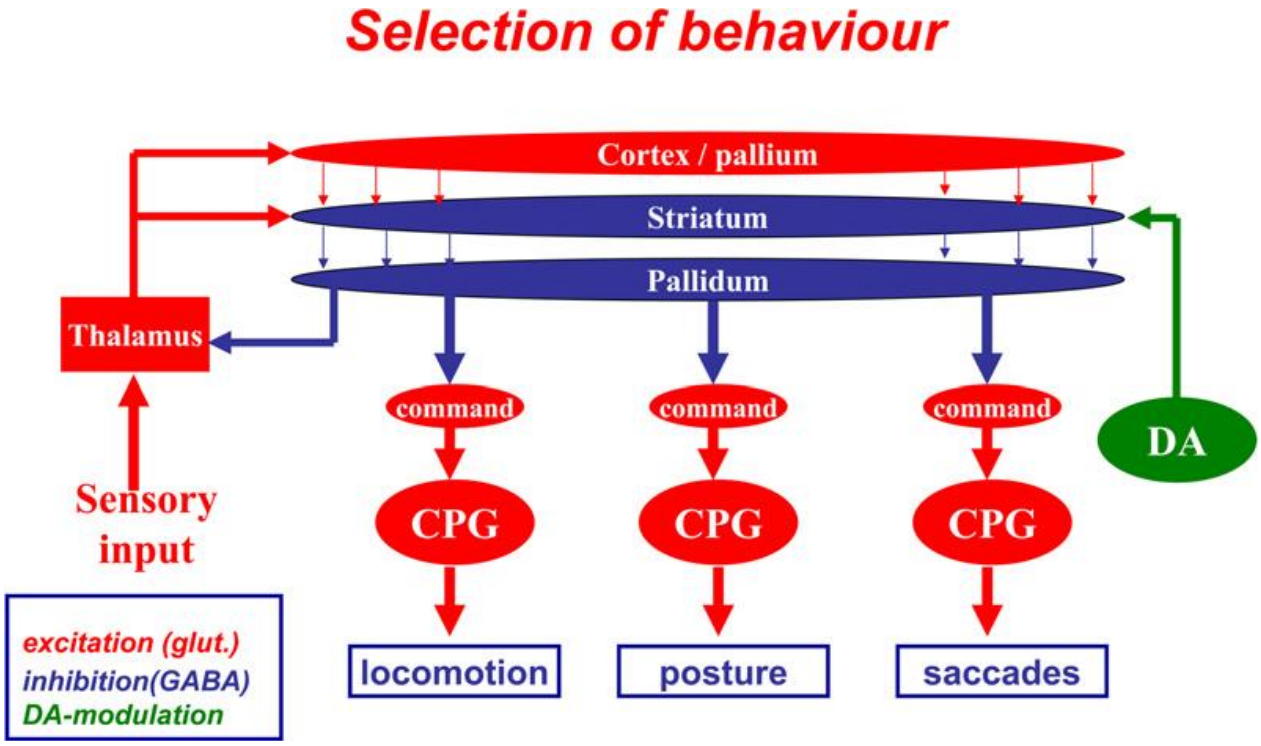

Fig. 5 Scheme of selection of specific behaviour by basal ganglia (Grillner, 2006)

Two regions which may be associated with initiating locomotor behaviours in different behavioural context are medial and lateral hypothalamus. Medial hypothalamus involves in escape or defensive locomotor behaviour, whereas lateral hypothalamus is involved in behavioural context when animal searches for food.

Neurons of mesencephalic locomotor region (MLR) project to the medial reticular formation in the lower brain stem which further projects its neurons onto locomotor CPG in the spinal cord to execute locomotion as shown in Fig. 6.

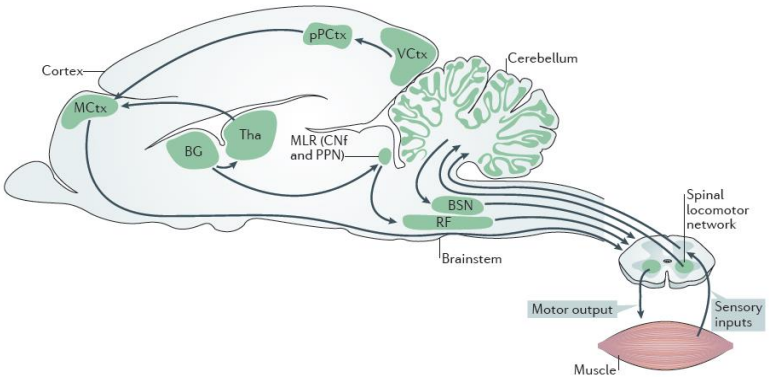

Fig. 6 Scheme of organization of neural structures controlling locomotion (Kiehn, 2016)

The next query is the initiation of locomotion once selected by basal ganglia...

The output layer of basal ganglia, pallidum, projects its neurons onto MLR in mesencephalon (midbrain) (Fig. 6). After the selection of locomotion, the high resting activity of globus pallidus neurons declines, which relieve the tonic GABAergic inhibition of these neurons in MLR. After the release of inhibition, MLR becomes active and initiate locomotion.

Neurons in MLR are excitatory. The pedunculopontine nucleus (PPN) is located in the ventrolateral portion of caudal MLR and is composed of neurons comprising glutamate and acetylcholine (ACh) (Clements & Grant, 1990; Lavoie & Parent, 1994; Takakusaki et al., 1996; Mena-Segovia et al., 2008; Takakusaki et al., 2016). Previous studies have suggested that cholinergic neurons are important in maintaining the rhythm of locomotion and postural muscle tone (Bohnen & Albin, 2011; Takakusaki et al., 2011). These glutamatergic and cholinergic input signals arising from MLR may control the excitability of reticulospinal neurons that project to spinal CPGs to initiate stepping (Le Ray et al., 2011; Skinner et al., 1990).

There are two main systems involved in the execution of locomotion: Glutamatergic and serotonergic locomotor pathways as previously been studied in mammals (Guertin, 2009; Ghosh & Damien, 2014). Therefore, it seems that there are parallel pathways, at least in mammals, activating the spinal locomotor networks.

The next point to discuss is the localization of CPG in the spinal cord of mammals…

CPG locomotor networks are localized in the ventromedial part of spinal cord (Fig. 7) which is distributed along the lumbar segment of mice (Nishimaru et al., 2000) and humans (Dimitrijevic et al., 1998). Locomotor activity is specifically found in the gray matter intermediate zone, ventral horn and central canal areas (e.g., Kjaerulff et al., 1994; Cina and Hochman, 2000). Locomotor CPG neurons have been identified as the populations of HB9 (Wilson et al., 2005), EphA4 (Kullander et al., 2003), V0 (Lanuza et al., 2004), V1 (Gosgnach et al., 2006), V2 a/b (Lundfald et al., 2007), V3 (Zhang et al., 2008), excitatory Ib (Guertin et al., 1995; Angel et al., 2005), lamina VII-IN (Jankowska

et al., 1967a,b), ChAT-positive/c-fos-labeled ascending (Huang et al., 2000), rhythmic interneurons which are activated by group II afferent (Edgley and Jankowska, 1987) and descending commissural interneurons (dCIN) (Butt et al., 2002) (See Fig. 7).

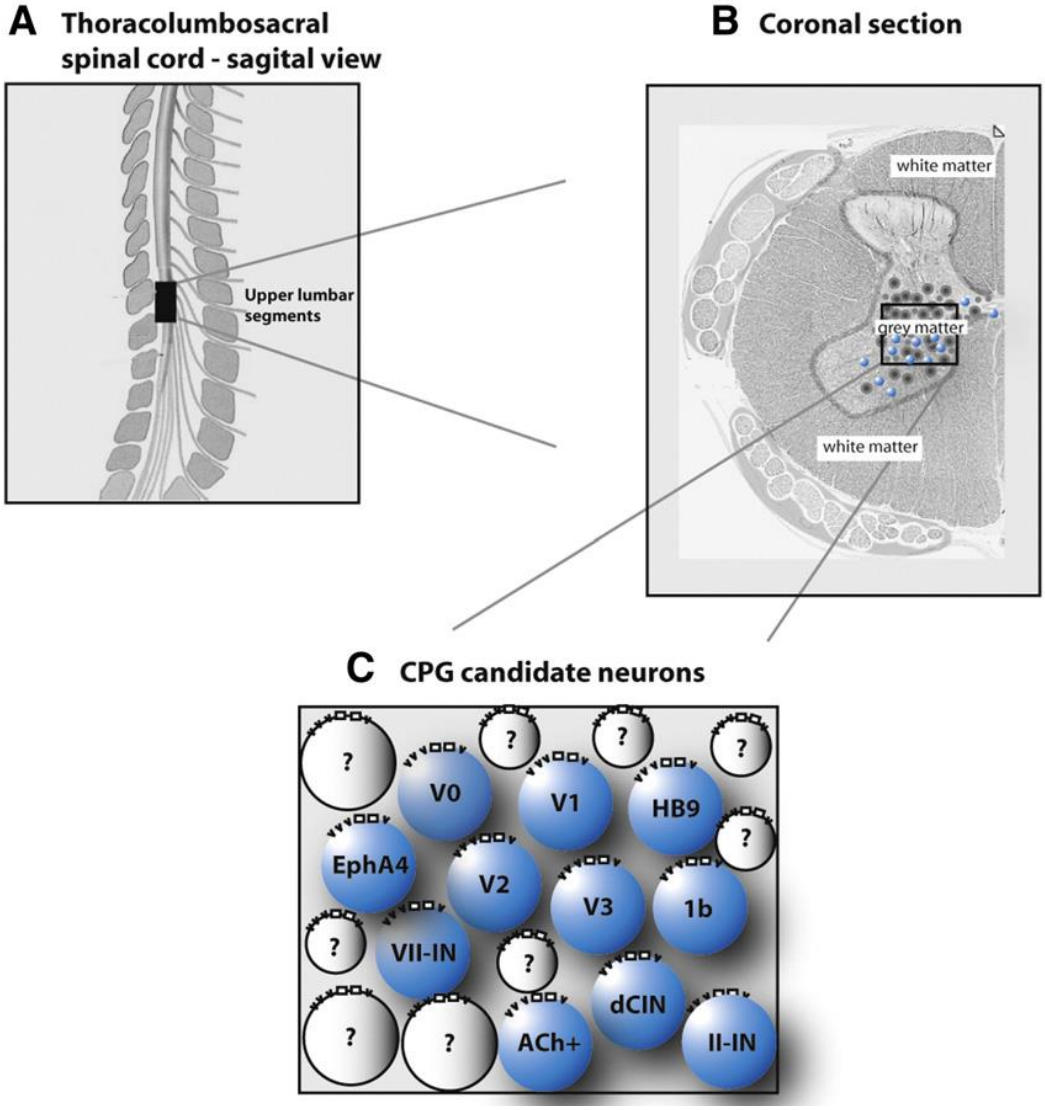

Fig. 7 Localization of spinal networks (Guertin, 2009)

3.1.3 Generation of rhythm and pattern of locomotor behaviour

Rhythm generation in mammals is more complex than lower vertebrates (Grillner, 1985; Guertin, 2009). There are two main aspects with control the coordination of limbs.

- The left-right pattern generating circuits – maintain the coordination during movement on both sides of the body along with, rhythm-generating circuits – which drive the activity and modulate the speed in non-limbed locomotion.
- Flexor–extensor pattern-generating circuits – which maintain intra-limb coordination in limbed locomotion. Limbed locomotion also requires left-right pattern generating circuits (in addition to flexor-extensor circuits) for locomotor movement to occur.

- ***Left–right coordination circuits***

Commissural neurons (CNs) play an important role in providing left-right coordination during locomotion at different frequencies (speeds). CNs that are associated with motor control in mammals are localized in at the ventral part of spinal cord and composed of inhibitory (GABA and glycine) and excitatory (glutamate) neurotransmitters (Bannatyne et al., 2003; Weber et al., 2007; Restrepo et al., 2009).

V0 CNs evolved from p0 progenitor domain in the ventral horn of cord. Five progenitor domains are present in ventral (p0-p3, pMN) and six in the dorsal horn (pd1-pd6) (Jessell, 2000; Alaynick et al., 2011) (Fig. 8). After maturation, these progenitor cells differentiate into neurons and motoneurons. The V0 neurons split into inhibitory dorsal $V0_D$ and excitatory ventral $V0_V$ neurons and produce left-right alternations. $V0_D$ neurons maintain hindlimb alternation at a lower speed of locomotion and $V0_V$ control hindlimb alternation at high frequencies (Kiehn, 2016). According to previous in vitro genetic studies on mice, ablation of V0 resulted in lack of hindlimb alternations in mice (Fig. 9 A) (Talpalar et al., 2013). When studied in vivo in mice model, mice explicit four basic gaits (two alternating gaits, walk and trot; one synchronous gait, bound and an intermediate gait, gallop) in the

presence of V0 neurons ($V0_D$ and $V0_V$) (Fig. 9 B). These four gaits occurred at different locomotion speeds. Walk is expressed at a minimum (1-4 Hz) and bound at the maximum (10-14 Hz) speed (Fig. 9 B). When both V0 CNs were deleted mice expressed only bound gait in which pairs of hindlimbs and pairs of forelimbs are moved in synchrony. When $V0_D$ were deleted mice died before birth. However, when $V0_V$ were deleted mice were able to walk, gallop, bound but unable to trot.

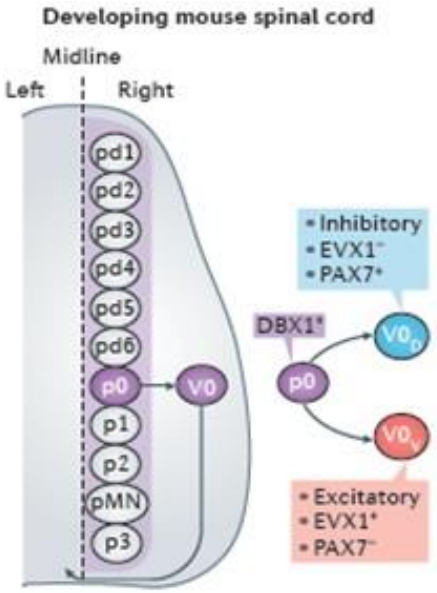

Fig. 8 Development of CNs from progenitor domain in the mouse spinal cord (Kiehn, 2016)

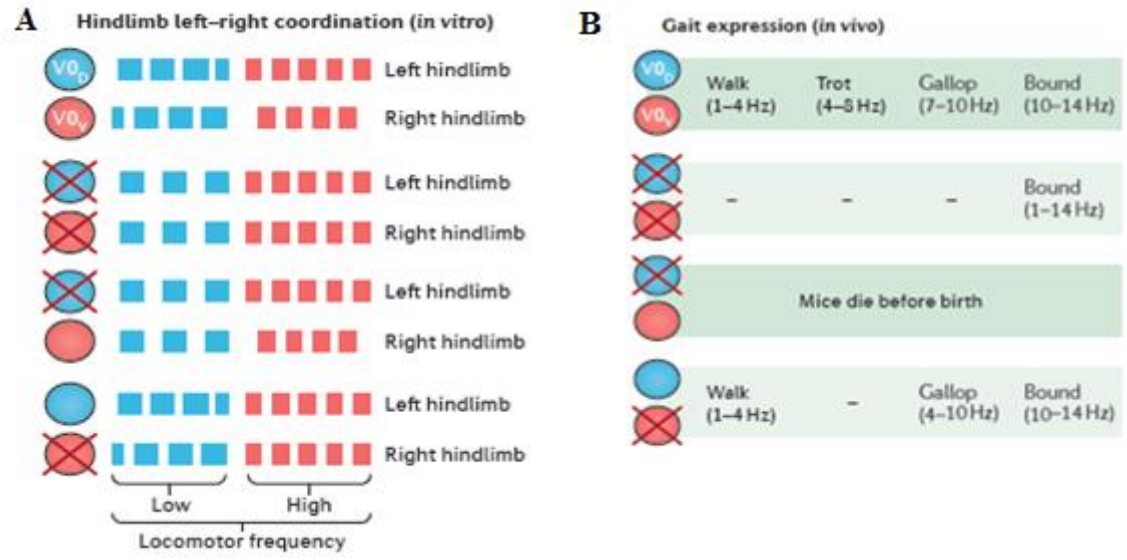

Fig. 9 Genetic ablation studies of V0 CNs in vitro (a) and in vivo (b) in mouse spinal cord (Kiehn, 2016)

Further, these $V0_D$ and $V0_V$ neurons are recruited in ascending order as the locomotor speed increases (Fig. 10). Therefore, at low speed like walking rhythm-generating neurons (R) activate $V0_D$ CNs on the same side of the spinal cord, which in turn inhibit motoneurons on the other side of the cord. At high speed of locomotion, $V0_V$ neurons are activated which leads to trot movement by inhibition of locomotor network circuits including motoneurons on the other side of the cord. At higher frequencies of locomotion, which lead to a bound movement, arises by the preservation of left-right synchrony by non-V0 neurons which might be V3 (Quinlan & Kiehn, 2007; Crone et al., 2008; 2009; Talpalar et al., 2013; Bellardita & Kiehn, 2015).

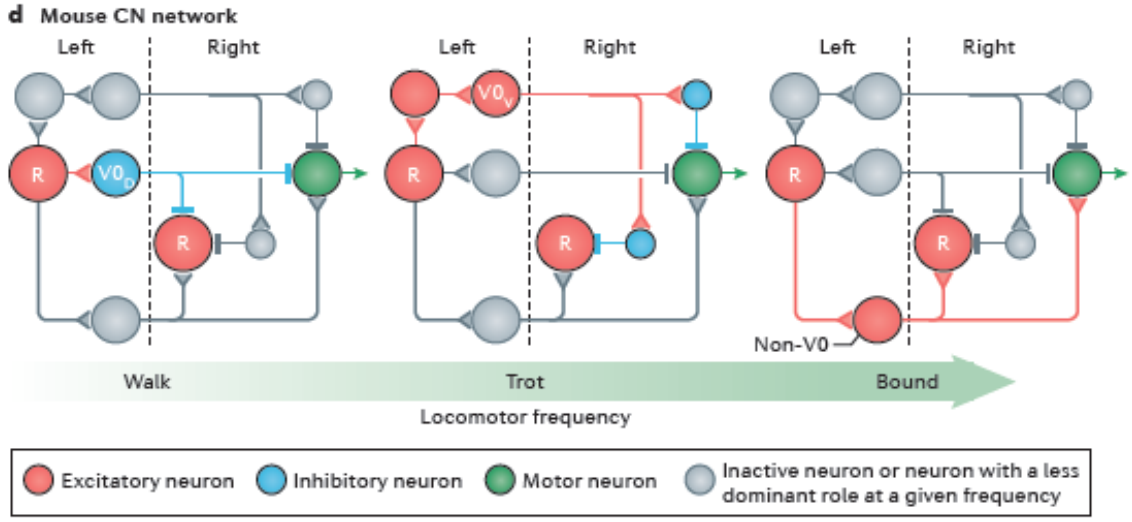

Fig. 10 Schematic diagram of hypothesized V0 CNs locomotor pathways activated with different speed of locomotion (Kiehn, 2016)

- ***Flexor-extensor coordination***

Motoneurons control flexor-extensor muscles during mammalian locomotion and these muscles are activated in alternation. This flexor-extensor coordination is produced by reciprocal Ia inhibitory neurons (rIa-INs), which reciprocally inhibit antagonist motoneurons and each other. These rIa-INs are one synapse away from flexor-extensor motoneurons (Fig. 11) and are activated by Ia afferents from muscle spindle. rIa-INs are

rhythmically active while locomotion (Hultborn, 1976). As they are reciprocally connected to extensor-flexor motoneurons, they have been proposed as originators of rhythmic inhibition of motoneurons during locomotor activity. Experiments on mice by genetically ablating glutamate networks showed that minimum inhibitory network is enough for flexor-extensor alternation (Fig. 11 a) (Talpalar et al., 2011). When V1 and V2b (inhibitory neurons) were removed, flexor-extensor alternations were absent, instead synchronous activity was observed (Fig. 11 b) (Zhang et al., 2014).

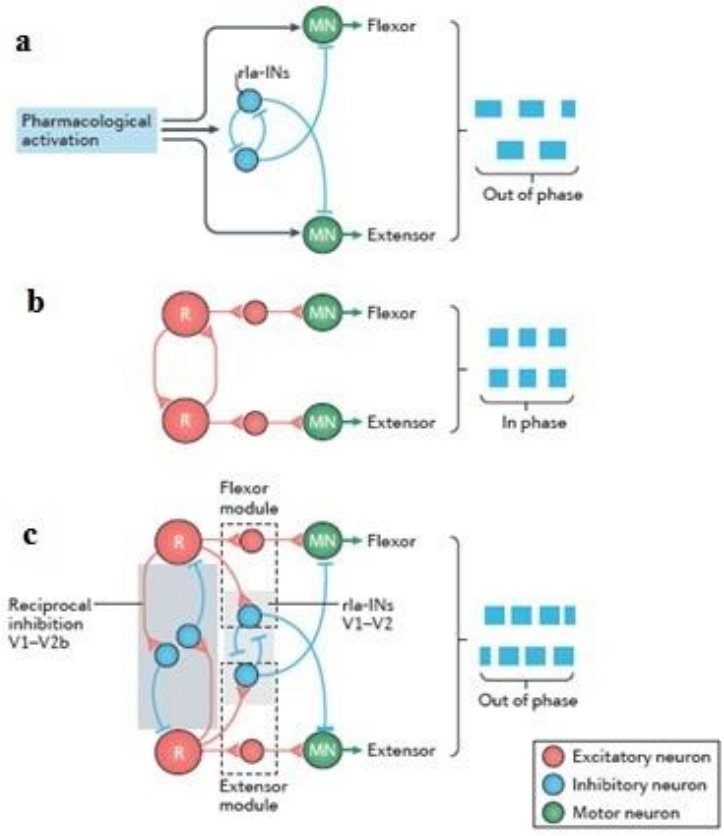

Fig. 11 Proposed scheme of flexor-extensor antagonism in mammals (Kiehn, 2016)

Fig. 11 c shows various levels of the intact circuit with all neuronal elements. Excitatory rhythm generating circuits (R) providing inputs to excitatory neurons and rIa-INs (which also belong to V1 and V2b neurons) which are further reciprocally providing rhythmic excitation and inhibition to flexor-extensor muscles respectively. Therefore, these V1 and V2b inhibitory neurons evoke reciprocal inhibition between flexor and extensor rhythm generators (Endo & Kiehn, 2008; Talpalar et al., 2011; Zhang et al., 2014).

❖ ***Rhythm generating circuits***

Akoi and his co-workers have explained slow rhythm generating circuits in lamprey spinal cord (Akoi et al., 2001) (Fig. 12). They proposed that, apart from network providing the swimming rhythm in the lamprey cord, there is also a network generating slow reciprocal alternation into dorsal and ventral parts of the myotome. During steering movement, the dorsal and ventral myotomes are selectively triggered and the neural networks generating the slow rhythm may depict activity in the spinal machinery used for steering (Fig. 12).

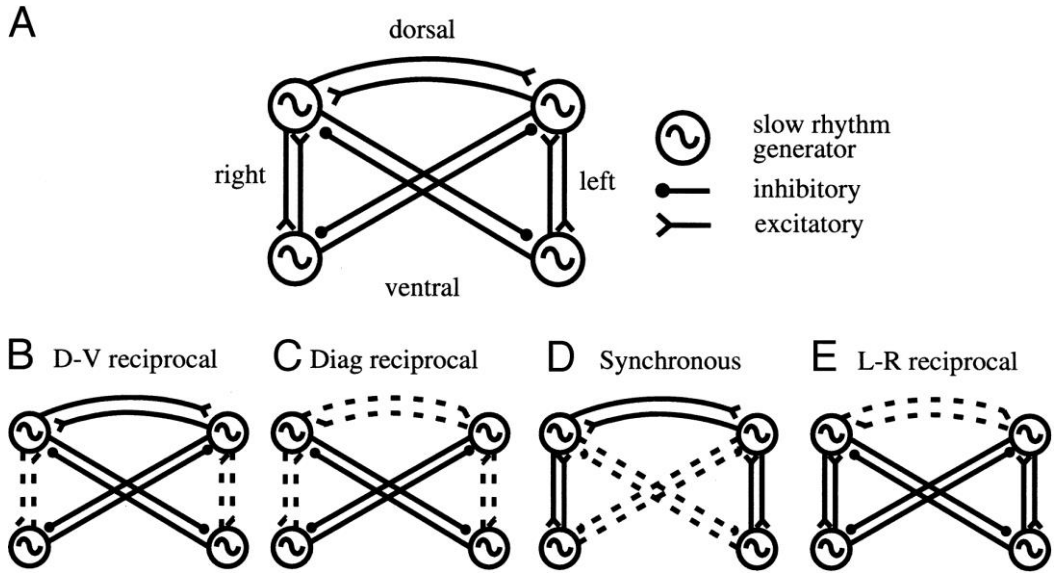

Fig. 12 Scheme of slow rhythm generating networks in the lamprey spinal cord. A) Four slow oscillators for dorsal and ventral myotomes are present on both sides, which are connected in three ways: diagonal inhibitory, ipsilateral excitatory and contralateral excitatory coupling. B) Dorsal-ventral reciprocal patterns are produced by lowering the strength (dashed line) of ipsilateral excitatory connections with respect to the other couplings. C) Diagonal reciprocal patterns are evoked by decreasing all excitatory couplings relative to diagonal inhibitory couplings. D) The synchronous patterns are induced by reducing the diagonal inhibitory connections. E) Left-right reciprocal patterns are evoked by decreasing the contralateral excitatory coupling.

Rhythm generating circuits (in the mammalian spinal cord) contain neurons which express short stature homeobox protein 2 (SHOX2) (Fig. 13). These circuits also drive left-right coordinating circuits like non-V (which might be V3) neurons, V2a and V2a SHOX2+ (Crone et al., 2008; 2009). It is evident from optogenetic studies that blocking SHOX2+ synaptic output disturbs the rhythm without completely abolishing it which shows that some unknown excitatory interneuron is still generating the rhythm (Dougherty et al., 2013).

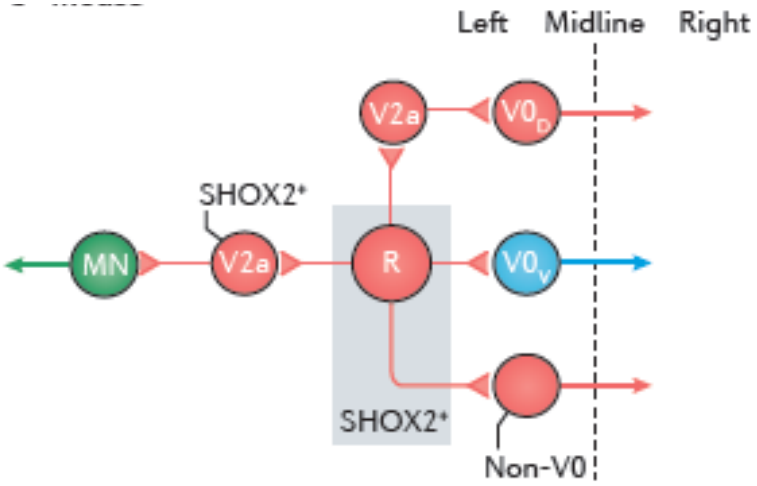

Fig. 13 Organizational and molecular delineation of rhythm-generating circuits (extracted from Kiehn, 2016)

3.1.4 Dis-inhibited activity in an isolated spinal cord

Locomotors like rhythmic activity, which is termed as fictive locomotion can be evoked in an isolated neonatal rat spinal cord in a ventrally located pre-motoneuronal network (Kjaerulff & Kiehn, 1996) by application of N-methyl-D-aspartate (NMDA) (Kudo & Yamada 1987) and serotonin (5-HT) (Cazalets et al., 1992) or high K^+ solutions (Bracci et al., 1998) or dopamine (Kiehn & Kjaerulff, 1996). The relation of disinhibited rhythm to the locomotor activity is of particular interest and has been investigated previously (Beato & Nistri, 1999). The isolation (split-bath) experiments revealed strong synergy between disinhibited rhythm and locomotor pattern. This synergy is expressed in the presence of typical alternation between locomotor-like patterns produced during each interburst interval even in the absence of 5HT or/and NMDA, despite the presence of strychnine

and bicuculline in the caudal area (5HT or/and NMDA applied to the rostral region). Moreover, it is also evident that organotypic rat spinal cultures show synchronous bursting by blocking $GABA_A$ and glycine receptors (Streit, 1993). These studies have suggested that spinal rhythmic generators could work even in the absence of synaptic inhibition although inhibition is important for temporal phasing of motor patterns (Bracci et al., 1996b). Further, $GABA_B$ receptors were not necessary for rhythm generation. Therefore, Bracci (Bracci et al., 1996b) hypothesized mechanisms that might be involved in primary discharge could be the activation of AMPA receptors at excitatory synapses and for late oscillations, ascribed to dendritic calcium spikes (Traub et al., 1993).

3.1.5 Reflex pathways in the spinal cord

The gray matter neurons form spinal reflex pathways (also called reflex arc) which are simpler than locomotor circuits. These spinal arcs are associated with classical reflexes. In vertebrates, most sensory neurons do not pass directly into the brain; instead make direct synapses in the spinal cord, which allow faster reflex actions via activation of spinal motor neurons. Activation of a simple reflex in response to a corresponding specific stimulus typically leads to rapid, repeated, stereotyped and involuntary motor reaction. They could be simple mono-, di- or polysynaptic reflexes with their corresponding neurons (i.e., interneurons and motoneurons). Simple reflexes may have an autonomic (eyes, blood vessels, etc.) or somatic (skeletal muscle responses) origin. Somatic spinal reflexes have been studied in detail in cats and Ia, Ib, II, FRA (flexion reflex afferent) reflexes were described, however, their function in control of locomotion remain incompletely understood.

- ***Monosynaptic reflexes***

Monosynaptic reflexes are evoked by primary afferents (Ia) in response to muscle stretch (from muscle spindles) like tendon jerk (knee or ankle) or tap or myotatic reflex. Ia afferent (sensory) signal enters the spinal cord from dorsal horn and forms a single synaptic connection with homonymous α-motoneuron in the ventral horn of gray matter of cord (Fig. 14). In response to muscle elongation, this excitatory reflex will cause

muscles to contract. Apart from homonymous α-motoneurons, Ia afferents also make monosynaptic connections with synergistic α-motoneurons. It has previously been experimentally demonstrated that monosynaptic activity level depends on task and circumstances like the amplitude of H reflex is more in standing position and decreases while walking. Also, H reflex has more amplitude in extension phase than flexion (swing) phase (Stein and Capaday, 1988). Moreover, the precise analysis of Ia monosynaptic reflex could provide important information about the neuropathological conditions (Matthews, 1972; 1991; Henneman, 1974).

Ib reflex (inverse myotatic reflex or autogenic inhibitory reflex) is connected to peripheral afferent inputs via Ib afferent fibres (Golgi tendon organs). It has found to be silent during locomotion and replaced by other Ib afferent reflex pathway, which induces more excitation to homonymous and synergistic α-motoneurons (at lower extremities; Gossard et al., 1994; Guertin et al., 1995). Moreover, clasp knife reflex may be caused by communication between Ia monosynaptic excitatory and Ib autogenic inhibitory actions on α-motoneurons in spastic patients (with descending tracts injury).

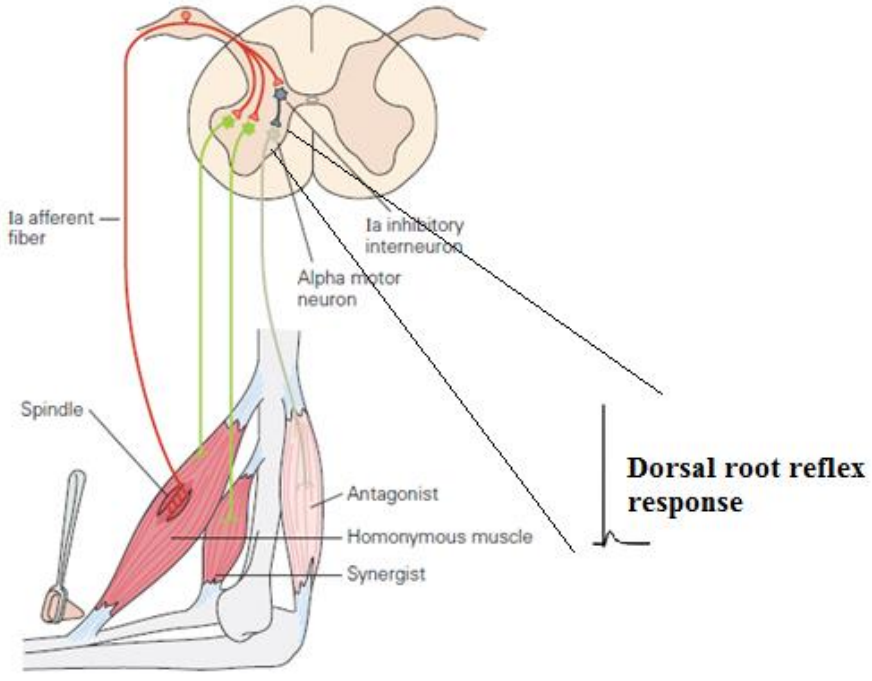

Fig. 14 Monosynaptic reflex pathways mediate stretch reflexes (http://www.krigolsonteaching.com/uploads/4/3/8/4/43848243/chapter_35-_spinal_reflexes.pdf)

❖ ***Polysynaptic reflexes***

Flexion (withdrawal) reflex pathways are activated in response to high threshold, A and C fibres. It consists of two interneurons (3 or more synapses) in many segments of cord and α-motoneurons of many flexor muscles. In response to an intense (painful) stimulus, it causes the withdrawal of limb (Fig. 15). Precisely it consists of two excitatory interneurons (3 synapses) for ipsilateral flexor and two interneurons for ipsilateral extensor (1 excitatory and 1 inhibitory) motoneurons inhibition. Contralateral pathways are activated with a more intense stimulus which results in cross-extension reflex, further producing an extension of the contralateral limb. Cross-extension pathways are involved in enhancing the postural support while withdrawing a limb from the harsh stimulus. Its corresponding interneurons are proposed to be a part of locomotor CPGs (Jankowska et al., 1967 a, b).

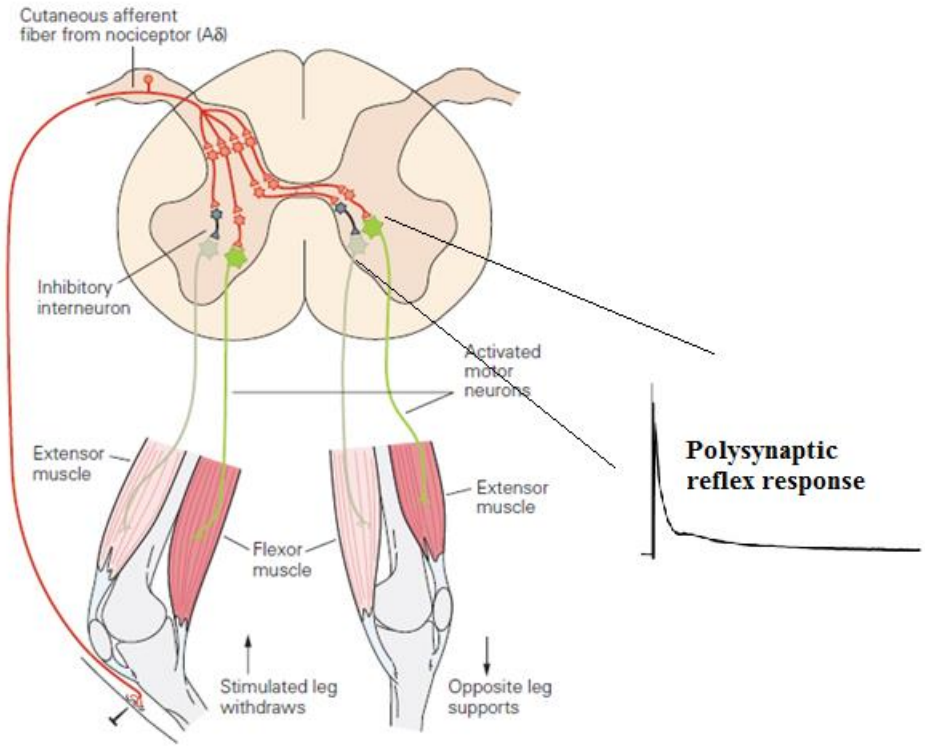

Fig. 15 Polysynaptic reflexes mediate flexion and crossed-extension reflexes (http://www.krigolsonteaching.com/uploads/4/3/8/4/43848243/chapter_35-_spinal_reflexes.pdf)

3.2 Spinal cord injury

Spinal cord injury (SCI) is considered to be an incurable condition despite extensive advancement in medical and surgical treatment strategies. Traumatic SCI is divided into 2 groups: 1) penetrative in which damage to the spinal cord by any sharp object, 2) non – penetrative in which compression is caused by accident. Acute SCI occurs due to a traumatic injury to the spine that fractures or dislocates vertebrae which leads to bruising, partially or completely tearing of ligaments in the spinal cord tissue. SCI is a common cause of permanent disability and death in children and adults. Recent clinical data indicate that in addition to traumatic SCI, there is growing etiopathogenetic importance of non-traumatic injuries (McKinley et al., 1999; van den Berg et al., 2010) which may occur because of degeneration of spinal column, inflammation, infection, tumour/cancer etc. Non-traumatic SCI is more often seen in elderly (Sekhon & Fehlings, 2001). SCI is also classified into complete or incomplete, no matter of its origin. With the complete injury, the spinal cord is unable to deliver signals below or above the level of injury, which ultimately leads to paralysis. With the incomplete injury, some sensation is still present below the level of injury (Ryan et al., 2014).

According to American spinal injury association (ASIA) impairment scale, it is classified into five grades:

- *Grade A* = Complete injury, where no function, whether sensory or motor, is preserved in S4-S5 (sacral) segments.

- *Grade B* = Sensory incomplete, where sensory (not motor) functions are preserved below injury including sacral segments.
- *Grade C* = Motor incomplete, in which motor functions are preserved below the injury and most key muscles below the level of cord injury have a muscle grade less than 3.

- *Grade D* = Motor incomplete, where motor functions are preserved below the injury and at least half of the key muscles below the neurological level have a muscle grade of 3 or more.

- *Grade E* = Normal, where no motor or sensory deficits, but deficits existed in the past.

3.2.1 Epidemiology

The quantification of incidence and prevalence of SCI is necessary to gain better potential impact of healthcare management strategies and health policies to prevent and minimize the consequences of injury. In the past, many studies have reviewed the worldwide incidence and prevalence of SCI. In 2004, Ackery reviewed and reported the annual incidences of injury from 11.5- 57.8 cases/million (Ackery et al., 2004). Later in 2006, Wyndaele & Wyndaele reported SCI incidences range from 10.4 – 83 cases/million population (Wyndaele & Wyndaele, 2006). Then in 2010, Cripps and his colleagues reported prevalence varied from 236 to 1009 cases/million, and the annual incidences in North America, Australia, and Western Europe were reported as 39, 16, and 15 cases/million population, respectively (Cripps et al., 2010). Recently, Chiu and his fellows reported the injury incidence ranges from 13.1 to 52.2 cases/million population yearly among 13 different countries (Chiu et al., 2010). More recently, van den Berg found incidence rates varied from 12.1 to 57.8 cases/million population in different countries (van den Berg et al., 2010). These figures indicate that it is difficult to compare data from distinct countries as different methods are used to report SCI incidences. Table1 shows the incidence of SCI in different countries within Europe (Fulran et al., 2013).

All studies have shown SCI cases are more prevalent among males than females. However, in Manitoba, the male to female ratio was significantly reduced from 12:1 to 4:4:1 from the 1980s to 2000s due to more cases of motor vehicle injuries among females (McCammon & Ethans, 2011). Fig. 16 shows motor vehicle accidents being the leading

cause of injury worldwide followed by falls, sports and so on. The injury ratio in Alaska was 5:1 (Warren, 1995). The average age of injury varies from 15 -30 years (Price et al., 1994; Warren et al., 1995; Dryde et al., 2003). According to the National SCI database, length of stay in hospitals in the acute care unit has declined from 24 days to 11 days since the year 1970 to 2010, respectively. Substantial downward trends are also noted for days in the rehabilitation unit (from 98 to 36 days). Neurologic level and extent of lesion: the most frequent neurologic category is incomplete tetraplegia followed by incomplete paraplegia, complete paraplegia, and complete tetraplegia. Less than 1% of persons experienced complete neurologic recovery by the time they were discharged from hospital (National SCI Statistical Center, 2014).

Table 1 SCI cases in Europe (extracted from Fulran et al., 2013)

Reference (N)	Geographic Area	Inclusion and exclusion criteria	Incidence rates by year
(33) N=29	Greenland	1965-1986 Admissions to rehabilitation hospital in Hornback with traumatic SCI	26/million/year
(34) N=360	Kingdom of Denmark	1975-1984 Admission to national specialized rehabilitation hospitals.	9.2/million/year
(35) N=79	Iceland	1973-1989 Patients admitted to rehabilitation unit in Reykjavik.	24/million/year (1973-1982) 18/million/year (1983-1989)
(36) N=207	Iceland	1975-2009 Landspitali University Hospital, the single referral center for SCIs in Iceland	30/million/year (1975-1979) 12.5 million/year (1995-1999) 33.5/million/year (2005-2009)
(37) N=>3000	Estonia	1997-2007 Medical records from 22 Estonian hospitals	39.7/million/year (1997-2007)
(38) N=980	Plovdiv region, Bulgaria	1983-1992 Treatment for SCI at 2 clinics in Plovdiv region.	130.6/ million/year
(39) N=46	Ireland	2000 Patients admitted to National Rehabilitation Hospital.	13.1/ million/year
(40) N=126	Netherlands	1994 Defined SCI cases within national registration system Exclusion Criteria: Spinal contusions with no or temporary neurological symptoms.	12.1/million/year
(41) N=539	Anatolia, Turkey	1990-1999 Four hospitals that were major referral centers for trauma in South-eastern Anatolia.	12.1/million/year
(42) N=75	Southeast Turkey	1994 Traumatic SCI in Southeast Turkey.	16.9/million/year
(43) N=152	Istanbul, Turkey	1992 All new patients with SCI, including pediatrics.	20.8/million/year
(44) N=581	Turkey	1992 Nation-wide survey of SCI admissions to medical institutions. Exclusion Criteria: Patients who died before hospitalization.	12.7/million/year
(45) N= 398	Central Region of Portugal	1989-1992 Two hospitals that treat all SCI in the central region of Portugal. Including pediatric cases. Cases without neurological lesion, rehospitalization and vertebral lesions were excluded	57.8/million/year
(46) N=366	Western Norway	1952-2001 Discharges from 8 hospitals in region with SCI.	6.2/million/year (1952-1956) 26.3/million/year (1997-2001)
(47) N=336	Norway	1952-2001 Individuals with SCI in the Hordaland and Sogn og Fjordane counties	6.2/million/year (1952-1956) 13.6/million/year (1972-1976) 26.3/million/year (1997-2001)
(48) 1970 N=29 2004 N=228	Finland	1970-2004 All persons aged 50 or older admitted to Finnish hospitals for treatment of a fall induced severe cervical spine injury,	52.0/million/year (1970) 120.0/million/year (2004)
(49) N=1647	Finland	1976-2005 Käpylä Rehabilitation Centre database.	13.8/million/year (1976-2005)
(50) N=412	Bucharest, Romania	1992-1993 SCI patients admitted to Dr Gh. Marinescu Hospital.	28.5/million/year
(51) N=4431	Federal Republic of Germany	1983 Hospitalizations, Hamburg's Central Office for Paraplegic Patients, German Workmen's compensation, and General Local Health Insurance Cia.	36.0/million/year
(52) N=577	Veneto, Italy	1994-1995 New cases of traumatic SCI and non-traumatic spinal cord disease treated in regional hospitals.	14.3/million/year
(53) N=1010	Spain	1984-1985 (Every traumatic and non-traumatic SCI patient in specialized Spanish hospitals)	8.0/million/year
(54) N=540	Aragon, Spain	1972-2008 Hospital admission in Aragon.	8.2/million/year (1972-1980) 13.8/million/year (1981-1990) 12.9/million/year (1991-2000) 13.4/million/year (2001-2008)
(55) N=10,274	Spain	2000-2009 The National Hospital Discharge Register	23.5/million/year (2000-2009)
(56) N=934	France	2000 (Survey of rehab units in France Patients with SCI (≥ 15 yo) admitted for first stay. Exclusion Criteria: Non-traumatic SCI; neurological impairment due to peripheral nervous lesion; follow-up or readmissions to rehab unit)	19.4/million/year

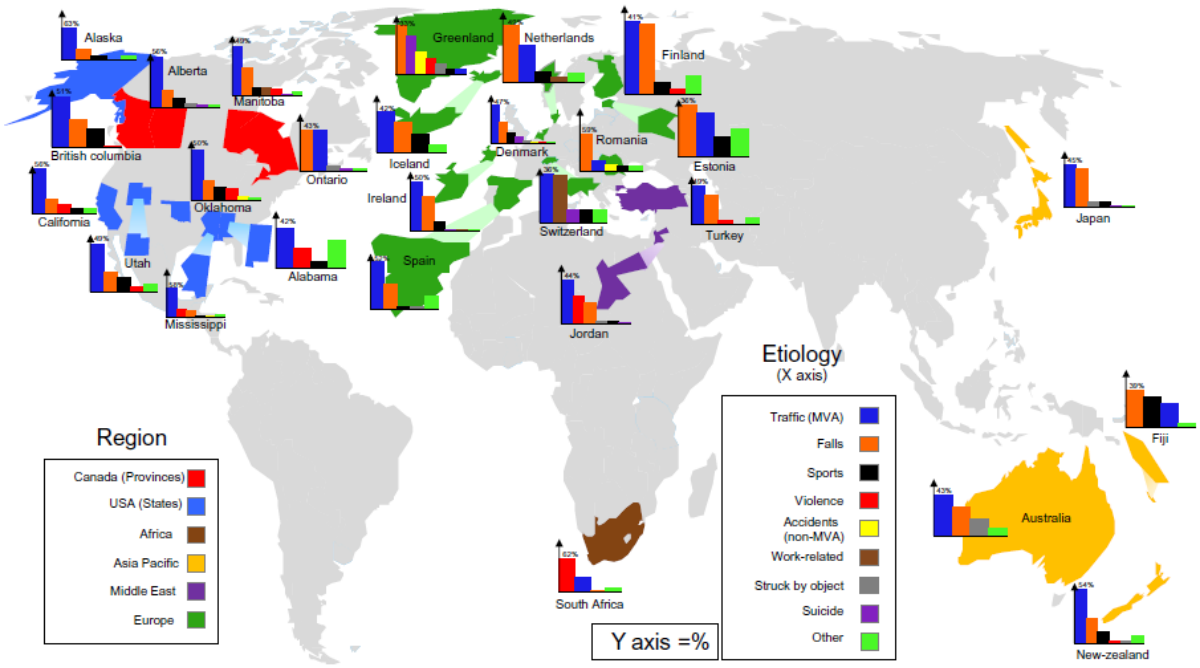

Fig. 16 Causes of SCI cases in different countries around the globe (Singh et al., 2014)

Lifetime costs: The average annual health care and living expenses and the estimated cost over a lifetime vary according to the severity of the injury as shown in Table 2.

Severity of Injury	Average Yearly Expenses (in November 2013 dollars)		Estimated Lifetime Costs by Age At Injury (discounted at 2%)	
	First Year	Each Subsequent Year	25 years old	50 years old
High Tetraplegia (C1–C4) AIS ABC	$1,048,259	$182,033	$4,651,158	$2,556,197
Low Tetraplegia (C5–C8) AIS ABC	$757,459	$111,669	$3,398,426	$2,090,336
Paraplegia AIS ABC	$510,883	$67,677	$2,274,396	$1,492,617
Motor Functional at Any Level AIS D	$342,112	$41,554	$1,553,878	$1,096,770

Table 2 Average yearly expenses and lifetime cost of SCI (Economic Impact of SCI published in the journal *Topics in Spinal Cord Injury Rehabilitation*, Volume 16, Number 4, in 2011)

3.2.2 Pathophysiology

Pathophysiology of SCI is divided into two phases: primary and secondary phase of injury.

Primary injury refers to direct mechanical injury to the cord. Primary injury is further classified into four types: 1) concussion (transitory spinal cord dysfunction in the absence of structural damage), 2) contusion (where the damage is because of vertebral disc displacement), 3) compression (similar to contusion although the continuity of columns are immediately restored without any intervention (Bailey, 1971; Jaillenger, 1976) and 4) laceration (where the injury is due to vertebral fracture). It can last up to 2 h. The initial insult tends to damage central gray matter with relative sparing of white matter, especially at the periphery (Wolman, 1965). Haemorrhage within the spinal cord develops early followed by disruption of blood flow after the initial mechanical injury, resulting in local infarction because of hypoxia and ischemia. This particularly damages the gray matter due to high metabolic requirements. Neurons near the injury site are disrupted and myelin thickness diminished (Young, 1993). Nerve transmission is also disrupted due to oedema (Anderson & Hall, 1989; Geiser et al., 1991; Lapcak et al., 2001).

In most clinical situations, ***secondary injury*** following the primary insult is a therapeutic target for preventing extension of injury (Rowland et al., 2008). Secondary injury begins in minutes after the primary insult and lasts from days to even months. It is further divided into three phases: 1) Acute (2h – 2 weeks), 2) Sub-acute (intermediate; 1-2 months post-injury) and 3) chronic phase (> 6 months) (Fig. 17).

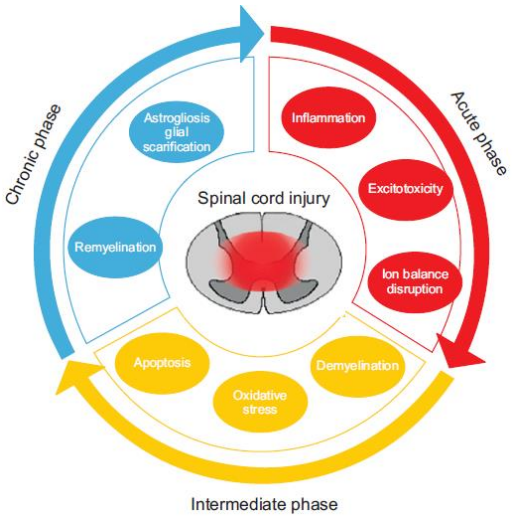

Fig. 17 Phases of secondary insult after SCI (Young et al., 2017)

Secondary injury causes the activation of local factors such as vascular effects (leading to hemorrhage, increased permeability, ischemia and formation of free radicals; Xiong et al., 2007; Donnelly & Polovich, 2008), glutamate release (causes excitotoxicity because of overactivation of glutamate receptors, which further changes the membrane potential and activation) (Li & Styts, 2000) and inflammation (leads to activation of microglia and neutrophils which further changes the gene expression) (Fig. 18). All these factors ultimately converge to apoptosis and finally cell death (Li et al., 1999; Park et al., 2004).

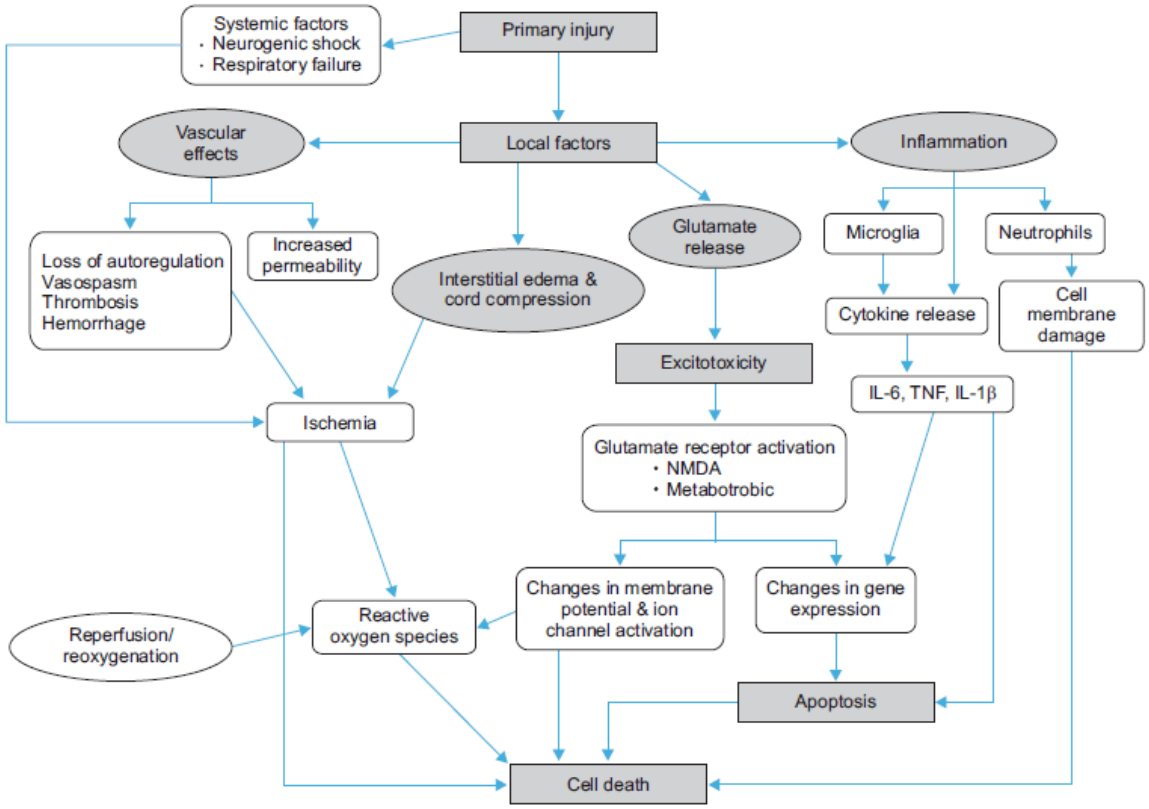

Fig. 18 Pathophysiology of secondary SCI (Young et al., 2017)

"The time window between primary and secondary injury gives us an opportunity to develop neuroprotective strategies combat spinal injury".

In recent years our lab has developed an in vitro model of rat SCI. The usefulness of using this in vitro preparation is its survival for up to 24 h in physiological conditions. It provides us with an opportunity to study the secondary phase of injury for 24 h. In 24 h, we are able to study the mechanisms of neuroprotection produced by treating the preparation with different drugs after lesion. The lesion is induced by application of either glutamate agonist, ***kainate for 1 h***, which induces excitotoxicity at the gray matter of spinal cord or ***pathological medium*** (PM) which produces hypoxia-like conditions, leading to white matter damage. Also, Kuzhandaivel in 2011 has reported, despite kainate washout, the secondary lesion progresses within first few hours (Kuzhandaivel et al., 2011) which enable us to test locomotor spinal networks and imply pharmacological treatment for the injury.

3.3 Glucocorticoid system

Corticoids (or corticosteroids) are steroid hormones produced by the adrenal cortex of vertebrates, as well as the synthetic analogues of these hormones. They are classified into two groups: ***mineralocorticoids*** and ***glucocorticoids***.

Mineralocorticoids: such as aldosterone (produced in the adrenal cortex), helps in the regulation of electrolyte and water balance in kidneys by regulating ion transport in renal tubules (Lui et al., 2013).

Glucocorticoids (GCs): also known as glucocortico-steroids are hormones synthesized and released by the adrenal cortex in a circadian manner and in response to stress. The secretion of these hormones is maintained by the hypothalamic-pituitary-adrenal (HPA) axis (Fig. 19). Hypothalamus secretes corticotropin-releasing hormone (CRH), in response to internal and external stimuli which acts on the anterior pituitary to stimulate the synthesis and secretion of adrenocorticotropic hormone (ACTH). ACTH further acts on the adrenal cortex to secrete glucocorticoids. It is present in all vertebrate animal cells. The name glucocorticoid (glucose + cortex + steroid) is composed of its role in the regulation of glucose metabolism. Glucocorticoids play important role in regulation of homeostasis, metabolism, immune functions, skeletal growth, cardiovascular function, reproduction and cognition, etc (Barnes, 1998; Sapolsky et al., 2000). GCs are also important part of feedback mechanism in immune system where they release in response to stress and help in reduction of inflammation. Hence they are also used as a medicine to treat diseases where the immune system is over-activated like in autoimmune diseases, asthma and various allergies etc.

They show anti-inflammatory effects by inhibiting inflammatory mediators (by transrepression) and inducing anti-inflammatory mediators (called as transactivation) (Häggström & Richfield, 2014). Their vaso-constrictive effects are mediated by blocking the action of inflammatory mediators (histidine) (Häggström & Richfield, 2014). GCs also help in immunosuppression effects by suppressing delayed hypersensitivity reactions

(by acting directly on T-lymphocytes). Further their anti-proliferative effects are induced by inhibition of DNA synthesis and epidermal cells turnover (Häggström & Richfield, 2014).

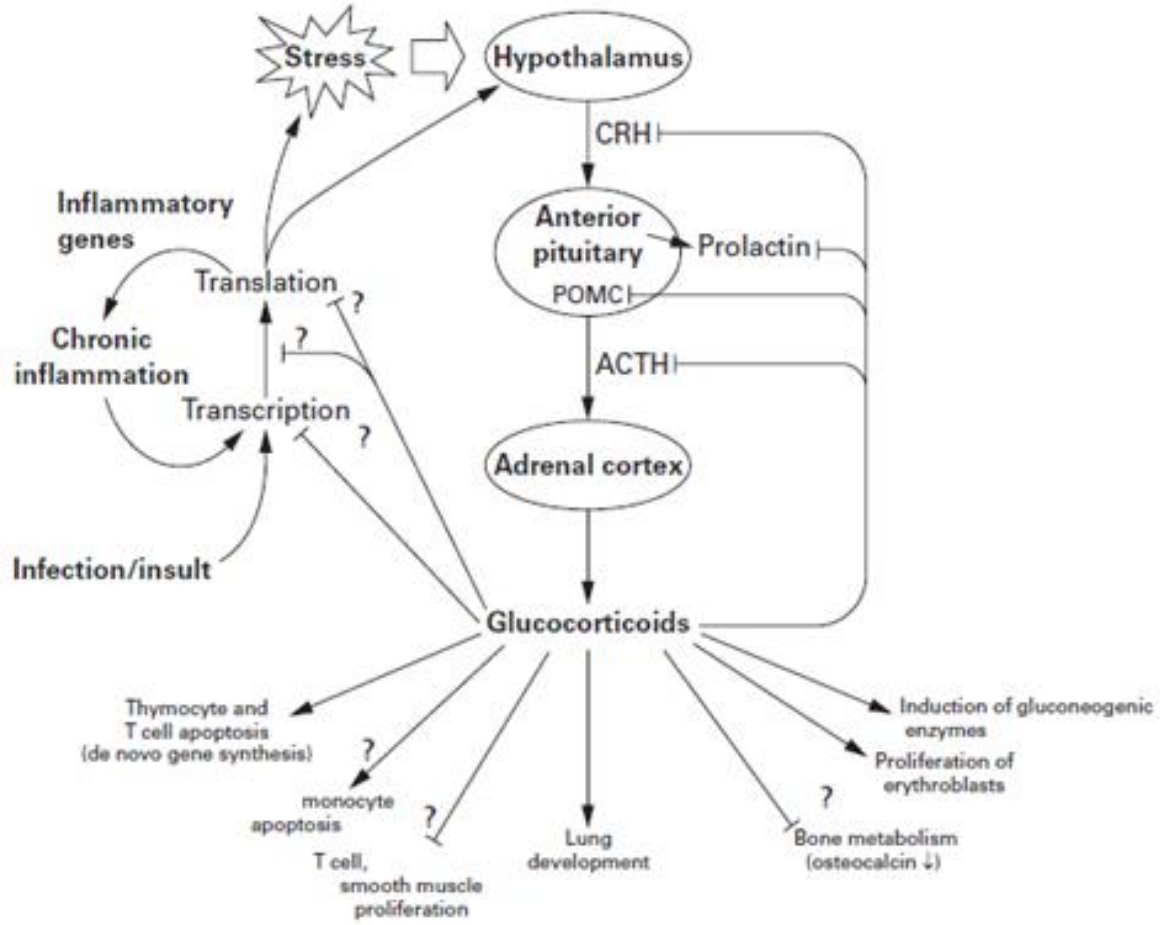

Fig. 19 Effects of glucocorticoids on Hypothalamus-Pituitary-Adrenal (HPA) axis. The scheme represents sites of synthesis and the targets of action of glucocorticoid. Question marks indicate uncertainty as to the mechanism of action. Corticotropin-releasing hormone (CRH) (also known as a corticotropin-releasing factor, CRF), adrenocorticotropic hormone (ACTH) and pro-opiomelanocortin (POMC) (extracted from Newton, 2000)

Once in the bloodstream, GCs diffuse into tissues and cells and bind to glucocorticoid (GR) or mineralocorticoid nuclear receptors (MR). In normal conditions, GC binding favours MRs, even though GRs are still occupied by GCs at low levels (Spencer et al., 1990). When the level of GCs increases in response to stress, they bind to GRs at higher levels. Unbound GRs are present in the cytoplasm in complex with heat

shock proteins, HSP90 and HSP70, and FK506-binding proteins, FKBP51. When GCs bind to GRs, these receptors undergo a conformational change and nuclear translocation to induce gene transcription (Sanchez, 1990; Oakley & Cidlowski, 2011; Maiarù et al., 2016). GRs mediate gene transcription by binding to glucocorticoid response elements (GREs) (Datson et al., 2008; Revollo & Cidlowski, 2009). Many transcriptional GR targets block the release of cytokines (like TNFα and IL-1β) making GR activation a powerful tool to suppress inflammation (Joyce et al., 1997; Revollo & Cidlowski, 2009). Therefore, GCs are prescribed to treat acute and chronic inflammatory diseases, autoimmune diseases and after an organ transplant (Oakley & Cidlowski, 2011).

In the CNS, GRs are expressed in neurons throughout the brain and spinal cord. Hippocampal CA1 neurons have maximum expression of GRs (McEwen et al., 1968; Herman et al., 1989). Moreover, all glia express GRs. Schwann cells (the myelinating cells of the peripheral nervous system, PNS), brain and spinal cord microglia (originate from bone marrow-derived monocytes and are the resident macrophages of CNS), oligodendrocytes (myelinating cells of CNS) and astrocytes (major support cells to CNS neurons) all bind synthetic GR agonists and are positive to GR immunoreactivity (Warembourg et al., 1981; Vielkind et al., 1990; Sierra et al., 2008; Shaqura et al., 2016). MRs co-localize with calcitonin gene-related peptidergic (CGRP) nociceptive neurons in the spinal cord and dorsal root ganglia (Shaqura et al., 2016) and not present in spinal astrocytes, microglia and oligodendrocytes. In contrast, oligodendrocytes, spinal cord astrocytes, and microglia are mostly absent of MR immunoreactivity (Matsusue et al., 2014; Shaqura et al., 2016). It may be possible that cells lacking MRs have more GRs (Shaqura et al., 2016; Shaqura et al., 2016). It has been reported that spinal microglia are activated in response to stress/GCs (Alexander et al., 2009), providing evidence for direct stress/GC-induced plasticity in microglia.

Unfortunately, its therapeutic benefits are limited by side effects like re-appearance of inflammation or pain, abdominal obesity, glaucoma, growth retardation in children, and hypertension (Oakley & Cidlowski, 2011; 2013). Apart from this, GCs uptake may lead to neuropsychiatric disorders like depression mood imbalance and anxiety (Dubovsky et al., 2012). However, agonists of GCs are still prescribed in hospitals because of their beneficial effects.

Prednisone is one of the commonly prescribed steroid drug for chronic conditions (the structure is shown in Fig. 20). It is more popular also because of its low cost. It is a prodrug which is biotransformed to an active metabolite, prednisolone after incorporation. Thus it is available only for oral use that allows for first-pass metabolism during absorption.

Betamethasone is available in markets in many forms: betamethasone dipropionate (branded as Diprosone, Diprolene, Celestamine, Procort (in Pakistan), and others), betamethasone sodium phosphate (branded as Bentelan in Italy) and betamethasone valerate (branded as Audavate, Betnovate, Celestone, Fucibet, and others). In the United States and Canada, betamethasone is mixed with clotrimazole and sold as Lotrisone and Lotriderm etc. Its molecular structure is depicted in Fig. 20. Betamethasone was approved for medical purpose in the United States in 1961 (The American Society of Health-System Pharmacists, 2015). Betamethasone may suppress astrocytes activation and elevate TNF-α and IL-1β levels in neuropathic pain of rat. Local injection of betamethasone leads to a small increase in spinal GR expression and thus relieve from pain as compared to intrathecal injection (Wang et al., 2013).

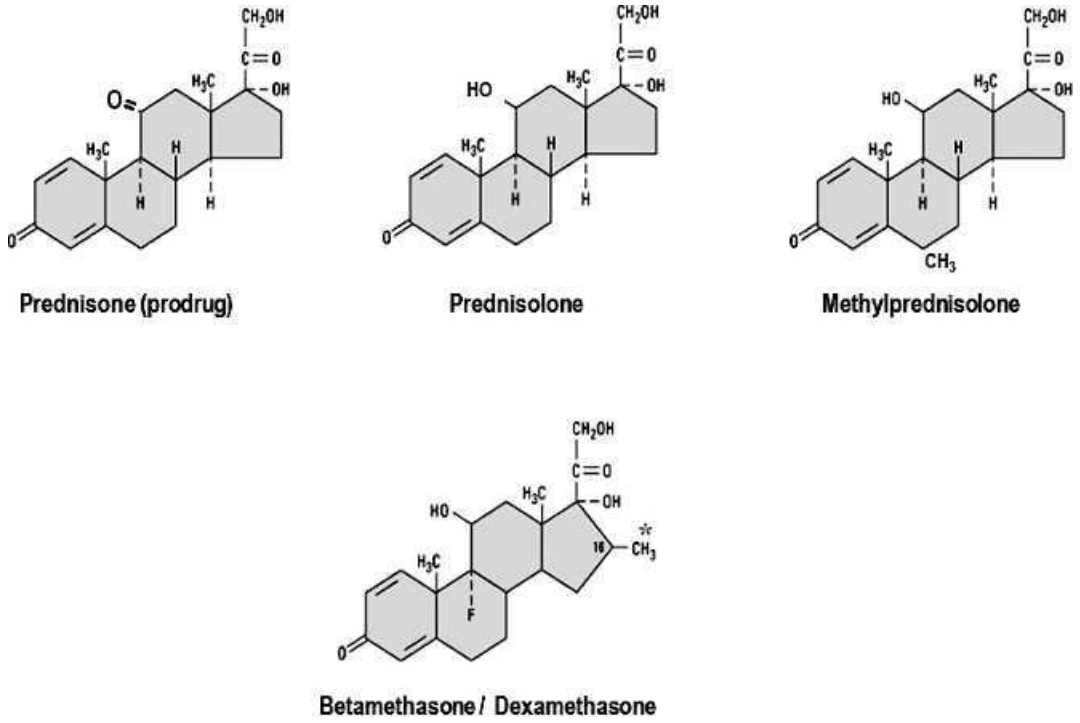

Fig. 20 Molecular structures of some glucocorticoids (Becker DE, 2013)

Methylprednisolone (MP, Medrol) is a widely used medication for the treatment of patients with chronic SCI (Hurlbert et al., 2013; Fallah et al., 2016; Fehlings et al., 2017). It is available to administer orally or via injection. Methylprednisolone has also been reported to promote recovery of neurological function after spinal cord injury in rats (Lu et al., 2016). The neuroprotective effect of MP on SCI may be because of the activation of the Wnt/β-catenin signalling pathway and this inhibition of apoptosis, providing a novel molecular mechanism underlying the role of MP for the treatment of SCI (Lu et al., 2016) (Fig. 21).

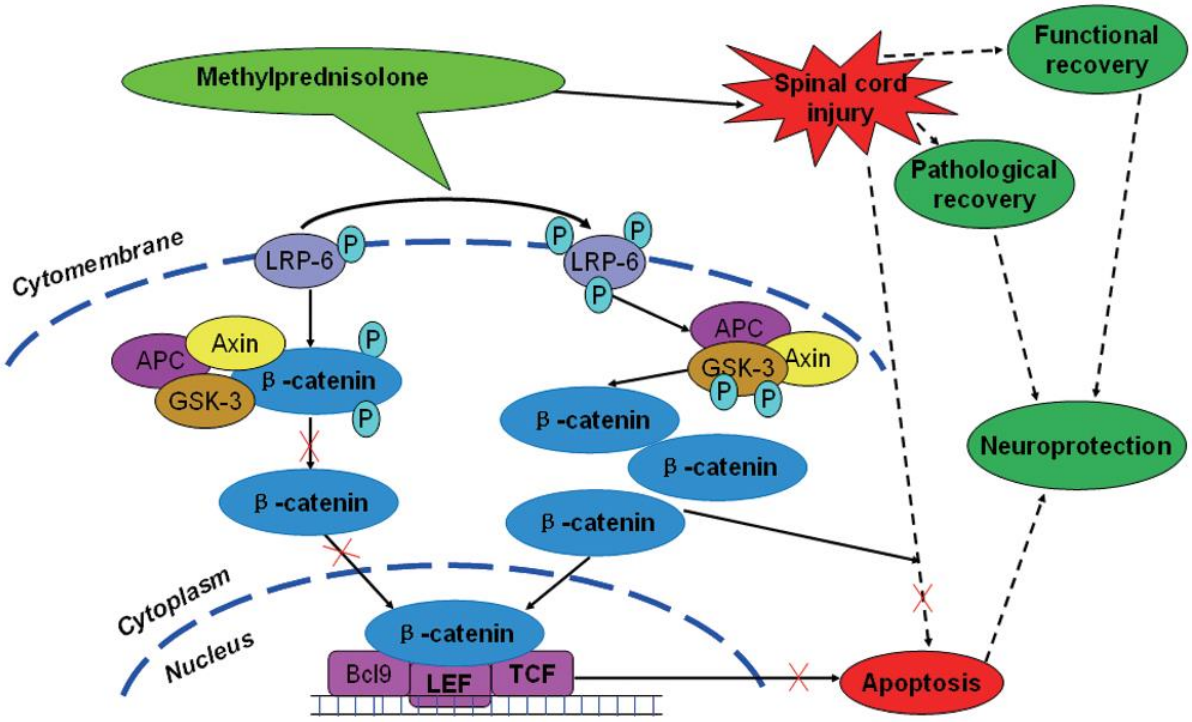

Fig. 21 Neuroprotective effect of MP after SCI in vitro (Lu et al., 2016)

It also exhibits antioxidant properties and inhibits lipid peroxidation (Hall & Springer, 2004) (Fig. 22).

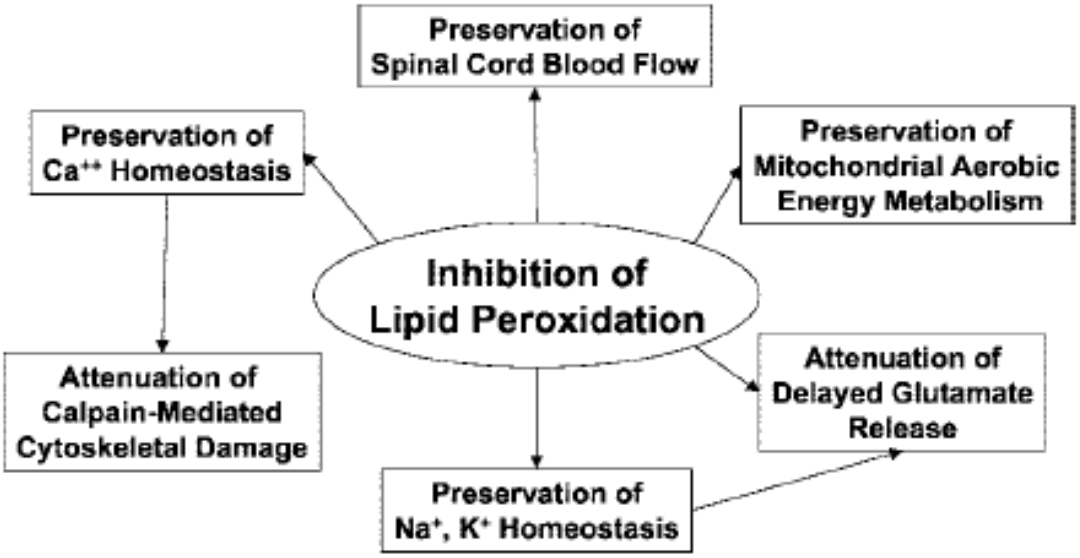

Fig. 22 Hypothesized role of inhibition of lipid peroxidation by MP and production of neuroprotective effect after acute SCI (Springer & Hall, 2004)

However, due to its side effects which makes it as a controversial drug of choice. We tested this drug on our in vitro rat SCI model (Sámano et al., 2016) to investigate its pros and cons on the lesioned spinal cord in vitro.

3.4 General anesthetics

An ancient Greek surgeon Dioscorides who originally used the term “anaesthesia” and it was resurrected by Dr Oliver Wendell Holmes in 1846 which means lack of sensation produced by inhalation of ether (Nuland, 1988; Kissin, 1997). The objectives of general anaesthesia include amnesia, unconsciousness (also termed hypnosis), and immobilization. According to its definition, it reversibly produces all of these three therapeutic effects (Grasshoff et al., 2005; Mashour et al., 2005).

General anaesthetic drugs include inhaled gases as well as intravenous agents. Other classes of drugs used to achieve specific clinical goals during surgery (Woodbridge, 1957) could be the use of selective blockers of neuromuscular transmission to restrict movement of patients while surgery.

These anaesthetics have been broadly divided into three groups based on relative potencies for distinct clinical endpoints and their impact on electroencephalogram (EEG) (Forman & Chin, 2008).

Group 1: consists of etomidate, propofol, and barbiturates, intravenous drugs, which can potentially produce unconsciousness than immobilization. For example in case of propofol unconsciousness (hypnosis) is attained at 3 µg/ml of plasma concentration whereas immobility (during skin incision) is achieved with four times higher concentration of the drug (Smith et al., 1994). They shift EEG (recorded from cortex) to lower frequencies which enable to reproduce correlation with anaesthetic depth (Kuizenga et al., 2001).

Group 2: composed of gaseous (volatile) anaesthetics such as nitrous oxide (N_2O), xenon and cyclopropane, along with ketamine, an intravenous agent. They are capable to induce analgesia however hypnotic and immobilizing ability is weak. N_2O and ketamine may increase the EEG frequencies however, the anaesthetic depth monitored via EEG is not

stable (Rampil et al., 1998; Anderson & Jakobsson, 2004). There are some contradictory data for xenon based on EEG monitoring (Goto et al., 2000; Laitio et al., 2008).

Group 3: consists of the volatile halogenated anaesthetics: halothane, isoflurane, sevoflurane, desflurane and methoxyflurane. They produce amnesia, hypnosis and immobility in a predictable manner (Campagna et al., 2003; Mashour et al., 2005). They reduce the frequency of EEG and anaesthetic depth monitors show reliable correlations with the level of consciousness.

It has extensively been studied that anaesthetics produce neuroprotective effects on spinal neurons and motoneurons (Salzman et al., 1993; Sooner et al., 2003; Baranović et al., 2014; Ishikawa et al., 2014; Bao et al., 2017). Therefore our lab has recently tested the volatile anesthetic, methoxyflurane (Shabbir et al., 2015), which is less frequently used these days because of its toxic effects (Paul et al., 1976; Wharton et al., 1980), showed strong neuroprotective effects on spinal motoneurons and fictive locomotion has recovered back by this drug. Back in 2005, the Food and Drug Administration (FDA) disapproved its usage in the market because of safety concerns (Mazze, 2006). However, it is still used in Australia for emergency purposes as an analgesic for the initial management of pain due to acute trauma.

On the other hand, an intravenous anaesthetic, propofol (Fig. 23) which is a widely used drug these days in hospitals by surgeons to induce anaesthesia before surgery. More usage is because of its fast recovery of consciousness, however, fast recovery means eye-opening (Grundmann et al., 2001) and not complete recovery of cognitive functions (Mirski et al., 1995). Propofol also exerts other advantages such as minimal side effects, controllable anaesthetic state and quick onset (Glen, 1980; Glen & Hunter, 1984). Further it also exerts non-anaesthetic effects (stimulates constitutive nitric oxide (NO) production and inhibits inducible NO production, produce anxiolytic effects, has antioxidant, immunomodulatory, analgesic, antiemetic and neuroprotective effects) reported in animals (Rossi et al., 1996; Pain et al., 1999; Yamasaki et al., 1999; Ishii et al., 2002; Wang et al., 2002; Kurt et al., 2003; Nishiyama et al., 2004; Kushida et al., 2007; Sanchez-Conde et al., 2008) as well as in humans (Zacny et al., 1996; Aoki et al., 1998; Grouzmann et al., 2000; Veselis et al., 2004; Gonzalez-Correa et al., 2008; Veselis et al., 2008).

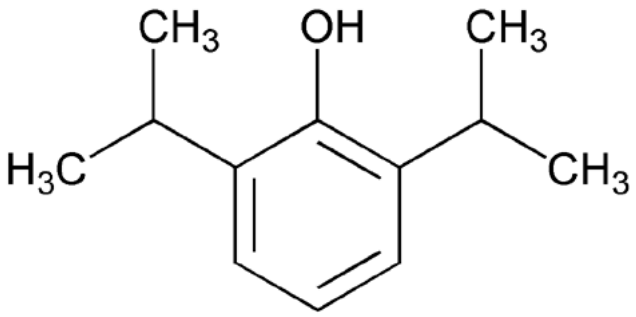

Fig. 23 Structure of propofol (also known as 2, 6-di-isopropylphenol or Diprivan or Disoprofol or Disoprivan) (http://www.drugfuture.com/pharmacopoeia/usp32/pub/data/v32270/usp32nf27s0_m70460.html)

Mechanism of action of neuroprotective effect of propofol

Propofol shows neuroprotective effect via potentiation of $GABA_A$ (β2 and β3 subunits) mediated receptor responses (Fig. 24) (Belelli et al., 1997; Forman & Chin, 2008; Bajrektarevic & Nistri, 2016) and depressed the glutamate (mainly NMDA) mediated one (Vasileiou et al., 2009).

GABA receptors are a class of receptors which respond by binding of the inhibitory neurotransmitter, GABA. GABA receptors are classified into two groups: $GABA_A$ and $GABA_B$. $GABA_A$ receptors are ligand-gated ion channels also called as ionotropic receptors [which also include nicotinic acetylcholine receptors (nAChR), the 5-hydroxytryptamine (5-HT) type-3 receptors, and the glycine receptors], whereas $GABA_B$ receptors are G protein-coupled receptors (also known as metabotropic receptors).

$GABA_A$ receptors are made up of five subunits that belong to different subclasses (α, β, γ, δ, ε, π, θ, ρ) (Fig. 24). The subunits exhibit a 60–70% homology within each class, however, the homology between the classes is 30–40% (Sieghart, 1995; Barnard et al., 1998). So far, a total of six α-, three β-, three γ-, one δ-, one ε-, one π-, one θ-, and

three ρ-subunits of $GABA_A$ receptors and alternatively spliced isoforms of these subunits have been cloned and sequenced from the mammalian CNS (Sieghart, 1995; Barnard et al., 1998). In the human brain, this subunit seems to be final as no new $GABA_A$ receptors were detected by applying search algorithms from human to nematodes (Simon et al., 2004).

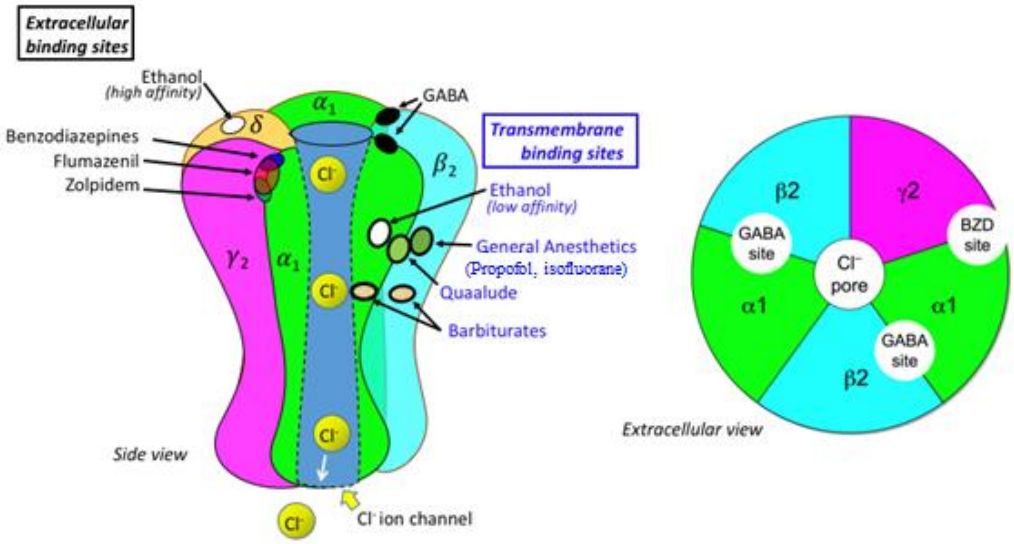

Fig. 24 Structure of $GABA_A$ receptor-chloride (Cl^-) channel complex with binding sites for different drugs in CNS. GABA binds to two sites located between α and β subunits, trigger the opening of the Cl^- channel, which produces membrane to hyperpolarize resulting in a reduction of neuronal firing rate (http://tmedweb.tulane.edu/pharmwiki/doku.php/overview_of_cns_neurotransmitters)

3.5 Nicotinic Acetylcholine Receptors

The importance of nicotinic acetylcholine receptors (nAChRs) to regulate biological functions lies in their ability to bind endogenous agonist, acetylcholine (ACh), which makes the receptor in motion and gates the channel allowing the flow of ions and thus produces a cellular response. In 1936, Henry Dale and Otto Loewi shared the Nobel prize in Physiology and Medicine for their pioneering research on chemical neurotransmission; in particular, the discovery of first identified neurotransmitter, ACh. The history of this neurotransmitter was based on critical experiments performed by H. Dale (Dale, 1914) who determined the role of ACh in vasodepression and O. Loewi (Loewi, 1921), who described the chemical neurotransmission in frog nerve-heart preparation. This story was concluded after 15 years when ACh was actually found in mammalian organs (Dale & Dudley, 1929). Since that time, the history of ACh in neuroscience has been of extreme advancement to our knowledge in various functions in the nervous system and in neuropathologies.

The name ACh is derived from its chemical structure as it is an ester of acetic acid and choline with chemical formula, $CH_3COOCH_2N^+(CH_3)_3$. In cholinergic neurons, it is synthesized from choline and acetyl-CoA by the enzyme choline acetyltransferase, located in the cytosol. Choline is supplied from extracellular space by the high-affinity active transport system, whereas acetyl-CoA is synthesized in mitochondria. After synthesis, ACh is stored into synaptic vesicles along with ATP. Upon nerve stimulation, it is released into the synaptic cleft, by exocytosis through the synaptic vesicles, where it may activate cholinergic receptors or be rapidly degraded by acetylcholinesterases to choline and acetate.

3.5.1 Receptor types and distribution

The key molecules to which ACh bind are cholinergic ***muscarinic*** (mAChRs) and ***neuronal nicotinic acetylcholine receptors*** (nAChRs). Muscarinic receptors were named

as such because they are sensitive to muscarine and nicotinic receptors for their sensitivity to nicotine. Both are expressed by either neuronal or non-neuronal cells throughout the body. These two receptors are structurally and functionally different.

mAChRs occur primarily in CNS and belong to a family of G-protein coupled receptors. They use an intracellular secondary messenger system which increases intracellular calcium resulting in the transmission of signals inside the cells. Upon ACh binding to mAChRs causes conformational changes at the receptors leading to activation of intracellular G-protein and conversion of GTP to GDP (in order to become activated and dissociate from the receptor). The active G-Protein acts as an enzyme to further catalyze downstream signalling cascades. These receptors play an important role in modulating various physiological functions like the release of neurotransmitter, contraction of smooth muscles and heart rate etc. They are classified into five types of metabotropic receptors: M1 to M5 (Bonner et al., 1987; Peralta et al., 1987; Bonner et al., 1988; Bonner, 1989; Caulfield et al., 1998). M1-M5 are localized in CNS, M1-M4 are also found in many tissues like M1 receptors are localized in salivary glands, M2 in cardiac tissues where they play a crucial role in closing calcium channels and therefore reduce the force and rate of contraction and M3 receptors are found in smooth muscles and secretion glands. M1, M3 and M5 are involved in activation of phospholipase C and thus produce two secondary messengers, Inositol trisphosphate (IP_3) and diacylglycerol (DAG) eventually causing an increase of intracellular calcium (Wess, 1996; et al., 1998). M2 and M4 inhibit adenylate cyclase and thus causing the low production of cAMP which is a second messenger (Scarr, 2012).

nAChRs are a member of the superfamily of cysteine-loop of pentameric ligand-gated ion channels, widely expressed in both central and peripheral nervous system (Sine & Engel, 2006; Albuquerque et al., 2009). They are expressed in both neuronal and in non-neuronal systems (Dani & Bertrand, 2007; Wessler & Kirkpatrick, 2008). So far, seventeen vertebrate subunits (α1-10, β1-4, γ, δ, and ε) have been identified in the nervous system and muscles nevertheless, only the subunits expressed in the mammalian CNS are reviewed here.

12 genes have been identified, encode for neuronal nAChR subunits, α2–α10 (contain 2 adjacent cys-residues crucial for binding ACh) and β2–β4 (lack cys-residues) (Le Novere & Changeux, 1995; Lindstrom, 2000). Further, these receptors are mainly

divided into 2 categories, low affinity receptors (mainly α7 nAChRs) that bind the agonist with low affinity (with μM concentration) and high affinity (majorly α4β2 nAChRs) that bind receptors with high (with nM concentration) affinity in the chick (Whiting & Lindstrom, 1986a) and rat brain (Whiting & Lindstrom, 1986b; Whiting & Lindstrom, 1987). In CNS, cholinergic transmission acts via nAChRs and modulates various activities such as cell excitability, neurotransmitter release etc and also control physiological functions like cognition, pain, anxiety, fatigue, reward, learning, memory (Changeux & Edelstein, 2001; Hogg et al., 2003; Christie et al., 2008). The ***brain cholinergic system*** is formed of a number of subsystems consisting of eight major and highly overlapping groups of cells, where dendrites of one cell are making contacts with a number of other cells. Therefore it can be assumed that these network interconnections may lead to firing of a group of neurons altogether in coordination and consequently to the activation of different cholinergic subsystems (Mesulam & Geula, 1988; Mesulam et al., 1989; Woolf, 1991).

- ***Magnocellular basal complex***: The most important group of cholinergic neurons, providing input to cortical and hippocampal neurons.

- ***Pedunculopontine-laterodorsal tegmental complex:*** The second significant cholinergic complex in brain. The neurons are localized at the pedunculopontine tegmental nucleus and innervating the thalamus and midbrain dopaminergic (DA) neurons.

- ***Striatum:*** Dense cholinergic fibres evolving from inner cholinergic neurons located in the caudate nucleus and they do not innervate beyond striatum.

- ***Lower brain stem:*** Cholinergic neurons localized in brainstem reticular formation and spinal intermediate gray matter which innervate the superior colliculus, cerebellum and cortical nuclei.

- ***Habenula–interpeduncular system:*** Cholinergic neurons present in the medial habenula project to the interpeduncular nucleus. Thalamus is providing input signals to habenula and thus it is a significant point through which the brainstem reticular formation is being influenced by the limbic system.

- ***Autonomic nervous system:*** The preganglionic neurons in sympathetic and parasympathetic systems are cholinergic. The parasympathetic preganglionic cells are present in encephalic trunk nuclei and in S2–S4 segments of the spinal cord and are innervating to target organs. The sympathetic preganglionic neurons are located in the intermediolateral gray matter (T1–L3 segments) of the spinal cord and innervating to paravertebral sympathetic ganglia.

3.5.2 Structure and topology of nAChR

The pentameric neuronal nAChRs (Fig. 25 B) encode for peptides having hydrophilic extracellular -NH_2 domain (M1-M3), a large intracellular loop and a fourth hydrophobic transmembrane domain (M4) (Sargent, 1993; Hogg et al., 2003) (Fig. 25 A). During evolution, these receptor subunits are highly conserved with < 80% amino acid identity of the same subunit among different vertebrate species (Le Novere & Changeux, 1995). These nAChRs are further divided into 2 classes: homomeric (consisting of single types of subunits; made of α7– α9 subunit homo-pentamers) or heteromeric (composed of several subunit types; made up of α7, α8 or α9, α10 subunit hetero-pentamers). Although, nAChRs, which contain the α2– α6 and β2– β 4 subunits form only heteromeric receptors that bind to the agonists with high affinity (Lindstrom, 2000) (Fig. 25 C). nAChR subunits are organized around the central canal, where the receptor has binding sites for a ligand, ACh. ACh has two components, principal and complementary. In heteromeric nAChRs, α2– α4 and α6 subunits carry principal component and β2 or β4 subunits carry the complementary component. In case of homomeric receptors, each subunit has both components to bind ACh (Changeux & Edelstein, 1998; Corringer et al., 2000; Fig. 25 C). However, these components are absent in α5 and β3 subunits, therefore, called as

auxiliary subunits. nAChRs are permeable to Na^+, K^+, and in some cases, Ca^{2+} ions. The channel opens immediately (with a time constant of about 20 μs) upon binding of least two ACh molecules to the receptor. In the open state, the nAChR channel has a pore diameter of 9-10 Å with a conductance in the range from 5 to 35 pS.

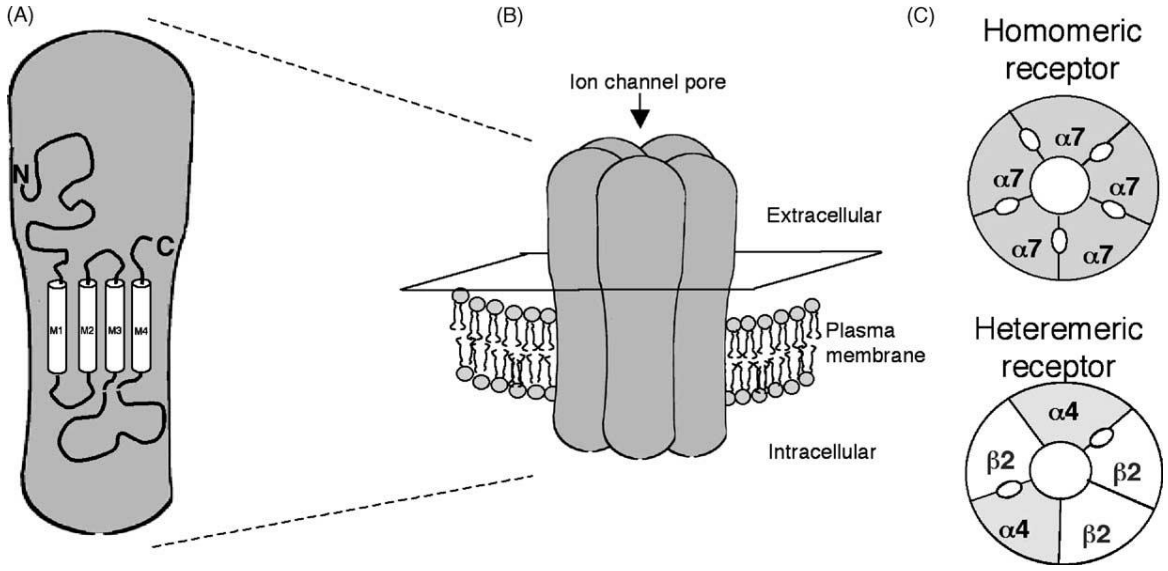

Fig. 25 The structure of neuronal nAChRs. (A) Scheme of transmembrane topology of nAChR subunits. (B) An assembled pentameric arrangement of nAChR receptor subunits. (C) Subunit arrangement in the homomeric α7 and heteromeric α4β2 subtypes, and localization of the ACh binding site (Gotti & Clementi, 2004)

3.5.3 Ligands –Agonists of nAChRs

There are several molecules being reported to activate nAChRs exemplified in Fig. 26:

- Nicotine acts as an agonist at most nicotinic nAChRs (IUPHAR Database, 2004; Malenka et al., 2009), except at two receptor subunits (α9 and α10) where it acts as a receptor antagonist. Nicotine is an alkaloid found in the nightshade family of plants. In smokers, the peak concentration of nicotine in blood plasma is about 0.31 μM (between 10 and 50 ng/ml), in the brain is about 1 μM, and after smoking

in lung fluids the concentration reaches to 60 μM (Clunes et al., 2008; Matta et al., 2006). After inhaling the cigarette smoke, nicotine reaches the brain within 8-10 s through arterial circulation. Its half-life is about 2 h, and of cotinine (the major nicotine metabolite) is about of 16 h (Benowitz, 2009). Other nAChR analogues are also synthesized from nicotine (shown in Fig. 26, compound 1) by replacing pyridine or pyrrolidine rings or by conformational flexibility.

- Compound 2 is highly selective for α4β2 receptor subtype (Romanelli & Gualtieri, 2003; Bunnelle et al., 2004; Jensen et al. 2005).

- Analogue in example 3 has nM affinity for β2-containing receptors (Wei et al., 2005).

- The compounds of general formula 4 and 5 (Pallavicini et al., 2004) possess affinity in μM range for the rat brain nAChRs labelled by [^{3}H]-epibatidine.

- Substitution of pyridine ring with a quinoline gives rise to compound 6 which behave as a nicotinic agonist in the hot-plate test on mice when injected intracerebroventricularly (i.c.v.) (Guandalini et al., 2006).

- Compounds 7–10 designed with the motive of discovering new analgesic drugs. Compounds of general formula 7, but not 8 or 9, showed significant analgesic activity in the writing test in mice (Zhang et al., 2006), whereas compound 10 showed analgesic activity in the formalin test on mice (Baraznenok et al., 2005).

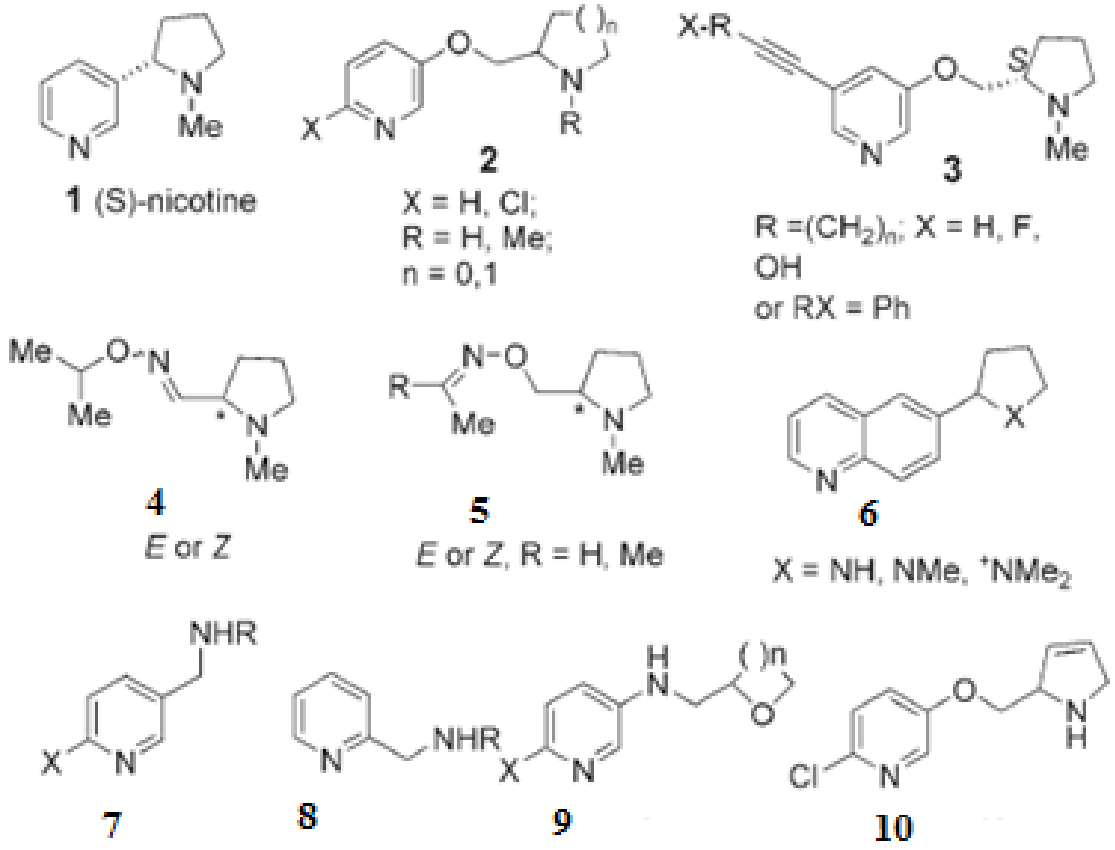

Fig. 26 Agonists of nAChRs (modified from Romanelli et al., 2007)

3.5.4 Desensitization of nAChR

Loss of physiological response after prolonged application of stimulus is termed desensitization. Desensitization of the nAChR is produced by prolonged exposure to agonists leading to inactivation of the channel. In spite of extensive studies on nAChRs, the detailed molecular mechanism of the nAChR desensitization is not known with certainty. Concerning desensitization, nAChRs in the mammalian nervous system can be divided into two main groups: α7-containing receptors which desensitize within milliseconds and non α7 nAChRs that desensitize slowly, in seconds (Quick & Lester,

2002; Giniatullin et al., 2005). Desensitization depends on agonist concentration and time of exposure.

nAChRs may exist in three distinct conformations: 1) the resting, 2) active and 3) desensitized states. Fig. 27 A, B demonstrates an idealized nicotinic cholinergic synapse where the presynaptic component composed of the neurotransmitter ACh (black dots) within synaptic vesicle and the postsynaptic membrane consists of the receptor. The receptor exists in an equilibrium mixture of two conformation states, resting (Re) and desensitized (D) state. The numbers below each conformation state imply amount or percent of each conformation state (Heidmann & Changeux, 1979; Boyd & Cohen, 1980). An action potential causes the release of ACh at the cleft produces conformational change resulting in an active state. As soon as ACh occupies all binding sites, the receptor affinity towards ACh increases which activates the D state.

In classical desensitization, the agonist is applied from medium to a high (μM to mM) concentration which activates and then desensitizes the receptors which subsequently recovers after the removal of agonist. Classical desensitization develops in tens of millisecond range (Fig. 27 C). High-affinity desensitization occurs with low agonist concentration without apparent receptor activation. Both phenomena are nAChR subunit and agonist-dependent (Giniatullin et al., 2005). Desensitization can be regulated by exogenous and endogenous substances and by covalent modifications of the receptor structure. Modulators could be non-competitive blockers such as calcium (Giniatullin et al., 2005), thymic hormone peptides, substance P and receptor phosphorylation. Phosphorylation is correlated with the regulation and desensitization of the receptor through various protein kinases (Changeux & Edelstein, 1998).

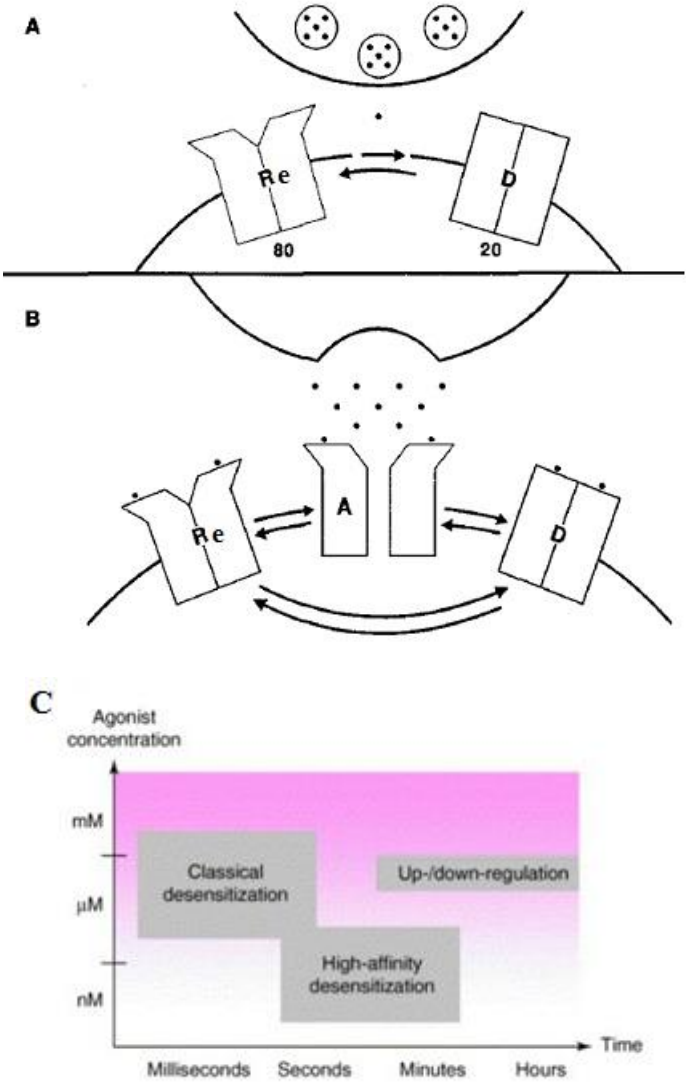

Fig. 27 (A, B) Mechanism of desensitization (Ochoa et al., 1988). (C) Different timings of desensitization with respect to agonist concentration and time of agonist application (Giniatullin et al., 2005)

3.5.5 Role in Neuroprotection

Previous studies have indicated that nAChRs are important targets to attempt neuroprotective strategies against pathological insults such as excitotoxicity or oxygen/glucose deprivation. The present study was raised with the recent observation of nicotine, an agonist of nACRs protection against excitotoxicity applied to rat brainstem

motoneurons. Due to lack of information on similar effects on the rat spinal cord, we applied this procedure to our model to test the effects of nicotine on SCI model. There are many studies which show promising neuroprotection by nicotine application. Kihara and his colleagues have proposed that the neuroprotection may be achieved by activation of PI_3-kinase-Akt system and upregulation of Bcl-2 in cultured cortical neurons (Kihara et al., 2001). Therefore, it could also be possible the involvement of PI3-kinase-Akt pathway in nAChR mediated neuroprotection in spinal motoneurons of rat (Nakamizo et al., 2005). It is also known that nAChR mediated neuroprotection against excitotoxicity is Ca^{2+} dependent (Donnelly-Roberts et al., 1996; Dajas-Bailador et al., 2000; Ferchmin et al., 2003) and does not involve inhibition of glutamate receptor function (Dajas-Bailador et al., 2000; Prendergast et al., 2001; Ferchmin et al., 2003).

3.6 Neuroprotection by a natural compound: Celastrol

Identification of some bioactive compounds extracted from medicinal plants has drawn substantial interest in recent years for their strong and exclusive anti-oxidant, anti-inflammatory, anticancer and neuroprotective properties. One classic example is Tripterygium wilfordii (TW) plant, widely used in Chinese medicine for the treatment of distinct chronic inflammatory and autoimmune diseases (Kannaiyan et al., 2011; Wong et al., 2012). TW or "lei gong teng" (called in Chinese) is also known as thunder god vine, is a vine used in traditional Chinese medicine. The roots of this plant contain various therapeutic compounds such as steroids, terpenoids and alkaloids. There are more than 46 diterpenoids (for example triptolide), 20 triterpenoids (like celastrol), 21 alkaloids (like euonine), and many other small molecules have been identified from TW. The most abundantly found bioactive compound extracted from its roots is celastrol, consisting of ample biological activities. Celastrol is a pentacyclic triterpenoid that belongs to the family of quinine methides (Fig. 28).

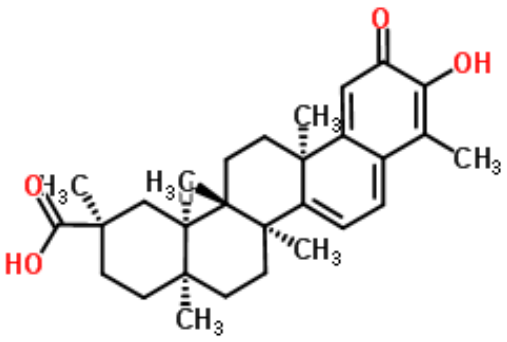

Fig. 28 Structure of celastrol (http://www.chemspider.com/Chemical-Structure.109405.html)

Numerous studies have shown the pharmacological effects celastrol on several diseases (Allison et al., 2001; Salminen et al., 2010; Kannaiyan et al., 2011). Celastrol exhibited effects in suppression of microglial activation, production of pro-inflammatory cytokines and inducible nitric oxide (Allison et al., 2001). China Food and Drug Administration (CFDA) has approved the TW drug for the treatment of rheumatoid arthritis in China. More recent studies on animals model have shown that celastrol has the

ability to attenuate multiple sclerosis (MS) by regulating Th17 responses, balancing the pro- and anti-inflammatory cytokines and downregulating the expression of factor kappa-B (NF-κB) (Abdin & Hasby, 2014; Wang et al., 2015). Celastrol has shown to potentially inhibit lipid peroxidation (Sassa et al., 1990; 1994) in rat liver mitochondrial membrane. Further, this drug has shown to exhibit neuroprotective effects in the rodent model of Huntington's and Parkinson's diseases by inducing heat shock protein 70 (HSP70) within dopaminergic neurons and reducing tumour necrosis factor-α and NF-κB and astrogliosis (Cleren et al., 2005). HSP70 is prominently induced during stress conditions and is also the best-conserved protein. It has demonstrated to be widely expressed in the CNS. It is expressed by neurons, glial cells (Brown et al., 1989; Nowak et al., 1990) and spinal motoneurons (Carmel et al., 2004; Cizkova et al., 2004) as well. Therefore we have investigated the neuroprotective effects of celastrol in our rat SCI model. We have pre-treated our preparations with celastrol (0.75 μM) for 6 h by making a hypothesis that during this time course celastrol with activate HSP70 expression and decrease NF-κB. This hypothesis is based on previous studies and our lab reports where Shabbir has shown the expression of HSP70 in spinal motoneurons and its role in neuroprotection (Shabbir et al., 2015). After pre-treating the spinal cords we have applied excitotoxic agent, kainate (50 μM) for 1 h to induce excitotoxicity and record its effects the day after.

4 AIMS

For any kind of rhythmic motor behaviour, like running or walking or swimming, CPGs have been presumed to be present (Grillner, 1986). Disturbance of finely tuned locomotor network within sensory input and pattern generation following central insult such as SCI, Parkinson disease, stroke, results in movement disorder. Therefore, it is important to understand the mammalian locomotor CPG in order to improve neuro-rehabilitation of patients with SCI (Rossignol et al., 1998; Edgerton et al., 2004). Without interpreting the spinal neuronal circuits which generate motor behaviours, it is hard to design suitable therapies to combat spinal lesion.

Using this fundamental therapeutic approach as a first step, by using an in vitro rat SCI model, thesis project focuses at:

- Gaining insight of early pathophysiological processes occurs after inducing spinal lesion by application of kainate (50 or 100 µM) (glutamate agonist, which is used to produce excitotoxicity by over-activation of glutamatergic system) or pathological medium (mimics dysmetabolic/hypoxic conditions after vascular dysfunction) for 1 h and studying the changes occurred in spinal reflexes, locomotor networks, neuronal and motoneuronal damage during injury by extracellular recordings, immuno-histochemistry and calcium imaging techniques.

The next step was to:

- Study the mechanisms of neuroprotection at the early phase of insult to prevent delayed pathological events by using pharmacological therapies.

- ***Methylprednisolone sodium succinate (6 &10 µM)*** – used to study how this drug could modulate fictive locomotor rhythms and attenuate neuronal, motoneuronal and astroglial damage.

- ***Propofol*** (***5 µM)*** – How this widely used intravenous anaesthetic could antagonize the effect of excitotoxicity by understanding its mechanism of action.

- ***Nicotine (0.5, 1, 2 & 10 µM)*** – A potent parasympathomimetic stimulant used to investigate (using in vitro rat spinal cord and organotypic spinal cultures):

    - The correct neuroprotective dose.

    - Its effects on spinal locomotor CPGs before and after lesion.

    - How this drug could modulate the damage evoked by stimulation of excitotoxic pathways.

    - Which receptors at the spinal level are involved in the neuronal and motoneuronal recovery after SCI.

- ***Celastrol (0.75 µM)*** – A bioactive extract used to examine the protective role of inducible HSP70 on spinal motoneurons against excitotoxic injury to rat spinal cord.

5 MATERIALS, METHODS AND RESULTS

(See enclosed papers)

Neuroscience 315 (2016) 136–149

A STUDY OF METHYLPREDNISOLONE NEUROPROTECTION AGAINST ACUTE INJURY TO THE RAT SPINAL CORD *IN VITRO*

C. SÁMANO,[a] J. KAUR[b] AND A. NISTRI[b,c]*

[a] *Departamento de Ciencias Naturales, Universidad Autónoma Metropolitana, Unidad Cuajimalpa, Mexico City, Mexico*

[b] *Neuroscience Department, International School for Advanced Studies (SISSA), Trieste, Italy*

[c] *SPINAL (Spinal Person Injury Neurorehabilitation Applied Laboratory) Laboratory, Istituto di Medicina Fisica e Riabilitazione, Udine, Italy*

Abstract—Methylprednisolone sodium succinate (MPSS) has been proposed as a first-line treatment for acute spinal cord injury (SCI). Its clinical use remains, however, controversial because of the modest benefits and numerous side-effects. We investigated if MPSS could protect spinal neurons and glia using an *in vitro* model of the rat spinal cord that enables recording reflexes, fictive locomotion and morphological analysis of damage. With this model, a differential lesion affecting mainly either neurons or glia can be produced via kainate-evoked excitotoxicity or application of a pathological medium (lacking O_2 and glucose), respectively. MPSS (6–10 μM) applied for 24 h after 1-h pathological medium protected astrocytes and oligodendrocytes especially in the ventrolateral white matter. This effect was accompanied by the return of slow, alternating oscillations (elicited by NMDA and 5-hydroxytryptamine (5-HT)) reminiscent of a sluggish fictive locomotor pattern. MPSS was, however, unable to reverse even a moderate neuronal loss and the concomitant suppression of fictive locomotion evoked by kainate (0.1 mM; 1 h). These results suggest that MPSS could, at least in part, contrast damage to spinal glia induced by a dysmetabolic state (associated to oxygen and glucose deprivation) and facilitate reactivation of spinal networks. Conversely, when even a minority of neurons was damaged by excitotoxicity, MPSS did not protect them nor did it restore network function in the current experimental model.

Key words: motoneuron, glial cells, glutamate, metabolic perturbation, excitotoxicity, fictive locomotion.

INTRODUCTION

The incidence of new cases of spinal cord injury (SCI) has remained at a high, stable level throughout the last decade (Jain et al., 2015) with poor long-term outcome for neurological recovery (Chen et al., 2013; Furlan et al., 2013). The acute phase of SCI (due to the primary insult of mechanical, vascular or dysmetabolic nature) rapidly evolves into secondary damage, characterized by excitotoxicity caused by massive release of glutamate, in turn triggering a complex pathophysiological cascade generating toxic compounds (Dumont et al., 2001; Park et al., 2004; Rowland et al., 2008; Forder and Tymianski, 2009; Fatima et al., 2014). Thus, neuroprotection against secondary injury is a major therapeutic target (York et al., 2013; Cox et al., 2014) to preserve the spinal gray (Lipton, 2006; Sámano et al., 2012) and white matter containing the long-fiber tracts (Kanellopoulos et al., 2000; Lee et al., 2008; Margaryan et al., 2010; Sun et al., 2010; Cox et al., 2014). Large-scale clinical trials proposed the early i.v. administration of the glucocorticosteroid methylprednisolone sodium succinate (MPSS) in high doses as the mainstay treatment especially directed to white matter protection (Bracken et al., 1990, 1992; Bracken, 2012). This approach stems from the potent anti-inflammatory and antioxidant properties of MPSS to reduce lipid peroxidation, and to alter gene transcription (Oudega et al., 1992; Hall, 1993).

After the publication of the National Acute Spinal Cord Injury Study trials (NASCIS I, II and III; Bracken et al., 1990; Bracken, 1992), the MPSS treatment has become controversial because the neurological improvements were modest (Harrop, 2014; Fehlings et al., 2014) and coupled to important side effects (Bydon et al., 2013; Harrop, 2014). Notwithstanding the debate about the clinical use of MPSS, this drug is still used in several centers as first approach to SCI (Nicholas et al., 2009; Bracken, 2012; Druschel et al., 2013; Miekisiak et al., 2014; Cheung et al., 2015). A large-scale clinical survey has very recently re-examined the usefulness of MPSS administration to SCI patients with debatable outcome in terms of short- or long-term motor control (Evaniew et al., 2015). Animal models of SCI have shown protection especially for white matter oligodendrocytes (Oudega et al., 1999; Lee et al., 2008; Xu et al., 2009; Sun et al., 2010). These observations raise the issue

*Correspondence to: A. Nistri, SISSA, Via Bonomea 265, 34136 Trieste, Italy. Tel: +39-040-3787718; fax: +39-040-3787702.
E-mail address: nistri@sissa.it (A. Nistri).

Abbreviations: ANOVA, analysis of variance; ChAT, choline acetyltransferase; DAPI, 4′,6-diamidino-2-phenylindole; DR, dorsal root; GABA, γ-aminobutyric acid; GFAP, glial fibrillary acidic protein; KA, kainate; l, left; L, lumbar; LWM, lateral white matter; MPSS, methylprednisolone sodium succinate; NeuN, Neuronal-specific nuclear protein; NMDA, N-methyl-D-aspartate; PBS, Phosphate-buffered saline; O4, oligodendrocyte progenitor marker; r, right; PM, pathological medium; RIP, oligodendrocyte and myelin sheath marker; ROI, region of interest; SCI, spinal cord injury; SD, standard deviation; SEM, standard error of the mean; S100, Ca^{2+}-binding protein; SMI-32, non-phosphorylated neurofilament H; VR, ventral root; VWM, ventral white matter; 5-HT, 5-hydroxytryptamine.

http://dx.doi.org/10.1016/j.neuroscience.2015.12.003

whether certain types of SCI might receive more benefit from MPSS than others.

In recent years we have developed an *in vitro* model of SCI in which transient application of the potent glutamate agonist kainate or a ''pathological medium" (PM; mimicking the dysmetabolic conditions occurring after a vascular dysfunction) evokes distinct alterations in locomotor networks with primary damage to gray or white matter, respectively (Taccola et al., 2008; Nasrabady et al., 2012). Useful features of this model are the limited tissue damage in analogy to the majority of the new SCI cases that are incomplete (Jain et al., 2015), and the study of how delayed drug administration (mimicking the clinical setting) might work. The model offers the distinctive advantage of direct investigation of locomotor spinal networks that express alternating motor patterns recorded from lumbar ventral roots (Grillner, 2006; Kiehn, 2006). Thus, the aims of the present study were to find out if, in our *in vitro* model, any neuroprotection by MPSS could be observed and if it might be differentially effective on white or gray matter (Taccola et al., 2008; Margaryan et al., 2009; Kuzhandaivel et al., 2010a,b).

EXPERIMENTAL PROCEDURES

Rat spinal cord preparation

The experiments were carried out on neonatal Wistar rats (ages 1–2 days). All efforts were directed toward minimizing the number of animals used for the experiments and their suffering. Under urethane anesthesia (0.2 ml i.p. of a 10% w/v solution), the spinal cords were carefully dissected out, superfused (7.5 ml/min) with Kreb's solution containing (in mM): 113 NaCl, 4.5 KCl, 1 $MgCl_2 \cdot 7H_2O$, 2 $CaCl_2$, 1 NaH_2PO_4, 25 $NaHCO_3$ and glucose 11; gassed with O_2 95%, CO_2 5%, pH 7.4 at room temperature (22 °C) (Taccola et al., 2008; Margaryan et al., 2009). The experiments were performed in accordance with the ethical guidelines for the care and use of laboratory animals of National Institutes of Health (NIH). All treatment protocols were approved by the Scuola Internazionale Superiore di Studi Avanzati (SISSA) ethics committee and are in accordance with the European Union guidelines on animal experimentation.

Electrophysiological recordings

In order to study reflexes and fictive locomotor rhythms, the experiments were based on DC coupled recordings with tight-fitting suction electrodes from lumbar (L) ventral roots (VRs) (Taccola et al., 2008). Signals were routinely recorded from L2 and L5 VRs carrying mainly flexor and extensor motor signals to hind limb muscles, respectively (Kiehn, 2006). Further analysis of recorded signals was done using pClamp software (version 9.2; Molecular Devices, Sunnyvale, CA, USA).

VR responses were evoked by stimulating a single ipsilateral dorsal root (DR) via a bipolar suction electrode once every 60 s. First, the minimum stimulus intensity was estimated to produce a VR threshold response homolaterally which is considered equivalent to 1× threshold to induce monosynaptic reflexes (Marchetti et al., 2001). Three times higher values of threshold were used to elicit polysynaptic responses (Baranauskas and Nistri, 1995). Generally a train of DR stimuli (30 pulse trains at 2-Hz frequency, 0.1-ms pulse duration) was given to electrically induce fictive locomotion. The responses were calculated by averaging the peak amplitude and area of 3–5 events. Alternatively, rhythmic cycles were recorded by application of N-methyl-D-aspartate (NMDA; 3–6 μM) and 5 hydroxytryptamine (5-HT; 10 μM) (Kiehn, 2006). The periodicity and amplitude of cycles were measured from 20 continuous oscillations as already described by Taccola et al. (2008). Disinhibited bursting was induced by continuous bath application of blockers of γ-aminobutyric acid (GABA)-A and glycine receptors, bicuculline (20 μM) and strychnine (1 μM), respectively. Burst parameters were analyzed in accordance with Bracci et al. (1996).

Protocols for spinal cord lesion and neuroprotection

Two experimental protocols were used: in the first one, spinal lesioning of the gray matter (with loss of fictive locomotion) was induced with 1-h application of the excitotoxic agent kainate (KA, 0.1 mM) in standard Krebs' solution (Taccola et al., 2008; Margaryan et al., 2009; Mazzone et al., 2010).With this approach white matter lesions are usually quite limited (Taccola et al., 2008).

The second protocol mimicked the condition of anoxia/aglycemia that mainly damages the white matter of the spinal cord and is thought to better simulate what occurs after a non-traumatic lesion (Taccola et al., 2008; Margaryan et al., 2009; Kuzhandaivel et al., 2010a). Thus, spinal cord preparations were subjected (for 1 h) to PM, namely a modified Kreb's solution containing 10 mM H_2O_2, 500 μM sodium nitroprusside (SNP), and lacking extracellular Mg^{2+}, glucose and oxygen (replaced by N_2). $NaHCO_3$ was replaced by 1 mM 4-(2-hydroxyethyl)-1-piperazine-ethanesulfonic acid (HEPES) to reach pH 6.75–6.80 (with 0.1 N NaOH), while the osmolarity was lowered to 230–240 mOsm. This solution is known to induce a pathological condition that includes locomotor network depression and spinal damage (Taccola et al., 2008; Margaryan et al., 2009).

With either protocol, we investigated any neuroprotection by MPSS (Pfizer, Italy) after the experimental (1 h) injury. MPSS was diluted with distilled sterile water to get a stock solution of 100 mM, from which test concentrations of 6 or 10 μM were made. The MPSS solution was used within 24 h, since the solution is unstable after 48 h as instructed by the manufacturer. The selection of MPSS concentrations (6 or 10 μM) was based on published clinical guidelines (Sauerland et al., 2000) and former reports with oligodendrocytes cell culture and an organotypic-based model of spinal cord damage (Guzmán-Lenis et al., 2009; Sun et al., 2010). After the application of kainate or PM was terminated with standard Krebs's solution washout, MPSS treatment (6 or 10 μM) started immediately and lasted for up to 24 h. Longer observation periods were prevented by the spontaneous deterioration of the spinal

cord *in vitro*. Control groups treated with MPSS alone were kept in standard Krebs's solution for 24 h *in vitro*. Sham spinal cord preparations run alongside the experimental group were maintained in standard Kreb's solution for up to 24 h (Taccola et al., 2008).

Immunohistochemistry procedure

At the end of the experiment, spinal cord preparations were fixed with 4% paraformaldehyde and cryoprotected in sucrose solution (30% w/v) for subsequent immunohistochemistry (Taccola et al., 2008). Transverse sections (30-μm-thick) of the spinal cord were cut with a sliding microtome at −20 °C and stored in phosphate-buffered saline (PBS) until use. In accordance with our former studies, we analyzed spinal regions of interest (ROI) between L1 and L2 segments where the main components of the locomotor central pattern generator (CPG) are located (Kiehn, 2006). Single or double immunohistochemical stainings were performed on the free-floating tissue sections or on the sections immobilized on Superfrost plus slides (Thermo Fisher Scientific GmbH, Germany) and processed in a humid atmosphere. Sections were preincubated for 1–2 h at room temperature in 5% normal goat serum (NGS) or 5% normal donkey serum/5% bovine serum albumin (BSA) and 0.3% Triton X-100, followed by overnight incubation at 4 °C in 1% NGS/1% BSA/0.1% Triton X-100 solution containing the primary antibodies listed in Table 1. Anti-NeuN (neuronal nucleus) recognizes a neuronal-specific nuclear protein (NeuN) to detect differentiated neurons (Taccola et al., 2008; Margaryan et al., 2009; Cifra et al., 2012). Anti-SMI32 recognizes a non-phosphorylated neurofilament in ventral motoneurons, and anti-choline acetyltransferase (ChAT) is the marker for choline acetyl transferase, the synthetic enzyme of acetylcholine. Both antibodies are clearly identifiable in motoneurons (Cifra et al., 2012).

Anti-S100 recognizes the protein S100 that belongs to the family of Ca^{2+}-binding proteins found in the cytoplasm and nuclei of astrocytes (Donato, 2003), while anti-GFAP recognizes the glial fibrillary acidic protein (GFAP), an intermediate filament protein characteristic for white matter astrocytes (Eng, 1985).The anti-O4 antibody is the earliest recognized marker specific for a sulfated glycolipid antigen of oligodendroglia (Sommer and Schachner, 1981). Oligodendrocyte and myelin sheath marker (RIP) antibody selectively stains oligodendrocytes and their processes containing myelin basic protein (Friedman et al., 1989) (Table 1).

Tissue sections were rinsed thrice for 10 min each in PBS–Triton X-100 (0.1 M PBS, 0.3% Triton X-100), and then incubated for 2 h with the appropriate secondary antibody, anti-mouse Alexa Fluor 488 or 594, or anti-rabbit Alexa Fluor 488 or 594, or anti-goat Alexa 488, or anti-donkey Alexa 488 antibodies. Finally, to identify pyknotic nuclei, the sections were stained with 1 μg/ml solution of 4′,6-diamidino-2-phenylindole (DAPI) (Sigma, Dorset, UK) for 10 min at room temperature and processed with fluorescence mounting medium (DAKO, Milan, Italy) for analysis with an epifluorescence microscope (Zeiss Axioskope 2, Carl Zeiss, Oberkochen, Germany). Selected spinal cord serial sections with double or triple labeling staining were further analyzed with confocal Leica (DMRI2, Wetzlar, Germany) equipped with Ar/Arkrypton laser and Metavue software (Molecular Devices, Sunnyvale, CA, USA).

Cell analysis

Pyknotic nuclei, neurons and astrocytes were identified and quantified with the cell counter software "eCELLence" (Glance Vision Tech, Trieste, Italy). For each experimental condition, 5–6 spinal cords were analyzed and for each spinal cord 10 transverse sections from T12 to L2 segments were examined. We quantified the percentage of pyknosis stained with DAPI, the number of NeuN-expressing cells, SMI32-labeled motoneurons, ChAT-positive motoneurons and the S100 immunoreactive astrocytes in each section according to four ROIs: (i) dorsal gray matter (Rexed laminae I–IV), (ii) central gray matter (Rexed laminae V–VII and X), (iii) ventral gray matter (Rexed laminae VIII–IX) and (iv) ventrolateral white matter. For each region, 5–7 fields of 350 × 350 μm (dorsal and central regions in the gray matter), 520 × 520 μm (ventral horn),

Table 1. Antibodies used for immunofluorescence labeling

Antibodies	Type of antibody	Coupled to	Dilution	Origin
Primary				
NeuN	Mouse monoclonal	—	1:50; 1:100	Millipore; Chemicon. Milan, Italy
SMI32	Mouse monoclonal	—	1:200	Covance. Emeryville, CA, USA
ChAT	Goat polyclonal	—	1:50	Millipore; Chemicon. Milan, Italy
S100	Rabbit polyclonal	—	1:200	Dako. Glostrup. Denmark
GFAP	Mouse monoclonal	—	1:200	Sigma–Aldrich
RIP	Mouse monoclonal	—	1:100; 1:200	Millipore; Chemicon. Milan, Italy R&D Systems. Minneapolis, MN, USA
O4	Mouse monoclonal	—	1:200	Millipore; Chemicon. Milan, Italy
Secondary				
α mouse IgG	Goat	Alexa Fluor 488	1:200; 1:250	Invitrogen. Milan, Italy
α mouse IgG	Goat	Alexa Fluor 594	1:200	Invitrogen. Milan, Italy
α rabbit IgG	Goat	Alexa Fluor 488	1:250; 1:500	Invitrogen. Milan, Italy
α goat IgG	Donkey	Alexa Fluor 488	1:200	Invitrogen. Milan, Italy

or 100 × 500 μm (white matter) were analyzed. Complete details of this analysis have been previously reported (Taccola et al., 2008; Cifra et al., 2012).

Quantification of immunofluorescence intensity (gray levels intensity expressed in arbitrary units, AU) was performed by Metamorph image analysis system (v.7.5.6; Universal Imaging Corporation, Molecular Devices, Downington, PA, USA) or Metavue imaging Software (Molecular Devices, Sunnyvale, CA, USA). Using the densitometry function we calculated mean specific immunofluorescence labels to GFAP, RIP and O4 that were more intense than the background level (i.e. > mean ± 2 SD) for each ROI (640 × 480 μm^2). The values are mean ± SD (at least three different fields in each one of three different sections from three different spinal cords).

Drugs

Kainate was purchased from Ascent Scientific (Bristol, UK); SNP was obtained from Sigma–Aldrich; H_2O_2 from Carlo Erba Reagents (Milan, Italy); and the drug MPSS was purchased as SOLU-MEDROL© (1000 mg/16 ml from Pfizer, Italy).

Statistical analysis

Statistical analysis was performed with Sigma Stat (Sigma Stat 3.1, Systat Software, Chicago, IL, USA). Histology and electrophysiology data were expressed as mean ± SEM. Parametric or non-parametric data distribution was first established with a normality test and the significance of differences between the means was evaluated with either an independent Student's *t*-test or Mann–Whitney test, respectively. ANOVA was used for analyzing multiple comparisons followed by a post hoc Mann–Whitney test. The accepted level of significance was set as $P < 0.05$.

RESULTS

MPSS decreased the number of pyknotic nuclei in the white matter after PM

Because previous reports indicate that PM induces early white matter damage (Taccola et al., 2008; Margaryan et al., 2009; Kuzhandaivel et al., 2010a), we first confirmed that 24 h after 1 h application of PM, the regions more prone to lesion were the dorsal and ventrolateral white matter. Fig. 1A, B exemplifies and quantifies the damage evoked by PM, reaching the maximum occurrence of pyknotic nuclei in the ventrolateral white matter ROI (61 ± 3%; $n = 9$) in comparison with sham preparations. MPSS (6 or 10 μM; 24 h) per se had no toxic effects on gray or white matter (Fig. 1A, B). When MPSS (6 or 10 μM) was applied for 24 h immediately after PM washout, it could significantly attenuate the number of pyknotic nuclei in ventrolateral white matter regions (Fig. 1A, B) in comparison with the effect of PM alone (Fig. 1A, B). The concentrations of 6 and 10 μM were equieffective (47 ± 3% and 45 ± 3% pyknosis, respectively, vs. PM preparations).

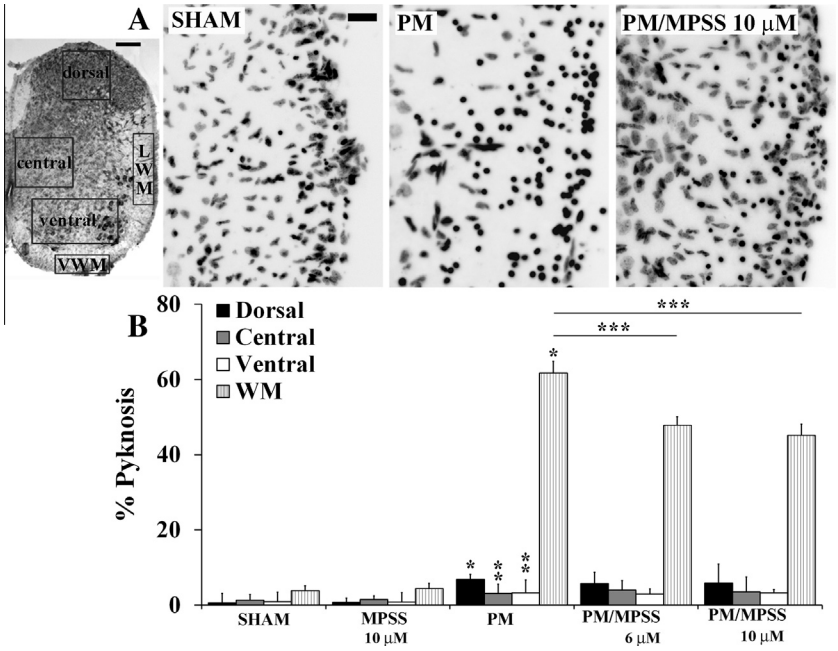

Fig. 1. Characterization of methylprednisolone sodium succinate (MPSS) effect on hypoxic-dysmetabolic-perturbation (PM) damage after 24 h. (A) Upper panel (left) shows a spinal cord half section with ROIs used for cell counting based on DAPI-staining. Bar = 100 μm. Right panels depict representative images of the lateral white matter (WM) of sham, PM or PM- followed by MPSS (10 μM)-treated spinal cords stained with DAPI. Bar = 50 μm. (B) Graph showing percent occurrence of pyknosis (as percentage of total count cell nuclei) in each ROI analyzed (dorsal, central, ventral and ventro-lateral white matter) of the spinal cord for sham preparations in standard Kreb's solution; MPSS (10 μM); PM and washout PM followed by two different concentrations of MPSS (6 or 10 μM). A statistically significant increase in all four spinal cord regions is observed with the pyknotic cell number in the samples treated with PM alone versus sham preparations ($^{*}P < 0.05$, and $^{**}P < 0.01$). MPSS significantly reduces ($^{***}P < 0.001$) the number of pyknotic cells vs. PM alone in white matter regions. Data are averages taken from nine sections from three rats. The Mann–Whitney test was used after performing One-Way Analysis of Variance test.

MPSS protected white matter glial cells from PM damage

As previously reported by Margaryan et al. (2009) and Kuzhandaivel et al. (2010a,b)***, and in accordance with data reported in Fig. 1, glial cells of the white matter are the most vulnerable to PM. Thus, using markers for spinal neurons (NeuN), astrocytes (GFAP or S100), and oligodendrocytes (O4 and RIP), we investigated the cell protection specificity by MPSS 24 h after the PM insult. In line with our former reports (Margaryan et al., 2009; Kuzhandaivel et al., 2010a; Bianchetti et al., 2013) that demonstrate good neuronal preservation after PM application, we observed that the number of NeuN-immunopositive cells was unchanged throughout the gray matter regions (data not shown). On the other hand, while MPSS per se had no toxic action, PM application significantly decreased the immunofluorescence intensity of GFAP-positive fibers of ventrolateral white matter regions (40%) compared to sham preparations (Fig. 2A, B), in coincidence with widespread pyknosis. However, when MPSS was applied immediately after PM, the GFAP signal intensity significantly increases by 27% and 29%, respectively, vs. data after PM alone (Fig. 2B).

We also wished to explore whether the MPSS (6 or 10 μM) treatment after PM could protect oligonde ndrocytes. Since O4 (like GFAP) staining is non-nuclear, O4 immunofluorescence intensity was expressed as average AU in the white matter ROI. Oligondendrocytes suffered PM-induced damage because the signal intensity for O4 or RIP staining was weak in the ventral white matter (VWM) ROI and represented 42% and 49%, respectively, of the values observed in sham preparations (Fig. 2C–F). When MPSS (6 or 10 μM) was applied for 24 h immediately after PM washout, the O4 immunofluorescence intensity increased significantly vs. PM preparations, by 15% and 18%, respectively (Fig. 2D). Similar increases were found with RIP staining (16% and 18%; Fig. 2F).

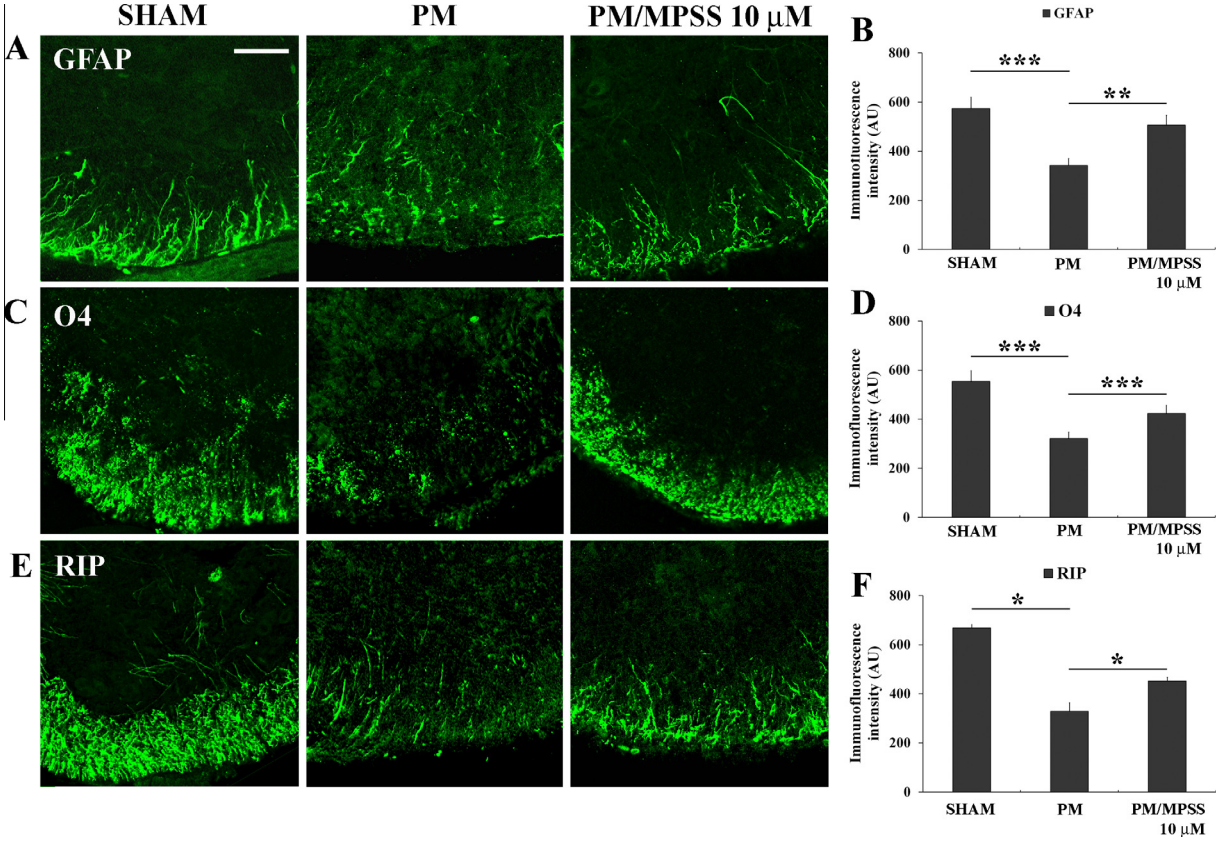

Fig. 2. MPSS administration followed by metabolic perturbation (PM) protects astrocytes and oligodendrocytes in the ventrolateral white matter region. (A) Micrographs showing examples of GFAP positive fibers detected after 24 h in sham, PM alone for 1 h, or PM followed by MPSS treatment (PM/MPSS 10 μM) for 24 h. Note that PM triggers loss of GFAP signal, while PM/MPSS (10 μM) treatment induces some protection by increasing the GFAP fiber signal. Bar = 100 μm. (B) Plots of immunostaining intensity (expressed in arbitrary units; AU) from GFAP positive fibers of sham, PM- or PM/MPSS (10 μM)-treated spinal cords. Comparisons of data from treated spinal cords with PM alone are significantly different from sham samples with $^{***}P < 0.001$ and $^{**}P < 0.01$ for those treated with PM followed by MPSS 10 μM vs. PM alone. (C, E) Panels show examples of the O4 and RIP positive elements (oligodendrocytes) in the same region of GFAP analysis from sham, PM- or PM/MPSS- (10 μM)-treated spinal cords. Note PM application induces large loss of O4 and RIP immunoreactivity, while PM/MPSS (10 μM) treatment increases significantly the fluorescence signal of both markers. Scale bar = 100 μm. (D, F) Histograms quantifying immunofluorescence intensity (AU) from O4 or RIP signals of sham, PM- or PM/MPSS (10 μM)-treated spinal cords. The loss of O4 or RIP signal is significantly different from sham preparations, $^{***}P < 0.001$ and $^{*}P < 0.05$, respectively. The fluorescence signal from both markers in preparations treated with MPSS (10 μM) after PM vs. PM alone is significantly different, being $^{***}P < 0.001$ and $^{*}P < 0.05$, respectively. For all experiments, data are from six spinal sections from three rats. The Mann–Whitney test was used after performing One-Way Analysis of Variance test.

To further quantify white matter astrocytes, we also stained them with the antibody S100 that recognizes all astrocytes (white matter GFAP-positive astrocytes, and gray matter protoplasmic GFAP-negative astrocytes). Twenty-four hours after PM, significant loss of ventrolateral white matter astrocytes was apparent together with preservation of gray matter astrocytes (Fig. 3A, B). This result is in accordance with the GFAP signal (Fig. 2A, B). Fig. 3A, B demonstrates that MPSS (6 or 10 μM) significantly protected ventrolateral S100 positive glial cells (118 ± 8; 111 ± 4 cells, respectively) compared to PM treatment (91 ± 7 cells). In summary, these results show that the early toxic effect produced by PM on astrocytes and oligodendrocytes of white matter could be attenuated by the immediate application of MPSS for 24 h.

Poor neuroprotection by MPSS after kainate-mediated excitotoxicity

We have previously shown that kainate (1 h) primarily produces extensive spinal network damage with loss of fictive locomotion, and lesion of gray matter affecting neurons and motoneurons with very limited destruction of white matter glia (Taccola et al., 2008; Margaryan et al., 2009; Kuzhandaivel et al., 2010b; Sámano et al., 2012). We first explored if MPSS neuroprotection could be achieved after a moderate excitotoxic insult, namely 1 h application of 0.1 mM kainate. An example of the extent of pyknosis ($n = 6$) 24 h after washout of kainate is provided in Fig. 4A. When MPSS (6 or 10 μM) was applied for 24 h immediately after kainate, no change in gray matter pyknosis in dorsal, central and ventral ROIs

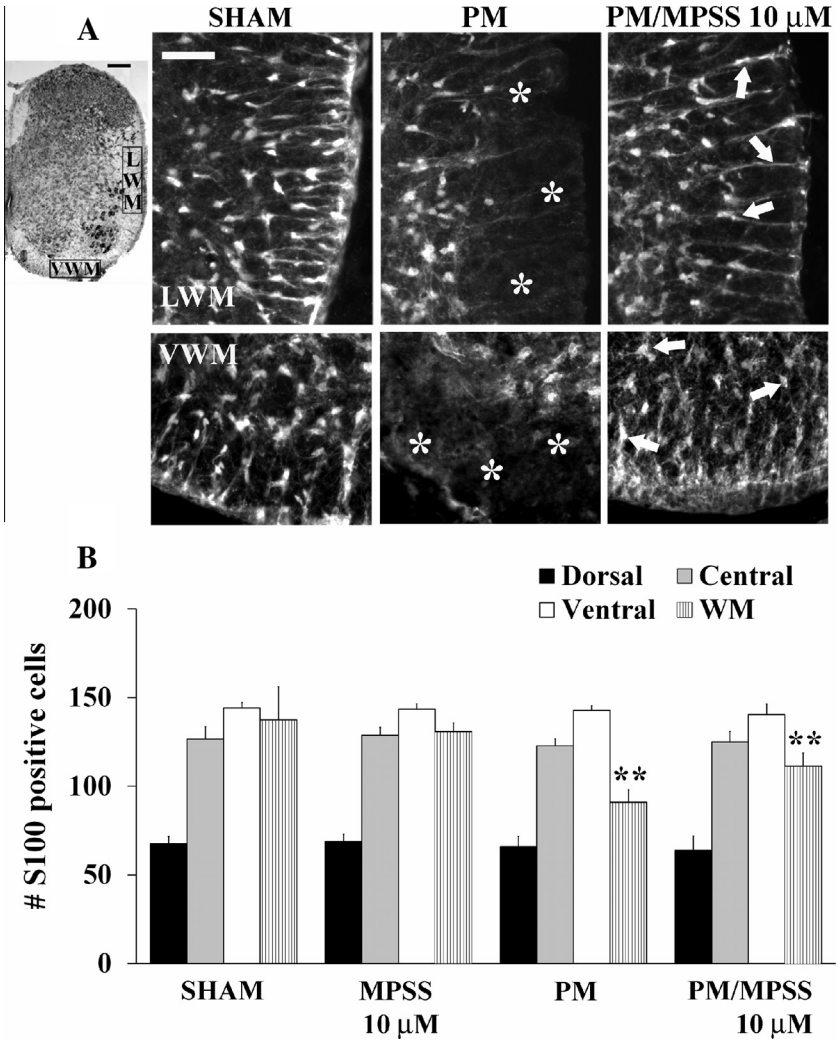

Fig. 3. Quantification of effect of MPSS after metabolic perturbation (MP). (A) Inset shows a spinal cord half section of the white matter areas analyzed (lateral and ventral white matter; LWM, VWM). Bar = 100 μm. The panels show examples of S100-immunoreactivity in the L2 LWM (upper) and VWM (lower) ROIs in sham (left), PM (middle) or PM followed by MPSS (10 μM) after 24 h (right). The asterisks show lack of S100 staining in ventrolateral white matter of spinal cords treated with PM alone. The arrows show that following treatment with 10 μM MPSS (after 1 h of PM application), some fibers and cell bodies are present in ventrolateral WM regions, compared to PM alone. Bar = 50 μm. (B) Histograms showing total number of S100-positive cell bodies in sham, MPSS (10 μM), PM or MPSS after PM toxicity (PM/MPSS 10 μM)-treated spinal cord. Dorsal (filled bars), central (gray bars), ventral (open bars) and white matter (WM; dashed bars) regions were analyzed. For all experiments, data are from six spinal sections from three rats. The Mann–Whitney test was used after performing One-Way Analysis of Variance test; comparison between PM data vs. sham gave $^{**}P < 0.05$; comparing PM/MPSS 10 μM vs. PM alone also gave $^{**}P < 0.05$.

was observed. Nonetheless, there was a slight reduction in pyknosis in the white matter ROI for both concentrations of MPSS (4.0 ± 1% with 6 μM, and 3.1 ± 1% with 10 μM) compared to kainate alone (6.9 ± 2%) (Fig. 4A, B).

We also quantified the number of NeuN-positive neurons in dorsal, central and ventral ROIs after kainate washout and treatment with MPSS (6 or 10 μM). Table 2 lists neuronal loss elicited by excitotoxicity and the unchanged outcome 24 h after MPSS administration. In the ventral horn ROI, motoneurons analyzed with ChAT (ACh synthetic enzyme) immunopositivity were highly vulnerable to kainate and not rescued by MPSS (Table 2).

Effects of MPSS on electrophysiological network properties

To further verify any neuroprotective effect by MPSS from a functional viewpoint, we investigated whether this drug could protect against neuronal damage evoked by kainate (0.1 mM) or PM. Kainate or PM was applied for 1 h followed by washout and subsequent administration of MPSS for 24 h. The electrophysiological responses were recorded 24 h later (Taccola et al., 2008; Margaryan et al., 2009).

Fig. 5 summarizes data related to monosynaptic (A) or polysynaptic (B) reflexes elicited by DR stimulation. These responses were largely depressed 24 h after either kainate or PM application with no significant recovery in peak amplitude after MPSS administration (Fig. 5C, D). Nevertheless, a significant improvement in the area of polysynaptic reflexes was detected in KA or PM solution followed by MPSS ($P = < 0.001$; $P = 0.015$, respectively) (Fig. 5B, E).

We next tested DR pulse trains to induce fictive locomotion expressed as alternating oscillations superimposed on cumulative depolarization (Marchetti et al., 2001). These effects were severely depressed by kainate or PM (Fig. 6A). As illustrated in Fig. 6A–D, subsequent application of MPSS had little impact on the electrophysiological outcome. In fact, just minimal oscillations were seen in 5 out 11 preparations treated with MPSS after kainate solution ($P < 0.001$) (Fig. 6A, B).

Table 2. Vulnerability of neurons to kainate-mediated excitotoxicity was not rescued by MPSS treatment

IR	ROI	Sham	0.1 mM KA	KA/MPSS 6 μM	KA/MPSS 10 μM
NeuN	D	197 ± 4	127 ± 6*	125 ± 8	126 ± 8
NeuN	C	170 ± 2	143 ± 2*	136 ± 2	134 ± 2
NeuN	V	195 ± 6	175 ± 3*	176 ± 5	176 ± 6
ChAT	V	30 ± 2	21 ± 1**	21 ± 3	22 ± 2
SMI-32	V	13 ± 2	5 ± 2**	5 ± 1	5 ± 2

* Indicates the significant difference ($P < 0.001$) between kainate 0.1 mM (KA) vs. sham for NeuN immunoreactivity (IR).

** $P < 0.01$ for 0.1 mM KA ($n = 3$) vs. sham for both motoneurons markers (ChAT and SMI-32). No statistically-significant difference is apparent among groups treated with kainate followed by methylprednisolone (MPSS 6 or 10 μM) vs. kainate alone. For all experiments, data are from six spinal cords sections from three rats; the Mann–Whitney test was used after performing One-way analysis of Variance test. D, C and V denote dorsal, central and ventral ROIs, respectively.

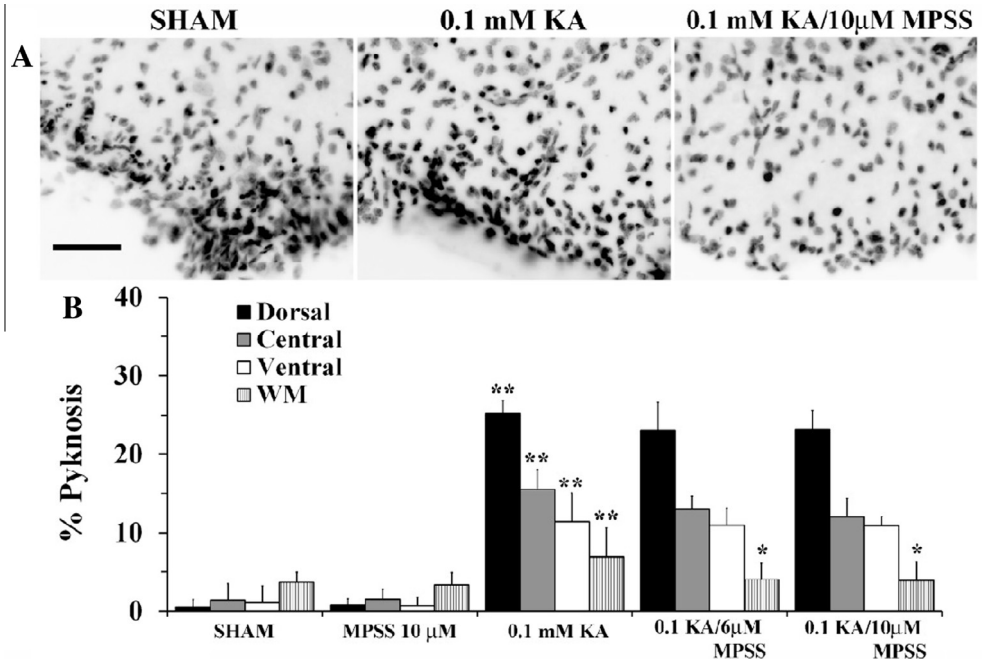

Fig. 4. Limited neuroprotection by MPSS after kainate-mediated excitotoxicity. (A) Micrographs of DAPI staining showing pyknosis in the ventral white matter part of the rat lumbar spinal cord. Sham (left), 0.1 mM kainate (KA; middle) or kainate followed by MPSS (KA/MPSS 10 μM; right). Bar = 50 μm. (B) Histograms showing the percent of pyknotic nuclei counted in dorsal (filled bars), central (dark gray bars), ventral (open bars) and ventrolateral white matter (striped bars) regions, in sham, MPSS alone (10 μM), 0.1 mM KA (1 h), or KA followed by 24 h MPSS (6 or 10 μM). Average from six spinal sections from three rats; the Mann–Whitney test was used after performing One-Way Analysis of Variance test. Comparisons were KA vs. sham and KA/MPSS 6 μM or KA/MPSS 10 μM vs. KA alone; *$P < 0.05$ and **$P < 0.001$.

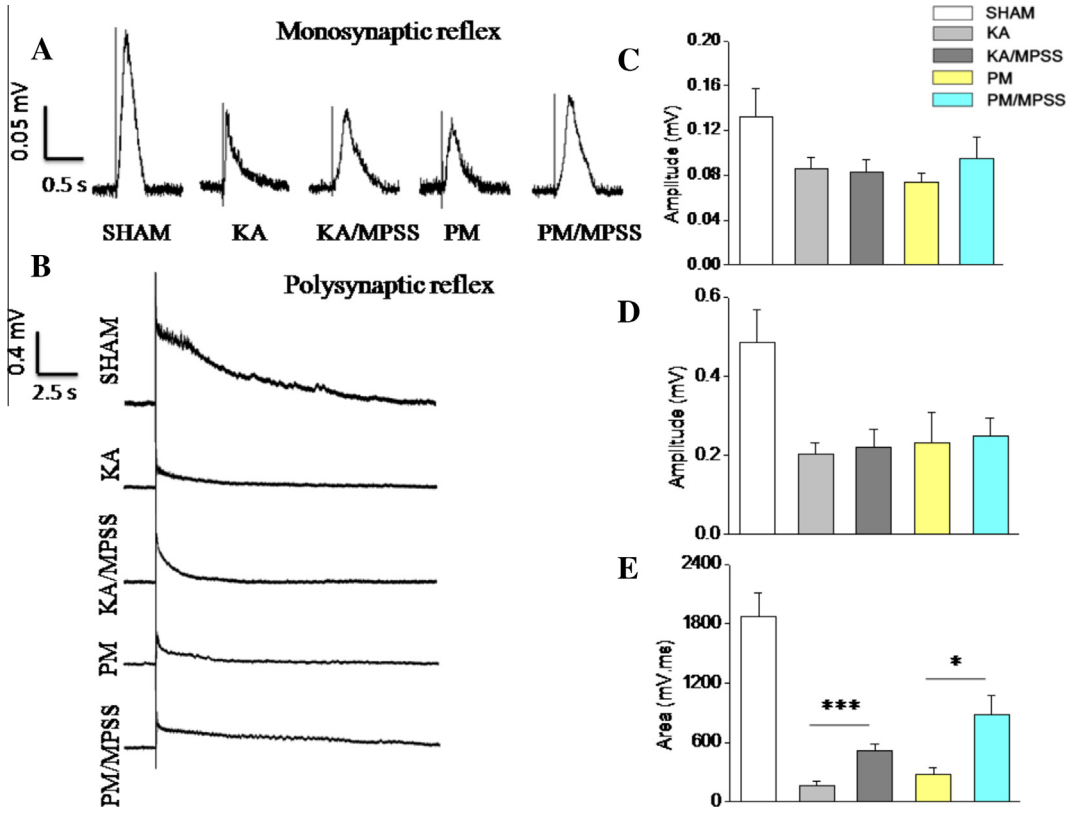

Fig. 5. Effect of MPSS (10 μM) application on reflex responses recorded after 24 h from exposure to kainate (KA) (0.1 mM) or pathological medium (PM) for 1 h. (A, B) Examples of average monosynaptic (A) or polysynaptic (B) responses recorded from L2 homolateral VRs in control (sham), kainate (KA, 1 h), kainate followed by MPSS (KA/MPSS) for 24 h, pathological medium (PM, 1 h) and PM followed by MPSS (PM/MPSS) for 24 h. (C, D) Histograms representing the peak amplitude (mV) of monosynaptic (C) and polysynaptic (D) responses after KA (n = 11), KA/MPSS (n = 11), PM (n = 9), PM/MPSS (n = 9) treatment compared to sham (n = 10). Note that there is significant fall in amplitude of only polysynaptic reflexes (D) in treated preparations as compared to sham (P = 0.006; One Way Analysis of Variance test) but no significant change in case of amplitude of monosynaptic reflexes (C). (E) Histograms showing the area (mV ms) of polysynaptic responses of KA- or PM-treated spinal cords. MPSS application for 24 h significantly increases the reflex area after kainate or PM vs data after either treatment ($^{***}P < 0.001$, $^{*}P = 0.015$, respectively; t-test). All values of polysynaptic reflex area in treated spinal cords were different from sham ($P < 0.001$; One-Way Analysis of Variance test).

Modest recovery (P = 0.042) in the area of cumulative depolarization was also detected (Fig. 6A, D).

As indicated in Fig 7A, kainate application (1 h) blocked rhythmic oscillations induced by NMDA and 5HT. The majority of preparations (8/11 spinal cords) could not generate any cyclic discharge after superfusion with kainate (1 h) despite increasing the NMDA concentration in the 2–6 μM range. In the remaining three preparations, sporadic oscillatory cycles without any alternation were observed. These oscillations were not restored after MPSS (24 h) treatment (Fig. 7A–C). On the other hand, following application of PM, few (7–10), slow oscillations without alternation were recorded in five out of nine spinal cords (Fig. 7). This condition was improved after MPSS administration because rhythmic, alternating oscillations were present in eight out of nine preparations, even if they remained slow by comparison with sham spinal cords (Fig. 7A, C).

Fig. 8A, B summarizes data concerning the spinal cord intrinsic rhythmicity (disinhibited bursting) studied after pharmacological block of synaptic inhibition (Bracci et al., 1996). Kainate application resulted in a comparatively lower number of bursts (of smaller size) vs sham preparations. This condition was not significantly ameliorated by a 24-h application of MPSS. After PM application followed by 24-h MPSS, the number of bursts was significantly reduced because their duration and amplitude had increased when compared to the spinal cords treated with PM alone.

DISCUSSION

The principal finding of this report is that, within the first 24 h from an experimental lesion, any neuroprotection by MPSS was limited in extent and regionally restricted to the ventrolateral white matter when damaged by PM. Conversely, MPSS could not contrast excitotoxic neuronal damage. In either case no good recovery in locomotor network function was observed.

Regional and cellular specificity of MPSS protection

The underlying mechanisms of MPSS action against SCI secondary damage remain unclear. Various suggestions have been proposed including decrease in oxygen radical-induced lipid peroxidation of cell membranes, scavenging of free radicals, attenuation of Ca^{2+} influx

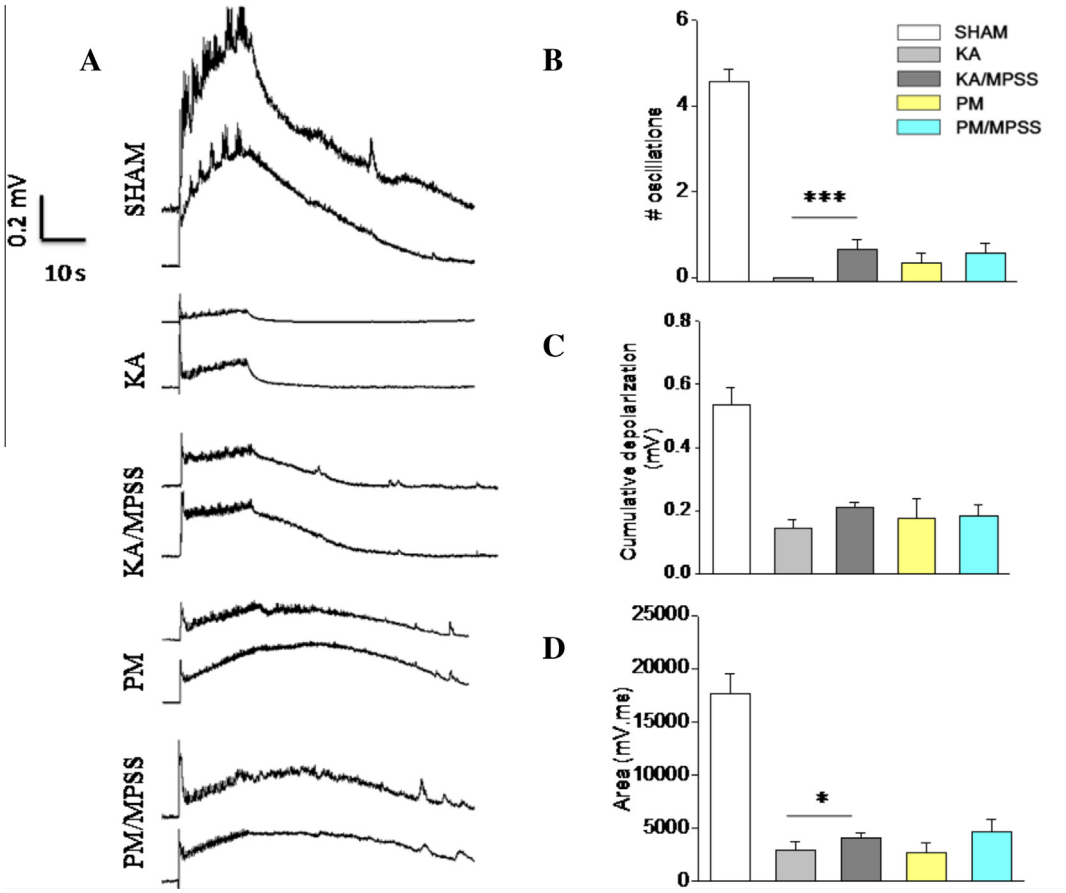

Fig. 6. Effect of MPSS (10 μM) application on fictive locomotion evoked by a train of DR stimuli. Data recorded after 24 h from spinal cords exposed to kainate (KA) or pathological medium (PM) for 1 h. Same preparations as analyzed in Fig. 5. (A) Representative records of electrically evoked cumulative depolarization with superimposed oscillations (fictive locomotion) of sham, kainate (KA), kainate followed by MPSS (KA/MPSS), PM and PM followed by MPSS (PM/MPSS). (B) Histograms depicting number of oscillations evoked by DR stimulation. There is a small, yet significant recovery of DR oscillations in kainate-treated spinal cords after application of MPSS (24 h) ($^{***}P < 0.001$; *t*-test). (C) Bar graph showing no significant improvement by MPSS administration (24 h) in cumulative depolarization recorded from kainate- or PM-treated preparations. (D) Histograms showing significant recovery of cumulative depolarization area after kainate followed by MPSS for 24 h ($^{*}P = 0.042$; *t*-test). Note the significant change in number of oscillations as well as in the amplitude and area of cumulative depolarization seen in all treated preparations in comparison to sham ($P < 0.001$; One-Way Analysis of Variance test).

and enhancement of spinal blood flow (Hall, 2011; Tohda and Kuboyama, 2011; Bains and Hall, 2012). The rationale for MPSS use in SCI is based on the destructive processes affecting the white matter as consequence of ischemia, edema and lipid peroxidation (Liu et al., 1997; Kanellopoulos et al., 2000). Astrocytes and oligodendrocytes are very sensitive to injury that induces demyelination and cell death by apoptosis (Kim et al., 2003; Kuzhandaivel et al., 2010a). Our standard protocol for inducing experimental SCI *in vitro* attempted to mimic a clinical scenario whereby the initial injury (whether of mechanical or dysmetabolic nature) is promptly addressed with emergency care that involves correction of ongoing metabolic dysregulation and support of life-critical functions. The use of a neonatal mammalian SCI *in vitro* preparation is helpful to investigate neuronal network properties because of its well-defined inputs via DR fibers and motor output via VR axons. Spinal networks can generate, even in the absence of external stimuli, a repertoire of rhythmic activities that represent an advantageous model to explore the delayed action of excitotoxicity and metabolic perturbation. Additionally, the model can also be useful for better understanding the pathological processes related to child SCI, a scarcely researched field. In fact, clinical studies report a relatively high occurrence of SCI among very young children (Bilston and Brown, 2007; Pieretti-Vanmarcke et al., 2009), even at perinatal age (Vialle et al., 2008).

Thus, our protocols used a transient application of a pathological medium or of the excitotoxic agent kainate (Kuzhandaivel et al., 2011) followed by a 24-h washout with oxygenated Kreb's that, in the present study, included MPSS (6 or 10 μM that corresponds to the clinical use). Cell protection by MPSS application was mainly expressed as a significant decrease in the number of pyknotic nuclei in the ventrolateral white matter, although a substantial number of dead cells remained. In this area MPSS could reverse the loss of astrocytes, and, to a lesser extent, the fall in oligodendrocytes. The present data accord with *in vivo* studies of the rat-transected

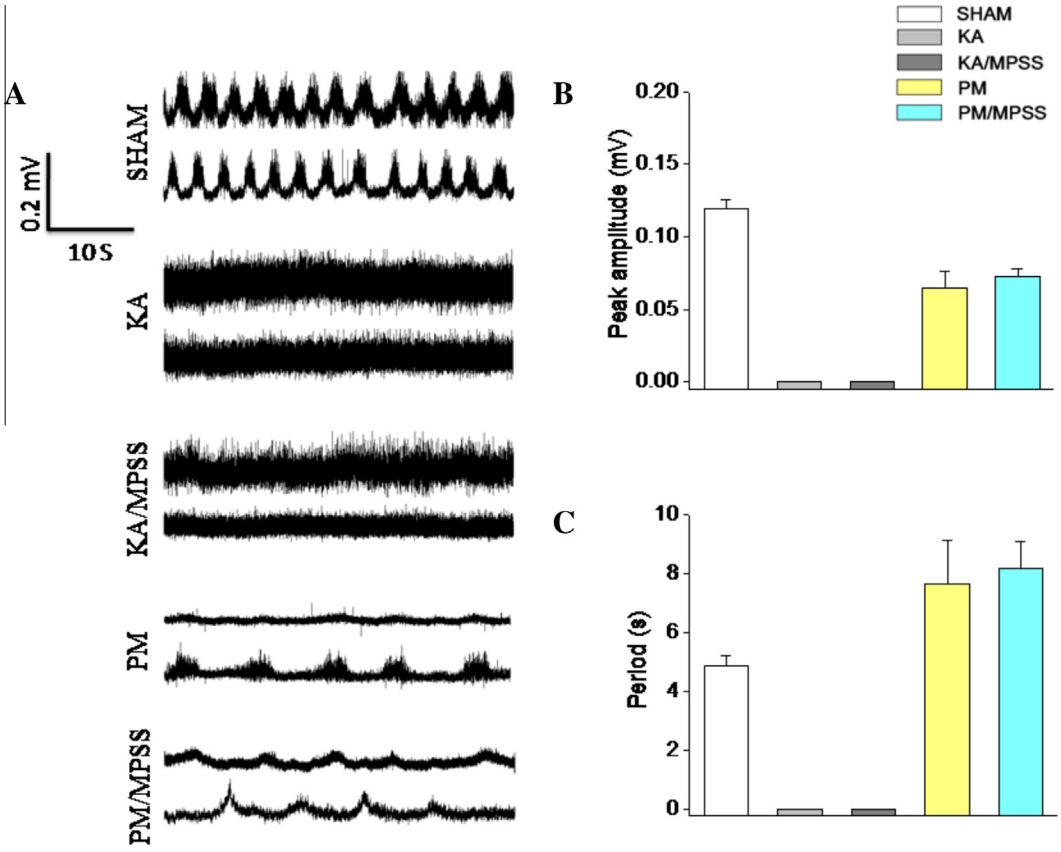

Fig. 7. Changes in chemically induced fictive locomotor rhythms after kainate or PM (1 h) followed by MPSS (24 h). (A) Representative records of oscillatory cycles alternating between left (l) and right (r) L2 VRs in the presence of NMDA and 5-HT. After kainate exposure, fictive locomotion has irreversibly stopped and no recovery is observed after MPSS application. Only 3 out of 11 preparations show some oscillatory cycles without any alternation both after kainate and kainate followed by MPSS. Few oscillations (8–12) without any alternation and with longer periodicity are observed in five out of nine spinal cords exposed to PM, whereas after MPSS application oscillations with alternations in eight out of nine preparations are detected. (B, C) Bar graphs summarizing averaged data for peak amplitude and periodicity of fictive locomotion of kainate or PM exposed preparations followed by MPSS (24 h). Note that a significant change in peak amplitude and period of oscillations is observed in treated spinal cords as compared with sham ($P < 0.001$; One-Way Analysis of Variance test). MPSS does not alter the effects observed after KA or PM.

spinal cord indicating that MPSS treatment can reduce spinal tissue loss (Oudega et al., 1999). In particular, MPSS is reported to attenuate cell death of oligodendrocytes in a dose-dependent manner and to inhibit axonal demyelination (Lee et al., 2008). Several investigations have targeted oligodendrocytes for protection after experimental SCI (Lee et al., 2008; Sun et al., 2010). The question, however, remains whether glial cells within the gray or white matter are differentially sensitive to lesion.

Our former investigations have detailed the type and extent of glial damage evoked by kainate and/or PM applications to the rat isolated spinal cord or organotypic spinal slices. Immunohistochemical analysis has indicated that, within the gray and white matter, excitotoxicity induced by kainate has rather limited effects on astroglia and oligodendroglia (Kuzhandaivel et al., 2010a,b; Mazzone and Nistri, 2011, 2014; Mazzone et al., 2013), though microglia becomes activated early (Taccola et al., 2010). Loss of myelination within 24 h from the insult is scant and is not associated with a significant decrease in action potential generation by isolated VRs (Taccola et al., 2008). Furthermore, when the lesion is restricted to one spinal segment, descending or ascending fibers coursing through it can be electrically stimulated to generate polysynaptic reflexes at segments above or below the lesion, demonstrating that impulse propagation via long axons is well preserved (Taccola et al., 2010). Contusive injury to the rat dorsal spinal cord *in vivo* elicits early, patchy demyelination (mainly in central laminae) followed by chronic demyelination interrupted by phases of remyelination and variable functional recovery (Totoiu and Keirstead, 2005).

The PM protocols of the present study evoked significant loss of astroglia and oligodendroglia (and limited neuronal damage) together with depression of fictive locomotor patterns in accordance with our former reports (Taccola et al., 2008; Margaryan et al., 2010; Kuzhandaivel et al., 2010b). Globally, these observations validate the functionally-negative consequence of even moderate neuronal losses, but they also raise the issue of the impact of glia on locomotor network activity.

Studies of the locomotor circuitry in the lamprey spinal cord have suggested that glia may play a role in regulating the efficiency of network function (Baudoux and Parker, 2008). In the mouse spinal cord, glial cells are proposed to dynamically release ATP that is degraded extracellularly to adenosine that, in turn, negatively controls the frequency of locomotor output (Witts et al., 2012; Acton and

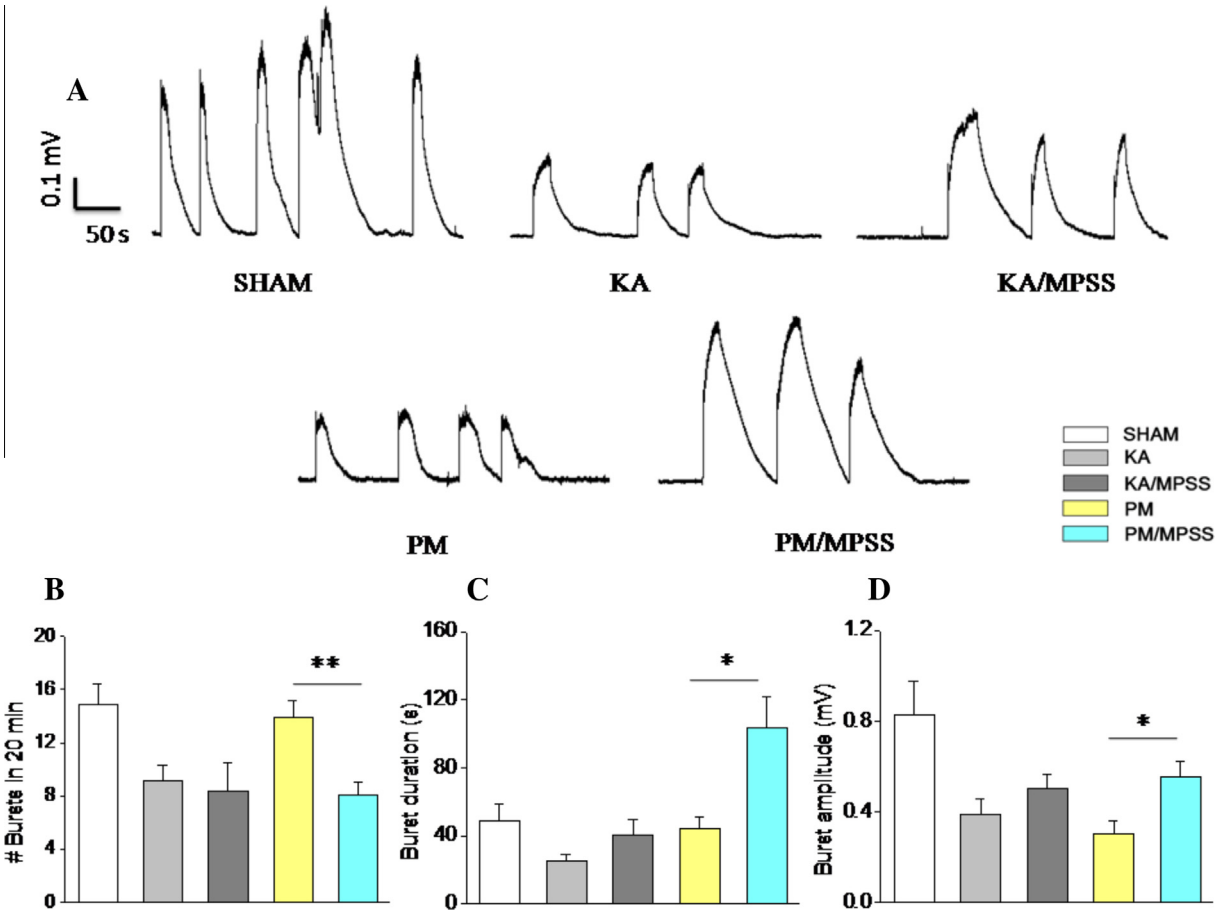

Fig. 8. Disinhibited bursting after MPSS (24 h) application. (A) Sample recordings of disinhibited bursts obtained from sham ($n = 7$), kainate (KA) ($n = 7$), kainate followed by MPSS (KA/MPSS) ($n = 5$), PM ($n = 7$) and PM- followed by MPSS (PM/MPSS) ($n = 9$)-treated preparations. (B–D) Histograms representing significant change induced by MPSS in the number of bursts during a 20-min epoch ($^{**}P = 0.002$; *t*-test) (B), duration of bursts ($^{*}P = 0.02$; *t*-test) (C), and burst amplitude ($^{*}P = 0.02$; *t*-test) (D) after kainate or PM.

Miles, 2015). In the present report the only partial retention of locomotor cycles and disinhibited bursting after PM application suggests that, against a relatively limited neuronal loss, glia damage might have significantly enhanced the network dysfunction not predicted on the basis of the quite modest neuronal damage. The small improvement in astroglia survival with MPSS treatment was, however, insufficient to restore the standard locomotor output.

Excitotoxic damage is distinct from PM-evoked damage because the former primarily affects neurons rather than glia (Kuzhandaivel et al., 2011). In the kainate-lesioned model, MPSS exerted no neuronal protection and modest inhibition of the limited white matter pyknosis. Previous studies have, however, indicated that motoneurons could be protected by MPSS in SCI *in vitro* or *in vivo* (Guzmán-Lenis et al., 2009; Yin et al., 2013). This discrepancy may be attributable to: (*i*) distinct models of SCI with differential distribution and timecourse of MPSS action; (*ii*) the degree of excitotoxic stimulation and the timing of MPSS application; (*iii*) the different outcome parameters investigated (Wittstock et al., 2015). These considerations led us to test the electrophysiological network activity after experimental lesion and MPSS administration.

MPSS and functional deficit of spinal networks

In accordance with previous studies (Taccola et al., 2008; Margaryan et al., 2009), mono and polysynaptic reflexes were partially depressed 24 h after kainate or PM application. The same result was obtained when repeated DR stimuli generated cumulative depolarization that lacked oscillations. Fictive locomotion induced by NMDA and 5HT was blocked after kainate and consistently depressed after PM. This functional scenario of network function inhibition by either lesion protocol was not accompanied by massive cell loss. In fact, the largest incidence of gray matter pyknosis was observed in the dorsal horn following kainate application and amounted to less than 30%. With PM application the damage was even more limited. These observations suggest that spinal networks operate in a condition of criticality (Massobrio et al., 2015; Valverde et al., 2015) whereby even modest losses are transduced into major functional deficit. This notion is consistent with the view of minimal network membership necessary to express locomotor patterns (Kuzhandaivel et al., 2011). Once that value is surpassed, no locomotor activity can be observed anymore.

This adverse condition was only partly changed by MPSS. Thus, the polysynaptic reflex area increased,

perhaps suggestive of more residual connections left within the premotoneuron circuitry. Likewise, a small improvement was observed with the cumulative depolarization area and superimposed oscillations. These were minimal gains in the presence of MPSS and could not be carried over to any strong recovery in locomotor network function particularly after kainate application. The outcome appeared more favorable when fictive locomotion was monitored following PM and MPSS as slow alternating oscillations could re-emerge.

Studying these network phenomena cannot clarify if a beneficial, albeit small, effect by MPSS was produced at the level of discrete elements of the white or gray matter. Hence, it seemed useful to minimize the size of the spinal circuitry by blocking synaptic inhibition (Streit, 1993; Bracci et al., 1996; Darbon et al., 2002) and observing spontaneous rhythmic bursting that reflects the intrinsic excitability of the ventral area predominantly through glutamatergic transmission (Bracci et al., 1996). In this case, MPSS did not change the depression elicited by kainate, although it contrasted PM effects by increasing burst amplitude and duration (with consequently fewer bursts per unit of time). The latter observation suggests slightly improved functional connectivity within the network.

CONCLUSIONS

Management of acute SCI is a difficult task because the origin, duration and extent of the primary lesion vary considerably, making it complicated issuing guidelines for a standard therapeutic treatment. Furthermore, SCI grows in size and severity in a time-dependent fashion, thus demanding rapid intervention that so far has been useful only when performing early neurosurgery (Fehlings et al., 2012). The benefits of MPSS have been long debated because of the contrasting results in human trials (Tohda and Kuboyama, 2011; Bracken, 2012; Harrop, 2014). The present study suggests that MPSS may exert a modest beneficial action in a non-excitotoxic lesion of the spinal cord by preserving a number of glial cells. This phenomenon is not, however, translated into a rapid functional protection of spinal networks.

Acknowledgment—This work was supported by a grant (SPINAL project) from the Friuli Venezia Giulia Region government.

REFERENCES

Acton D, Miles GB (2015) Stimulation of glia reveals modulation of mammalian spinal motor networks by adenosine. PLoS One 10: e0134488.

Bains M, Hall ED (2012) Antioxidant therapies in traumatic brain and spinal cord injury. Biochim Biophys Acta 1822:675–684.

Baranauskas G, Nistri A (1995) Membrane potential oscillations of neonatal rat spinal motoneurons evoked by electrical stimulation of dorsal root fibres. Eur J Neurosci 7:2403–2408.

Baudoux S, Parker D (2008) Glial-toxin-mediated disruption of spinal cord locomotor network function and its modulation by 5-HT. Neuroscience 153:1332–1343.

Bianchetti E, Mladinic M, Nistri A (2013) Mechanisms underlying cell death in ischemia-like damage to the rat spinal cord in vitro. Cell Death Dis 4:e707–e718.

Bilston LE, Brown J (2007) Pediatric spinal injury type and severity are age and mechanism dependent. Spine 32:2339–2347.

Bracci E, Ballerini L, Nistri A (1996) Localization of rhythmogenic networks responsible for spontaneous bursts induced by strychnine and bicuculline in the rat isolated spinal cord. J Neurosci 16:7063–7076.

Bracken MB (1992) Pharmacological treatment of acute spinal cord injury: current status and future prospects. Paraplegia 30:102–107.

Bracken MB (2012) Steroids for acute spinal cord injury. Cochrane Database Syst Rev 18:1–51.

Bracken MB, Shepard MJ, Collins WF, Holford TR, Young W, Baskin DS, Eisenberg HM, Flamm E, Leo-Summers L, Maroon J (1990) A randomized, controlled trial of methylprednisolone or naloxone in the treatment of acute spinal-cord injury: results of the Second National Acute Spinal Cord Injury Study. N Engl J Med 322:1405–1411.

Bracken MB, Shepard MJ, Collins WF, Holford TR, Baskin DS, Eisenberg HM, Flamm E, Leo-Summers L, Maroon JC, Marshall LF, Perot PL, Piepmeier J, Sonntag VKH, Wagner FC, Wilberger JL, Winn HR, Young W (1992) Methylprednisolone or naloxone treatment after acute spinal cord injury: 1-year follow-up data. Results of the second National Acute Spinal Cord Injury Study. J Neurosurg 76:23–31.

Bydon M, Lin J, Macki M, Gokaslan ZL, Bydon A (2013) The current role of steroids in acute spinal cord injury. World Neurosurg 82:848–854.

Chen Y, Tang Y, Vogel LC, Devivo MJ (2013) Causes of spinal cord injury. Top Spinal Cord Inj Rehabil 19:1–8.

Cheung V, Hoshide R, Bansal V, Kasper E, Chen CC (2015) Methylprednisolone in the management of spinal cord injuries: Lessons from randomized, controlled trials. Surg Neurol Int 6:142.

Cifra A, Mazzone GL, Nani F, Nistri A, Mladinic M (2012) Postnatal developmental profile of neurons and glia in motor nuclei of the brainstem and spinal cord, and its comparison with organotypic slice cultures. Dev Neurobiol 72:1140–1160.

Cox A, Varma A, Banik N (2014) Recent advances in the pharmacologic treatment of spinal cord injury. Metab Brain Dis 30:473–482.

Darbon P, Scicluna L, Tscherter A, Streit J (2002) Mechanisms controlling bursting activity induced by disinhibition in spinal cord networks. Eur J Neurosci 15:671–683.

Donato R (2003) Intracellular and extracellular roles of S100 proteins. Microsc Res Tech 60:540–551.

Druschel C, Schaser KD, Schwab JM (2013) Current practice of methylprednisolone administration for acute spinal cord injury in Germany: a national survey. Spine 38:e669–e677.

Dumont RJ, Okonkwo DO, Verma S, Hurlbert RJ, Boulos PT, Ellegala DB, Dumont AS (2001) Acute spinal cord injury, part I: pathophysiologic mechanisms. Clin Neuropharmacol 24:254–264.

Eng LF (1985) Glial fibrillary acidic protein (GFAP): the major protein of glial intermediate filaments in differentiated astrocytes. J Neuroimmunol 8:203–214.

Evaniew N, Belley-Côté EP, Fallah N, Noonan V, Rivers CS, Dvorak MF (2015) Methylprednisolone for the treatment of patients with acute spinal cord injuries: a systematic review and meta-analysis. J Neurotrauma. Epub ahead of print.

Fatima G, Sharma VP, Das SK, Mahdi AA (2014) Oxidative stress and antioxidative parameters in patients with spinal cord injury: implications in the pathogenesis of disease. Spinal cord 53:3–6.

Fehlings MG, Vaccaro A, Wilson JR, Singh A, Cadotte DW, Harrop JS, Aarabi B, Shaffrey C, Dvorak M, Fisher C, Arnold P, Massicotte EM, Lewis S, Rampersaud R (2012) Early versus delayed decompression for traumatic cervical spinal cord injury: results of the Surgical Timing in Acute Spinal Cord Injury Study (STASCIS). PLoS One 7:e32037.

Fehlings MG, Wilson JR, Cho N (2014) Methylprednisolone for the treatment of acute spinal cord injury: counterpoint. Neurosurgery 1:36–42.

Forder JP, Tymianski M (2009) Postsynaptic mechanisms of excitotoxicity: involvement of postsynaptic density proteins, radicals, and oxidant molecules. Neuroscience 158:293–300.
Friedman B, Hockfield S, Black JA, Woodruff KA, Waxman SG (1989) In situ demonstration of mature oligodendrocytes and their processes: an immunocytochemical study with a new monoclonal antibody, Rip. Glia 2:380–390.
Furlan JC, Sakakibara BM, Miller WC, Krassioukov AV (2013) Global incidence and prevalence of traumatic spinal cord injury. Can J Neurol Sci 40:456–464.
Grillner S (2006) Biological pattern generation: the cellular and computational logic of networks in motion. Neuron 52:751–766.
Guzmán-Lenis MS, Navarro X, Casas C (2009) Drug screening of neuroprotective agents on an organotypic-based model of spinal cord excitotoxic damage. Restor Neurol Neurosci 27:335–349.
Hall ED (1993) Neuroprotective actions of glucocorticoid and nonglucocorticoid steroids in acute neuronal injury. Cell Mol Neurobiol 13:415–432.
Hall ED (2011) Antioxidant therapies for acute spinal cord injury. Neurotherapeutics 8:152–167.
Harrop JS (2014) Spinal cord injury: debating the efficacy of methylprednisolone. Neurosurgery 61:30–31.
Jain NB, Ayers GD, Peterson EN, Harris MB, Morse L, O'Connor KC, Garshick E (2015) Traumatic spinal cord injury in the United States, 1993–2012. JAMA 313:2236–2243.
Kanellopoulos GK, Xu XM, Hsu CY, Lu X, Sundt TM, Kouchoukos NT (2000) White matter injury in spinal cord ischemia: protection by AMPA/kainate glutamate receptor antagonism. Stroke 31:1945–1952.
Kiehn O (2006) Locomotor circuits in the mammalian spinal cord. Annu Rev Neurosci 29:279–306.
Kim DH, Vaccaro AR, Henderson FC, Benzel EC (2003) Molecular biology of cervical myelopathy and spinal cord injury: role of oligodendrocyte apoptosis. Spine J 3:510–519.
Kuzhandaivel A, Margaryan G, Nistri A, Mladinic M (2010a) Extensive glial apoptosis develops early after hypoxic-dysmetabolic insult to the neonatal rat spinal cord in vitro. Neuroscience 169:325–338.
Kuzhandaivel A, Nistri A, Mladinic M (2010b) Kainate-mediated excitotoxicity induces neuronal death in the rat spinal cord in vitro via a PARP-1 dependent cell death pathway (Parthanatos). Cell Mol Neurobiol 30:1001–1012.
Kuzhandaivel A, Nistri A, Mazzone GL, Mladinic M (2011) Molecular mechanisms underlying cell death in spinal networks in relation to locomotor activity after acute injury in vitro. Front Cell Neurosci. 5:9.
Lee JM, Yan P, Xiao Q, Chen S, Lee KY, Hsu CY, Xu J (2008) Methylprednisolone protects oligodendrocytes but not neurons after spinal cord injury. J Neurosci 28:3141–3149.
Lipton SA (2006) Paradigm shift in neuroprotection by NMDA receptor blockade: memantine and beyond. Nat Rev Drug Discov 5:160–170.
Liu XZ, Xu XM, Hu R, Du C, Zhang SX, McDonald JW, Dong HX, Wu YJ, Fan GS, Jacquin MF, Hsu CY, Choi DW (1997) Neuronal and glial apoptosis after traumatic spinal cord injury. J Neurosci 17:5395–5406.
Marchetti C, Beato M, Nistri A (2001) Alternating rhythmic activity induced by dorsal root stimulation in the neonatal rat spinal cord in vitro. J Physiol 530:105–112.
Margaryan G, Mladinic M, Mattioli C, Nistri A (2009) Extracellular magnesium enhances the damage to locomotor networks produced by metabolic perturbation mimicking spinal injury in the neonatal rat spinal cord in vitro. Neuroscience 163:669–682.
Margaryan G, Mattioli C, Mladinic M, Nistri A (2010) Neuroprotection of locomotor networks after experimental injury to the neonatal rat spinal cord in vitro. Neuroscience 165:996–1010.
Massobrio P, Pasquale V, Martinoia S (2015) Self-organized criticality in cortical assemblies occurs in concurrent scale-free and small-world networks. Sci Rep 5:10578.
Mazzone GL, Nistri A (2011) Effect of the PARP-1 inhibitor PJ 34 on excitotoxic damage evoked by kainate on rat spinal cord organotypic slices. Cell Mol Neurobiol 31:469–478.
Mazzone GL, Nistri A (2014) S100β as an early biomarker of excitotoxic damage in spinal cord organotypic cultures. J Neurochem 130:598–604.
Mazzone GL, Margaryan G, Kuzhandaivel A, Nasrabady SE, Mladinic M, Nistri A (2010) Kainate-induced delayed onset of excitotoxicity with functional loss unrelated to the extent of neuronal damage in the in vitro spinal cord. Neuroscience 168:451–462.
Mazzone GL, Mladinic M, Nistri A (2013) Excitotoxic cell death induces delayed proliferation of endogenous neuroprogenitor cells in organotypic slice cultures of the rat spinal cord. Cell Death Dis 31:e902.
Miekisiak G, Kloc W, Janusz W, Kaczmarczyk J, Latka D, Zarzycki D (2014) Current use of methylprednisolone for acute spinal cord injury in Poland: survey study. Eur J Orthop Surg Traumatol 24: S269–273.
Nasrabady SE, Kuzhandaivel A, Akrami A, Bianchetti E, Milanese M, Bonanno G, Nistri A (2012) Unusual increase in lumbar network excitability of the rat spinal cord evoked by the PARP-1 inhibitor PJ-34 through inhibition of glutamate uptake. Neuropharmacology 63:415–426.
Nicholas JS, Selassie AW, Lineberry LA, Pickelsimer EE, Haines SJ (2009) Use and determinants of the methylprednisolone protocol for traumatic spinal cord injury in South Carolina acute care hospitals. J Trauma 66:1446–1450.
Oudega M, Marani E, Thomeer RT (1992) Transient expression of stage-specific embryonic antigen-1 (CD15) in the developing dorsal rat spinal cord. Histochem J 24:869–877.
Oudega M, Vargas CG, Weber AB, Kleitman N, Bunge MB (1999) Long-term effects of methylprednisolone following transection of adult rat spinal cord. Eur J Neurosci 11:2453–2464.
Park E, Velumian AA, Fehlings MG (2004) The role of excitotoxicity in secondary mechanisms of spinal cord injury: a review with an emphasis on the implications for white matter degeneration. J Neurotrauma 21:754–774.
Pieretti-Vanmarcke R, Velmahos GC, Nance ML, Islam S, Falcone Jr RA, Wales PW, Brown RL, Gaines BA, McKenna C, Moore FO, Goslar PW, Inaba K, Barmparas G, Scaife ER, Metzger RR, Brockmeyer DL, Upperman JS, Estrada J, Lanning DA, Rasmussen SK, Danielson PD, Hirsh MP, Consani HF, Stylianos S, Pineda C, Norwood SH, Bruch SW, Drongowski R, Barraco RD, Pasquale MD, Hussain F, Hirsch EF, McNeely PD, Fallat ME, Foley DS, Iocono JA, Bennett HM, Waxman K, Kam K, Bakhos L, Petrovick L, Chang Y, Masiakos PT (2009) Clinical clearance of the cervical spine in blunt trauma patients younger than 3 years: a multi-center study of the American association for the surgery of trauma. J Trauma 67:543–549.
Rowland JW, Hawryluk GW, Kwon B, Fehlings MG (2008) Current status of acute spinal cord injury pathophysiology and emerging therapies: promise on the horizon. Neurosurg Focus 25:E2.
Sámano C, Nasrabady SE, Nistri A (2012) A study of the potential neuroprotective effect of riluzole on locomotor networks of the neonatal rat spinal cord in vitro damaged by excitotoxicity. Neuroscience 222:356–365.
Sauerland S, Nagelschmidt M, Mallmann P, Neugebauer EA (2000) Risks and benefits of preoperative high dose methylprednisolone in surgical patients: A systematic review. Drug Saf 23: 449–461.
Sommer I, Schachner M (1981) Monoclonal antibodies (O1 to O4) to oligodendrocyte cell surfaces: an immunocytological study in the central nervous system. Dev Biol 83:311–327.
Streit J (1993) Regular oscillations of synaptic activity in spinal networks in vitro. J Neurophysiol 70:871–878.
Sun YY, Wang CY, Hsu MF, Juan SH, Chang CY, Chou CM, Yang LY, Hung KS, Xu J, Lee YH, Hsu CY (2010) Glucocorticoid protection of oligodendrocytes against excitotoxin involving hypoxia-inducible factor-1α in a cell-type-specific manner. J Neurosci 30:9621–9630.
Taccola G, Margaryan G, Mladinic M, Nistri A (2008) Kainate and metabolic perturbation mimicking spinal injury differentially contribute to early damage of locomotor networks in the in vitro neonatal rat spinal cord. Neuroscience 155:538–555.

Taccola G, Mladinic M, Nistri A (2010) Dynamics of early locomotor network dysfunction following a focal lesion in an in vitro model of spinal injury. Eur J Neurosci 31:60–78.
Tohda C, Kuboyama T (2011) Current and future therapeutic strategies for functional repair of spinal cord injury. Pharmacol Ther 132:57–71.
Totoiu MO, Keirstead HS (2005) Spinal cord injury is accompanied by chronic progressive demyelination. J Comp Neurol 486:373–383.
Valverde S, Ohse S, Turalska M, West BJ, Garcia OJ (2015) Structural determinants of criticality in biological networks. Front Physiol 6:127.
Vialle R, Piétin-Vialle C, Vinchon M, Dauger S, Ilharreborde B, Glorion C (2008) Birth-related spinal cord injuries: a multicentric review of nine cases. Childs Nerv Syst 24:79–85.
Witts EC, Panetta KM, Miles GB (2012) Glial-derived adenosine modulates spinal motor networks in mice. J Neurophysiol 107:1925–1934.
Wittstock M, Rommer PS, Schiffmann F, Jügelt K, Stüwe S, Benecke R, Schiffmann D, Zettl UK (2015) Effect of methylprednisolone on mammalian neuronal networks in vitro. Cell Mol Neurobiol 35:111–114.
Xu J, Chen S, Chen H, Xiao Q, Hsu CY, Michael D, Bao J (2009) STAT5 mediates antiapoptotic effects of methylprednisolone on oligodendrocytes. J Neurosci 29:2022–2026.
Yin Y, Sun W, Li Z, Zhang B, Cui H, Deng L, Xie P, Xiang J, Zou J (2013) Effects of combining methylprednisolone with rolipram on functional recovery in adult rats following spinal cord injury. Neurochem Int 62:903–912.
York EM, Petit A, Roskams AJ (2013) Epigenetics of neural repair following spinal cord injury. Neurotherapeutics 10:757–770.

(Accepted 1 December 2015)
(Available online 14 December 2015)

EJN European Journal of Neuroscience

FENS Federation of European Neuroscience Societies

European Journal of Neuroscience, pp. 1–13, 2016 doi:10.1111/ejn.13353

Neuroprotective effect of propofol against excitotoxic injury to locomotor networks of the rat spinal cord *in vitro*

Jaspreet Kaur,[1,*] Javier Flores Gutiérrez[1,*] and Andrea Nistri[1,2]
[1]Neuroscience Department, International School for Advanced Studies (SISSA), Via Bonomea 265, 34136 Trieste, Italy
[2]SPINAL (Spinal Person Injury Neurorehabilitation Applied Laboratory), Istituto di Medicina Fisica e Riabilitazione, Udine, Italy

Keywords: general anaesthetic, kainic acid, motoneuron, spinal cord injury

Edited by Paul Bolam
Received 14 April 2016, accepted 11 July 2016

Abstract

Although neuroprotection to contain the initial damage of spinal cord injury (SCI) is difficult, multicentre studies show that early neurosurgery under general anaesthesia confers positive benefits. An interesting hypothesis is that the general anaesthetic itself might largely contribute to neuroprotection, although *in vivo* clinical settings hamper studying this possibility directly. To further test neuroprotective effects of a widely used general anaesthetic, we studied if propofol could change the outcome of a rat isolated spinal cord SCI model involving excitotoxicity evoked by 1 h application of kainate with delayed consequences on neurons and locomotor network activity. Propofol (5 μM; 4–8 h) enhanced responses to GABA and depressed those to NMDA together with decrease in polysynaptic reflexes that partly recovered after 1 day washout. Fictive locomotion induced by dorsal root stimuli or NMDA and serotonin was weaker the day after propofol application. Kainate elicited a significant loss of spinal neurons, especially motoneurons, whose number was halved. When propofol was applied for 4–8 h after kainate washout, strong neuroprotection was observed in all spinal areas, including attenuation of motoneuron loss. Although propofol had minimal impact on recovery of electrophysiological characteristics 24 h later, it did not further depress network activity. A significant improvement in disinhibited burst periodicity suggested potential to ameliorate neuronal excitability in analogy to histological data. Functional recovery of locomotor networks perhaps required longer time due to the combined action of excitotoxicity and anaesthetic depression at 24 h. These results suggest propofol could confer good neuroprotection to spinal circuits during experimental SCI.

Introduction

Traumatic spinal cord injury (SCI) produces long-term effects associated with severe motor disability (Furlan *et al.*, 2013). Although acute management of SCI has been improved, only about 5% of patients with complete SCI will walk again (Dobkin & Havton, 2004). The primary insult triggers a sequence of pathological events (secondary injury) lasting a few hours or even days (Sekhon & Fehlings, 2001; Park *et al.*, 2004; Rowland *et al.*, 2008). This time window creates the opportunity for a potentially successful clinical intervention to prevent damage expansion.

One major mechanism contributing to cell loss during the secondary phase is excitotoxicity due to excessive activation of glutamate receptors (Rossignol *et al.*, 2007) with subsequent neuronal degeneration (Mandir *et al.*, 2000; David *et al.*, 2009; Kuzhandaivel *et al.*, 2010): this is, thus, an important target for neuroprotection. To investigate the pathophysiological events occurring after SCI, we have developed an *in vitro* model of SCI based on the application of kainate, a potent glutamate receptor agonist that evokes delayed neuronal loss especially affecting motor networks (Taccola *et al.*, 2008; Nasrabady *et al.*, 2011b; Nistri, 2012). One major advantage of this model is that it allows studying any correlation between electrophysiological activity and histological damage. Although previous reports indicate limited neuroprotective success with various strategies (Nasrabady *et al.*, 2011a, 2012), more encouraging data have recently emerged by testing the volatile anaesthetic methoxyflurane (Shabbir *et al.*, 2015). These results raised the question whether neuroprotection is an intrinsic property of a volatile anaesthetic (less frequently employed because of toxicity) or whether another general anaesthetic may produce a similar effect. The present study explored the potential protection by the intravenous anaesthetic propofol widely used to induce and maintain general anaesthesia (Acton, 2011). Studies investigating its neuroprotective action on *in vitro* and *in vivo* models of brain ischaemia have provided positive results (Pittman *et al.*, 1997; Young *et al.*, 1997; Ito *et al.*, 1999; Gelb *et al.*, 2002; Velly *et al.*, 2003; Engelhard *et al.*, 2004b). Proprofol pre-treatment also protects against spinal cord ischaemia *in vivo* (Sahin *et al.*, 2015). The underlying mechanism of neuroprotection by propofol is related to potentiation of $GABA_A$-mediated inhibition of synaptic transmission (Hales & Lambert, 1991; Xu, 1999; Bajrektarevic & Nistri, 2016), direct inhibition of glutamate release (Orser

Correspondence: Professor A. Nistri, as above.
E-mail: nistri@sissa.it

*Joint first authors.

et al., 1995) and antioxidant properties (Hans *et al.*, 1997; Ansley *et al.*, 1998; Stratford & Murphy, 1998). While propofol attenuates damage to the motoneurons of organotypic spinal slice cultures (Bajrektarevic & Nistri, 2016), it is unknown what functional impact on locomotor networks this phenomenon may have. The novel findings of the present investigation are that propofol protected spinal neurons, and motoneurons in particular, from damage even when it was applied for a few hours after kainate. Recovery in locomotor network function was not, however, observed probably because of the lingering depression of circuit activity by the sustained application of this anaesthetic. It is noteworthy that this protocol simulates the clinical setting of acute SCI by applying the anaesthetic agent only after having provoked the damage.

Materials and methods

Spinal cord preparation

Spinal cords were carefully dissected from 0- to 2-day-old Wistar rats under terminal anaesthesia with i.p. urethane (0.2 mL i.p. of a 10% w/v solution) according to the guidelines for the care and use of laboratory animals of National Institute of Health (NIH). Because urethane produces non-selective depression of excitatory amino acid or dorsal root-evoked depolarization of isolated spinal cords (Evans & Smith, 1982) and is not clinically used due to liver toxicity, this drug was employed only for terminal anaesthesia rather than as a test agent for neuroprotection. Rats were supplied by the animal house of the International School for Advanced Studies (SISSA) through their in-house breeding facility. A total of 87 animals were used. All experimental protocols were approved by the ethics committee for animal experimentation of SISSA. All efforts were made to minimize the number of the animals used for the experiments as well as their suffering. Once dissected, spinal cords were continuously superfused with Krebs solution (in mM: 113 NaCl, 4.5 KCl, 1 $MgCl_2 \cdot 7H_2O$, 2 $CaCl_2$, 1 NaH_2PO_4, 25 $NaHCO_3$, 11 glucose; gassed with 95% O_2 and 5% CO_2, pH 7.4 at room temperature at 7.5 mL/min) as described previously (Taccola & Nistri, 2006a). After dissection, to obtain full functional recovery, spinal cords were incubated in Krebs solution for about 2 h to recover before proceeding to experimentation. Recovery from urethane is reported to occur during 30-min washout *in vitro* (Bagust & Kerkut, 1981; Evans & Smith, 1982).

Protocol for drug application, lesion and neuroprotection

In order to mimic the *in vitro* spinal lesion of grey matter, kainate (100 μM) was applied for 1 h (Taccola *et al.*, 2008; Margaryan *et al.*, 2010; Mazzone *et al.*, 2010). This concentration was chosen to fully abolish fictive locomotion elicited by DR train pulses or NMDA + 5-HT when tested 24 h after injury (Nasrabady *et al.*, 2011b). Propofol (Frenesius Kabi Italia – SPA, NDC 63323-0270-50, Verona, Italy) was diluted in Krebs solution and to ensure its full solubilization, vigorous mixing for at least 3 min was performed before application. Several studies have demonstrated that propofol clinical effects are achieved at concentrations from 0.5 to 10 μM (Gredell *et al.*, 2004; Matute *et al.*, 2004; Wakita *et al.*, 2013; Eckle *et al.*, 2015). As propofol had never been tested before in this type of experiment, we chose the mid-range value of 5 μM.

The effect of propofol (5 μM) was first studied electrophysiologically by applying it for 4 h on day 1. The polysynaptic reflex activity was recorded every 10 min during 4 h, and its area and amplitude were analysed. The same experiments were also done by doubling the duration of propofol (5 μM) application. Thereafter, preparations were kept in standard Krebs solution overnight and recorded on the subsequent day (Fig. S1). Furthermore, we used a different protocol to find out the effect of propofol on the ventral root (VR) depolarization induced by exogenously applied neurotransmitter agents (2 min application): GABA (10 μM, 20 μM, and 30 μM; $n = 7$); glycine (30 μM and 50 μM; $n = 5$); AMPA (5 μM, 7.5 μM and 10 μM; $n = 5$); NMDA (10 μM, $n = 5$; 20 μM, $n = 6$, and 25 μM, $n = 6$). We also tested responses to GABA or NMDA after application of tetrodotoxin (TTX; initially 1 μM and then 0.1 μM for maintenance) to pharmacologically isolate motoneuronal responses from neuronal networks. GABA was applied at 10 μM and 20 μM ($n = 6$), while NMDA was at 10 μM ($n = 4$), 20 μM ($n = 6$), 25 μM ($n = 6$) and 30 μM ($n = 8$).

The excitotoxic protocol was based on kainate (100 μM) applied for 1 h and then washout with either Krebs solution or propofol (5 μM) solution for 4–8 h. These spinal cords were later superfused for 16–24 h with standard Krebs solution. Electrophysiological and immunohistochemical data were compared among the following six groups after 24 h: sham (untreated), kainate 100 μM/1 h, propofol 5 μM/4 h, propofol 5 μM/8 h and the two corresponding kainate treatments followed by propofol-treated groups (see scheme in Fig. S1).

Electrophysiological recordings

DC-coupled recordings from lumbar (L) ventral roots (VR) using Ag/AgCl suction electrodes were employed to study fictive locomotor rhythms from flexor (L2) and extensor (L5) motor pools. Data were acquired with pClamp software (version 9.2; Molecular devices, Sunnyvale, CA, USA).

In order to generate polysynaptic responses, single electrical stimuli (0.1 ms duration) were applied to an individual ipsilateral homosegmental dorsal root (DR) once every 1 min. We first determined the minimum stimulus intensity to elicit the VR threshold response homolaterally. As previously reported by Marchetti *et al.* (2001), thrice threshold stimuli were used to produce polysynaptic responses (Baranauskas & Nistri, 1995). Data were analysed by averaging three to five consecutive responses. Cumulative depolarization was induced by stimulating (0.1 ms) a single DR with 30 pulse trains (2 Hz) that elicited a series of alternating discharges typical of electrically induced fictive locomotion (Marchetti *et al.*, 2001). Fictive locomotion was also elicited chemically by applying NMDA (3–6 μM) and 5-HT (10 μM) (Kiehn, 2006). A minimum of 20 VR cycles alternating homolaterally between flexor and extensor motor pools or from side to side at the same segmental level was considered as a criterion to observe fictive locomotion evoked by NMDA and 5-HT (Taccola *et al.*, 2008). Disinhibited bursting was elicited by co-applying blockers of $GABA_A$ and glycine receptors, bicuculline (20 μM) and strychnine (1 μM) respectively (Bracci *et al.*, 1996a). All the recorded parameters were digitized and analysed as previously reported (Sámano *et al.*, 2016).

Immunohistochemical procedure

Spinal cords from all experimental groups were fixed in paraformaldehyde approximately 24 h after dissection, then cryoprotected with 30% sucrose and finally sectioned (30 μm) with a sliding microtome at −20 °C. Immunostaining was performed with a free-floating method on T13-L5 segments, which contain the principal elements of the locomotor networks, in accordance with former studies from our laboratory (Cifra *et al.*, 2012; Bianchetti *et al.*,

2013; Shabbir *et al.*, 2015). As a routine, after incubation in blocking solution (5% normal goat serum, 5% bovine serum albumin, 0.3% Triton-X 100, 1% phosphate buffer saline) for 2 h at room temperature, spinal cord sections were incubated overnight at 4 °C with one of these primary antibodies: anti-NeuN (neuron-specific protein, mouse monoclonal, 1 : 50 dilution; Chemicon, Millipore, Billerica, MA), anti-SMI32 (specific non-phosphorylated neurofilament protein, mouse monoclonal, 1 : 200 dilution; Chemicon, Millipore) and anti-ChAT (choline acetyltransferase, goat polyclonal, 1 : 50 dilution; Chemicon, Millipore). Anti-NeuN antibody was used to identify differentiated neurons, whereas anti-SMI32 and anti-ChAT antibodies were used to specifically stain motoneurons visualized as large (>20 μm) cells in the ventral horn. All these antibodies have been validated for immunostaining with this preparation in our laboratory (Taccola *et al.*, 2008; Cifra *et al.*, 2012; Bianchetti *et al.*, 2013; Shabbir *et al.*, 2015). Primary antibodies were visualized using secondary donkey anti-goat Alexa fluor 594 and donkey anti-mouse Alexa fluor 488 (1 : 500, Invitrogen, Carlsbad, CA, USA). Sections were finally incubated with 4′,6-diamidino-2-phenylindole (DAPI) for 30 min and analysed as detailed below.

Cell death analysis

The methods for cell counting are the same as used before in our laboratory and described in detail (Bianchetti *et al.*, 2013; Shabbir *et al.*, 2015). We used either a Zeiss Axioskop2 epifluorescence microscope (Oberkochen, Germany) or a confocal Leica TCS SP2 microscope (Wetzlar, Germany) to obtain bidimensional histological images. Cell counting was performed by an observer blinded to the experimental protocols after DAPI, NeuN, ChAT and SMI32 staining, for nuclei, neurons and motoneurons, respectively, using 'eCELLence' software (Glance Vision Tech., Trieste, Italy) and the 'cell counter' plugin for ImageJ (Kurt De Vos, University of Sheffield, UK). For neuron counting, the NeuN nuclear antibody enabled quantifying their number in discrete regions of interest (ROI; dimensions indicated below) regardless of the neuron size: nuclear staining was confirmed with DAPI staining. Clearly damaged nuclei were discarded from counting. Pyknosis was readily observed as a change in nuclear morphology characterized by an intense nuclear condensation with strong refractivity (Burgoyne, 1999; Taccola *et al.*, 2008) corresponding to type 1 cell death as stated by the international Nomenclature Committee on Cell Death (NCCD) classification (Galluzzi *et al.*, 2007, 2012).

For each histological section of the spinal cord, three different ROIs were investigated as previously reported (Mazzone *et al.*, 2010; Cifra *et al.*, 2012; Bianchetti *et al.*, 2013): dorsal grey matter (Rexed laminae I–IV), central grey matter (Rexed laminae V–VII and X) and ventral grey matter (Rexed laminae VIII–IX) (Fig. S2). In each region, two fields of 125 × 100 μm were analysed. For each experimental group, at least three spinal cords were analysed and, for each spinal cord, at least 10 different sections were examined.

Statistics

Statistical analysis was done using Sigma Stat 3.5 software (Systat Software, Chicago, IL, USA). Electrophysiology and immunohistochemical data are shown as mean ± SEM; n is the number of spinal cord preparations. From each histological experiment that yielded several sections, we calculated the mean for one spinal cord and repeated the same approach with the other spinal cords so that we could finally calculate the mean of the experimental group.

After applying a normality test to differentiate between parametric and non-parametric data, the values were evaluated with either a two-tailed Student's t-test or a Mann–Whitney test respectively. Analysis of variance (anova) test was used to compare multiple groups (through Kruskal–Wallis or Holm–Sidak tests or Dunn's method). The acceptance level of significance was $P < 0.05$.

Results

Early changes in responses to exogenously applied neurotransmitters in the presence of propofol

Previous reports have shown that propofol acts as a positive modulator of $GABA_A$ and glycine receptors (Hales & Lambert, 1991; Xu, 1999). Furthermore, propofol can decrease glutamate and NMDA-mediated responses of mouse cultured hippocampal neurons (Orser *et al.*, 1995). To validate that these observations are applicable to the rat spinal cord as well, we tested if propofol differentially affected network depolarizations evoked by GABA, glycine, AMPA or NMDA recorded sequentially from lumbar VRs on the first day *in vitro* as exemplified in Fig. 1A. Thus, propofol (5 μm) potentiated the GABA (20 μm)-mediated response that was characterized by an early peak followed by fade presumably due to receptor desensitization (Fig. 1A). Responses to glycine or AMPA were not significantly changed, while NMDA-mediated depolarization was decreased (Fig. 1A). Figure 1D (filled circles) indicates that average responses to 10–20 μm GABA ($F_{5,34} = 2.657$, $^*P = 0.039$; Holm–Sidak test, calculated from raw data) were enhanced by propofol, while larger responses were less potentiated. On the same preparations, propofol had no significant effect on glycine ($F_{3,14} = 0.114$, $P = 0.950$; one-way analysis of variance test, calculated from raw data) or AMPA ($F_{5,24} = 0.617$, $P = 0.688$; one-way analysis of variance test, calculated from raw data)-mediated responses (Fig. 1C). A reduction in depolarization amplitude was observed when NMDA (10–30 μm) was tested in the presence of propofol (Fig. 1A and E; $F_{5,24} = 3.747$, $P = 0.012$; Holm–Sidak test, calculated from raw data). As shown by the sample depolarizations depicted in Fig. 1A, these network responses had complex origin and time-course arising from co-activation of premotoneurons and motoneurons. In order to minimize the indirect network contribution to the observed VR effects, TTX was pre-applied to block propagated network activity. Responses, therefore, reflected motoneuron population depolarization as exemplified in Fig. 1B. VR depolarizations of similar amplitude evoked by GABA or NMDA were differentially modulated by propofol because the first ones were increased and the latter ones depressed (Fig. 1B,D and E; $H_{(3)} = 8.978$, $P = 0.03$ and $H_{(7)} = 24.893$, $^{***}P = <0.001$; Kruskal–Wallis one-way analysis of variance on ranks test, respectively, calculated from raw data). Hence, the present results suggest that, in the rat spinal cord, GABA receptor-mediated responses were upregulated by propofol that concomitantly depressed NMDA-mediated ones.

Delayed application of propofol protected from cell death evoked by kainate

The protocol to assess whether propofol could be neuroprotective against kainate-elicited excitotoxicity involved observing the histological characteristics of three ROIs (see Fig. S2A) of the spinal cord 24 h after applying kainate (1 h). Thus, we used 100 μm kainate that is damaging neurons (identified with NeuN immunopositivity) rather than glia with particular vulnerability of motoneurons (immunoreactive to ChAT or SMI32; Mazzone *et al.*, 2010; Cifra

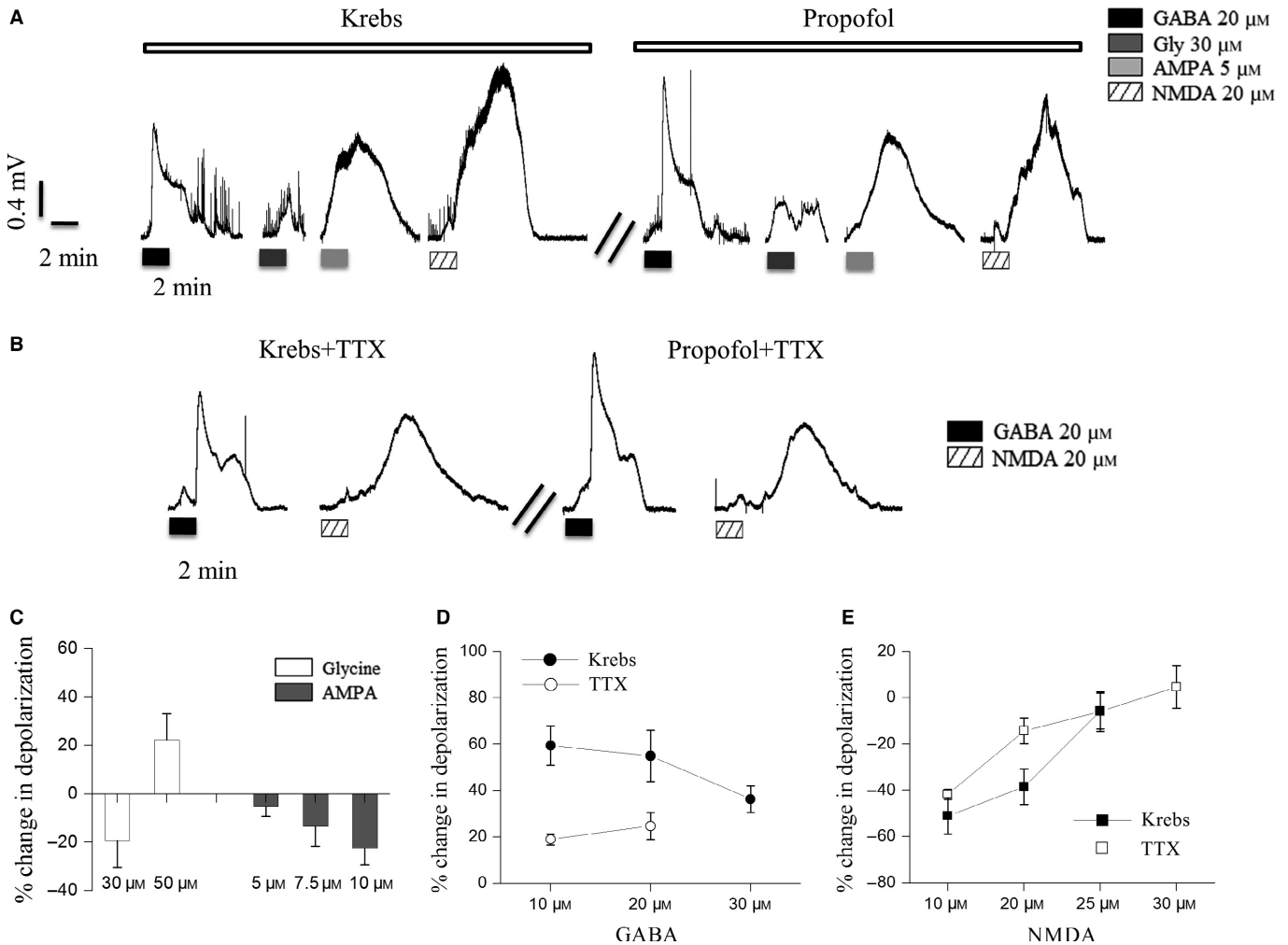

FIG. 1. Effect of propofol (5 μM) on VR depolarization induced by exogenously applied neurotransmitter agonists. (A) Examples of responses recorded from a single lumbar VR following superfusion with GABA (20 μM), glycine (30 μM), AMPA (5 μM) or NMDA (20 μM) in standard Krebs solution (control) and subsequently with propofol. Application times are indicated by horizontal bars. (B) Representative records of lumbar VR responses evoked by GABA (20 μM) or NMDA (20 μM) in TTX solution followed by propofol + TTX. Data exemplify propofol-mediated potentiation of GABA and suppression of NMDA responses. (C) Bar graph showing per cent change (vs. control) in VR depolarization recorded in the presence of propofol following application of glycine (30 μM, $n = 6$, $U = 13$, $P = 0.485$ and 50 μM, $n = 3$, $U = 6$, $P = 0.700$; Mann–Whitney test) or AMPA (5 μM, $t_8 = 0.681$, $P = 0.515$; 7.5 μM, $t_8 = 0.494$, $P = 0.635$ and 10 μM, $t_8 = 1.356$, $P = 0.212$; $n = 5$). No significant alteration in such responses was obtained. (D) Line graph depicting per cent increase in GABA-mediated VR depolarization after application of propofol alone (filled symbols) (GABA = 10, 20 and 30 μM) in Krebs solution or in TTX solution (open symbols) (GABA = 10 and 20 μM) when compared with the amplitude detected with GABA alone. Applying the Student's *t*-test to raw data, a significant increase in peak amplitude was observed with 10 μM GABA and propofol ($n = 7$, $t_{12} = -2.634$, $^*P = 0.022$) and 10 μM GABA + propofol + TTX ($n = 4$, $t_6 = -3.125$, $P = 0.02$). However, there was no significance change in response to 20 and 30 μM GABA with propofol (20 μM, $n = 7$, $t_{12} = -1.926$, $P = 0.078$; 30 μM, $n = 6$, $t_{10} = -1.315$, $P = 0.218$) and 20 μM GABA + propofol + TTX ($n = 4$, $U = 13$, $P = 0.200$; Mann–Whitney test). (E) Line graph illustrating per cent decrease in NMDA-mediated VR depolarization in the presence of propofol (NMDA = 10, 20, 25; μM) as well as propofol + TTX (NMDA = 10, 20, 25, 30; μM) vs. responses evoked by NMDA alone. Applying the Student's *t*-test to raw data indicated that propofol significantly depressed 10 and 20 μM NMDA-mediated responses in Krebs (10 μM, $n = 6$, $t_{10} = 2.729$, $P = 0.021$ and 20 μM, $n = 5$, $t_8 = 2.649$, $P = 0.029$ respectively), whereas propofol applied with TTX significantly depressed only 10 μM NMDA responses ($n = 5$, $t_6 = 3.089$, $P = 0.021$). Responses to 25 μM NMDA applied with propofol ($n = 4$, $t_6 = 0.263$, $P = 0.801$) and 20, 25, 30 μM NMDA + propofol + TTX (20 μM, $n = 6$, $t_{10} = 0.475$, $P = 0.645$; 25 μM, $n = 6$, $t_{10} = 0.0673$, $P = 0.948$; 30 μM, $n = 8$, $t_{14} = -0.312$, $P = 0.759$) were not significantly different from their subsequent control groups.

et al., 2013). Figure 2A provides general data concerning the toxicity of kainate and its antagonism by propofol in the three spinal ROIs. The examples for ventral ROI shown in Fig. 2C indicate a pyknotic cell (see the arrow in inset pointing to a DAPI-stained cell with compacted nuclear chromatin) next to a standard neuron, suggesting scattered damage. In general, the % value of pyknotic cells was significantly lower when kainate application was followed by propofol for 4 or 8 h (Fig. 2A and C). One example of pyknotic nuclei is shown in Fig. S2B.

By analysing actual neuronal numbers in the three ROIs (Fig. 2B and C), it became apparent that, 24 h after kainate, the number of neurons was lowered in all regions as a consequence of kainate toxicity (see also Taccola *et al.*, 2008; Mazzone *et al.*, 2010) and that this effect was significantly prevented by propofol applied for 4 or 8 h after washout of kainate. It is noteworthy that propofol per se applied for the same length of time had no deleterious effect (Fig. 2A–C). Figure 3A and B shows results for motoneurons immunolabeled with the ChAT antibody (or SMI32; see Fig. S3):

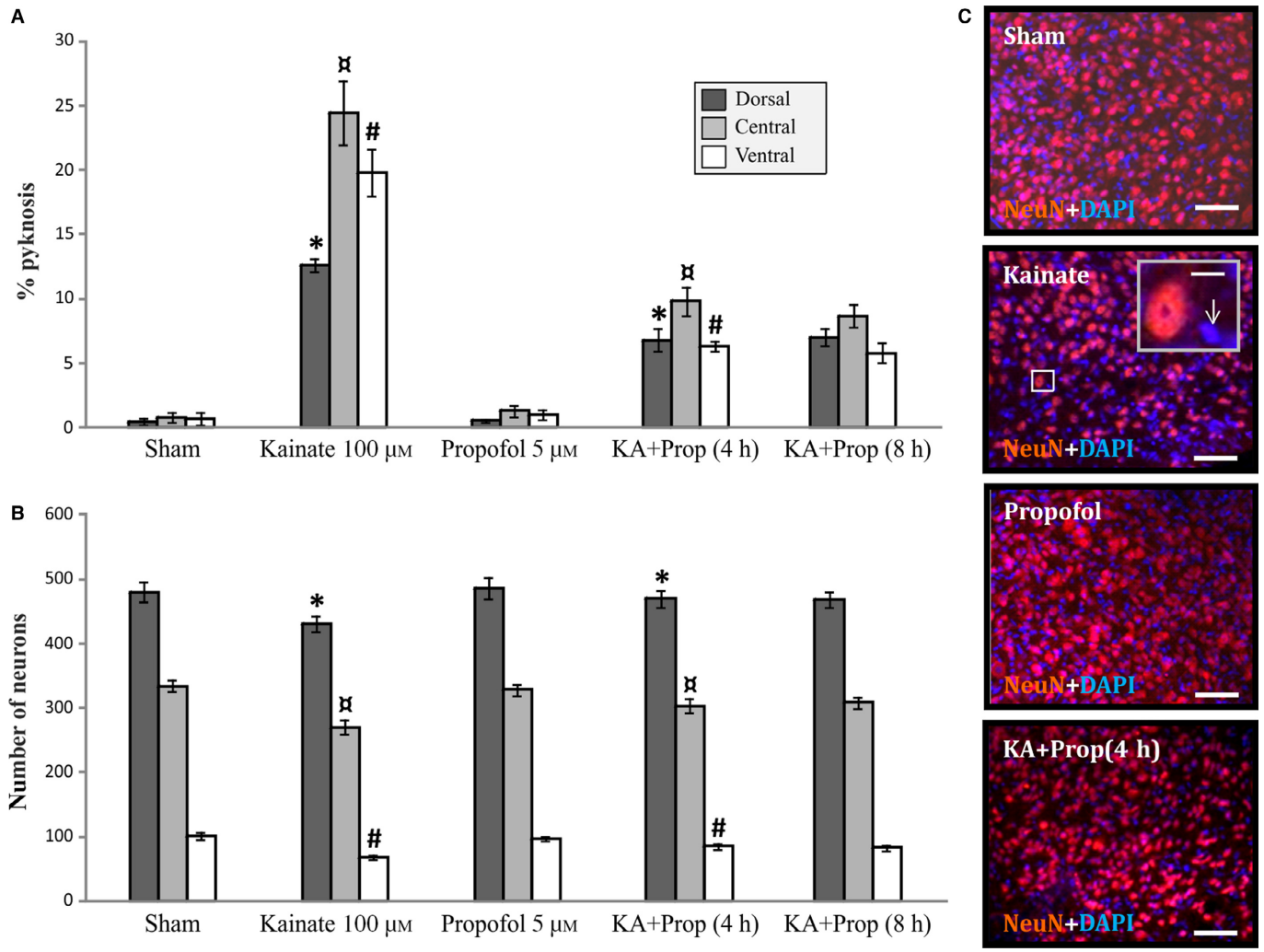

FIG. 2. Histological neuroprotection by propofol (Prop; 5 μM) against kainate (KA; 100 μM)-evoked excitotoxicity. (A) Histograms showing percentage of pyknotic cells in the different ROIs (dorsal, central and ventral) after kainate application and/or propofol treatment. Note statistically significant decrease of pyknosis percentage in all three ROIs when anaesthetic propofol was applied (4 or 8 h) after kainate, compared to sham or application of kainate alone. Thus, using the Mann–Whitney test, the observed significance level was for KA + Prop 4 h vs. KA alone was $P = 0.0009$ ($U = 238$), $P = 0.0003$ ($U = 835$) and $P = 0.0002$ ($U = 990$) for dorsal, central and ventral ROI respectively. For KA + Prop 4 h vs. sham, significance levels were: $P = 0.0003$ ($U = 652$), $P = 0021$ ($U = 681$) and $P = 0.0009$ ($U = 636$) for dorsal, central and ventral ROI respectively. Equivalent results were obtained when Mann–Whitney test was performed for comparing KA + Prop 8 h vs. KA alone and KA + Prop 8 h vs. sham. All data are the average from 10 to 15 sections of 3–5 rat spinal cords and are represented as mean ± SEM. Likewise symbols represent a significant difference between groups (for more details see Material and Methods section). (B) Histograms showing number of neurons in the same ROIs after kainate application and/or propofol treatment. Also here, a significant neuroprotective effect of propofol is shown. Thus, using a two-tailed Student's *t*-test, the observed significance level was for KA + Prop 4 h vs. KA alone: $P = 0.048$ ($t_{36} = 2.056$), $P = 0.004$ ($t_{52} = 3.076$) and $P = 0.0008$ ($t_{39} = -3.645$) for dorsal, central and ventral ROI respectively. For KA + Prop 4 h vs. sham, significance levels were: $P = 0.2070$ ($t_{31} = 1.281$), $P = 0.135$ ($t_{40} = 1.541$) and $P = 0.002$ ($t_{27} = 3.469$) for dorsal, central and ventral ROI respectively. Equivalent results were obtained when a two-tailed Student's *t*-test was performed for comparing the number of neurons in KA + Prop 8 h vs. KA alone and KA + Prop 8 h vs. sham. All data are the average from 10 to 15 sections of 3–5 rat spinal cords and are represented as mean ± SEM. Likewise symbols represent a significant difference between groups (for more details see Material and Methods section). (C) Examples of ventral horn NeuN and DAPI staining. In the kainate group example, the inset shows at larger magnification an apparently normal neuron next to one pyknotic nucleus (indicated by an arrow). Scales bars: 20 μm and 2.5 μm. For protocols of drug applications see Fig. S1.

against a very strong loss of motoneurons induced by kainate, a significant neuroprotection by 4–8 h propofol was observed.

Long-lasting effect of propofol on network synaptic transmission

While previous studies have reported the relatively early effect of propofol on spinal dorsal (Jewett *et al.*, 1992) and ventral (Kungys *et al.*, 2009; Eckle *et al.*, 2015) horn neurons and reflexes (Baars *et al.*, 2006), it was first necessary to investigate what changes in synaptic transmission were caused by administration of this anaesthetic extended for a few hours even in the absence of excitotoxicity. Hence, we monitored polysynaptic reflexes over several hours following 4- (Fig. 4A upper row, B) or 8-h (Fig. 4A lower row, C) application of propofol. During the 4-h application, the reflex amplitude did not significantly change (Jewett *et al.*, 1992), while the area fell with minimal recovery over the following 3-h washout (Control vs. Prop 4 h, $t_9 = 3.587$, $^{**}P = 0.006$; Control vs. Wash, $t_9 = 2.977$, $^{*}P = 0.016$; *t*-test; Fig. 4A and B). When the application of

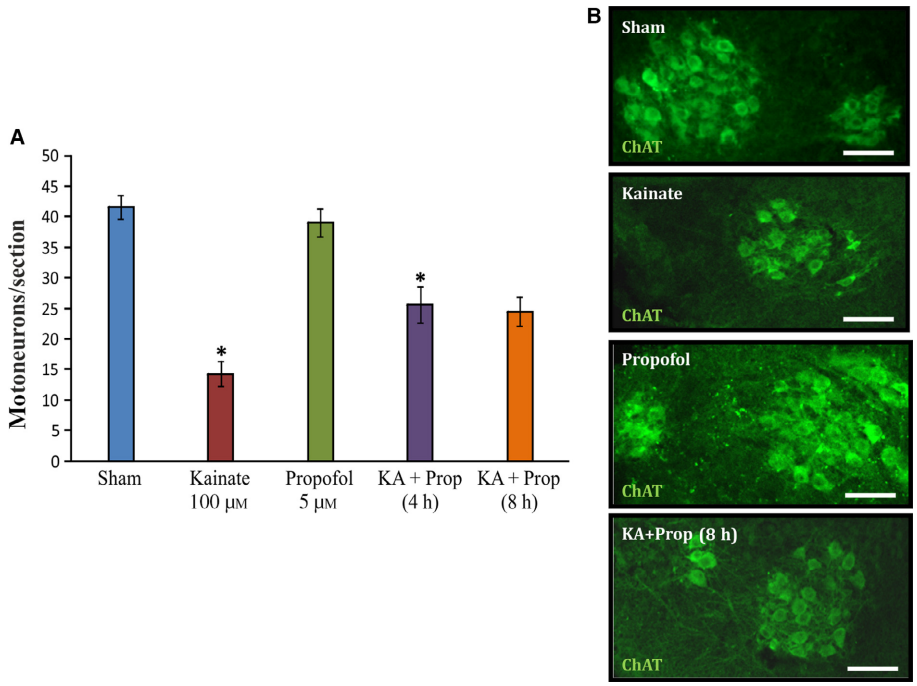

FIG. 3. Histological neuroprotection of ChAT-positive motoneurons by propofol (Prop; 5 μM) against kainate (KA; 100 μM) evoked excitotoxicity. (A) Histogram showing number of motoneurons in ventral ROI. Note significantly larger number of motoneurons from samples treated with propofol for 4 or 8 h after kainate vs. sham or kainate alone. Thus, by using a two-tailed Student's *t*-test, the observed significance level for KA + Prop 4 h vs. KA alone was: $P = 0.002$ ($t_{18} = 3.729$) and for KA + Prop 4 h vs. sham, $P = 0.00001$ ($t_{28} = 5.321$). When compared KA + Prop 8 h vs. KA alone through the same test, the obtained significance was $P = 0.004$ ($t_{16} = 2.808$) and for KA + Prop 8 h vs. sham, $P = 0.0001$ ($t_{26} = 4.489$). All data are the average from 10 to 15 sections of 3–5 rat spinal cords and are represented as mean ± SEM. Star symbols represent a significant difference between groups (for more details see Material and Methods section). (B) Examples of ChAT immunopositive cells using such protocols. Scale bar: 50 μm. For paradigms of drug applications see Fig. S1.

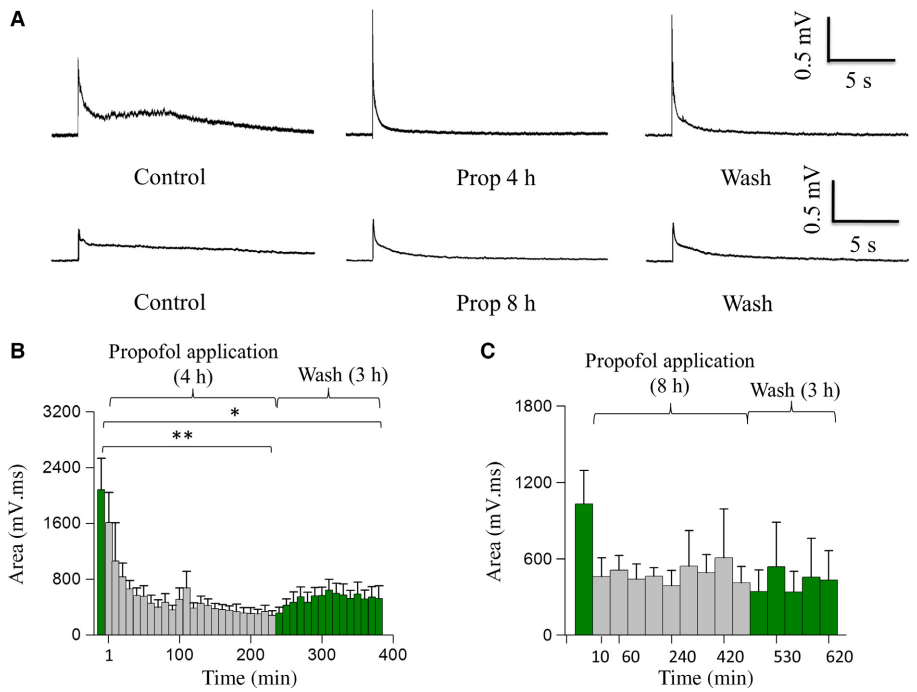

FIG. 4. Long-lasting effect of propofol (5 μM) on polysynaptic responses. (A) Upper row: sample recordings of reflex responses evoked by single DR stimulation in Krebs (Control), at 4 h application of propofol (Prop 4 h) and washed out with Krebs for 3 h (Wash). Lower row: sample recordings of responses in Krebs (Control), at 8-h propofol application (Prop 8 h) and washed out with Krebs for 3 h (Wash). (B, C) Histograms showing the area of average polysynaptic reflex responses at 10 min (B) or 1 h (C) intervals while propofol was continuously applied for 4 h ($n = 6$) and 8 h ($n = 6$), respectively, and then washed out with Krebs solution for further 3 h. Green bars depict superfusion with Krebs, whereas grey bars show propofol application (4 and 8 h). Recordings (A) and bar graphs (B, C) indicate that the area was reduced after propofol application (4 and 8 h) with modest recovery during wash (Control vs. Prop 4 h, $t_9 = 3.587$, $^{**}P = 0.006$; Control vs. Wash, $t_9 = 2.977$, $^{*}P = 0.016$). No apparent recovery was observed at 3 h washout after 8 h propofol (Control vs. Prop 8 h, $t_{10} = 2.121$, $P = 0.060$; Control vs. Wash, $U = 20$, $P = 0.114$, Mann–Whitney test).

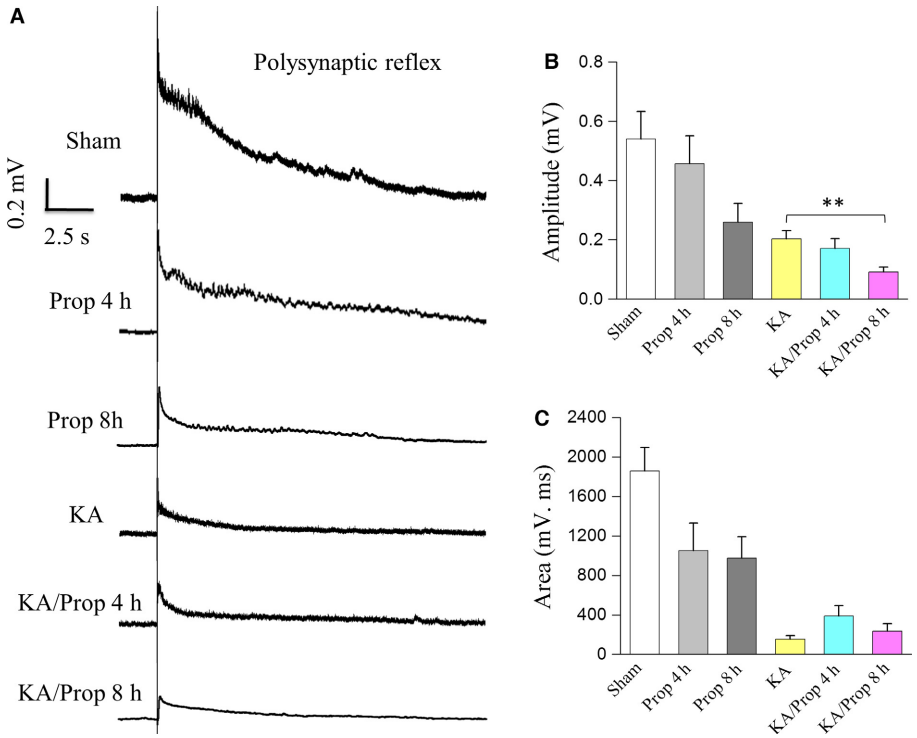

FIG. 5. Effect of propofol (5 μM) application on polysynaptic reflex responses recorded 24 h after exposure to kainate (KA, 100 μM). (A) Examples of polysynaptic responses recorded from L5 VRs in sham (control for day 2), propofol applied for 4 h (Prop 4 h), propofol applied for 8 h (Prop 8), kainate applied for 1 h (KA), kainate (1 h) followed by propofol for 4 h (KA/Prop 4 h) and kainate (1 h) followed by propofol for 8 h (KA/Prop 8 h). (B, C) Histograms illustrating the peak amplitude (B) and area (C) of reflex responses after KA (n = 11), KA/Prop 4 h (n = 10), KA/Prop 8 h (n = 14) treatment compared to sham (n = 8), Prop 4 h (n = 9) and Prop 8 h (n = 8). Note the significant fall in peak amplitude (U = 24, $^{**}P$ = 0.004; Mann–Whitney test) of preparations treated with propofol for 8 h after kainate application as compared to kainate alone. All values of reflex peak amplitude and area in treated spinal cords were significantly different from sham (H_5 = 32.163, P = 0.001; H_5 = 30.521, P = 0.001; Kruskal–Wallis one-way analysis of variance on ranks test respectively).

propofol was extended to 8 h, the response area was persistently decreased with no apparent recovery over the next 3 h wash (Fig. 4A lower row, C; Control vs. Prop 8 h, t_{10} = 2.121, P = 0.060, t-test; Control vs. Wash, U = 20, P = 0.114, Mann–Whitney test). Figure 5A–C shows that 24 h later, reflex characteristics, when compared with sham preparations, were depressed after previous exposure to propofol (on the first day) especially in terms of area despite the observation that no histological deficit was detected (see Figs 2 and 3). These observations suggested prolonged functional depression by propofol despite washout.

Functional activity of locomotor networks following kainate and propofol application

We next explored whether propofol depression of synaptic transmission was additive to any neurotoxic action by kainate or whether it could actually reverse it, at least in part. Figure 5A–C indicates that reflex depression was more intense after kainate alone than after propofol *per se*. Furthermore, although 4–8 propofol administration was inhibiting reflexes, its application after kainate did not intensify the reflex reduction, indeed it either occluded the overall fall in amplitude or actually counteracted the area shrinkage. This phenomenon was readily apparent with 4-h propofol and less manifested with 8-h propofol (Fig. 5A–C). Nevertheless, no additive neurodepression caused by excitotoxicity plus propofol was observed.

We next queried if the propofol-dependent histological preservation, despite innate decrease in network transmission, could shape the output of locomotor networks activated by trains of DR stimuli or NMDA + 5HT. Thus, DR stimulation-evoked fictive locomotion (expressed as alternating oscillations recorded from pairs of VRs) was readily apparent in sham preparations 24 h later (Fig. 6A and B), yet completely absent after kainate with no recovery in the oscillations (bottom traces in Fig. 6A). As expected from previous reports (Taccola *et al.*, 2008), the cumulative depolarization amplitude and area were severely decreased by the previous kainate application (Fig. 6C and D). After application of propofol alone, on the subsequent day, oscillations could still be elicited by DR stimulus trains as indicated in Fig. 6A. In fact, the number of oscillations although decreased was still close to the value detected in sham preparations (Fig. 6B) (Sham vs. Propofol 4 h, Q = 0.262; Sham vs. Propofol 8 h, Q = 0.369; Dunn's method). Despite this preservation of electrically evoked fictive locomotion, no oscillations were present when propofol was applied after kainate (Fig. 6A and B).

Fictive locomotion was also tested by co-applying NMDA (3–6 μM) and 5-HT (10 μM) 24 h after kainate (1 h) followed by propofol (4 or 8 h). Figure 7 illustrates that alternating oscillations were observed the day after application of propofol alone even if their periodicity was longer (Sham vs. Propofol 4 h, U = 66, P = 0.005) and after the 8-h treatment (U = 61, P = 0.001, Mann–Whitney test), the cycle amplitude was also decreased (Sham vs. Propofol 8 h, t_{14} = 3.313, P = 0.005, Student t-test) (Fig. 7A–C). When the 4-h propofol application paradigm was employed after 1-h kainate administration, in 5 out of 10 spinal cords, there was emergence of sporadic oscillations at slow period as exemplified in Fig. 7A (middle panels). This effect was not typical of fictive locomotion and was absent after 8-h propofol following kainate application (Fig. 7A–C).

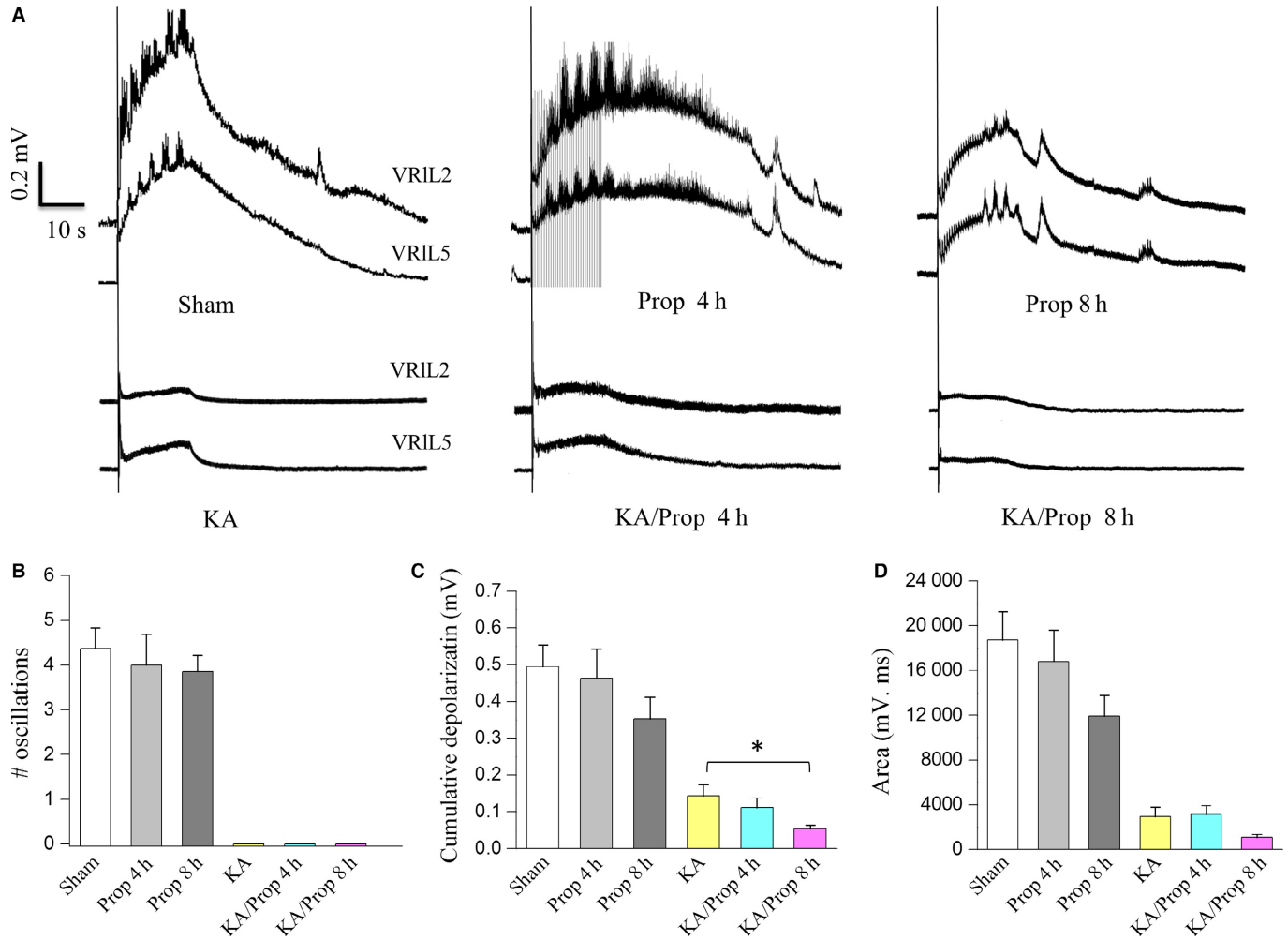

FIG. 6. Changes in electrically induced fictive locomotor oscillations elicited by DR stimuli recorded on day 2 after kainate (1 h) exposure followed by propofol for 4 or 8 h. (A) Representative records of electrically evoked cumulative depolarization of sham (n = 7), propofol applied for 4 h (Prop 4 h, n = 7), propofol applied for 8 h (Prop 8, n = 8), kainate applied for 1 h (KA, n = 11), kainate (1 h) followed by propofol for 4 h (KA/Prop 4 h, n = 10) and kainate (1 h) followed by propofol for 8 h (KA/Prop 8 h, n = 14) protocols. Traces show typical alternating VR cycles between homolateral L2 and L5 motor pools: these oscillations are superimposed over the slowly developing cumulative depolarization due to non-linear summation of synaptic responses (Marchetti *et al.*, 2001). (B) Bar graph representing number of alternating oscillations elicited by DR stimulation. Although propofol alone does not change oscillations, no emergence of oscillations is observed after kainate with or without subsequent application of propofol for 4 or 8 h. (C) Histogram representing significant depression in cumulative depolarization after treating spinal cords with kainate: this effect was unchanged by 4-h propofol (t_{19} = 0.792, P = 0.438) and intensified by 8 h of the same anaesthetic (U = 31, *P = 0.013; Mann–Whitney test). (D) Histogram depicting a decrease in cumulative depolarization area of the same preparations shown in C. Note the significant change in number of oscillations, cumulative depolarization and area of all treated preparations in comparison to sham (H_5 = 51.806, P = <0.001; H_5 = 37.673, P = <0.001; H_5 = 41.110, P = <0.001; Kruskal–Wallis one-way analysis of variance on ranks test, respectively).

Figure 8A summarizes the data involving network rhythmicity that appears when synaptic inhibition is blocked by strychnine and bicuculline (Bracci *et al.*, 1996b). Figure 8A–C shows persistence of bursting 1 day after propofol application even though with smaller amplitude and longer period. When kainate application was followed by propofol (4 h or 8 h), the burst amplitude remained very depressed (t_{13} = 3.087, P = 0.009; U = 4, P = 0.004; Mann–Whitney test), while the periodicity improved in comparison to kainate alone.

Discussion

The principal finding of the present study is the novel demonstration that the anaesthetic propofol induced significant neuroprotection of spinal neurons against excitotoxicity even when administered after the excitotoxic stimulus (i.e. kainate application) had been terminated. This protection was also extended to motoneurons as the number of survivors approached the control level. Using the *in vitro* preparation enabled us testing the proof of principle that propofol might neuroprotect independently from vascular (or peripheral) effects. While these beneficial effects were observed after 24 h from excitotoxic stimulation, they were not, however, associated with significant recovery in locomotor network output, a phenomenon we attributed to the rather slow recovery of motor networks from the depressant effect of propofol.

Effects of propofol per se *on spinal networks*

In line with previous studies (Kotani *et al.*, 2008), we observed that the concentration of propofol used in the present investigation partly depressed polysynaptic transmission (Jewett *et al.*, 1992), potentiated GABA-evoked responses (Adodra & Hales, 1995; Reynolds &

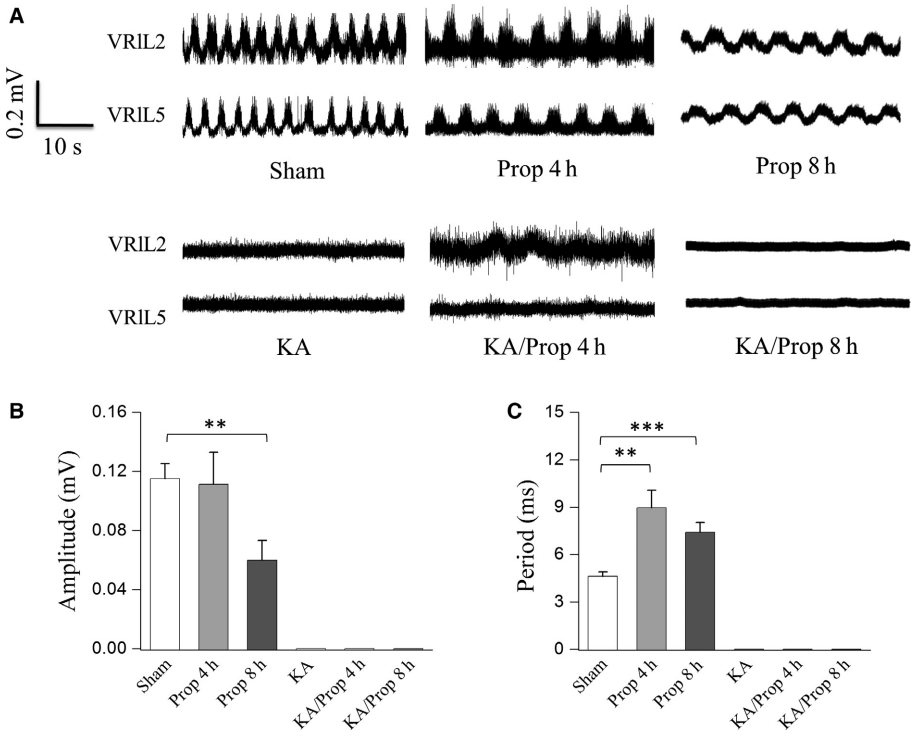

FIG. 7. Changes in chemically induced fictive locomotion after exposure to kainate (1 h) followed by propofol (4 or 8 h). Data recorded on day 2 after treatment. (A) Sample recordings of fictive locomotion induced by NMDA and 5-HT in sham (n = 8), propofol applied for 4 h (Prop 4 h, n = 9), propofol applied for 8 h (Prop 8 h, n = 8), kainate applied for 1 h (KA, n = 6), kainate (1 h) followed by propofol for 4 h (KA/Prop 4 h, n = 10) and kainate (1 h) followed by propofol for 8 h (KA/Prop 8 h, n = 11). Traces show typical alternating VR cycles between homolateral L2 and L5 motor pools. Although smaller in amplitude and slower, these cycles are still present the day after treatment with propofol alone (4 or 8 h). (B, C) Bar graphs illustrate the peak amplitude of oscillatory cycles (B) whose amplitude was decreased after application of propofol (8 h) in comparison to sham (t_{14} = 3.313, $^{**}P$ = 0.005; Student t-test), and period of oscillations (C) has increased by application of propofol for 4 h (U = 66, P = 0.005; Mann–Whitney test) and for 8 h (U = 61, $^{***}P$ = 0.001; Mann–Whitney test). After kainate application, alternating oscillatory cycles irreversibly stopped in most cases. However, 5–15 sporadic oscillations (typically limited to a single VR) could be detected in spinal cord preparations (5/10) after propofol administration for 4 h. No recovery in the preparations treated with propofol for 8 h after kainate exposure (1 h) was found. Note a significant change in all the values of amplitude and period vs. sham (B and C) (H_5 = 38.038, P = <0.001 and H_5 = 40.923, P = 0.001; Kruskal–Wallis one-way analysis of variance on ranks test respectively).

Maitra, 1996) and depressed NMDA-mediated ones (Orser *et al.*, 1995). These effects on GABA or NMDA depolarizations were at least in part attributable to a direct effect on motoneurons as they persisted after block of network activity with TTX. Human studies corroborate this notion as propofol has been shown to reduce spinal motoneuron excitability (Kakinohana *et al.*, 2002; Kammer *et al.*, 2002). Long-term effects by propofol on synaptic transmission investigated over several hours suggested that the reduction in reflex area was perhaps due to a combinatorial phenomenon of facilitated GABA action (that on neonatal spinal neurons is depolarizing, yet inhibitory; Vinay & Jean-Xavier, 2008) plus NMDA receptor antagonism as these receptors contribute to the late component of excitatory transmission onto motoneurons (Evans *et al.*, 1982). It is noteworthy that even prolonged washout of propofol (for at least 16 h) did not fully restore synaptic transmission, although within the 24 h timeframe of the present study, fictive locomotion evoked by DR stimuli or neurochemicals (albeit of slow rate and small intensity) could still be observed together with lack of histochemical damage to spinal networks. It is surprising that details of reversibility of propofol depression on polysynaptic transmission induced by DR stimulation in the rat spinal cord are lacking, although a former study seemed to indicate partial recovery (Matute *et al.*, 2004). Previous experiments have indicated that propofol depresses cumulative depolarization (Matute *et al.*, 2004), a phenomenon consistent with the proposed analgesic action of this drug.

Propofol contrasted excitotoxic damage to spinal networks

In accordance with the view that propofol is neuroprotective against brain ischaemia (Kawaguchi *et al.*, 2005), the present study observed that delayed application of propofol was an effective strategy to largely prevent the development of neuronal damage in all three spinal ROIs and was especially striking in the case of motoneurons. As we found no difference in the histological outcome when propofol was applied for 4 or 8 h, we propose that its neuroprotective effect was exerted during the early phase of secondary injury that involves (within the first few hours) activation of non-apoptotic cell death mechanisms (Kuzhandaivel *et al.*, 2011). The question then arises about the mode of action of propofol. We favour the possibility that propofol enhanced GABA-mediated inhibition and thereby decreased network excitability in a persistent fashion (Jewett *et al.*, 1992). This phenomenon is somewhat reminiscent of the action by the anaesthetic methoxyflurane that depresses network activity by activating background K^+ conductances (Elliott *et al.*, 1992; Sirois *et al.*, 2000) and thus, protects spinal neurons from injury (Shabbir *et al.*, 2015).

Hence, the simplest interpretation is that, regardless of the cellular mode of action of the general anaesthetic drug, intense network depression elicited by either a gas or an i.v. anaesthetic drug can exert largely beneficial actions on spinal networks even when administered following the excitotoxic insult. This notion accords with the

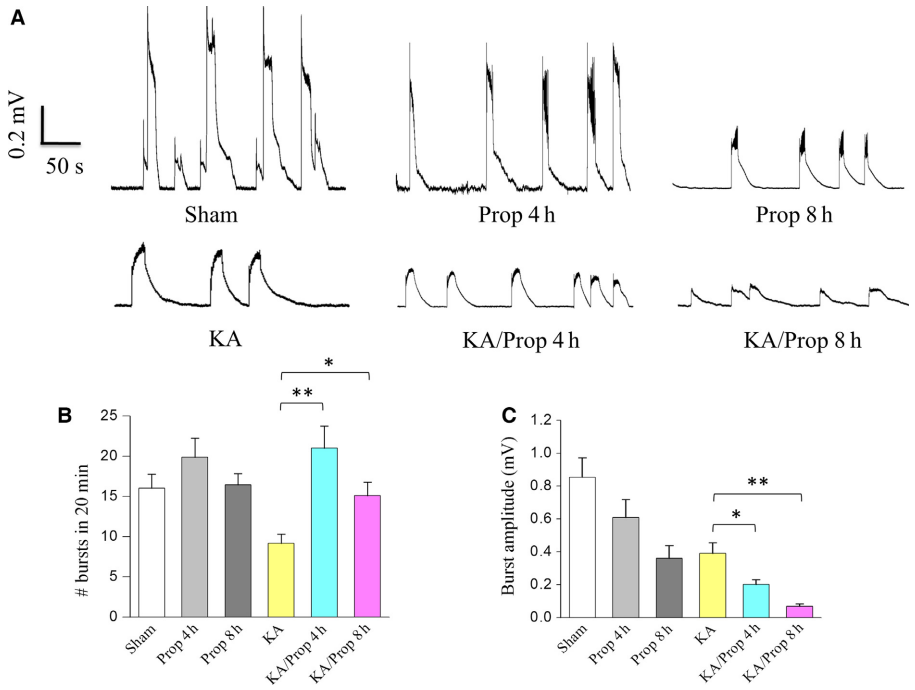

FIG. 8. Disinhibited bursts recorded on day 2 after kainate (1 h) followed by propofol (4 or 8 h) treatment. (A) Sample recordings obtained from sham (n = 8), propofol applied for 4 h (Prop 4 h; n = 9), propofol applied for 8 h (Prop 8; n = 7), kainate applied for 1 h (KA; n = 7), kainate (1 h) followed by propofol for 4 h (KA/Prop 4 h; n = 9), and kainate (1 h) followed by propofol for 8 h (KA/Prop 8 h; n = 9). After kainate or propofol alone bursts are smaller, although no further decrease is observed when these two treatments were sequentially applied (A–C). Note significant recovery in number of bursts during 20-min epoch after kainate followed by propofol treatment both for 4 and 8 h (t_{14} = −3.622, **P = 0.003 and t_{14} = −2.793, *P = 0.014 respectively) in comparison to kainate alone, although their corresponding amplitude was significantly reduced after propofol for 4 and 8 h (t_{13} = 3.087, P = 0.009; U = 4, P = 0.004; Mann–Whitney test respectively). Note a significant change in number of bursts (in 20 min) and burst amplitude in treated preparations in comparison to sham ($F_{5,43}$ = 4.100, P = 0.004, one-way analysis of variance test; H_5 = 36.563, P = <0.001, Kruskal–Wallis one-way analysis of variance on ranks test, respectively).

observations that neuronal damages after kainate are not immediately caused by necrotic death as they emerge during the first few hours after washout of this excitotoxic drug and concern a certain populations of neurons only (Kuzhandaivel *et al.*, 2010). Testing other general anaesthetics like chloralose or barbiturates that are not clinically used would also pose problems of data interpretation due to the rather slow recovery of the *in vitro* spinal cord from their effects even when applied for relatively short times (Bagust & Kerkut, 1981).

It is also noteworthy that pharmacological block of GABA-induced inhibition largely aggravates kainate-evoked damage (Bajrektarevic & Nistri, 2016). The propofol-mediated antagonism of NMDA responses was less likely to contribute to neuroprotection because we have previously shown that NMDA receptor blockers *per se* are not efficacious in this model (Margaryan *et al.*, 2010). The present results suggest that depression of network excitability is an important strategy for damage limitation even after the excitotoxic stimulus has been removed. Conversely, decrease in the release of the excitatory transmitter glutamate by applying for instance riluzole is far less effective (Sámano *et al.*, 2012) perhaps because significant background release of glutamate continues (Mazzone & Nistri, 2011) to support ongoing cell death processes.

Network function after kainate and propofol

Twenty-four hours after kainate followed by propofol application, there was no recovery in integrated network function, in particular cumulative depolarization evoked by DR stimuli, or fictive locomotion induced by electrical pulses or NMDA + 5-HT. This was not totally unexpected in view of the long-lasting depression evoked by propofol *per se*: there was, however, no additive depression by kainate and propofol on synaptic transmission, indicating that further deterioration had been blocked. In fact, disinhibited bursting that reflects the intrinsic rhythmicity of spinal networks (Streit, 1993; Bracci *et al.*, 1996a) showed improved periodicity when 4-h propofol administration followed kainate washout. The simplest interpretation is that, when network output required activation of a limited circuitry (Bracci *et al.*, 1996b), the protective action of propofol was manifested more efficiently than over a very wide locomotor network with complex connections extending over several segments (Kiehn, 2006, 2016) and, therefore, with a much higher probability of failure. These observations are consistent with our view (Sámano *et al.*, 2016) that spinal networks operate in a condition of criticality (Massobrio *et al.*, 2015; Valverde *et al.*, 2015), so that even moderate cell losses trigger a major functional deficit. Thus, we propose that there is a minimal network membership necessary to express locomotor patterns (Kuzhandaivel *et al.*, 2011) below which locomotor output is lost.

Following the pioneer clinical work by Kay & Rolly (1977) who used propofol for rapid induction of anaesthesia in man, this drug is widely used in surgery because of the relatively fast recovery of patient's consciousness after the end of i.v. administration (Grundmann *et al.*, 2001): this phenomenon is normally assessed as awareness ("eye opening") rather than locomotor function, and is apparently due to the drug fast redistribution to body fat stores rather than metabolic inactivation (Mirski *et al.*, 1995). In fact, in humans, the propofol plasma half-life is about 5 h, indicating slow drug elimination with delayed concentration peaks perhaps responsible for potential changes in cardiovascular activity (Kay *et al.*,

1986). Earlier investigations report that patients may experience side effects even 24–48 h after a single 10-min administration of propofol (Sanders *et al.*, 1991). Anaesthesiological studies also demonstrate that full motor recovery in humans is incomplete for many hours after propofol (Münte *et al.*, 2001; Haavisto & Kauranen, 2002), leading to the general advice that dizziness and drowsiness may persist for 24 h and to caution against driving (http://www.rxlist.com/diprivan-drug/patient-images-side-effects.htm). Thus, our interpretation is that poor recovery of *in vitro* network function after kainate and propofol was not due to neuronal damage but to lingering consequences of long-lasting propofol administration. One limitation of the present model is the length of *in vitro* survival that is restricted to 24 h, as at later times, tissue deterioration and loss of locomotor network activity emerge as earlier reported by Kerkut & Bagust (1995). This condition makes it difficult to extend the timeframe of our experimental observations to support our view about the late consequences of propofol administration.

In conclusions, recent clinical reports suggest that general anaesthetics may be neuroprotective for the spinal cord especially during aortic surgery when blood supply to the spinal cord is compromised (Kakinohana, 2014). Our current data support the notion that a general anaesthetic applied even after an excitotoxic stimulus to the *in vitro* spinal cord can provide large neuroprotection of locomotor networks (Shabbir *et al.*, 2015; Bajrektarevic & Nistri, 2016), whose functional recovery might depend on the actual pharmacokinetic characteristics of the anaesthetic used. It should be interesting to extent these studies to *in vivo* animals to better identify their translational impact. Furthermore, multicentre clinical trials will be required to find out whether propofol should be the preferred drug of choice for early management of traumatic SCI apart from its use for spinal cord ischaemia (Kakinohana, 2014).

Supporting Information

Additional supporting information can be found in the online version of this article:

Fig. S1. Scheme of experimental procedures.

Fig. S2. (A) Regions of interest (ROIs) for immunohistochemical analysis.

Fig. S3. Histological neuroprotection of motoneurons (SMI32) by propofol (Prop; 5 μM) against kainate (KA; 100 μM) evoked excitotoxicity.

Acknowledgements

This work was supported by an intramural SISSA grant.

Abbreviations

5-HT, 5-hydroxytryptamine; AMPA, α-amino-3-hydroxy-5-methyl-4-isoxazolepropionic acid; ANOVA, analysis of variance; ChAT, choline acetyltransferase; DAPI, 4′,6-diamidino-2-phenylindole; DR, dorsal root; GABA, γ aminobutyric acid; i.v., intravenous; KA, kainate; L, lumbar; NeuN, neuronal-specific nuclear protein antibody; NIH, National Institute of Health; NMDA, N-methyl-D-aspartate; Prop, propofol; ROI, region of interest; S100, subgroup of Ca^{2+}-binding proteins marker; SCI, spinal cord injury; SEM, standard error of the mean; SMI32, neurofilament H non-phosphorylated antibody; TTX, tetrodotoxin; VR, ventral root.

References

Acton, Q.A. (2011) Chapter 3: propofol. In Acton, Q.A. (Ed), *General Anesthetics: Advances in Research and Application*. QA Scholarly Editions, Atlanta, GA, USA, pp. 30–95.

Adodra, S. & Hales, T.G. (1995) Potentiation, activation and blockade of $GABA_A$ receptors of clonal murine hypothalamic GT1-7 neurones by propofol. *Brit. J. Pharmacol.*, **115**, 953–960.

Ansley, D.M., Lee, J., Godin, D.V., Garnett, M.E. & Qayumi, A.K. (1998) Propofol enhances red cell antioxidant capacity in swine and humans. *Can. J. Anaesth.*, **45**, 233–239.

Baars, J.H., Dangel, C., Herold, K.F., Hadzidiakos, D.A. & Rehberg, B. (2006) Suppression of the human spinal H-reflex by propofol: a quantitative analysis. *Acta Anaesth. Scand.*, **50**, 193–200.

Bagust, J. & Kerkut, G.A. (1981) Observations on the use of anaesthetics in the preparation of in vitro CNS material. *Neuropharmacology*, **20**, 73–88.

Bajrektarevic, D. & Nistri, A. (2016) Delayed application of the anesthetic propofol contrasts the neurotoxic effects of kainate on rat organotypic spinal slice cultures. *Neurotoxicology*, **54**, 1–10.

Baranauskas, G. & Nistri, A. (1995) Membrane potential oscillations of neonatal rat spinal motoneurons evoked by electrical stimulation of dorsal root fibres. *Eur. J. Neurosci.*, **7**, 2403–2408.

Bianchetti, E., Mladinic, M. & Nistri, A. (2013) Mechanisms underlying cell death in ischemia-like damage to the rat spinal cord *in vitro*. *Cell Death Dis.*, **4**, e707–e718.

Bracci, E., Ballerini, L. & Nistri, A. (1996a) Spontaneous rhythmic bursts induced by pharmacological block of inhibition in lumbar motoneurons of the neonatal rat spinal cord. *J. Neurophysiol.*, **75**, 640–647.

Bracci, E., Ballerini, L. & Nistri, A. (1996b) Localization of rhythmogenic networks responsible for spontaneous bursts induced by strychnine and bicuculline in the rat isolated spinal cord. *J. Neurosci.*, **16**, 7063–7076.

Burgoyne, L.A. (1999) The mechanisms of pyknosis: hypercondensation and death. *Exp. Cell Res.*, **248**, 214–222.

Cifra, A., Mazzone, G.L., Nani, F., Nistri, A. & Mladinic, M. (2012) Postnatal developmental profile of neurons and glia in motor nuclei of the brainstem and spinal cord, and its comparison with organotypic slice cultures. *Dev. Neurobiol.*, **72**, 1140–1160.

Cifra, A., Mazzone, G.L. & Nistri, A. (2013) Riluzole: what it does to spinal and brainstem neurons and how it does it. *Neuroscientist*, **19**, 137–144.

David, K.K., Andrabi, S.A., Dawson, T.M. & Dawson, V.L. (2009) Parthanatos, a messenger of death. *Front Biosci.*, **14**, 1116–1128.

Dobkin, B.H. & Havton, L.A. (2004) Basic advances and new avenues in therapy of spinal cord injury. *Annu. Rev. Med.*, **55**, 255–282.

Eckle, V.S., Rudolph, U., Antkowiak, B. & Grasshoff, C. (2015) Propofol modulates phasic and tonic GABAergic currents in spinal ventral horn interneurones. *Brit. J. Anaesth.*, **114**, 491–498.

Elliott, J.R., Elliott, A.A., Harper, A.A. & Winpenny, J.P. (1992) Effects of general anaesthetics on neuronal sodium and potassium channels. *Gen. Pharmacol.*, **23**, 1005–1011.

Engelhard, K., Werner, C., Eberspächer, E., Pape, M., Stegemann, U., Kellermann, K., Hollweck, R., Hutzler, P. *et al.* (2004b) Influence of propofol on neuronal damage and apoptotic factors after incomplete cerebral ischemia and reperfusion in rats: a long-term observation. *Anesthesiology*, **101**, 912–917.

Evans, R.H. & Smith, D.A. (1982) Effect of urethane on synaptic and amino acid-induced excitation in isolated spinal cord preparations. *Neuropharmacology*, **21**, 857–860.

Evans, R.H., Francis, A.A., Jones, A.W., Smith, D.A. & Watkins, J.C. (1982) The effects of a series of omega-phosphonic alpha-carboxylic amino acids on electrically evoked and excitant amino acid-induced responses in isolated spinal cord preparations. *Brit. J. Pharmacol.*, **75**, 65–75.

Furlan, J.C., Sakakibara, B.M., Miller, W.C. & Krassioukov, A.V. (2013) Global incidence and prevalence of traumatic spinal cord injury. *Can. J. Neurol. Sci.*, **40**, 456–464.

Galluzzi, L., Maiuri, M.C., Vitale, I., Zischka, H., Castedo, M., Zitvogel, L. & Kroemer, G. (2007) Cell death modalities: classification and pathophysiological implications. *Cell Death Differ.*, **14**, 1237–1243.

Galluzzi, L., Vitale, I., Abrams, J.M., Alnemri, E.S., Baehrecke, E.H., Blagosklonny, M.V., Dawson, T.M., Dawson, V.L. *et al.* (2012) Molecular definitions of cell death subroutines: recommendations of the Nomenclature Committee on Cell Death 2012. *Cell Death Differ.*, **19**, 107–120.

Gelb, A.W., Bayona, N.A., Wilson, J.X. & Cechetto, D.F. (2002) Propofol anesthesia compared to awake reduces infarct size in rats. *Anesthesiology*, **96**, 1183–1190.

Gredell, J.A., Turnquist, P.A., Maciver, M.B. & Pearce, R.A. (2004) Determination of diffusion and partition coefficients of propofol in rat brain tissue: implications for studies of drug action in vitro. *Brit. J. Anaesth.*, **93**, 810–817.

Grundmann, U., Silomon, M., Bach, F., Becker, S., Bauer, M., Larsen, B. & Kleinschmidt, S. (2001) Recovery profile and side effects of remifentanil-

based anaesthesia with desflurane or propofol for laparoscopic cholecystectomy. *Acta Anaesth. Scand.*, **45**, 320–326.
Haavisto, E. & Kauranen, K. (2002) Psychomotor performance after short-term anaesthesia. *Eur. J. Anaesth.*, **19**, 436–441.
Hales, T.G. & Lambert, J.J. (1991) The actions of propofol on inhibitory amino acid receptors of bovine adrenomedullary chromaffin cells and rodent central neurones. *Brit. J. Pharmacol.*, **104**, 619–628.
Hans, P., Deby-Dupont, G., Deby, C., Pieron, F., Verbesselt, R., Franssen, C. & Lamy, M. (1997) Increase in antioxidant capacity of plasma during propofol anesthesia. *J. Neurosurg. Anesth.*, **9**, 234–236.
Ito, H., Watanabe, Y., Isshiki, A. & Uchino, H. (1999) Neuroprotective properties of propofol and midazolam, but not pentobarbital, on neuronal damage induced by forebrain ischemia, based on the $GABA_A$ receptors. *Acta Anaesth. Scand.*, **43**, 153–162.
Jewett, B.A., Gibbs, L.M., Tarasiuk, A. & Kendig, J.J. (1992) Propofol and barbiturate depression of spinal nociceptive neurotransmission. *Anesthesiology*, **77**, 1148–1154.
Kakinohana, M. (2014) Protective effects of anesthetics on the spinal cord. *Curr. Pharm. Des.*, **20**, 5744–5750.
Kakinohana, M., Fuchigami, T., Nakamura, S., Kawabata, T. & Sugahara, K. (2002) Propofol reduces spinal motor neuron excitability in humans. *Anesth. Analg.*, **94**, 1586–1588.
Kammer, T., Rehberg, B., Menne, D., Wartenberg, H.C., Wenningmann, I. & Urban, B.W. (2002) Propofol and sevoflurane in subanesthetic concentrations act preferentially on the spinal cord: evidence from multimodal electrophysiological assessment. *Anesthesiology*, **97**, 1416–1425.
Kawaguchi, M., Furuya, H. & Patel, P.M. (2005) Neuroprotective effects of anesthetic agents. *J. Anesth.*, **19**, 150–156.
Kay, B. & Rolly, G. (1977) I.C.I. 35868, a new intravenous induction agent. *Acta Anaesth. Belg.*, **28**, 303–316.
Kay, N.H., Sear, J.W., Uppington, J., Cockshott, I.D. & Douglas, E.J. (1986) Disposition of propofol in patients undergoing surgery. A comparison in men and women. *Brit. J. Anaesth.*, **58**, 1075–1079.
Kerkut, G.A. & Bagust, J. (1995) The isolated mammalian spinal cord. *Prog. Neurobiol.*, **46**, 1–48.
Kiehn, O. (2006) Locomotor circuits in the mammalian spinal cord. *Annu. Rev. Neurosci.*, **29**, 279–306.
Kiehn, O. (2016) Decoding the organization of spinal circuits that control locomotion. *Nat. Rev. Neurosci.*, **17**, 224–238.
Kotani, Y., Shimazawa, M., Yoshimura, S., Iwama, T. & Hara, H. (2008) The experimental and clinical pharmacology of propofol, an anesthetic agent with neuroprotective properties. *CNS Neurosci. Ther.*, **14**, 95–106.
Kungys, G., Kim, J., Jinks, S.L., Atherley, R.J. & Antognini, J.F. (2009) Propofol produces immobility via action in the ventral horn of the spinal cord by a GABAergic mechanism. *Anesth. Analg.*, **108**, 1531–1537.
Kuzhandaivel, A., Nistri, A. & Mladinic, M. (2010) Kainate-mediated excitotoxicity induces neuronal death in the rat spinal cord in vitro via a PARP-1 dependent cell death pathway (Parthanatos). *Cell. Mol. Neurobiol.*, **30**, 1001–1012.
Kuzhandaivel, A., Nistri, A., Mazzone, G.L. & Mladinic, M. (2011) Molecular mechanisms underlying cell death in spinal networks in relation to locomotor activity after acute injury in vitro. *Front. Cell. Neurosci.*, **5**, 9.
Mandir, A.S., Poitras, M.F., Berliner, A.R., Herring, W.J., Guastella, D.B., Feldman, A., Poirier, G.G., Wang, Z.Q. *et al.* (2000) NMDA but not non-NMDA excitotoxicity is mediated by Poly(ADP-ribose) polymerase. *J. Neurosci.*, **20**, 8005–8011.
Marchetti, C., Beato, M. & Nistri, A. (2001) Alternating rhythmic activity induced by dorsal root stimulation in the neonatal rat spinal cord in vitro. *J. Physiol.*, **530**, 105–112.
Margaryan, G., Mattioli, C., Mladinic, M. & Nistri, A. (2010) Neuroprotection of locomotor networks after experimental injury to the neonatal rat spinal cord in vitro. *Neuroscience*, **165**, 996–1010.
Massobrio, P., Pasquale, V. & Martinoia, S. (2015) Self-organized criticality in cortical assemblies occurs in concurrent scale-free and small-world networks. *Sci. Rep.*, **5**, 10578.
Matute, E., Rivera-Arconada, I. & López-García, J.A. (2004) Effects of propofol and sevoflurane on the excitability of rat spinal motoneurones and nociceptive reflexes in vitro. *Brit. J. Anaesth.*, **93**, 422–427.
Mazzone, G.L. & Nistri, A. (2011) Electrochemical detection of endogenous glutamate release from rat spinal cord organotypic slices as a real-time method to monitor excitotoxicity. *J. Neurosci. Meth.*, **197**, 128–132.
Mazzone, G.L., Margaryan, G., Kuzhandaivel, A., Nasrabady, S.E., Mladinic, M. & Nistri, A. (2010) Kainate-induced delayed onset of excitotoxicity with functional loss unrelated to the extent of neuronal damage in the in vitro spinal cord. *Neuroscience*, **168**, 451–462.
Mirski, M.A., Muffelman, B., Ulatowski, J.A. & Hanley, D.F. (1995) Sedation for the critically ill neurologic patient. *Crit. Care Med.*, **23**, 2038–2053.
Münte, S., Münte, T.F., Kuche, H., Osthaus, A., Herzog, T., Heine, J., Leuwer, M. & Piepenbrock, S. (2001) General anesthesia for interventional neuroradiology: propofol versus isoflurane. *J. Clin. Anesth.*, **13**, 186–192.
Nasrabady, S.E., Kuzhandaivel, A., Mladinic, M. & Nistri, A. (2011a) Effects of 6(5H)-phenanthridinone, an inhibitor of poly(ADP-ribose)polymerase-1 activity (PARP-1), on locomotor networks of the rat isolated spinal cord. *Cell. Mol. Neurobiol.*, **31**, 503–508.
Nasrabady, S.E., Kuzhandaivel, A. & Nistri, A. (2011b) Studies of locomotor network neuroprotection by the selective poly(ADP-ribose) polymerase-1 inhibitor PJ-34 against excitotoxic injury to the rat spinal cord in vitro. *Eur. J. Neurosci.*, **33**, 2216–2227.
Nasrabady, S.E., Kuzhandaivel, A., Akrami, A., Bianchetti, E., Milanese, M., Bonanno, G. & Nistri, A. (2012) Unusual increase in lumbar network excitability of the rat spinal cord evoked by the PARP-1 inhibitor PJ-34 through inhibition of glutamate uptake. *Neuropharmacology*, **63**, 415–426.
Nistri, A. (2012) An innovative spinal cord injury model for the study of locomotor networks. *Eur. J. Phys. Rehab. Med.*, **48**, 91–98.
Orser, B.A., Bertlik, M., Wang, L.Y. & MacDonald, J.F. (1995) Inhibition by propofol (2,6 di-isopropylphenol) of the N-methyl-D-aspartate subtype of glutamate receptor in cultured hippocampal neurones. *Brit. J. Pharmacol.*, **116**, 1761–1768.
Park, E., Velumian, A.A. & Fehlings, M.G. (2004) The role of excitotoxicity in secondary mechanisms of spinal cord injury: a review with an emphasis on the implications for white matter degeneration. *J. Neurotrauma*, **21**, 754–774.
Pittman, J.E., Sheng, H., Pearlstein, R., Brinkhous, A., Dexter, F. & Warner, D.S. (1997) Comparison of the effects of propofol and pentobarbital on neurologic outcome and cerebral infarct size after temporary focal ischemia in the rat. *Anesthesiology*, **87**, 1139–1144.
Reynolds, J.N. & Maitra, R. (1996) Propofol and flurazepam act synergistically to potentiate $GABA_A$ receptor activation in human recombinant receptors. *Eur. J. Pharmacol.*, **314**, 151–156.
Rossignol, S., Schwab, M., Schwartz, M. & Fehlings, M.G. (2007) Spinal cord injury: time to move? *J. Neurosci.*, **27**, 11782–11792.
Rowland, J.W., Hawryluk, G.W., Kwon, B. & Fehlings, M.G. (2008) Current status of acute spinal cord injury pathophysiology and emerging therapies: promise on the horizon. *Neurosurg. Focus*, **25**, E2.
Sahin, M., Gullu, H., Peker, K., Sayar, I., Binici, O. & Yildiz, H. (2015) Does the intrathecal propofol have a neuroprotective effect on spinal cord ischemia? *Neural Regen. Res.*, **10**, 1825–1829.
Sámano, C., Nasrabady, S.E. & Nistri, A. (2012) A study of the potential neuroprotective effect of riluzole on locomotor networks of the neonatal rat spinal cord in vitro damaged by excitotoxicity. *Neuroscience*, **222**, 356–365.
Sámano, C., Kaur, J. & Nistri, A. (2016) A study of methylprednisolone neuroprotection against acute injury to the rat spinal cord in vitro. *Neuroscience*, **315**, 136–149.
Sanders, L.D., Clyburn, P.A., Rosen, M. & Robinson, J.O. (1991) Propofol in short gynaecological procedures. Comparison of recovery over 2 days after anaesthesia with propofol or thiopentone as sole anaesthetic agent. *Anaesthesia*, **46**, 451–455.
Sekhon, L.H. & Fehlings, M.G. (2001) Epidemiology, demographics, and pathophysiology of acute spinal cord injury. *Spine*, **15**, S2–S12.
Shabbir, A., Bianchetti, E. & Nistri, A. (2015) The volatile anesthetic methoxyflurane protects motoneurons against excitotoxicity in an in vitro model of rat spinal cord injury. *Neuroscience*, **285**, 269–280.
Sirois, J.E., Lei, Q., Talley, E.M., Lynch, C. 3rd & Bayliss, D.A. (2000) The TASK-1 two-pore domain K^+ channel is a molecular substrate for neuronal effects of inhalation anesthetics. *J. Neurosci.*, **20**, 6347–6354.
Stratford, N. & Murphy, P. (1998) Antioxidant activity of propofol in blood from anaesthetized patients. *Eur. J. Anaesth.*, **15**, 158–160.
Streit, J. (1993) Regular oscillations of synaptic activity in spinal networks in vitro. *J. Neurophysiol.*, **70**, 871–878.
Taccola, G. & Nistri, A. (2006a) Fictive locomotor patterns generated by tetraethylammonium application to the neonatal rat spinal cord in vitro. *Neuroscience*, **137**, 659–670.
Taccola, G., Margaryan, G., Mladinic, M. & Nistri, A. (2008) Kainate and metabolic perturbation mimicking spinal injury differentially contribute to early damage of locomotor networks in the in vitro neonatal rat spinal cord. *Neuroscience*, **155**, 538–555.
Valverde, S., Ohse, S., Turalska, M., West, B.J. & Garcia-Ojalvo, J. (2015) Structural determinants of criticality in biological networks. *Front. Physiol.*, **6**, 127.

Velly, L.J., Guillet, B.A., Masmejean, F.M., Nieoullon, A.L., Bruder, N.J., Gouin, F.M. & Pisano, P.M. (2003) Neuroprotective effects of propofol in a model of ischemic cortical cell cultures: role of glutamate and its transporters. *Anesthesiology*, **99**, 368–375.

Vinay, L. & Jean-Xavier, C. (2008) Plasticity of spinal cord locomotor networks and contribution of cation-chloride cotransporters. *Brain Res. Rev.*, **57**, 103–110.

Wakita, M., Kotani, N., Nonaka, K., Shin, M.C. & Akaike, N. (2013) Effects of propofol on GABAergic and glutamatergic transmission in isolated hippocampal single nerve-synapse preparations. *Eur. J. Pharmacol.*, **718**, 63–73.

Xu, T.L. (1999) Gamma-aminobutyric acid-induced responses in acutely dissociated neurons from the rat sacral dorsal commissural nucleus. *J. Auton. Nerv. Syst.*, **75**, 156–163.

Young, Y., Menon, D.K., Tisavipat, N., Matta, B.F. & Jones, J.G. (1997) Propofol neuroprotection in a rat model of ischaemia reperfusion injury. *Eur. J. Anaesth.*, **14**, 320–326.

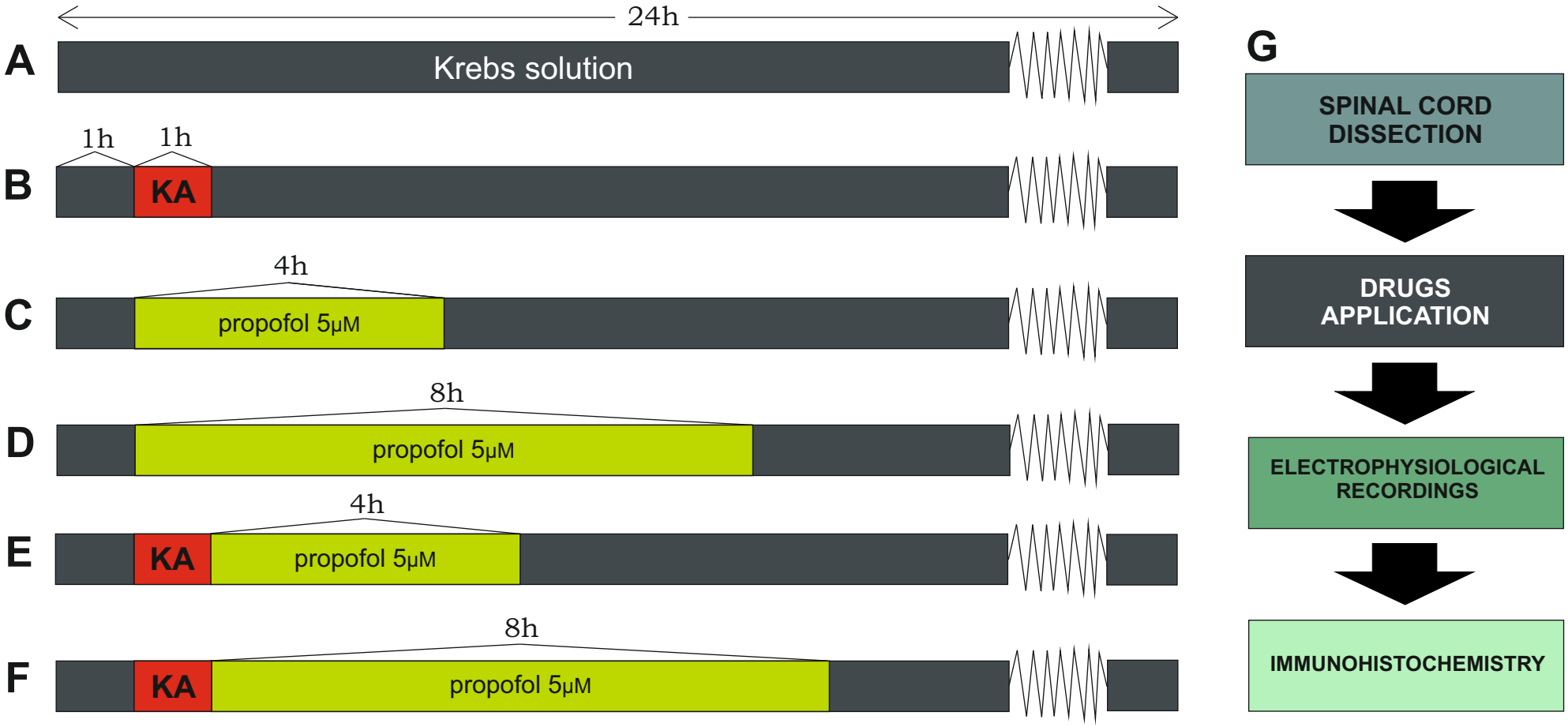

Supplemental Fig. 1. Scheme of experimental procedures. (A-F) Schematic diagrams to illustrate the timing of the different protocols of drug application and (G) related processing. All experimental groups were run in parallel: (A) sham, (B) kainate (KA; 100 µM), (C) 4-hour propofol, (D) 8-hour propofol, (E) 4-hour propofol treatment after kainate and (F) 8-hour propofol treatment after kainate.

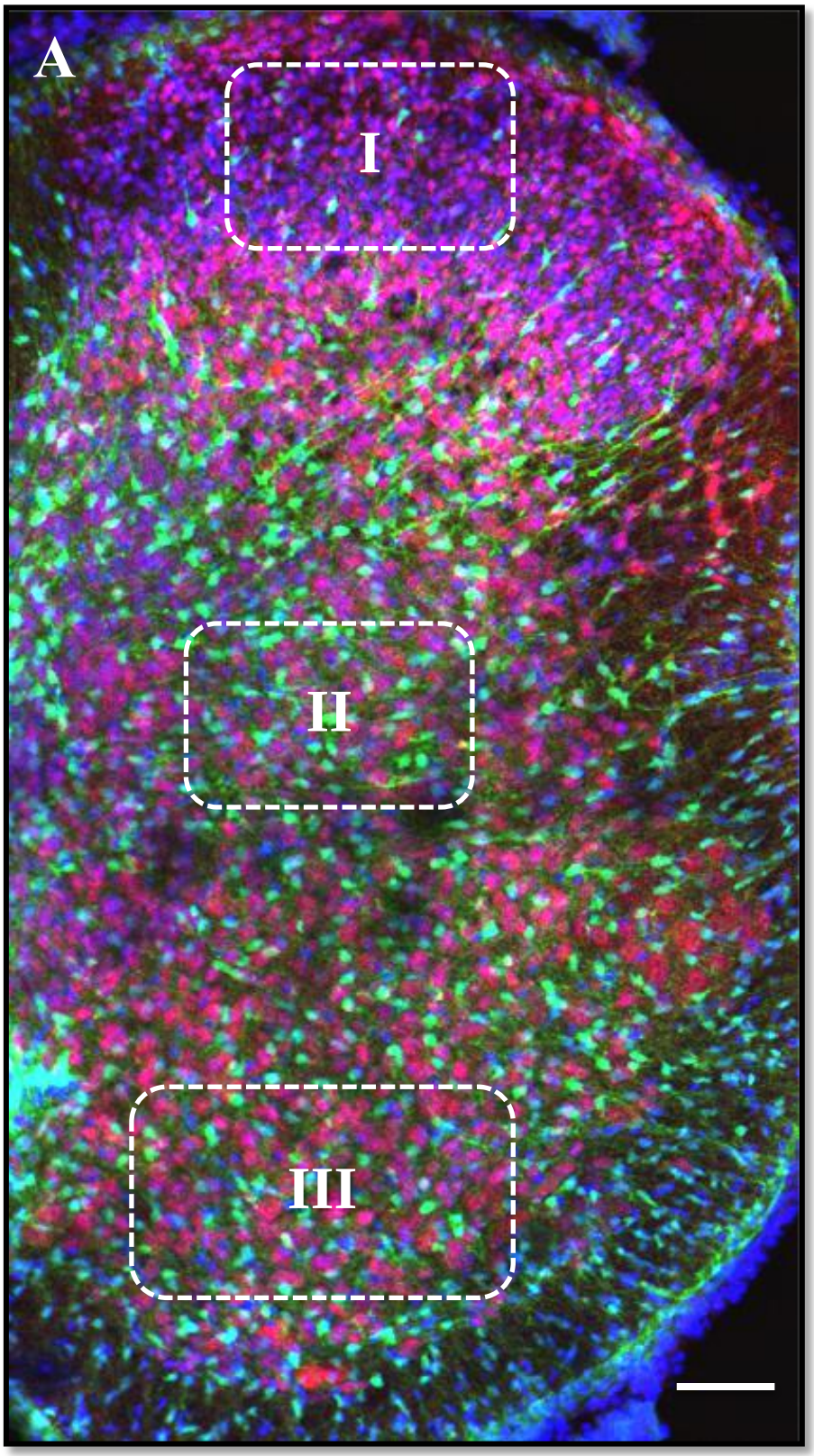

Supplemental Fig. 2. (A) Regions of interest (ROIs) for immunohistochemical analysis. Cross section of rat spinal cord to show spinal ROIs selected for analysis: (I) dorsal horn, (II) central area, (III) ventral horn. Anti-NeuN antibodies were used to mark neurons (red), whereas anti-S100B antibodies were used to mark astrocytes (green). Cell nuclei were marked with fluorescent stain 4',6-diamidino-2-phenylindole (DAPI, blue). Scale bar: 100 µm. **(B)** Examples of pyknotic cells in the dorsal horn of the rat spinal cord in vitro following transient (1 h) application of excitotoxic glutamatergic agonist kainate. Only DAPI staining was used.

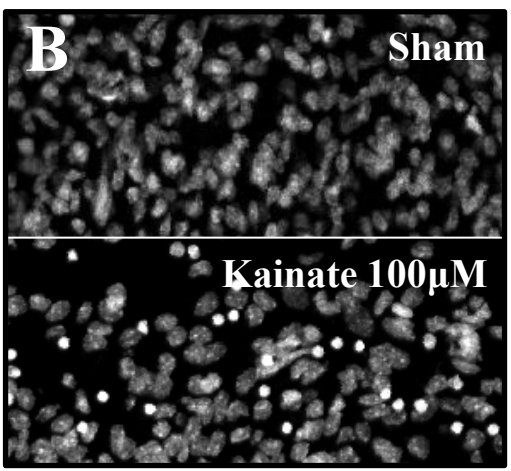

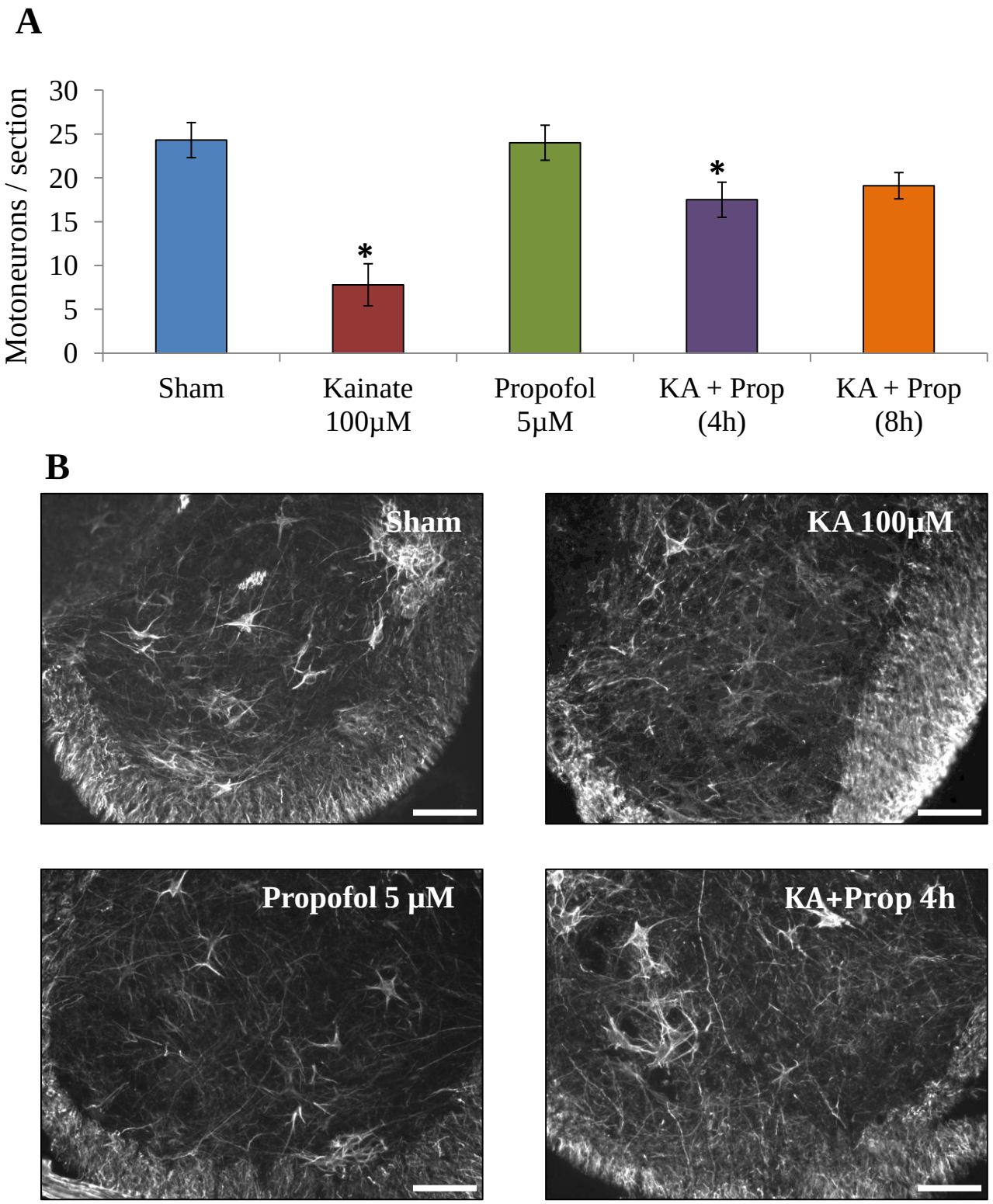

Supplementary Fig. 3. Histological neuroprotection of motoneurons (SMI32) by propofol (Prop; 5µM) against kainate (KA; 100µM) evoked excitotoxicity. (A) Histogram showing number of motoneurons in ventral ROI. Note significantly larger number of motoneurons from samples treated with propofol for 4 or 8 h after kainate versus sham or kainate alone. Thus, by using a two-tailed Student's *t*-test, the observed significance level for KA+Prop 4h vs KA alone was P=0.002 (t_{17}=3.693) and for KA+Prop 4h vs sham, P=0.021 (t_{24}=-2.487). When comparing KA+Prop 8h vs KA alone with the same test, the significance level was P=0.003 (t_{19}=3.538), and for KA+Prop 8h vs sham P=0.003 (t_{26}=2.351). Data are the average from 10-15 sections of 3-5 rat spinal cords and are represented as mean ± SEM. Stars represent a significant difference between groups (for more details see Material and Methods section). (B) Examples of SMI32 immunopositive cells using such protocols. Scale bar: 100 µm. For paradigms of drug applications see Supplemental Fig. 1.

EJN European Journal of Neuroscience FENS Federation of European Neuroscience Societies

Nicotine-mediated neuroprotection of rat spinal networks against excitotoxicity

Journal:	*European Journal of Neuroscience*
Manuscript ID	EJN-2017-09-24941
Manuscript Type:	Research Report
Date Submitted by the Author:	14-Sep-2017
Complete List of Authors:	Kaur, Jaspreet; SISSA, Neurobiology Rauti, Rossana; SISSA, Neurobiology Nistri, Andrea; SISSA, Neurobiology;
Key Words:	motoneuron, kainic acid, nicotinic receptor, locomotor network, spinal reflexes

Section: Clinical and Translational Neuroscience

Nicotine-mediated neuroprotection of rat spinal networks against excitotoxicity

Jaspreet Kaur[a], Rossana Rauti[a], Andrea Nistri[a]

[a]Department of Neuroscience, International School for Advanced Studies (SISSA), via Bonomea, 265, 34136 Trieste, Italy.

Correspondence to: Prof. Andrea Nistri, SISSA, Via Bonomea 265, 34136 Trieste, Italy; e-mail: nistri@sissa.it. tel. +39 040 3787718; fax +39 040 3787702

Email addresses: jaspreetkaur1306@gmail.com (Jaspreet Kaur), rrauti@sissa.it (Rossana Rauti), nistri@sissa.it (Andrea Nistri).

Running title: nicotine neuroprotection

Total number of pages = 35

Number of figures = 14+4 Supplemental Figs.

Number of words (i) in whole manuscript = 12,597

(ii) in abstract = 247

Keywords: motoneuron; kainic acid; nicotinic receptor; locomotor networks; spinal reflexes

Abstract

Activation of neuronal nicotinic acetylcholine receptors (nAChRs) by nicotine is reported to protect brain neurons from glutamate excitotoxicity. We inquired whether a similar phenomenon can occur in the rat isolated spinal cord (or spinal slice culture) challenged by a transient (1 h) application of kainate (a powerful glutamate receptor agonist) to induce excitotoxicity mimicking spinal injury in vitro. We recorded spinal reflexes and fictive locomotion generated by the locomotor central pattern generator before and 24 h after applying kainate. We also monitored network activity with Ca^{2+} imaging and counted neurons and glia with

immunohistochemical methods. In control conditions nicotine (1 μM; 4 h) depressed reflexes and fictive locomotion with slow recovery and no apparent neurotoxicity at 24 h although synchronous Ca^{2+} transients appeared in slice cultures. Kainate nearly halved neuron numbers (while sparing glia), decreased reflexes and Ca^{2+} transients, and suppressed fictive locomotion. When nicotine was applied (4 h) after washout of kainate, fictive locomotor cycles appeared 24 h later though with low periodicity, and significant protection of neurons, including motoneurons, was observed. Nicotine applied together with kainate and maintained for further 4 h yielded better neuroprotection, improved fictive locomotion expression, and reversed the depression of Ca^{2+} transients. nAChR antagonists did not intensify kainate neurotoxicity and inhibited the neuroprotective effects of nicotine. These data suggest that nicotine was efficacious to limit histological and functional excitotoxic damage probably because it activated and then desensitized nAChRs on excitatory and inhibitory network neurons to prevent triggering intracellular cell death pathways.

Introduction

The functional role of neuronal nicotinic acetylcholine receptors (nAChRs) was first observed at the motoneuron-Renshaw cell synapse, thus making the spinal cord exemplary for investigating the expression of nAChRs previously studied on peripheral tissues only (Eccles et al., 1954). nAChRs (α4β2 and α7 subtypes) are widely expressed in the dorsal (Kiyosawa et al., 2001; Khan et al., 2003; Genzen & McGehee, 2003; 2005; Takeda et al., 2007) and ventral horns (Roth & Berg, 2003; Nakamizo et al., 2005). These receptors mediate cation fluxes responsible for depolarization and firing, although these phenomena are attenuated by receptor desensitization (Fenster et al., 1999). There are also similar intracellular nAChRs on the outer membrane of mitochondria to control mitochondrial activity and energy supply (Skok et al., 2016). Mitochondrial receptors can be activated by nicotine that readily passes across cell membranes. From a functional viewpoint, spinal nAChRs are involved in physiological responses like pain (Khan et al., 1998) and locomotion (Perrins and Roberts, 1995; Nishimaru et al., 2006) to which motoneuron/Renshaw cell synapses make an important contribution (Lamotte d'Incamps et al., 2012; Enjin et al., 2017).

nAChRs are implicated in neuroprotection mechanisms against acute cell distress (Bencherif, 2009) induced by excitotoxicity, namely a process of over-activation of glutamate receptors considered as a paradigm of neurodegeneration (Choi 1992; 1994). Nicotine mediated neuroprotection has been reported in vitro (Garrido et al., 2003), in vivo (Xue et al., 2014) and in epidemiological studies (Quik et al., 2012), suggesting potential strategies to contrast neuronal death. On brainstem motoneurons nicotine protects against excitotoxicity by activating nAChRs that trigger intracellular pathways to block reactive oxygen species (ROS) and by normalizing mitochondrial metabolism (Corsini et al., 2016; Tortora et al., 2017). Since nicotine depolarizes rat spinal motoneurons via direct and indirect effects (Blake et al., 1987), this drug might be neuroprotective for the spinal cord by acting on a broad spectrum of targets. To explore this issue, we used an excitotoxic model of the isolated rat spinal cord kept in vitro for up to 24 h (Taccola et al., 2008). We measured the output of locomotor networks as fictive locomotion by recording oscillatory patterns from lumbar ventral roots (VRs), and investigated locomotor network activity and neuronal survival after excitotoxicity and nicotine application. For this purpose, we initially analyzed the acute and delayed effects of nicotine on synaptic transmission, fictive locomotion and cell composition to identify the most suitable concentration of nicotine. Thereafter, we applied the excitotoxic protocol based on a transient application of kainate, a potent glutamate analogue, to find out the best regimen of nicotine administration for functional and structural neuroprotection of spinal networks. Since the neurotoxicity evoked by kainate peaks after its washout (Kuzhandaivel et al., 2010), we investigated the impact of nicotine administration applied together with kainate or after its washout. Finally, we studied if the subtype selective nAChR antagonists Di-hydro-β-erythroidine (DHβE) and methyllycaconitine (MLA) (Arias, 1997; Gotti & Clementi, 2004) could change spinal network activity as well as influence any beneficial action by nicotine toward excitotoxic damage.

Materials and methods

Ethical approval

All the experimental procedures were approved by SISSA ethical committee (prot. 3599, 28th May 2012) and were performed in accordance with the guidelines provided by European Union

rules for animal experimentation. All attempts were made to reduce the number of animals used and their sufferings.

Spinal cord preparation and drug application protocol

Experiments were carried out with *in vitro* spinal cord preparations from 0-2 day old wistar rats (n = 111, where n is the number of animals used in the whole study) by rapidly decapitating under anesthesia with urethane (0.2 mL i.p. of a 10% w/v solution). Thoraco-lumbar spinal cord preparations were carefully isolated in continuously oxygenated Krebs solution (in mM; 113 NaCl, 4.5 KCl, 1 $MgCl_2.7H_2O$, 2 $CaCl_2$, 1 NaH_2PO_4, 25 $NaHCO_3$, 11 glucose; gassed with 95% oxygen and 5% CO_2; pH 7.4 at room temperature at 7.5 mL/min) as previously published (Taccola & Nistri, 2006a; Taccola et al., 2008; Margaryan et al., 2009). After dissection, spinal cords were kept in Krebs for 2 h to recover functional activity before starting with experimentation. To mimic excitotoxic damage of gray matter, kainate was applied at 50 μM concentration to partially abolish fictive locomotor rhythms induced by DR train pulses and NMDA+5HT when tested the subsequent day. Initially the protocol of nicotine concentration was optimized by using different concentrations of nicotine (10, 2, 1, 05; μM) for 4 h on day 1 and recorded polysynaptic reflex responses and fictive locomotor patterns every 15-20 min during 4 h. After all concentrations trails, on an *in vitro* spinal cord preparation, nicotine with 1 μM concentration was selected for further continuing experimentation with spinal lesion and neuroprotection protocols. Thereafter, spinal cords were kept in Krebs overnight and recorded monosynaptic reflexes, polysynaptic reflexes, electrically induced and chemically induced fictive locomotion 24 h after wash.

Excitotoxicity was induced by bath application of kainate (for 1 h; 50 μM, from Tocris), glutamate agonist, followed by either Krebs or nicotine (1 μM) administered for 4 h on day 1. These preparations were then superfused with Krebs solution overnight and reflexes and fictive locomotion were recorded on subsequent day. Electrophysiological and immunohistochemical data were compared among the following 5 groups; Sham (day 2 control), nicotine 1 μM applied for 4 h (N, from Sigma-Aldrich), kainate administered for 1 h, kainate (1 h) followed by nicotine for 4 h (KA/N 4h), kainate co-applied with nicotine for 1 h followed by nicotine for 4 h (KA+N/N 4h) (see supplemental fig. 1).

To further ensure the neuroprotective effect of nicotine and the involvement of specific nicotinic acetylcholine receptors i.e. α4β2 and α7 in spinal neuroprotection, nAChR antagonists, dihydro-β-erythroidine, 10 μM (DHβE, from Tocris) and methyllycaconitine, 10 nM (MLA, from Sigma-Aldrich, Saint Louis, MO, USA), were applied in the following 9 combinations; DHβE applied alone for 4 h (D), DHβE co-applied with kainate for 1 h (KA+D), DHβE administered with kainate and nicotine for 1 h followed by DHβE and nicotine for 4 h (KA+D+N/D+N 4 h), MLA applied for 4 h (M), MLA co-administered with kainate for 1 h (KA+M), MLA administered with kainate and nicotine for 1 h followed by MLA and nicotine for 4 h (KA+M+N/M+N 4 h), DHβE and MLA were co-applied for 4 h (D+M), DHβE+MLA coapplied with kainate for 1 h (KA+D+M), DHβE and MLA were administered with kainate and nicotine for 1 h followed by DHβE+MLA+nicotine for 4 h (KA+D+M+N/D+M+N 4 h) (supplemental fig. 1).

Electrophysiological recordings

By using tight fighting monopolar suction Ag/AgCl electrodes, DC coupled recordings were acquired from L2 and L5 ventral roots (VRs) which carry flexor and extensor motor pools to hind limbs (Taccola & Nistri, 2006a; Taccola et al., 2008). VR responses were elicited (at 10 KHz) by delivering electrical square pulses with 0.1 ms duration to the dorsal root (L) through bipolar suction electrodes. Initially, minimum stimulus threshold was estimated by applying graded electrical stimuli and detecting the minimal response in ipsi-lateral and ispi-segmental VRs, equivalent to 1x threshold to induce monosynaptic reflex responses. 3x stimulus threshold was used to evoke polysynaptic reflexes. 3x threshold intensity to evoke DR induced fictive locomotion by stimulating 30 pulses of DR train at 2 Hz frequency (15 s) (Marchetti et al., 2001). Chemically induced fictive locomotion was evoked by bath application of N-methyl-D-aspartate (NMDA) (3-6 μM) and 5-hydroxytryptamine (5-HT) (10 μM) (Kiehn & Kjaerulff, 1998; Kiehn 2006). Disinhibited bursts were evoked by applying γ-aminobutyric acid (GABA)-A and glycine receptors blockers, bicuculline (20 μM) and strychnine (1 μM) respectively. Signal records were acquired and processed with pClamp software 9.2, (Molecular Devices, Sunnyvale, CA, USA). Fictive locomotor rhythms and burst activity was measured in accordance with Taccola et al. (Taccola et al., 2008) and Bracci et al. (Bracci et al.,1996a,b) respectively.

Immunofluorescence, microscopy and analysis

Immunohistochemical experiments were performed in accordance with previous reports (Cifra et al. 2012; Sámano et al., 2016; Kaur et al., 2016). After electrophysiology recordings, spinal cords were fixed in 4% paraformaldehyde and then cryoprotected with 30 % (w/v) sucrose. 30 µm thick transverse sections of spinal cords were cut from T13-L5 segment of spinal cord with sliding microtome at –20 $^{\circ}$C and preserved in phosphate buffer saline (PBS) until use. Free floating immuno-fluorescence procedure was used where the sections were preincubated for 2 h with blocking solution (5% normal goat serum, 5% bovine serum albumin, 0.3 % Tritox X 100, 1% PBS) at room temperature. Spinal cords were immunolabelled with primary antibodies namely, anti-Neu N (Neuron specific neuronal marker; rabbit polyclonal; 1:500 dilution; Merck Millipore, Milan, Italy), anti-SMI 32 (specific non phosphorylated neurofilament H in spinal motoneurons; mouse monoclonal; 1:1000 dilution; Chemicon, Millipore, Milan, Italy), anti-S100 (specific for S100 protein, belongs to family of Ca^{2+} binding proteins in nuclei and cytoplasm of astrocytes, rabbit polyclonal; 1:1000; DAKO, Glostrup, Denmark) and anti-GFAP (specific for Glial fibrillary acidic protein (GFAP), member of class III intermediate filament protein family, expressed in astrocytes and certain other astroglia in the central nervous system; mouse monoclonal; 1:500; Sigma Aldrich) in antibody solution (containing 1% NGS, 1% BSA, 0.1 % Triton-X 100), kept overnight at 4 $^{\circ}$C. Sections were washed with 1x PBS and incubated with appropriated secondary antibodies, anti-mouse Alexa Flour 488 or 594, or anti-rabbi Alexa Fluor 488 or 594 and DAPI for 2 h. Finally they were mounted on glass and imaged with Leica DM6000 (20x magnification). Images were obtained from 3 to 6 spinal sections (5-10 sections/preparation) by selecting 3 regions of interest (ROIs); dorsal, central (D, C; 350x350 µm^2) and ventral (V; 300x230 µm^2) (Mazzone et al; 2010; Cifra et al., 2012; Sámano et al., 2016). Quantification (of cells, pyknotic nuclei, motoneurons and neurons) and immuno-fluorescence intensity (AU, of astrocytes and glia) was measured by ImageJ software.

Preparation of organotypic slice cultures

Organotypic spinal cultures were prepared from spinal cords of E13 day rat embryos as previously reported (Avossa et al., 2003; Mazzone et al., 2010; Mazzone and Nistri, 2011). Thus, 275 µm transverse slices were cut and fixed on a glass coverslip (Kindler, EU) with reconstituted chicken plasma clotted with 1 drop of thrombin (200 U/mL). The coverslips with spinal sections

were inserted into plastic tubes with 1 mL of medium comprised 82 % Dulbecco's modified eagle's medium, 8% sterile water with tissue culture, 10 % fetal bovine serum, osmolarity 300 mOsm, pH 7.35. About 40 slices (from thoraco-lumbar part) were prepared from single dissection. The tubes were kept for culturing for 22 days *in vitro* (DIV) in roller drum (120 x *g*/h) at 36.5 $^{\circ}$C, with 5% CO_2. Dulbecco's modified eagle's medium was applied with high glucose (DME/HIGH), penicillin and streptomycin (Euroclone, Devon, UK). Fetal calf serum (FBS) was purchased from Invitrogen (Carlsbad, CA, USA), nerve growth factor (NGF) from D.A.B Italia (Segrate, Italy), chicken plasma from Innovative (Novi, MI, USA) and thrombin from Merck (Darmstadt, Germany). Organotypic spinal cultures were treated after 22 days of culturing. There were four selected paradigms used on 22nd day, namely sham, nicotine 1 µM, kainate 50 µM and kainate coapplied with nicotine for 1 h followed by nicotine for 4 h (KA+N/N 4h). All the treatments were washed out with culture medium for 24 h before using the cultures for Ca^{2+} imaging experiments.

Ca^{2+} Imaging

In accordance with previous protocols for Ca^{2+} imaging (Fabbro et al., 2004; Sharifullina & Nistri, 2006; Corsini et al., 2017), organotypic spinal slices grown *in-vitro* for 3 weeks were incubated with fluorescent calcium dye Fluo 3-AM (4 µM, Molecular Probes, Invitrogen, Carlsbad, CA, USA) for 1 h at room temperature in Dulbecco's modified eagle's medium. The fluorescent dye was washed out with the same medium (Dulbecco's modified eagle's medium) containing strychnine and bicuculline for 30 min. Spinal cultures were then transferred to a recording chamber of the Nikon Eclipse T1 microscope (Nikon, Tokyo, Japan) and replaced the medium with 2 mL of oxygenated Krebs comprising strychnine (1 µM) and bicuculline (20 µM). We recorded Ca^{2+} signals from ventrally located neurons (somatic diameter > 20 µm; Fabbro et al., 2007). For each slice, only one region was analyzed, and 8 ± 3 number of fluorescent ventral neurons was selected (focused in the most superficial plane) to investigate changes in intracellular Ca^{2+} concentration. Ca^{2+} fluorescent emission was excited at a fixed wavelength of 488 nm generated by a Nikon intensilight C-HGFI lamp (Nikon) and detected with the digital CMOS camera ORCA-Flash 4.0 (Hamamatsu Photonic, Hamamatsu City, Japan). Images were acquired with the Fiji software (ImageJ, Wayne Rasband, National Institued of Health, USA; 62)

with 200 ms exposure time. Traces extrapolated with Igor Pro software (version 6.37, Wavemetrics, Lake Oswego, OR, USA) were analyzed with the software Clampfit 10.0 (Molecular Devices Corporation, Sunnyvale, CA, USA). Ca^{2+} transients were expressed as $\Delta F/F_0$ (the amplitude fractional increase), where ΔF is the fluorescence rise over baseline, and F_0 the baseline fluorescence level; $[Ca^{2+}]_i$ elevations were considered significant when they exceeded 5 times the noise standard deviation (Bosi et al., 2015; Rauti et al., 2016). The correlation between the Ca^{2+} events among active cells recorded from the same field was assessed by cross-correlation analysis. The value of cross correlation factor (CCF) was used to measure the strength of the correlation between cells, i.e. the relative probability that the peaks of calcium transients took place at the same time in all the cells. These values range between 1 (maximal correlation) and −1 (maximal anti-correlation), and were obtained using Igor Pro.

Statistical analysis

Electrophysiological, immuno-histochemical and calcium imaging data were statistically analyzed with SigmaStat 3.5 (Stat Software, Chicago, IL, USA). Values were expressed as mean±SEM, where n is the number of spinal cords or spinal slices used. As directed by software, normality test was applied to distinguish between parametric and non-parametric data, the values were evaluated by Student's *t-test* or Mann-Whitney test respectively. One-way Analysis of variance test (ANOVA) was applied for multiple comparisons (via Kruskal-Wallis or Holm Sidak tests). The acceptance significance level was $P < 0.05$.

Results

Acute effects of nicotine on reflexes, fictive locomotion and motoneuron depolarization of the rat spinal cord

Because the effects of nicotine are complex and could be manifested as either neuroprotective or toxic, initial experiments were performed to identify the most suitable time course and concentration of nicotine for experiments which spanned over several hours. Fig. 1 A shows changes in average polysynaptic reflexes recorded from a lumbar VR following homosegmental DR stimulation. While the response peak was stable for several h in Krebs solution, in the presence of nicotine there was a sustained depression of the amplitude with partial recovery at 1

h wash. Nicotine was applied continuously for 4 h since this would be the most suitable time to contrast the delayed onset of kainate excitotoxicity that starts within the first h and is fully expressed over the next 4 h (Kuzhandaivel et al., 2010). The largest depression by nicotine was observed with 2 μM (**P = 0.007, area; P = 0.006, amplitude; Control vs N 20 min, Student's t-test) or 10 μM (***P = 0.001, area; *P = 0.017, amplitude; Control vs N 20 min, Mann Whitney-test) concentrations of nicotine (Fig. 1 B, C). Fig. 1 B shows that the polysynaptic response area became smaller with anyone of the nicotine concentrations used however not significant with 1 and 0.5 μM nicotine (P = 0.089 and P = 0.838, Mann Whitney-test). The acute effect of nicotine was associated with depolarization recorded from VRs as shown in Fig. 2. Thus, by comparison with kainate (50 μM), depolarization evoked by 10 μM nicotine was clearly smaller (P = 0.001, KA vs N 10 μM; Student's t-test) and almost undetectable when 1μM was applied (P = 0.001, KA vs N 1 μM; Student's t-test) (Fig 2 A). Fig. 2 B summarizes average data indicating that depolarization evoked by nicotine was less than 1/3rd of the one evoked by kainate, and that it was only modestly dependent on the drug concentration, probably indicating that most effects had indirect origin within spinal networks. To minimize network depression and to avoid concentrations likely to produce toxicity, these data suggested the use of 1 μM nicotine for further, even longer tests.

Delayed effects by nicotine on spinal networks

Fig. 3 shows responses recorded on the second experimental day after spinal cords had been treated on day 1 with 1 μM nicotine (4 h) followed by washout (see scheme in supplementary Fig. 1). Monosynaptic reflexes were largely depressed by comparison with sham preparations (P = 0.003, Student's t-test) (Fig. 3 A, E). A similar effect was also detected when recording polysynaptic reflexes from the same preparations (P = 0.027, amplitude, Mann Whitney-test; P = 0.029, area, Student's t-test; sham vs N) (Fig. 3 B, F, G). We next tested trains of DR stimuli applied to a single DR to elicit cumulative depolarization with superimposed alternating VR oscillations reflecting the activation of the locomotor central pattern generator (Marchetti et al., 2001). Fig 3 C, H-J shows that cumulative depolarization amplitude and area values were similar after nicotine pretreatment and retained their ability to generate oscillations. FL cycles induced by the standard method of co-application of NMDA and 5-HT to elicit alternating VR

oscillations (Kiehn, 2006) had slightly slower periodicity and smaller amplitude (P = 0.001, Student's t-test) after prior day treatment with nicotine (Fig. 3 D, K).

These data suggested that, despite extensive wash, nicotine had left a functional signature on the activity of spinal networks which were operative at near normal level only when subjected to strong, sustained stimulation (DR trains or NMDA + 5-HT). This realization raised the issue of whether nicotine could replicate its effects when reapplied on the second day or whether nAChRs might have been inactivated or lost. Supplemental Fig. 2 A, B shows that nicotine retained its depressant effect on polysynaptic reflexes (amplitude: P = 0.002, $H_{(2)}$ = 12.244, Kruskal-Wallis one way analysis of variance on ranks test; area: P = 0.001, $F_{2,26}$ = 12.385, one way analysis of variance test). When compared to Fig. 1 A, B the action of nicotine was even stronger and was associated with a larger decrease in the area (P = 0.011, $F_{2,21}$ = 5.714, one way analysis of variance test) of cumulative depolarization and associated oscillations (P = 0.013, $H_{(2)}$ = 8.636, Kruskal-Wallis one way analysis of variance on ranks test) (Supplemental Fig. 2 C, D).

Fig. 4 shows that prior application of nicotine on day 1 did not significantly change cell populations within the lumbar spinal cord. Thus, as exemplified in Fig. 1 A for a section of the dorsal horn, good immunopositivity to NeuN was retained, an observation applicable to all three ROIs investigated (Dorsal: P = 0.001, t_{16} = –5.406; Central: P = 0.859, U = 43, Mann Whitney test; Ventral: P = 0.104, t_{16} = 1.726, respectively, sham vs nicotine, N) (Fig. 4 D). Similar data were obtained for SMI32 positive motoneurons (P = 0.001; t_{24} = –3.798, sham vs N) (Fig. B, E) and astroglia immunostained with S100 (Dorsal, P = 0.562; Central, P = 0.276; Ventral, P = 0.265) or GFAP (Dorsal: P = 0.715; Central: P = 0.675; Ventral: P = 0.801, respectively, sham vs N) antibodies (Fig. 4 C, F, G).

Neuroprotection by delayed application of nicotine

The potential translation value of pharmacological treatment should, *inter alia*, include administration of the drug under test after the excitotoxic stimulus. Thus, as indicated in Supplemental Fig. 1, we applied kainate on day 1 followed by washout and immediate application of 1 µM nicotine for 4 h. Extensive washout was then performed with Krebs solution

for the next 24 h when testing commenced. Fig. 5 A-D shows sample record of mono-, polysynaptic responses, cumulative depolarization and chemically-induced fictive locomotion 24 h after kainate alone or kainate followed by nicotine. While kainate consistently decreased all these responses (see control sham values in Fig. 3) in accordance with previous reports (Taccola et al., 2008; Mazzone et al., 2010), delayed application of nicotine attenuated the kainate-induced toxicity as depression of polysynaptic responses was less intense (amplitude: $P = 0.002$, $U = 23$; area: $P = 0.014$, $U = 37$, Mann Whitney-test, respectively; KA vs KA/N 4h) (Fig. 5 B, F, G), some recovery in cumulative depolarization ($P = 0.005$, $t_{22} = –3.092$) (Fig. 5 C, I, J) and oscillations ($P = 0.001$; $U = 0$, Mann Whitney-test) (Fig. 5 H) was detected, and small VR alternating cycles were present (amplitude, $P = 0.001$; $t_{19} = –6.563$; period, $P = 0.001$, $U = 28$, Mann Whitney-test) (Fig. 5 D, K). No change in monosynaptic responses was apparent (Fig. 5 A, E).

Histological data validated the partial neuroprotection by the delayed application of nicotine as shown in Fig. 6. Thus, pyknosis was less frequent ($P = 0.001$, $U = 108$, Mann Whitney-test) (Fig. 6 C), neuronal numbers were better preserved ($P = 0.001$, $t_{16} = –11.612$) especially in the dorsal ROI (Fig. 6 A, D), and more numerous motoneurons ($P = 0.001$, $U = 3$, Mann Whitney-test) were observed (Fig. 6 B, E). In line with our previous results, we found no significant damage by kainate to astroglia in the three ROIs and, therefore, no effect by subsequent application of nicotine (Supplemental Fig. 3, A, C, D).

Advancing the timing of nicotine application to improve neuroprotection

We wondered if better neuroprotection could be obtained by applying nicotine earlier, i.e. together with kainate (Supplemental Fig. 1). While this procedure would not confer much translational value to the data, we felt it would probably serve another purpose, namely to clarify if the intracellular pathways triggered by nicotine operate more slowly than the death pathways triggered by kainate. This approach has been employed with some success with the PARP-1 inhibitor PJ34 (Nasrabady et al., 2011).

Fig. 7 summarizes our observations with co-application of kainate and nicotine for 1 h, followed by 4 h nicotine and then washout with Krebs up to the next day. Thus, while monosynaptic

reflexes were similarly depressed by kainate alone or with the nicotine protocol (Fig. 7 A, E), improvement in polysynaptic reflexes was stronger when nicotine had been co-applied (amplitude: $P = 0.001$; area: $P = 0.001$, Mann Whitney-test, respectively; KA vs KA+N/N 4h) (Fig. 7 B, F, G). Likewise, the cumulative depolarization was larger ($P = 0.001$, $U = 5$, Mann Whitney-test) with the latter protocol (Fig. 7 C, H, I, J) and, in particular VR cycles evoked by NMDA plus 5HT emerged at slow periodicity (amplitude: $*P = 0.012$ and periodicity: $P = 0.004$, Mann Whitney-test) (Fig. 7 D, K). These data suggested that network excitability strongly lowered by kainate was better preserved with this nicotine protocol. One functional test in support of this hypothesis was the demonstration that the spontaneous disinhibited bursting, arising after pharmacological block of inhibition and relying on network glutamatergic transmission (Bracci et al 1996), was characterized by significantly larger burst amplitude ($P = 0.027$, Students *t*-test; KA vs KA+N/N 4h) (Fig. 8 A, B) when nicotine was co-applied even if the burst frequency remained unchanged ($P = 0.356$) (Fig. 8 C).

While isolated preparations of the spinal cord offer the advantage of studying the integrated network output in terms of reflexes and fictive locomotion, they are not well suited to provide data on the distribution of bursting and their long-term sensitivity to kainate and/or nicotine. With the aim of studying long-term spontaneous bursting as an index of distributed network activity, we recorded Ca^{2+} transients from neurons in spinal slice cultures (Fabbro et al., 2007; Sibilla et al., 2009) as exemplified in Fig. 9 A. Fig. 9 A shows the spatial resolution of ventral neurons that could be simultaneously traced within the same field of view, with single cell resolution. At 22 DIV Ca^{2+} oscillations elicited during disinhibited bursting were typically very slow by comparison to electrophysiological bursts and detected over a wide area (Fig. 9 B, top left; see also Fabbro et al., 2007; Sibilla et al., 2009; Streit, 1993). By simultaneous recording from distinct neurons, it was clear that these Ca^{2+} oscillations were synchronous as evaluated with their cross-correlation factor even when the cells were spaced 300 µm apart (Fig. 9 A, B, E). Nicotine applied at 1 µM concentration for 4 h (in analogy to the protocol earlier reported; Supplemental Fig. 1) largely enhanced the frequency of bursting ($P = 0.001$, $F_{3,19} = 38.639$, Holm sidak-test) recorded the day after with preserved synchronicity (Fig. 9 B, C, E). This delayed effect of nicotine was accompanied by a significant decrease in the length of single transients (Fig. 9 D) ($P = 0.002$, $H_{(3)} = 15.009$, Kruskal-Wallis one way analysis of variance on

ranks test). Kainate application was followed by a strong decrement in oscillatory activity and prolongation of Ca^{2+} transients, effects that were significantly and persistently reversed by nicotine that did not decrease their synchronicity (Fig. 9 B-D).

Histochemical experiments with the isolated spinal cord preparation showed that early nicotine administration together with kainate followed by nicotine for 4 h strongly blocked pyknosis (Fig. 10 A, C), and left the motoneuronal number nearly normal (P = 0.001, U = 3, Mann Whitney-test, KA vs KA+N/N 4h) (B, E), while the neuronal number was significantly improved vs kainate treatment for all three ROI, especially in the case of dorsal horn (P = 0.001, t_{16} = – 14.761, Student's t-test) (Fig. 10 D). With this protocol the number of neurons in the dorsal ROI was similar to the one observed when nicotine had been applied only after kainate (P = 0.705, t_{16} = 0.385, Student's t-test; KA/N 4h vs KA+N/N 4h) (see Fig. 6 D). The protocol with nicotine + kainate followed by nicotine conferred additional protection to neurons in central (P = 0.001, t_{16} = - 6.036, Student's t-test; KA/N 4h vs KA+N/N 4h) and ventral (P = 0.003, U = 75, Mann Whitney-test, KA/N 4h vs KA+N/N 4h) ROI when compared (see Fig. 6 D) with the delayed nicotine application after kainate. Conversely, no difference was observed in immunofluorescence intensity for S100 and GFAP signals between the protocols of kainate followed by nicotine and kainate+nicotine followed by nicotine (Supplemental Fig. 3 A-C).

Changes in spinal reflexes and fictive locomotion by nAChR antagonists

We next investigated whether application of nAChR antagonists might induce delayed changes in network function recorded on the second day in vitro. Fig 11 A, B shows sample averaged traces of monosynaptic and polysynaptic reflexes recorded 24 h after earlier application of antagonists alone (for 4 h). When compared to sham preparations at 24 h, monosynaptic reflexes were depressed after DHβE or MLA or DHβE+MLA (P = 0.045, $F_{3,26}$ = 3.314; Holm-Sidak-test) (Fig. 11 A, E). Vice-versa, polysynaptic reflexes, while retaining peak amplitude (P = 0.281, $F_{3,22}$ = 1.373; one way analysis of variance test) similar to sham, were strongly enhanced in area (P = 0.043, U = 8; P = 0.043, U = 8; P = 0.03, t_{12} = –2.469; D vs sham; M vs sham; D+M vs sham, respectively) (Fig. 11 B, F, G). The amplitude and area of cumulative depolarization evoked by DR trains were not significantly increased (Fig. 11 C, I, J), while the number of superimposed oscillations were reduced (P = 0.043, H_3 = 8.416; Kruskal-Wallis one way analysis

of variance on ranks test) (Fig. 11 C, H). Chemically-induced fictive locomotion was present on the second day after antagonist application (Fig. 11 D), although the cycle amplitude was depressed with unchanged periodicity when both antagonists were applied (P = 0.006, $F_{3,26}$ = 5.279, one way analysis of variance test, sham vs D; P = 0.009, H_3 = 11.580, sham vs M, Kruskal-Wallis one way analysis of variance on ranks test) (Fig. 11 K).

Can antagonists change the severity of KA toxicity?

We next examined if DHβE or MLA or DHβE+MLA application together with kainate for 1 h could modify the outcome of network activity caused by the excitotoxic challenge. No antagonist (alone or in combination) altered the severe decrease in monosynaptic (Fig. 12 A, E) and polysynaptic reflexes (Fig. 12 B, F, G) associated with kainate toxicity. Cumulative depolarization remained largely depressed in amplitude and area values (Fig. 12 C, H, I) with significant change in amplitude of cumulative depolarization (H) in case of DHβE+MLA when co-applied with KA in comparison to KA alone (P = 0.042, U = 10; Mann Whitney test). Interestingly, chemically-induced VR patterns were, however, observed (Fig. 12 D, J), even though with smaller amplitude in comparison to kainate alone (P = 0.024, $F_{3,17}$ = 4.296; one way analysis of variance test). (Fig. 12 D, J) and of slow periodicity. Interestingly, co-application of kainate with DHβE and MLA improved neuronal survival in the dorsal and central ROI with no improvement in the ventral ROI (Dorsal: P = 0.001, $F_{2,28}$ = 35.058, Holm Sidak test; Central: P = 0.001, $H_{(2)}$ = 20.031, Kruskal Wallis test; Ventral: P = 0.001, $H_{(2)}$ = 17.757, Kruskal Wallis test) (Supplemental Fig. 4).

nAChR antagonists and neuroprotection by nicotine

Former observations indicated that the most useful neuroprotective protocol with nicotine was to apply this alkaloid together with kainate and maintained it for 4 h during the kainate washout. To find out if this action by nicotine was dependent on nAChR activation, we also co-applied nAChR antagonists either in combination or as single drug application (Supplemental Fig. 1). Fig. 13 summarizes data with such protocols. Thus, monosynaptic reflexes remained thoroughly depressed (P = 0.215, $F_{3,22}$ = 1.631; one way analysis of variance test) (Fig. 13 A), while the protective effect by nicotine on polysynaptic reflex amplitude and area was antagonized by

DHβE alone (P = 0.013, $F_{3,22}$ = 4.653 and P = 0.05, $F_{3,23}$ = 3.087, respectively; one way analysis of variance test) (Fig. 13 B, C). The cumulative depolarization amplitude (improved by nicotine plus kainate followed by nicotine vs kainate alone) was significantly depressed by nAChR antagonist DHβE when co-applied with KA+N/N (P = 0.047, t_{12} = 2.212, Student's t-test; KA+N/N 4 h vs KA+D+N/D+N 4 h), the protective role of nicotine on the size of the area was remained lost with DHβE application (P = 0.044, t_{12} = 2.248, Student's t-test; KA+N/N 4h vs KA+D+N/D+N 4h) (Fig. 13 D, E), and oscillations remained absent. On the other hand, the moderate recovery in fictive locomotion evoked by nicotine was maintained in terms of cycle amplitude and periodicity when the antagonists were co-applied together or in isolation (P = 0.684. $F_{3,23}$ = 0.504 and P = 0.746, $F_{3,23}$ = 0.4, respectively; one way analysis of variance test) (Fig. 13 F).

We next investigated how nAChR antagonists might affect the histological neuroprotection elicited by nicotine. Fig. 14 shows average distribution of neuronal damage in three ROI (see sample image of dorsal ROI in A). Thus, in comparison with data with kainate+nicotine followed by nicotine, a significant deterioration in the number of NeuN-positive neurons was detected when the antagonists were applied alone or in combination (Dorsal: P = 0.001, t_{16} = 4.660; Central: P = 0.001, U = 0; Ventral: P = 0.001, U = 0.5; KA+N/N 4 h vs KA+D+N/D+N 4 h), (Dorsal: P = 0.001, t_{16} = 8.649; Central: P = 0.003, t_{16} = 3.541; Ventral: P = 0.001, U = 0; KA+N/N 4 h vs KA+M+N/M+N 4 h), (Dorsal: P = 0.001, U = 0; Central: P = 0.001, t_{16} = 4.360; Ventral: P = 0.001, U = 0; KA+N/N 4 h vs KA+D+M+N/D+M+N 4 h) (Fig. 14 C). This observation was further validated by counting the number of motoneurons (Fig. 14 B, D) as their protection by nicotine was largely impaired by DHβE, while it was left unchanged by MLA (P = 0.001, $H_{(3)}$ = 35.347; Kruskal-Wallis one way analysis of variance on ranks test).

Discussion

The principal finding of the present report is the demonstration that nicotine could protect spinal networks from kainate-evoked excitotoxicity with good histological preservation and moderate recovery in circuitry activities including fictive locomotion. The effects of nicotine were dependent on nAChRs that are widely expressed in the spinal cord. These data, therefore,

indicate nicotine as a pharmacological agent that, at least in an in vitro model of spinal cord injury, was beneficial to limit cell death and related dysfunction.

nAChRs in the mammalian spinal cord

In the central nervous system (CNS), cholinergic transmission acts via nAChRs to modulate cell excitability and neurotransmitter release with control over physiological functions like cognition, pain, anxiety, fatigue, reward, learning, memory (Changeux and Edelstein, 2001; Hogg et al., 2003; Christie et al., 2008). CNS nAChRs mainly belong to α7 nAChRs and α4β2 subtypes (Whiting & Lindstrom, 1986a,b; Whiting & Lindstrom, 1987).

Although various nAChR subunits have been identified in the rat spinal cord (Wada et al., 1989, 1990; Khan et al., 2003), α4β2 and α7 are the prominent receptor assemblies (Hsu et al., 1997; Berg & Conroy, 2002). Furthermore, α4β2 and α7 receptors play a role in nAChR mediated neuroprotection against excitotoxicity reported with rat dissociated spinal cultures (Nakamizo et al., 2005; Shimohama, 2009) and spinal neurons of chick embryos (Roth & Berg, 2003). Thus, antagonists for α4β2 and α7 receptors, DHβE and MLA respectively, were used in the present excitotoxicity model.

As the physiological role of spinal nAChRs is complex, it is no surprise that nicotine application can activate excitatory as well as inhibitory neurons (Cordero-Erausquin et al., 2004). Within the dorsal horn, nicotinic cholinergic transmission can control, in an inhibitory fashion, nociceptive inputs (Matsumoto et al., 2007). Yet at network level, nAChR synaptic activity can depress GABA (Genzen & McGehee, 2005) and glycine (Kiyosawa et al., 2001) mediated inhibition, thus leading to disinhibition. The latter phenomenon may account for the present observation that co-application of DHβE and MLA enhanced polysynaptic reflexes. nAChR antagonists per se, however, decreased monosynaptic responses, perhaps implying that presynaptic nAChRs were regulating fast synaptic transmission (Khan et al., 2003) from primary afferent fibres whose neurotransmitter is glutamate (Pook et al., 1992; Kerkut & Bagust, 1995). Of course, nicotine is expected to rapidly activate nAChRs and desensitize them (Khiroug et al., 1997, Sokolova et al., 2005), making difficult to dissect out, over an extended experimental protocol, which of these processes was the principal contributor to the delayed responses to nicotine. The present study,

therefore, reports the delayed histological and functional outcome of nicotine application rather than its complex mechanisms.

Nicotine for experimental neuroprotection

Although previous preclinical studies have indicated that nicotine can protect neurons against insults like excitotoxicity, or oxygen/glucose deprivation (Gahring et al., 2003; More and Dong, 2016), the present investigation was prompted by the recent observation of nicotine protection against excitotoxicity applied to rat brainstem motoneurons (Corsini et al., 2016, 2017). There was, however, no report of similar effects on the rat spinal cord, an issue that was explored by using an in vitro model of spinal cord injury fully validated in our laboratory. Although the model relies on a neonatal spinal cord preparation (or organotypic slice preparations), it should be borne in mind that acute spinal injuries are frequent in infants with profound consequences in terms of disability (Betz e al., 2004; Parent et al., 2011). The in vitro model based on 1 h application of kainate to evoke excitotoxicity followed by extensive wash with oxygenated Krebs attempts to mimic clinical settings when an acute spinal injury is usually treated after 1-2 h in life-saving intensive care to arrest the primary cause of damage. Furthermore, as the secondary injury develops slowly over a matter of hours through complex intracellular metabolic pathways (Oyinbo, 2011; Zhang et al., 2012), our model offers the opportunity to explore the potential for neuroprotection by drugs applied during/after the injury and to follow up the functional and histological evolution during the first 24 h. The present study required a lengthy phase of protocol design because, in addition to the choice of nicotine concentration, it was necessary to identify delayed effects by nicotine itself and the timing of nicotine application. This led us to testing various protocols with nicotine to be applied late or during the excitotoxic stimulation.

Early and late effects of nicotine on spinal networks

In the present experiments the motoneuron depolarization produced by bath-applied nicotine (at μM concentrations) was modest by comparison to the one by kainate, indicating that it probably originated within the network (Blake et al., 1987) and that desensitization was likely curtailing it. The overall impact of nicotine on spinal reflexes was a depressant one with slow recovery on washout. While the multiple expression of nAChRs and their kinetics on distinct neurons can be

probably responsible for this phenomenon, the present data clearly showed that applying nicotine for 4 h (a time that corresponds to the strong activation of cell death pathways in the excitotoxic protocol; Kuzhandaivel et al., 2010) was tolerated and reversible even though some depression of mono and polysynaptic reflexes was apparent the day after. Nonetheless, application of nicotine on the first experimental day led to delayed increased network excitability observed as widespread Ca^{2+} transients, indicating that there was no generalized network depression. Following earlier treatment with nicotine, spinal cords in vitro did retain their ability to express fictive locomotor patterns elicited by DR stimulation or neurochemicals like NMDA plus 5HT. In keeping with these results, neurons and motoneurons were histologically preserved, even better than in sham conditions perhaps because nicotine had delayed the deterioration of preparations maintained in vitro for sustained time.

The mechanisms underlying effects by nicotine are difficult to be resolved with the present preparation because we measured network responses (which by their nature are nonlinear and integrated) and neuronal numbers that provide only an endpoint for the neurotoxic phenomenon 24 h later. Delayed network hyperactivity evoked by nicotine was associated with decreased reflexes perhaps because of facilitation of inhibitory circuits and/or persistent desensitization of excitatory nAChRs. One further target for nicotine might have been mitochondrial nAChRs that, although not mediating cationic fluxes, are important for the correct functioning of cell energy metabolism. Thus, the present protocols were not designed to clarify the molecular processes responsible for the nicotine action (a subject for future work) rather to delineate a scenario to achieve histological and functional neuroprotection.

Nicotine and excitotoxicity

Kainate (50 μM) is a validated agent to elicit irreversible degeneration in the rat spinal cord in vitro (Taccola et al., 2010) and in vivo (Sun et al., 2006). Although at least 50 % neurons survive the initial insult, severe inhibition of reflexes and arrest of fictive locomotion ensue (Mazzone et al., 2010). When the 1 h application of kainate was followed by 4 h application of nicotine, significant improvement in polysynaptic reflexes was observed together with some recovery in oscillatory VR patterns induced by DR stimuli or NMDA plus 5HT. Histological preservation of neurons, including motoneurons, provided the structural substrate for functional protection. We

further attempted to improve nicotine neuroprotection by applying nicotine together with kainate. This protocol has been used before with our model on the assumption that drug access to neuronal structures located deeply within the spinal cord, like for example lamina X neurons believed to be important for the central pattern generator of locomotion (Kiehn, 2006; 2016), may be too slow to block the wave of excitotoxic depolarization spreading through spinal segments (Taccola et al., 2008, 2010). Indeed, when nicotine was co-applied with kainate, better functional and structural neuroprotection was detected.

Since early treatment with nicotine could restore at least in part the amplitude and frequency of disinhibited bursts or Ca^{2+} transients, these results indicate that certain elementary circuits relying on glutamatergic transmission for intrinsic rhythmicity (Bracci et al., 1996b) had been protected by nicotine and retained their connectivity because synchronicity was preserved even over a substantial distance. It was of particular interest to note that motoneuron numbers were rather close to control and that preservation of neurons had been attained throughout the three ROI. In this scenario the depression of monosynaptic reflexes was the only phenomenon not reversed by nicotine. While extracellular recording is not well suited to demonstrate the monosynaptic nature of excitatory transmission, former experiments have demonstrated that this protocol can actually generate monosynaptic excitatory potentials on motoneurons (Ostroumov et al., 2007). Hence, it seems likely that, despite near normalization of motoneuron numbers by nicotine, their ability to respond to weak inputs had remained impaired after kainate application.

nAChR antagonists, nicotine and excitotoxicity

The outcome of experiments based on co-application of antagonists with kainate (and nicotine) was complicated by the fact that, in the isolated spinal cord, effects due to administration of multiple drugs depend on individual drug kinetics, targets and intra-tissue distribution which are unavoidably dissimilar. Nonetheless, the broad depression of spinal responses by kainate was not arrested by either nAChR antagonist with only one exception, namely a partial preservation of chemically-induced fictive locomotion. We hypothesize that kainate-mediated excitation had led to release of endogenous ACh and that this phenomenon partly contributed to excitotoxicity at the level of the central pattern generator network. This suggestion is compatible with the modest protection by DHβE and it alludes to the possibility that at least part of the neuroprotection

exerted by nicotine itself was caused by its dual action on nAChRs, namely rapid activation and desensitization. In the presence of the antagonists and nicotine, the protection by nicotine toward fictive locomotion remained while the number of surviving neurons was intermediate between kainate toxicity and full protection. Furthermore, any protection of spinal reflexes was inhibited by the antagonists (with DHβE more efficacious than MLA).

We have formerly proposed that the locomotor central pattern generator operates according to the principle of "minimal membership", i.e. a critical number of neurons below which no function is generated (Kuzhandaivel et al., 2011). Hence, whenever nAChRs were inhibited by antagonists or nicotine-dependent desensitization, we might surmise that locomotor network membership remained just above threshold fictive locomotion (elicited by NMDA plus 5HT acting broadly on spinal neurons). Conversely, since electrically-evoked mono and polysynaptic reflexes depended on a lower number of activated neurons, in this instance losses induced by kainate had consistently larger impact on electrophysiological responses.

Conclusions

Attempts to obtain early spinal neuroprotection with pharmacological agents have been reported earlier with mixed results (Lee et al., 2003; Bagriyanik et al., 2008). Thus, among glutamate release inhibitors, riluzole is the only present-day treatment for motoneuron disease with a rather limited lifespan of clinical efficacy (Wokke, 1996; Cheah et al., 2010). In our experimental model, this drug cannot effectively contrast the excitotoxicity induced by kainate (Sámano et al., 2012). Another controversial drug is the glucocorticoid methylprednisolone sodium succinate (MPSS) that, in our tests, provides limited neuroprotection to the white matter only (Sámano et al., 2016). The poly (ADP-ribose) polymerase-1 (PARP-1) inhibitor PJ34 inhibits a non-apoptotic cell death process, yet it does not confer full functional protection to locomotor networks in vitro (Nasrabady et al., 2011). A more favourable outcome is observed with delayed application of the volatile anaesthethic methoxyflurane (Shabbir et al., 2015), and less efficiently with the i.v. anaesthetic propofol (Kaur et al., 2016). Hence, the present data suggest that modulation of spinal nAChRs is a potentially useful new tool to prevent neurodegeneration and should prompt further studies to devise novel pharmacological approaches in vitro and in vivo to limit the damage associated with spinal cord injury.

Acknowledgements

This work was supported by an intramural grant from SISSA. RR is the recipient of a research fellowship supported by the grant from the EU FP7-ICT-2013-FET-F GRAPHENE Flagship project (No. 696656). We thank Dr. Beatrice Pastore for her help with organotypic cultures.

Conflict of interest

The authors declare no conflict of interest.

Author Contributions

JK, AN, study design; JK, RR, data collection and analysis; JK, RR, AN, data interpretation and MS writing

Data Accessibility

Data accessibility will be possible via the repository service of the SISSA library

Supporting information

Supplemental Fig. 1: study design protocols. Supplemental Fig. 2: reproducibility of nicotine effects on the second day in vitro. Supplemental Fig. 3: effects of nicotine on glia following kainate evoked excitotoxicity. Supplemental Fig. 4: effect of nicotinic antagonists on neuronal numbers during excitotoxicity.

Abbreviations

ANOVA, analysis of variance; DAPI, 4', 6-diamidino-2-phenylindole; DR, dorsal root; VR, ventral root; GABA, γ aminobutyric acid; KA, kainate; L, lumbar; NeuN, neuronal specific nuclear protein antibody; NMDA, N-methyl-D-aspartate; ROI, region of interest; SCI, spinal cord injury; SEM, standard error of the mean; S100, subgroup of Ca2+ binding proteins marker; Glial fibrillary acidic protein, GFAP; SMI32, neurofilament H non-phosphorylated antibody; 5-HT, 5-hydroxytryptamine; Nicotine, N; dihydro-β-erythroidine, DHβE; methyllycaconitine, MLA; 5-hydroxytryptamine, 5-HT.

References

Arias, H.R. (1997) Topology of ligand binding sites on the nicotinic acetylcholine receptor. *Brain. Res. Brain. Res. Rev*., **25**, 133–191.

Avossa, D., Rosato-Siri, M.D., Mazzarol, F., Ballerini, L. (2003) Spinal circuits formation: a study of developmentally regulated markers in organotypic cultures of embryonic mouse spinal cord. *Neuroscience,* **122**, 391–405.

Bagriyanik, H.A., Ozogul, C., Alaygut, E., Gokmen, N., Kucukguclu, S., Gunerli, A., Yilmaz, O. (2008) Neuroprotective effects of ketorolac tromethamine after spinal cord injury in rats: an ultrastructural study. *Adv. Ther.,* **25**, 152-158.

Bencherif, M. (2009) Neuronal nicotinic receptors as novel targets for inflammation and neuroprotection: mechanistic considerations and clinical relevance. *Acta. Pharmacol. Sin.,* **30**, 702–714.

Berg, D.K., Conroy, W.G. (2002) Nicotinic alpha7 receptors: synaptic options and downstream signaling in neurons. *J. Neurobiol*., **53**, 512–523.

Betz, R.R., Mulcahey, M.J., D'Andrea, L.P., Clements, D.H. (2004) Acute evaluation and management of pediatric spinal cord injury. *J. Spinal. Cord. Med.,* **27**, S11–S15.

Blake, J.F., Evans, R.H., Smith, D.A. (1987) The effect of nicotine on motoneurones of the immature rat spinal cord in vitro. *Br. J. Pharmacol*., **90**, 167–173.

Bosi, S., Rauti, R., Laishram, J., Turco, A., Lonardoni, D., Nieus, T., Prato, M., Scaini, D., Ballerini, L. (2015) From 2D to 3D: novel nanostructured scaffolds to investigate signalling in reconstructed neuronal networks. *Sci. Rep.,* **5**, 9562.

Bracci, E., Ballerini, L. & Nistri, A. (1996a) Spontaneous rhythmic bursts induced by pharmacological block of inhibition in lumbar motoneurons of the neonatal rat spinal cord. *J. Neurophysiol.,* **75**, 640–647.

Bracci, E., Ballerini, L. & Nistri, A. (1996b) Localization of rhythmogenic networks responsible for spontaneous bursts induced by strychnine and bicuculline in the rat isolated spinal cord. *J. Neurosci.,* **16**, 7063–7076.

Changeux, J., Edelstein, S.J. (2001) Allosteric mechanisms in normal and pathological nicotinic acetylcholine receptors. *Curr. Opin. Neurobiol.,* **11**, 369–377.

Cheah, B.C., Vucic, S., Krishnan, A.V., Kiernan, M.C. (2010) Riluzole, neuroprotection and amyotrophic lateral sclerosis. *Curr. Med. Chem.,* **17**, 1942–1959.

Choi, D.W. (1992) Excitotoxic cell death. *J. Neurobiol.,* **23**, 1261–1276.

Choi, D.W. (1994) Glutamate receptors and the induction of excitotoxic neuronal death. *Prog. Brain. Res.,* **100**, 47–51.

Christie, D.F., Michael, A.A., and Paul, J.K. (2008) Subtypes of nicotinic acetylcholine receptors in nicotine reward, dependence, and withdrawal: Evidence from genetically modified mice. *Behav. Pharmacol.,* **19**, 461–484.

Cifra, A., Mazzone, G.L., Nani, F., Nistri, A. & Mladinic, M. (2012) Postnatal developmental profile of neurons and glia in motor nuclei of the brainstem and spinal cord, and its comparison with organotypic slice cultures. *Dev. Neurobiol.* **72**, 1140–1160.

Cordero-Erausquin, M., Pons, S., Faure, P., Changeux, J.P. (2004) Nicotine differentially activates inhibitory and excitatory neurons in the dorsal spinal cord. *Pain,* **109**, 308–318.

Corsini, S., Tortora, M., Nistri, A. (2016) Nicotinic receptor activation contrasts pathophysiological bursting and neurodegeneration evoked by glutamate uptake block on rat hypoglossal motoneurons. *J Physiol.,* **594**, 6777-6798.

Corsini, S., Tortora, M., Rauti, R. and Nistri, A. (2017) Nicotine protects rat hypoglossal motoneurons from excitotoxic death via downregulation of connexin 36. *Cell Death and Disease,* **8**, e2881.

Eccles, J.C., Fatt, P. & Koketsu, K. (1954) Cholinergic and inihibitorv synapses in a pathway from motor-axon collaterals to motoneurones. *J. Physiol.,* **126**, 524–562.

Enjin, A., Perry, S., Hilscher, M.M., Nagaraja, C., Larhammar, M., Gezelius, H., Eriksson, A., Leão, K.E., Kullander, K. (2017) Developmental Disruption of Recurrent Inhibitory Feedback Results in Compensatory Adaptation in the Renshaw Cell-Motor Neuron Circuit. *J. Neurosci.,* **37**, 5634–5647.

Fabbro, A., Skorinkin, A., Grandolfo, M., Nistri, A. & Giniatullin, R. (2004) Quantal release of ATP from clusters of PC12 cells. *J. Physiol.,* **560**, 505–517.

Fabbro, A., Pastore, B., Nistri, A., Ballerini, L. (2007) Activity-independent intracellular Ca^{2+} oscillations are spontaneously generated by ventral spinal neurons during development in vitro. *Cell Calcium,* **41**, 317–329.

Fenster, C.P., Whitworth, T.L., Sheffield, E.B., Quick, M.W., Lester, R.A. (1999) Upregulation of surface alpha4beta2 nicotinic receptors is initiated by receptor desensitization after chronic exposure to nicotine. *J. Neurosci.,* **19**, 4804–4814.

Gahring, L.C., Meyer, E.L., Rogers, S.W. (2003) Nicotine-induced neuroprotection against N-methyl-D-aspartic acid or beta-amyloid peptide occur through independent mechanisms distinguished by pro-inflammatory cytokines. *J. Neurochem.,* **87**, 1125–1136.

Garrido, R., King-Pospisil, K., Son, K.W., Hennig, B., Toborek, M. (2003) Nicotine upregulates nerve growth factor expression and prevents apoptosis of cultured spinal cord neurons. *Neurosci. Res.,* **47**, 349–355.

Genzen, J.R., McGehee, D.S. (2003) Short- and long-term enhancement of excitatory transmission in the spinal cord dorsal horn by nicotinic acetylcholine receptors. *Proc. Natl. Acad. Sci. U.S.A.,* **100**, 6807–6812.

Genzen, J.R., McGehee, D.S. (2005) Nicotinic modulation of GABAergic synaptic transmission in the spinal cord dorsal horn. *Brain. Res.,* **1031**, 229–237.

Gotti, C., Clementi, F. (2004) Neuronal nicotinic receptors: from structure to pathology. *Progress in Neurobiology,* **74**, 363–396.

Hogg, R.C., Raggenbass, M., Bertrand, D. (2003) Nicotinic acetylcholine receptors: from structure to brain function. *Rev. Physiol. Biochem. Pharmacol.,* **147**, 1–46.

Hsu, Y.N., Edwards, S.C., Wecker, L. (1997) Nicotine enhances the cyclic AMP-dependent protein kinase-mediated phosphorylation of alpha4 subunits of neuronal nicotinic receptors. *J. Neurochem.,* **69**, 2427–2431.

Kaur, J., Flores, G.J., Nistri, A. (2016) Neuroprotective effect of propofol against excitotoxic injury to locomotor networks of the rat spinal cord in vitro. *Eur. J. Neurosci.,* **44**, 2418–2430.

Kerkut, G.A., Bagust, J. (1995) The isolated mammalian spinal cord. *Prog. Neurobiol.,* **46**, 1–48.

Khan, I.M., Buerkle, H., Taylor, P., Yaksh, T.L. (1998) Nociceptive and antinociceptive responses to intrathecally administered nicotinic agonists. *Neuropharmacology,* **37**, 1515–1525.

Khan, I., Osaka, H., Stanislaus, S., Calvo, R.M., Deerinck, T., Yaksh, T.L., Taylor, P. (2003) Nicotinic acetylcholine receptor distribution in relation to spinal neurotransmission pathways. *J. Comp. Neurol.,* **467**, 44–59.

Khiroug, L., Giniatullin, R., Sokolova, E., Talantova, M., Nistri, A. (1997) Imaging of intracellular calcium during desensitization of nicotinic acetylcholine receptors of rat chromaffin cells. *Br. J. Pharmacol.,* **122**, 1323–1332.

Kiehn, O., Kjaerulff, O. (1998) Distribution of central pattern generators for rhythmic motor outputs in the spinal cord of limbed vertebrates. *Ann. N. Y. Acad. Sci.,* **860**, 110–129.

Kiehn, O. (2006) Locomotor circuits in the mammalian spinal cord. *Annu. Rev. Neurosci.,* **29**, 279–306.

Kiehn, O. (2016) Decoding the organization of spinal circuits that control locomotion. *Nat. Rev. Neurosci.,* **17**, 224–238.

Kiyosawa, A., Katsurabayashi, S., Akaike, N., Pang, Z.P., Akaike, N. (2001) Nicotine facilitates glycine release in the rat spinal dorsal horn. *J. Physiol.,* **536**, 101–110.

Kuzhandaivel, A., Nistri, A., Mladinic, M. (2010) Kainate-mediated excitotoxicity induces neuronal death in the rat spinal cord in vitro via a PARP-1 dependent cell death pathway (Parthanatos). *Cell Mol. Neurobiol.,* **30**, 1001–1012.

Kuzhandaivel, A., Nistri, A., Mazzone, G.L., Mladinic, M. (2011) Molecular Mechanisms Underlying Cell Death in Spinal Networks in Relation to Locomotor Activity After Acute Injury in vitro. *Front. Cell Neurosci.,***5**, 9.

Lamotte d'Incamps, B., Krejci, E., Ascher, P. (2012) Mechanisms shaping the slow nicotinic synaptic current at the motoneuron-renshaw cell synapse. *J. Neurosci.,* **32**, 8413–8423.

Lee, S.M., Yune, T.Y., Kim, S.J., Park, D.W., Lee, Y.K., Kim, Y.C., Oh, Y.J., Markelonis, G.J., Oh, T.H. (2003) Minocycline reduces cell death and improves functional recovery after traumatic spinal cord injury in the rat. *J. Neurotrauma,* **20**, 1017–1027.

Marchetti, C., Beato, M., Nistri, A. (2001) Alternating rhythmic activity induced by dorsal root stimulation in the neonatal rat spinal cord in vitro. *J. Physiol.,* **530**, 105–112.

Margaryan, G., Mladinic, M., Mattioli, C., Nistri, A. (2009) Extracellular magnesium enhances the damage to locomotor networks produced by metabolic perturbation mimicking spinal injury in the neonatal rat spinal cord in vitro. *Neuroscience,* **163**, 669–682.

Matsumoto, M., Xie, W., Inoue, M., Ueda, H. (2007) Evidence for the tonic inhibition of spinal pain by nicotinic cholinergic transmission through primary afferents. *Mol. Pain,* **3**, 41.

Mazzone, G.L., Margaryan, G., Kuzhandaivel, A., Nasrabady, S.E., Mladinic, M., Nistri, A. (2010) Kainate-induced delayed onset of excitotoxicity with functional loss unrelated to the extent of neuronal damage in the in vitro spinal cord. *Neuroscience,* **168**, 451–462.

Mazzone, G.L., Nistri, A. (2011) Effect of the PARP-1 inhibitor PJ 34 on excitotoxic damage evoked by kainate on rat spinal cord organotypic slices. *Cell Mol. Neurobiol.,* **31**, 469–478.

More, S.V. & Dong, D.K. (2016) Emerging preclinical pharmacological targets for Parkinson's disease. *Oncotarget.,* **7**, 29835–29863.

Nakamizo, T., Kawamata, J., Yamashita, H., Kanki, R., Kihara, T., Sawada, H., Akaike, A., Shimohama, S. (2005) Stimulation of nicotinic acetylcholine receptors protects motor neurons. *Biochem. Biophys. Res. Commun.,* **330**, 1285–1289.

Nasrabady, S.E., Kuzhandaivel, A., Nistri, A. (2011) Studies of locomotor network neuroprotection by the selective poly(ADP-ribose) polymerase-1 inhibitor PJ-34 against excitotoxic injury to the rat spinal cord in vitro. *Eur. J. Neurosci.,* **33**, 2216–2227.

Nishimaru, H., Restrepo, C.E., Kiehn, O. (2006) Activity of Renshaw cells during locomotor-like rhythmic activity in the isolated spinal cord of neonatal mice. *J. Neurosci.,* **26**, 5320–5328.

Ostroumov, K., Grandolfo, M., Nistri, A. (2007) The effects induced by the sulphonylurea glibenclamide on the neonatal rat spinal cord indicate a novel mechanism to control neuronal excitability and inhibitory neurotransmission. *Br. J. Pharmacol.,* **150**, 47–57.

Oyinbo, C.A. (2011) Secondary injury mechanisms in traumatic spinal cord injury: a nugget of this multiply cascade. *Acta. Neurobiol. Exp. (Wars),* **71**, 281–299.

Parent, S., Mac-Thiong, J.M., Roy-Beaudry, M., Sosa, J.F., Labelle, H. (2011) Spinal cord injury in the pediatric population: a systematic review of the literature. *J. Neurotrauma,* **28**, 1515-1524.

Perrins, R., Roberts, A. (1995) Cholinergic contribution to excitation in a spinal locomotor central pattern generator in Xenopus embryos. *J. Neurophysiol.,* **73**, 1013–1019.

Pook, P.C., Sunter, D.C., Udvarhelyi, P.M., Watkins, J.C. (1992) Evidence for presynaptic depression of monosynaptic excitation in neonatal rat motoneurones by (1S, 3S)- and (1S,3R). *ACPD,* **77**, 529–532.

Quik, M., Perez, X.A., and Bordia, T. (2012) Nicotine as a potential neuroprotective agent for Parkinson's disease. *Mov. Disord.,* **27**, 947–957.

Rauti, R., Lozano, N., León, V., Scaini, D., Musto, M., Rago, I., Ulloa, Severino. F.P., Fabbro, A., Casalis, L., Vázquez, E., Kostarelos, K., Prato, M., Ballerini, L. (2016) Graphene Oxide Nanosheets Reshape Synaptic Function in Cultured Brain Networks. *ACS Nano.,* **10**, 4459–4471.

Roth, A.L., Berg, D.K. (2003) Large clusters of alpha7-containing nicotinic acetylcholine receptors on chick spinal cord neurons. *J. Comp. Neurol.* **465**, 195–204.

Sámano, C., Nasrabady, S.E., Nistri, A. (2012) A study of the potential neuroprotective effect of riluzole on locomotor networks of the neonatal rat spinal cord in vitro damaged by excitotoxicity. *Neuroscience,* **222**, 356–365.

Sámano, C., Kaur, J. & Nistri, A. (2016) A study of methylprednisolone neuroprotection against acute injury to the rat spinal cord in vitro. *Neuroscience,* **315**, 136–149.

Shabbir, A., Bianchetti, E., Nistri, A. (2015) The volatile anesthetic methoxyflurane protects motoneurons against excitotoxicity in an in vitro model of rat spinal cord injury. *Neuroscience,* **285**, 269–280.

Sharifullina, E., Nistri, A. (2006) Glutamate uptake block triggers deadly rhythmic bursting of neonatal rat hypoglossal motoneurons. *J. Physiol.,* **572**, 407–423.

Shimohama, S. (2009) Nicotinic receptor-mediated neuroprotection in neurodegenerative disease models. *Biol. Pharm. Bull.,* **32**, 332–336.

Sibilla, S., Fabbro, A., Grandolfo, M., D'Andrea, P., Nistri, A., Ballerini, L. (2009) The patterns of spontaneous Ca^{2+} signals generated by ventral spinal neurons in vitro show time-dependent refinement. *Eur. J. Neurosci.,* **29**, 1543–1559.

Skok, M., Gergalova, G., Lykhmus, O., Kalashnyk, O., Koval, L., Uspenska, K. (2016) Nicotinic acetylcholine receptors in mitochondria: subunit composition, function and signaling. *Neurotransmitter,* **3**, e1290.

Sokolova, E., Matteoni, C., Nistri, A. (2005) Desensitization of neuronal nicotinic receptors of human neuroblastoma SH-SY5Y cells during short or long exposure to nicotine. *Br. J. Pharmacol.,* **146**, 1087–1095.

Streit, J. (1993) Regular oscillations of synaptic activity in spinal networks in vitro. *J. Neurophysiol.,* **70**, 871–878.

Sun, H., Kawahara, Y., Ito, K., Kanazawa, I., Kwak, S. (2006) Slow and selective death of spinal motor neurons in vivo by intrathecal infusion of kainic acid: implications for AMPA receptor-mediated excitotoxicity in ALS. *J. Neurochem.,* **98**, 782–791.

Taccola, G. & Nistri, A. (2006a) Fictive locomotor patterns generated by tetraethylammonium application to the neonatal rat spinal cord in vitro. *Neuroscience,* **137**, 659–670.

Taccola, G., Margaryan, G., Mladinic, M. & Nistri, A. (2008) Kainate and metabolic perturbation mimicking spinal injury differentially contribute to early damage of locomotor networks in the in vitro neonatal rat spinal cord. *Neuroscience,* **155**, 538–555.

Taccola, G., Mladinic, M., Nistri, A. (2010) Dynamics of early locomotor network dysfunction following a focal lesion in an in vitro model of spinal injury. *Eur. J. Neurosci.,* **31**, 60–78.

Takeda, D., Nakatsuka, T., Gu, J.G., Yoshida, M. (2007) The activation of nicotinic acetylcholine receptors enhances the inhibitory synaptic transmission in the deep dorsal horn neurons of the adult rat spinal cord. *Mol. Pain,* **3**, 26.

Tortora, M., Corsini, S., Nistri, A. (2017) Nicotinic receptors modulate the onset of reactive oxygen species production and mitochondrial dysfunction evoked by glutamate uptake block in the rat hypoglossal nucleus. *Neurosci. Lett.* **639**, 43–48.

Wada, E., Wada, K., Boulter, J., Deneris, E., Heinemann, S., Patrick, J., Swanson, L.W. (1989) Distribution of alpha2, alpha3, alpha4 and beta2 neuronal nAChR subunit mRNAs in the central nervous system: a hybridization histochemical study in the rat. *J. Comp. Neurol.,* **284**, 314–335.

Wada, E., McKinnon, D., Heinemann, S., Patrick, J., Swanson, L.W. (1990) The distribution of mRNA encoded by a new member of the neuronal nicotinic acetylcholine receptor gene family (α5) in the rat central nervous system. *Brain Res.,* **526**, 45–53.

Whiting, P.J., Lindstrom, J.M. (1986a) Purification and characterization of a nicotinic acetylcholine receptor from chick brain. *Biochemistry,* **25**, 2082–2093.

Whiting, P., Lindstrom, J. (1986b) Pharmacological properties of immuno-isolated neuronal nicotinic receptors. *J. Neurosci.,* **6**, 3061–3069.

Whiting, P., Lindstrom, J. (1987) Purification and characterization of a nicotinic acetylcholine receptor from rat brain. *Proc. Natl. Acad. Sci. U.S.A.,* **84**, 595–599.

Wokke, J. (1996) Riluzole. *Lancet,* **348**, 795–799.

Xue, M.Q., Liu, X.X., Zhang, Y.L., Gao, G.F. (2014) Nicotine exerts neuroprotective effects against β-amyloid-induced neurotoxicity in SH-SY5Y cells through the Erk1/2-p38-JNK-dependent signaling pathway. *Int. J. Mol. Med.,* **33**, 925-933.

Zhang, N., Yin, Y., Xu, S.J., Wu, Y.P., Chen, W.S. (2012) Inflammation & apoptosis in spinal cord injury. *Indian J. Med. Res.,* **135**, 287-296.

Figure Legends

Fig. 1. Dose dependent effect of nicotine on day 1 on the isolated spinal cord. (A) Sample records of polysynaptic reflexes during application of 10 µM (upper panel) and 1 µM (lower panel) nicotine (N) for 4 h followed by 1 h wash with standard Krebs solution. Plots of changes in polysynaptic reflex area (B) and amplitude (C) with respect to control (at 0 min) by application of different concentrations (10, 2, 1, 0.5; µM; n = 3, 4, 5, 3 respectively) of nicotine for 4 h (240 min) followed by 1 h wash. Note decline in polysynaptic area and amplitude with 10 µM (***P = 0.001, U = 1 and *P = 0.017, U = 10, respectively; Mann Whitney-test; Control vs N 20 min) and 2 µM (**P = 0.007, t_{12} = 3.278 and P = 0.006, t_{12} = 3.314, respectively; Control vs N 20 min) of nicotine applied for 20 min, whereas there was no significant change in polysynaptic area and amplitude with 1 and 0.5 µM nicotine after 20 min of application (P = 0.089, U = 27; P = 0.058, t_{22} = 2.004 and P = 0.838, U = 42; P = 0.775, U = 49; Mann Whitney-test, respectively; Control vs N 20 min). No recovery in reflex area and amplitude during wash after 10 and 2 µM nicotine (P = 0.075, t_{14} = 1.921; P = 0.218, t_{14} = –1.291 and P = 0.059, U = 39; 0.563, t_{12} = 0.595, respectively; Control vs Wash). Reflex area was significantly recovered during wash after 1 µM nicotine (4h) (P = 0.027, U = 23; Mann Whitney-test; Control vs wash).

Fig. 2. VR depolarization evoked by kainate (KA) or nicotine administration. (A) Sample record of depolarization induced by 50 μM KA or nicotine (10 and 1 μM). (B) Histograms depict maximum depolarization induced by KA (n = 10) or nicotine (10, 2, 1, 0.5 μM; n = 5, 4, 6, 4, respectively). No significant depolarization was evoked by 2, 1 and 0.5 μM nicotine (P = 0.343, t_8 = –1.009, 2N vs 1N; P = 0.432, t_6 = 0.842, 2N vs 0.5N; P = 0.749, t_8 = –0.332; Student's t-test). However, 10 μM nicotine induced a signficant depolarization in comparison to 2, 1 and 0.5 μM nicotine (***P = 0.001, t_7 = –5.211, 10 N vs 2 N; **P = 0.005, t_9 = 3.738, 10 N vs 1 N; P = 0.005, t_7 = –4.033, 10 N vs 0.5 N; μM; Student's t-test).

Fig. 3. Changes in DR stimulation evoked synaptic transmission and fictive locomotion after 24 (day 2) *in vitro*. (A-D) Representative records of monoynaptic (A), polysynaptic (B) reflexes, DR induced (C) and NMDA+5HT evoked (D) fictive locomotion in sham and 1 μM nicotine (N) solution (applied for 4 h on the preceding day). (E-G) Bar graphs showing significant depression of monosynaptic (**P = 0.003, t_{20} = 3.334; Student's t-test) (E) and polysynaptic reflex amplitude (F) and area (G) (*P = 0.027, U = 15, Mann Whitney-test; P = 0.029, t_{16} = 2.391, respectively; sham vs N; n = 10, sham; n = 7 for nicotine). (H-J) Histograms representing number of oscillations induced by DR stimulus trains in spinal cords treated with nicotine for 4 h (P = 0.013, U = 87.5, Mann Whitney-test; sham vs N). No change in cumulative depolarization and area of fictive locomotion was observed (P = 0.343, t_{19} = 0.973; P = 0.993, t_{19} = 0.00936, respectively; sham vs N). (K) Plot showing significant decline in amplitude (***P = 0.001, t_{15} = 5.410; sham vs N) and with no increase in periodicity (P = 0.430, t_{15} = –0.811, respectively; sham vs N) of chemically induced fictive locomotion by nicotine application for 4 h.

Fig. 4. Changes in neurons (identified with NeuN positivity, red), and motoneuron number (SMI32 staining, green) and immunofluorescence intensity of glia (immunolabeled with S100, green or GFAP, red) induced by previous (24 h earlier) 1 μM nicotine (4 h) treatment. DAPI (blue) was used as cell nuclear marker. (A-C) Histochemical examples of dorsal horn neurons (A), motoneurons (B), and dorsal horn glia (C). (D) Bar graphs quantify increased number of neurons in the dorsal horn after application of N (4 h) (***P = 0.001, t_{16} = –5.406; sham vs N), whereas no significant change was observed in central and ventral horn (P = 0.859, U = 43, Mann Whitney test; P = 0.104, t_{16} = 1.726, respectively, sham vs N). (E) Histograms illustrate

increase in number of motoneurons after N treatment (4 h) (P = 0.001; t_{24} = –3.798; sham vs N). (F, G) Bar graphs show no change in immunofluorescence intensity (AU) of glia after N (4h) treatment in all three ROI (GFAP- D: P = 0.715, t_8 = –0.379; C: P = 0.675, t_8 = –0.435; V: P = 0.801, t_8 = –0.260 and S100- D: P = 0.562, t_9 = 0.601; C: P = 0.276, t_9 = 1.159; V: P = 0.265, t_8 = 1.199, respectively, sham vs N) (n = 3-6 spinal cords; 3-10 sections/preparation). Scale bar = 100 µm.

Fig. 5. Reflexes and fictive locomotion recorded 24 h *in vitro* after KA or KA followed by nicotine for 4 h (KA/N 4 h). (A-D) Sample records of mono-, polysynaptic reflexes, electrically and chemically induced fictive locomotion after application of KA (n = 8) or KA/N 4 h (n = 8). (E) shows no change in monosynaptic responses (P = 0.874, U = 70, Mann Whitney-test), whereas a measurable rise in polysynaptic reflex amplitude and area (F,G) was detected after KA followed by N (**P = 0.002, U = 23; *P = 0.014, U = 37, Mann Whitney-test, respectively; KA vs KA/N 4h). (H-K) Significant increase in electrically (H-J) (number of oscillations, ***P = 0.001; U = 0, Mann Whitney-test; cumulative depolarization, P = 0.005, t_{22} = –3.092) and chemically induced (K) (amplitude, P = 0.001; t_{19} = –6.563; period, P = 0.001, U = 28, Mann Whitney-test) fictive locomotion. There was no significant change in the area of DR evoked cumulative depolarization (P = 0.081, U = 35) after N application to KA treated spinal cords.

Fig. 6. Histochemical damage 24 h after KA (1 h) or KA followed by nicotine (N, 4 h). (A, B) Micrographs depicting examples of high pyknosis (A, staining with DAPI, blue), low neuronal (A, NeuN, red) and motoneuronal numbers (B, green) after KA application: this effect was prevented by KA/N 4h (DAPI- Dorsal: ***P = 0.001, U = 108; Central: P = 0.001, U = 0; Ventral: P = 0.001, U = 189, Mann Whitney-test; NeuN- Dorsal: P = 0.001, t_{16} = –11.612; Central: **P = 0.01, t_{16} = –2.944; Ventral: *P = 0.05, t_{16} = –2.05; SMI32- P = 0.001, U = 3; comparisons were between KA vs KA/N 4h), n = 3-5 spinal cords; 3-10 sections/preparation. Scale bar = 100 µm.

Fig. 7. Improved neuroprotection recorded at day 2 *in vitro* after former pretreatment with nicotine and KA (n = 8). Sample records representing changes in reflex activity and fictive locomotor patterns by excitotoxicity, effects prevented by co-application of nicotine with kainate followed by nicotine alone for further 4 h (KA+N/N 4h, n =8). (E-G) Histograms illustrating

recovery in polysynaptic reflex amplitude (F) and area (G) (***P = 0.001, U = 3 and P = 0.001, U = 10, Mann Whitney-test, respectively; KA vs KA+N/N 4h), despite no improvement in monosynaptic reflex activity (P = 0.864, U = 80, Mann Whitey-test) (E). (H-K) Bar plots show presence of DR evoked (number of oscillations: P = 0.001, U = 0; cumulative depolarization: P = 0.001, U = 5 and area: P = 0.001, U = 11, Mann Whitney-test) and chemically evoked fictive locomotion (amplitude: *P = 0.012, U = 24 and periodicity: **P = 0.004, U = 32, Mann Whitney-test).

Fig. 8. Effect of co-application of nicotine with KA on disinhibited bursts recorded on day 2 *in vitro*. (A) Representative records obtained after KA (n = 8) or KA+N/N 4h (n = 8) application on the day before. (B, C) Histograms depicting raised burst amplitude after KA+N/N 4h treatment (*P = 0.027, t_{14} = –2.794; KA vs KA+N/N 4 h) with no change in the number of bursts (P = 0.356, t_{14} = 0.989).

Fig. 9. Changes in Ca^{2+} transients evoked by application of strychnine and bicuculline (Sham, n = 6; nicotine, N, n = 4; kainate, KA, n = 6 and KA+N/N 4h, n = 4; n is the number of slices, where 6-12 neurons analysed/slice) on day 2 in organotypic spinal cord slices *in vitro*. (A, B) In A snapshot of representative field of ventral horn neurons. Numbers indicate two representative cells whose Ca^{2+} transients are shown in B. Scale bar = 100 μm. In B representative Ca^{2+} events recorded in Sham, Nicotine, Kainate and KA+N/N 4h conditions (two sample neurons were selected from the same field). (C-E) KA induced a significant decrease in bursts number (C) (**P = 0.007, t_{10} = 3.353, sham vs KA; ***P = 0.001, t_8 = 7.822, N vs KA) and increased single burst duration (D) (*P = 0.03, U = 3, sham vs KA; P = 0.016, U = 20, N vs KA; Mann Whitney-test) without affecting cross-correlation factor (CCF) (E): this phenomenon was reversed by applying nicotine with KA(burst number: P = 0.001, t_8 = –10.055; burst duration: P = 0.016, U = 20, KA vs KA+N/N, Mann Whitney-test, respectively).

Fig. 10. Histological neuroprotection induced by co-application of nicotine with KA. (A, C, D) Example (A) and bar graphs show large reduction in excitotoxicity by co-application of nicotine with KA followed by nicotine for 4 h, and observed 24 h later. Note minimal pyknosis (A, C) when staining with DAPI (blue) (Dorsal: ***P = 0.001, U = 108; Central = P = 0.001, U = 0; Ventral: P = 0.001, U = 189, Mann Whitney-test; KA vs KA+N/N 4h). (A, D) shows good

preservation of neurons stained with NeuN antibody (red) (Dorsal: P = 0.001, t_{16} = –14.761; Central: P = 0.001, t_{16} = –7.122; Ventral: P = 0.001, t_{16} = –7.445) in all three ROI. (B, E) Sample images (B) and histograms (E) illustrate significant survival of motoneurons (tsained with SMI32; green) in ventral horn of spinal cord (P = 0.001, U = 3, Mann Whitney-test, KA vs KA+N/N 4h). Scale bar = 100 µm, n = 3-5 spinal cords; 3-10 sections/preparation.

Fig. 11. Effect of nAChR antagonists on VR reflexes and fictive locomotion after 24 h *in vitro*. (A-D) Representative records of alterations in reflexes (A, B) and fictive locomotion (C, D) produced by 4 h co-application of DHβE (10 µM, n = 5) and MLA (10 nM, n = 5) in comparison to sham. (A, E) DHβE, MLA or DHβE+MLA (n = 4) application depressed monosynaptic reflex which was significant with DHβE alone (*P = 0.035, t_{16} = 2.304, DHβE vs sham). (B, F, G) The polysynaptic area (G) has increased (P = 0.043, U = 8; P = 0.043, U = 8; P = 0.03, t_{12} = –2.469; D vs sham; M vs sham; D+M vs sham, respectively) with no significant change in amplitude (F) in comparison to sham (n = 13). (C, H-J) The number of oscillations (C, H) during electrically induced fictive locomotion was reduced by DHβE+MLA co-application in comparison to sham (**P = 0.006, U = 45.5; Mann Whitney-test, DHβE+MLA vs sham), with no significant change in the area and amplitude of cumulative depolarization. (D, K) The cycle amplitude of chemically induced fictive locomotion was significantly depressed in MLA and DHβE+MLA treated preparations (P = 0.02, t_{16} = 2.590; P = 0.004, t_{15} = 3.411, respectively, MLA vs sham, DHβE+MLA vs sham) while the periodicity was increased in MLA treated spinal cords (P = 0.001, t_{16} = -6.696, MLA vs sham).

Fig. 12. Effect of application of nAChR antagonists on spinal cord preparations studied *in vitro* on day 2 after kainate application. (A-D) Sample recordings of reflex responses (A, B) and fictive locomotor rhythms (C, D) following co-application of DHβE+MLA (1 h) together with KA or of KA alone. (E-J) Histograms representing no change in monosynaptic (E), and polysynaptic (F, G) reflexes and DR evoked fictive locomotion (H-J) in KA+D (n = 5), KA+M (n = 6) and KA+D+M (n = 4) treated preparations in comparison to KA (n = 8) alone. Note significantly larger amplitude of cumulative depolarization with KA+D+M treatment vs KA alone (*P = 0.042, U = 10; Mann Whitney test). (D, J) emergence of chemically induced fictive locomotor rhythms the day after application of antagonists with KA (cycle amplitude: ***P =

0.024, $F_{3,17}$ = 4.296; one way analysis of variance test). There was no significant difference in periodicity among various treatments while no cycles appeared after KA alone (D, J).

Fig. 13. Effects of nAChR antagonists on neuroprotection evoked by nicotine on spinal cords after 24 *in vitro*. (A-C) Despite no variation in monosynaptic responses, DHβE (4 h) depressed amplitude of polysynaptic reflexes when co-applied with nicotine+KA (*P = 0.019, t_{11} = 2.756, KA+N/N 4 h vs KA+D+N/D+N 4 h). Likewise, the combination of DHβE+MLA suppressed nicotine evoked neuroprotection in terms of polysynaptic amplitude (P = 0.05, t_9 = 2.203, KA+N/N 4 h, vs KA+D+M+N/D+M+N 4 h). MLA alone could not prevent the effect of nicotine+KA. (C) Significant change in reflex area was observed with DHβE was applied with nicotine+KA with no significant change with combination of DHβE+MLA (*P = 0.049, t_{12} = 2.190, KA+N/N 4h vs KA+D+N/D+N 4 h; P = 0.136, t_9 = 1.635, KA+N/N 4h vs KA+D+M+N/D+M+N 4 h). (D, E) In the presence of KA+nicotine, DHβE (4h) alone significantly reduced the amplitude and area (E) (P = 0.047, t_{12} = 2.212 and P = 0.044, t_{12} = 2.248, respectively; KA+N/N 4h vs KA+D+N/D+N 4h) of cumulative depolarization (that did not generate oscillations). (K) Chemically induced fictive locomotor patterns were observed in all preparations without any significant difference (amplitude: P = 0.684. $F_{3,23}$ = 0.504; Period: P = 0.746, $F_{3,23}$ = 0.4; one way analysis of variance test). n = 8, 6, 6, 4; KA+N/N 4 h, KA+D+N/D+N 4h, KA+M+N/M+N 4h, KA+D+M+N/D+M+N 4 h, respectively.

Fig. 14. Histological damage evoked by co-application of nAChR antagonists with KA and nicotine. (A, C) Co-application of DHβE and MLA with KA+N/N 4 h treatment exaggerated the neuronal loss detected with NeuN staining (red) (D: ***P = 0.001, $F_{3,36}$ = 20.527; C: P = 0.001, $F_{3,35}$ = 32.380; V: P = 0.001, $H_{(3)}$ = 29.851; one way analysis of variance test; KA+N/N 4 h vs KA+D+N/D+N 4 h; KA+N/N 4 h vs KA+M+N/M+N 4 h; KA+N/N 4 h vs KA+D+M+N/D+M+N 4 h). (B, D) DHβE (4 h) and DHβE+MLA when co-applied with KA+N/N 4h enhanced motoneuronal loss detected with SMI32 staining (green) (P = 0.001, t_{29} = 4.736; *P = 0.028, t_{28} = –2.314; P = 0.001, t_{28} = 6.197, respectively; KA+N/N 4 h vs KA+D+N/D+N 4 h; KA+N/N 4 h vs KA+D+M+N/D+M+N 4 h), whereas MLA co-application with KA+N/N 4h did not change the effect of KA+nicotine (D). Scale bar = 100 µm, n = 3-5 spinal cords; 3-10 sections/preparation.

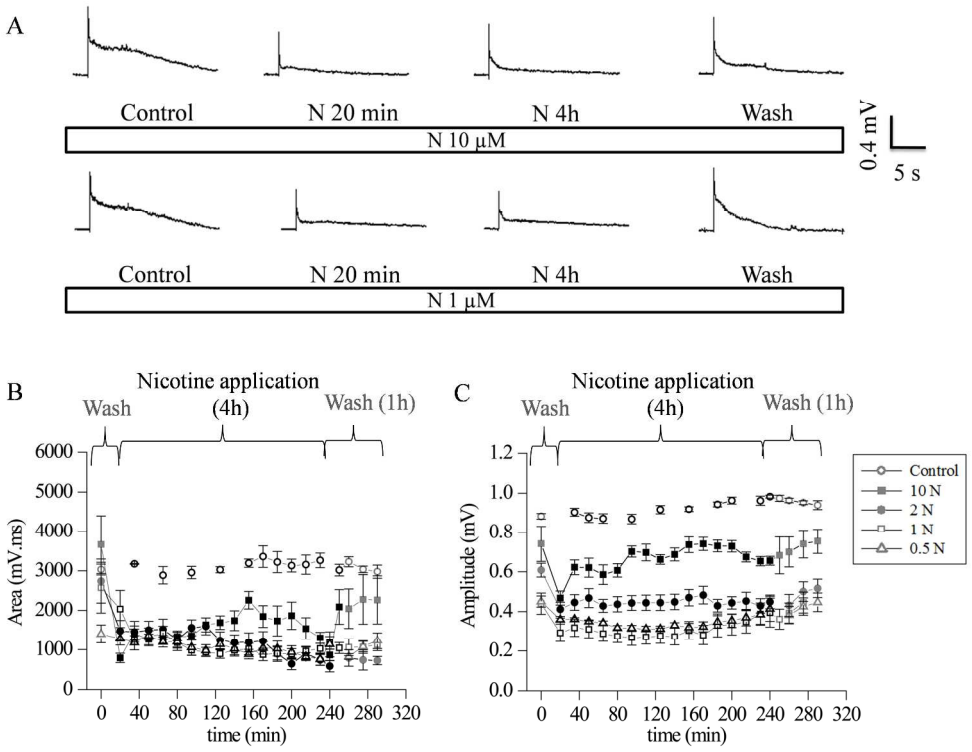

Figure 1

254x190mm (300 x 300 DPI)

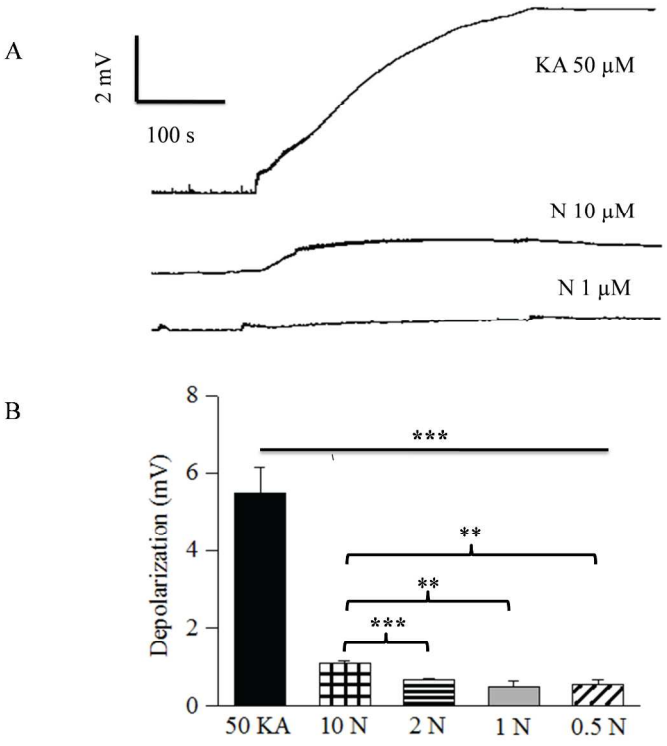

Figure 2

254x190mm (300 x 300 DPI)

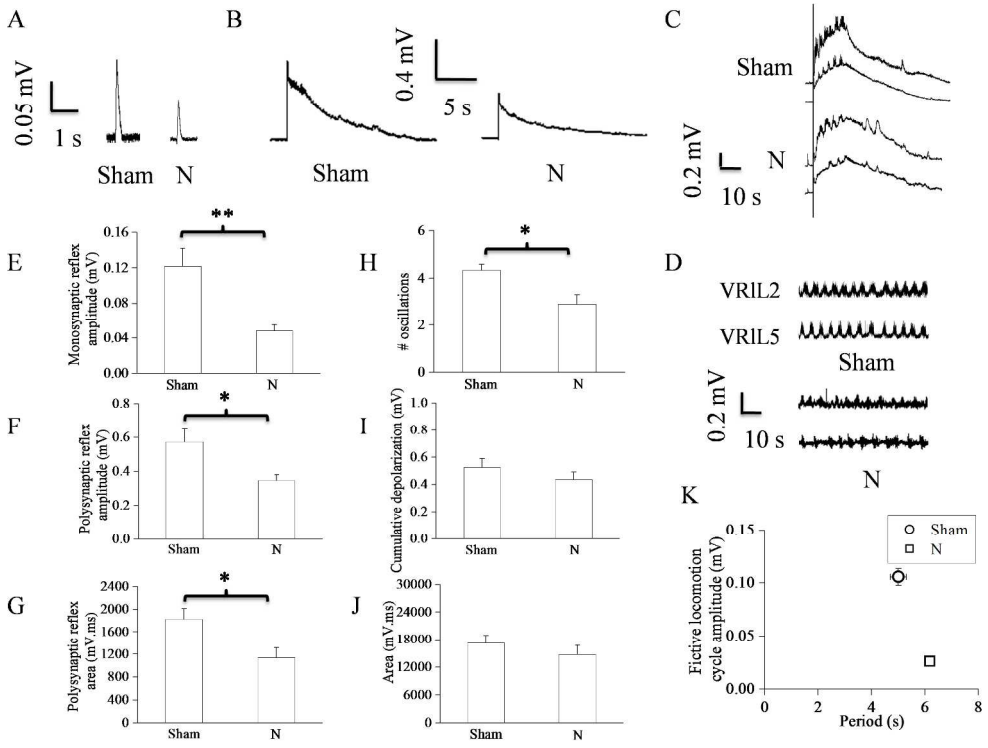

Figure 3

254x190mm (300 x 300 DPI)

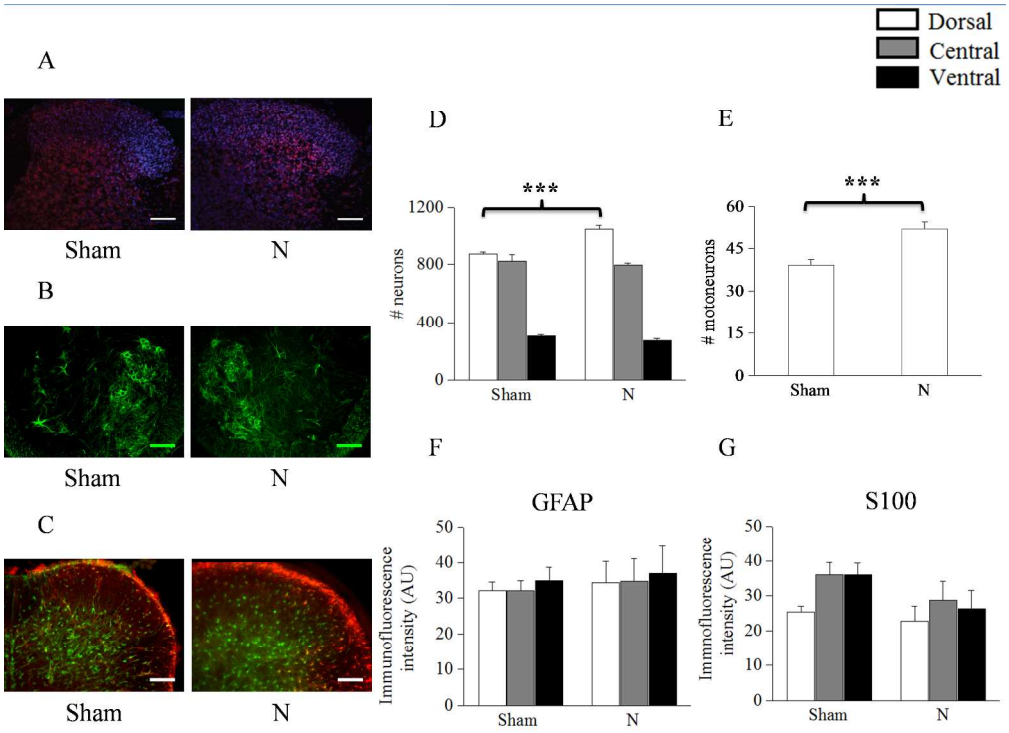

Figure 4

254x190mm (300 x 300 DPI)

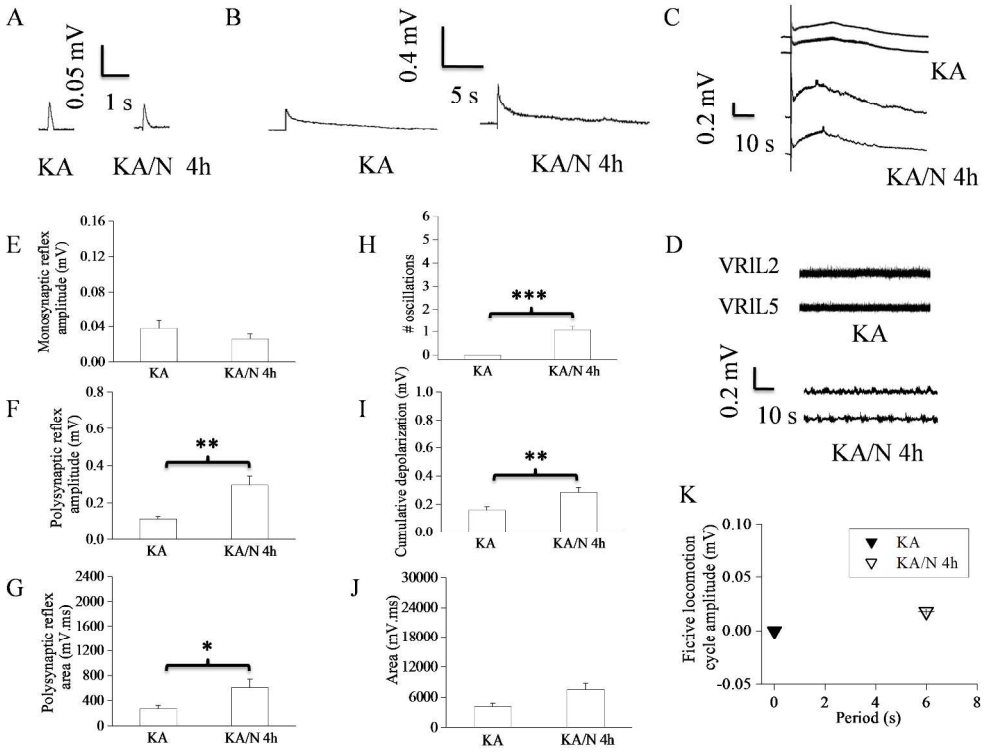

Figure 5

254x190mm (300 x 300 DPI)

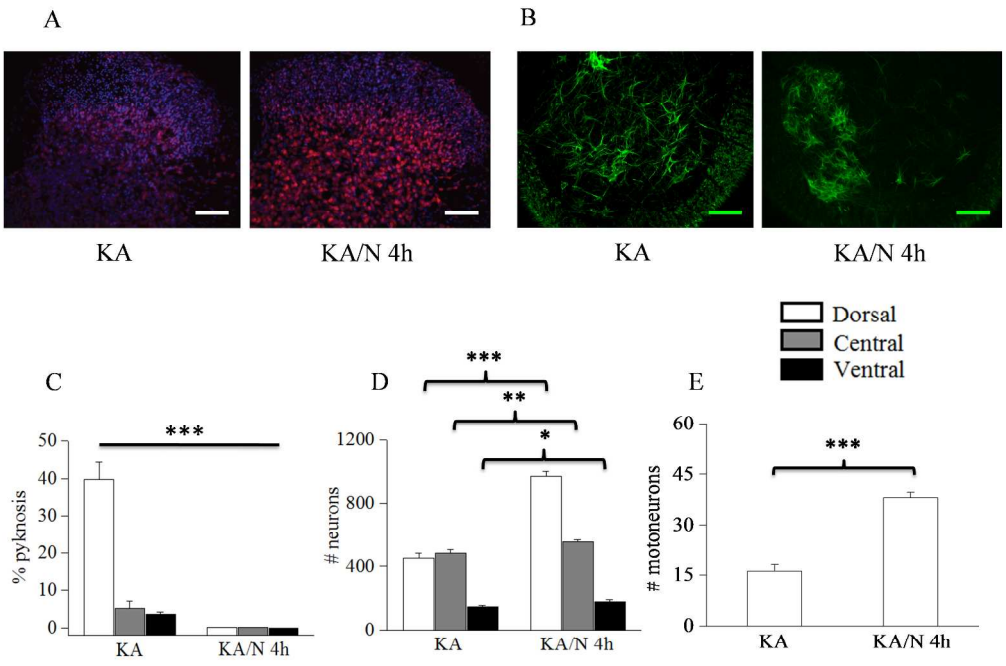

Figure 6

254x190mm (300 x 300 DPI)

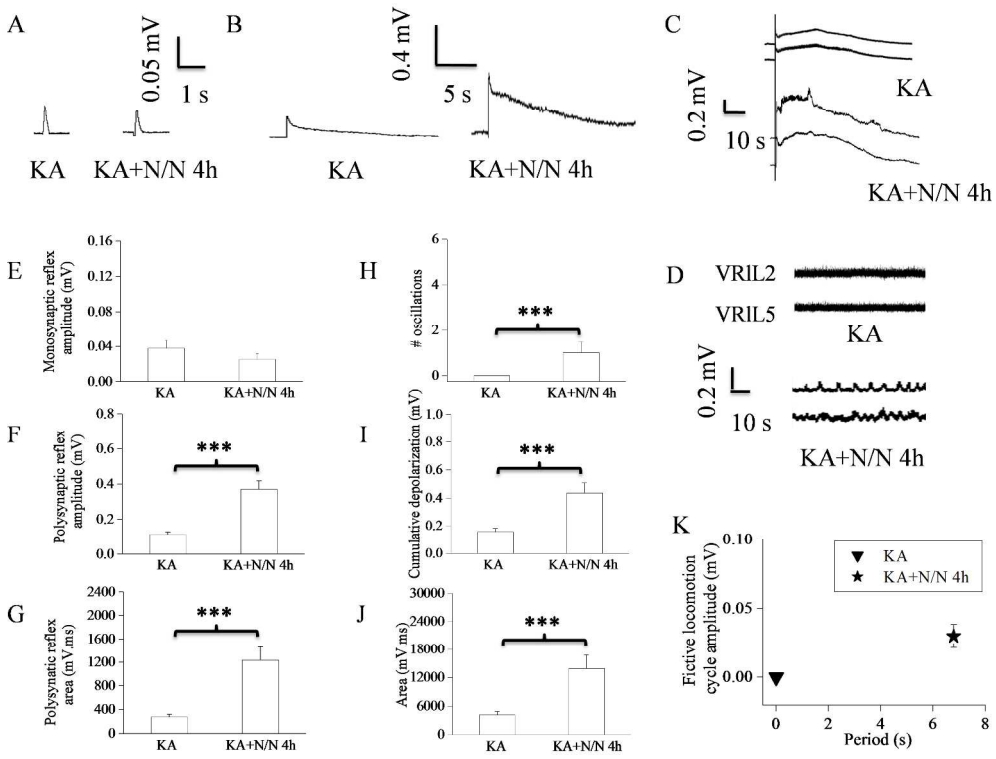

Figure 7

254x190mm (300 x 300 DPI)

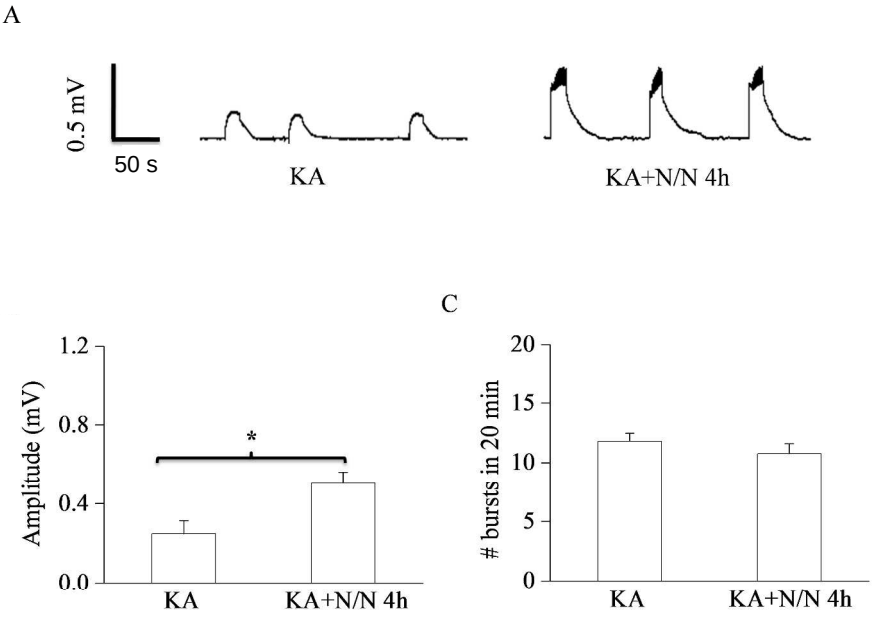

Figure 8

254x190mm (300 x 300 DPI)

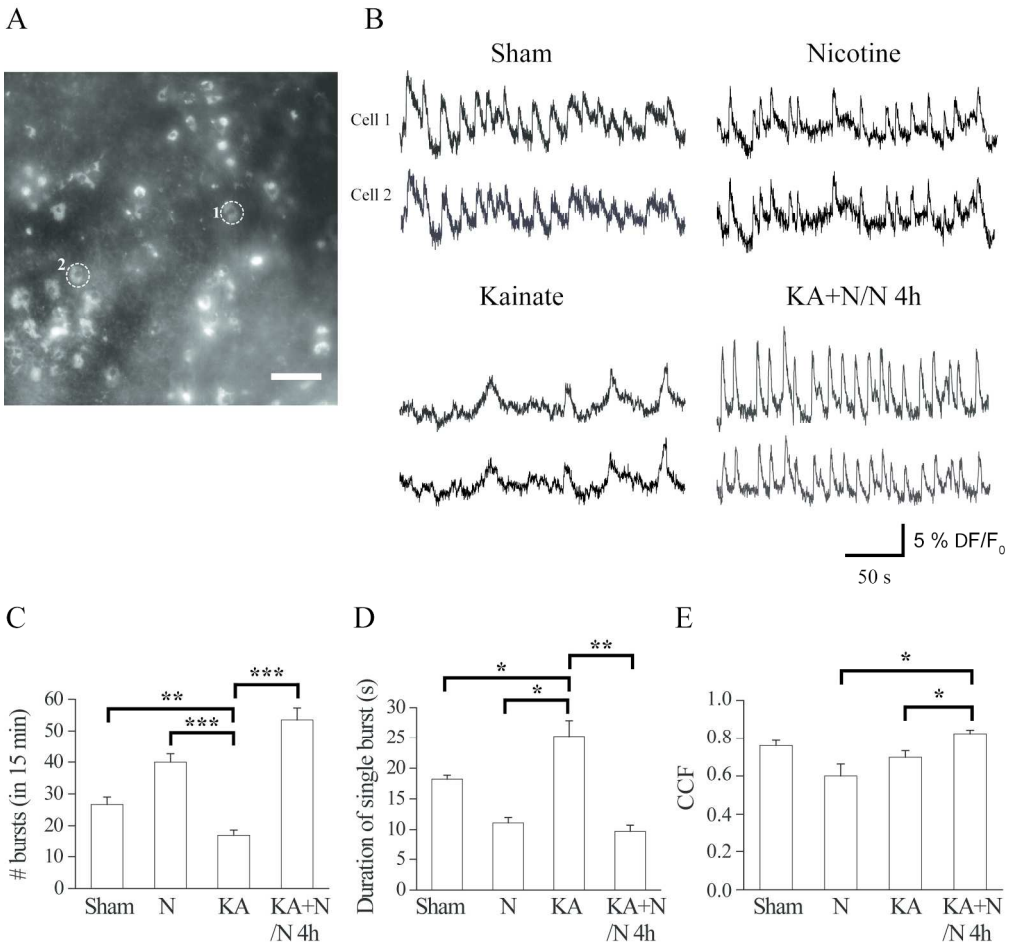

Figure 9

207x195mm (300 x 300 DPI)

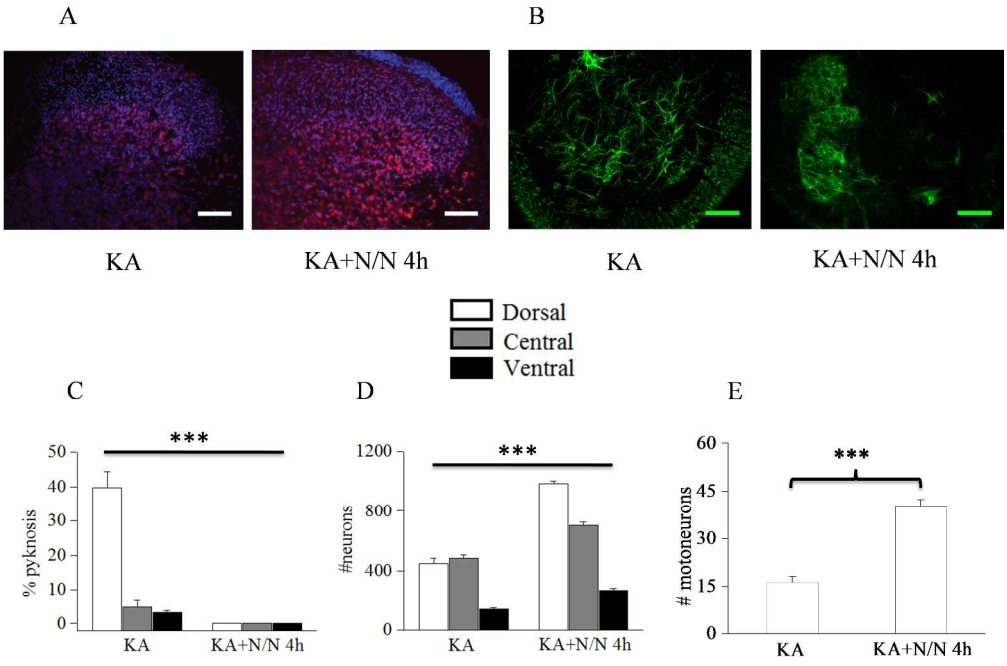

Figure 10

254x190mm (300 x 300 DPI)

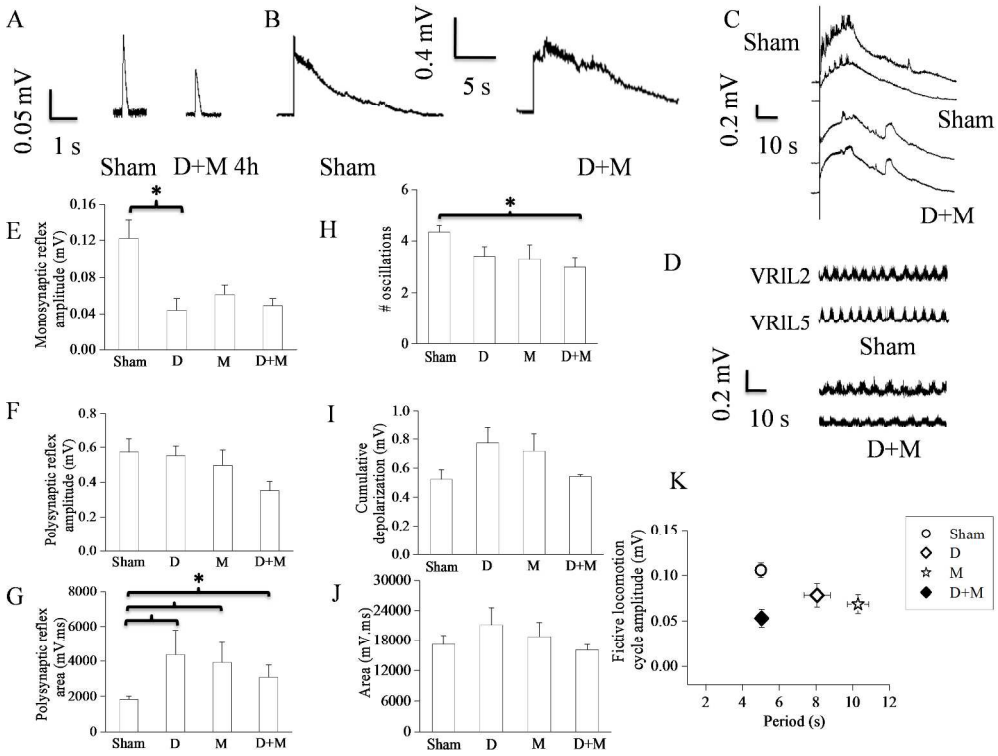

Figure 11

254x190mm (300 x 300 DPI)

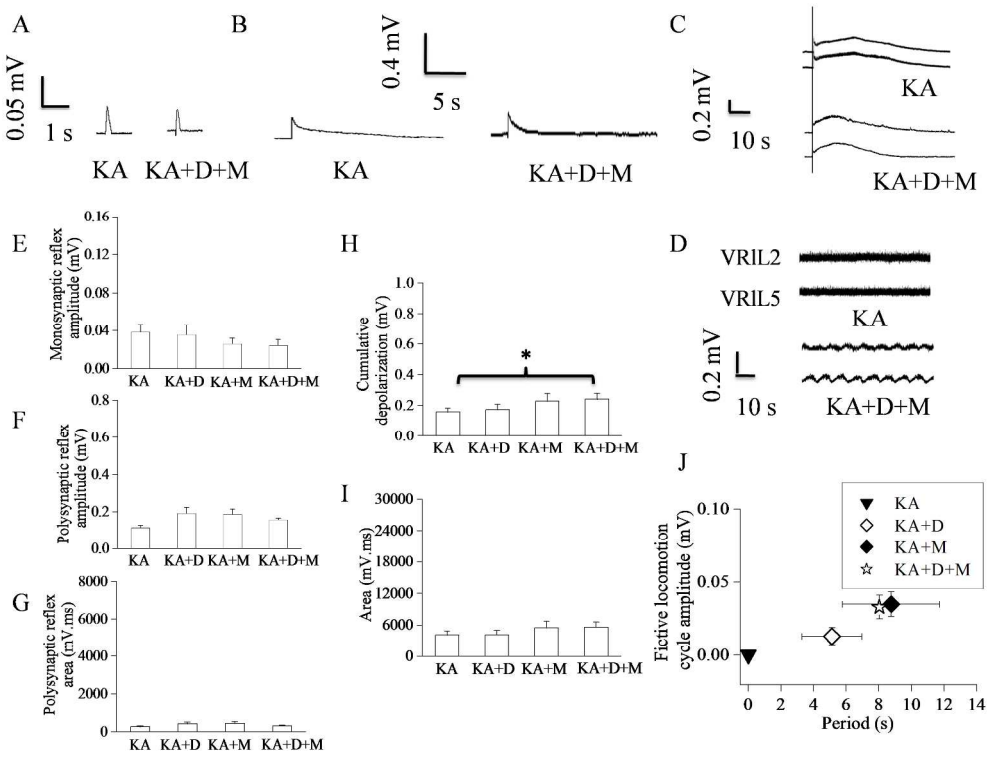

Figure 12

254x190mm (300 x 300 DPI)

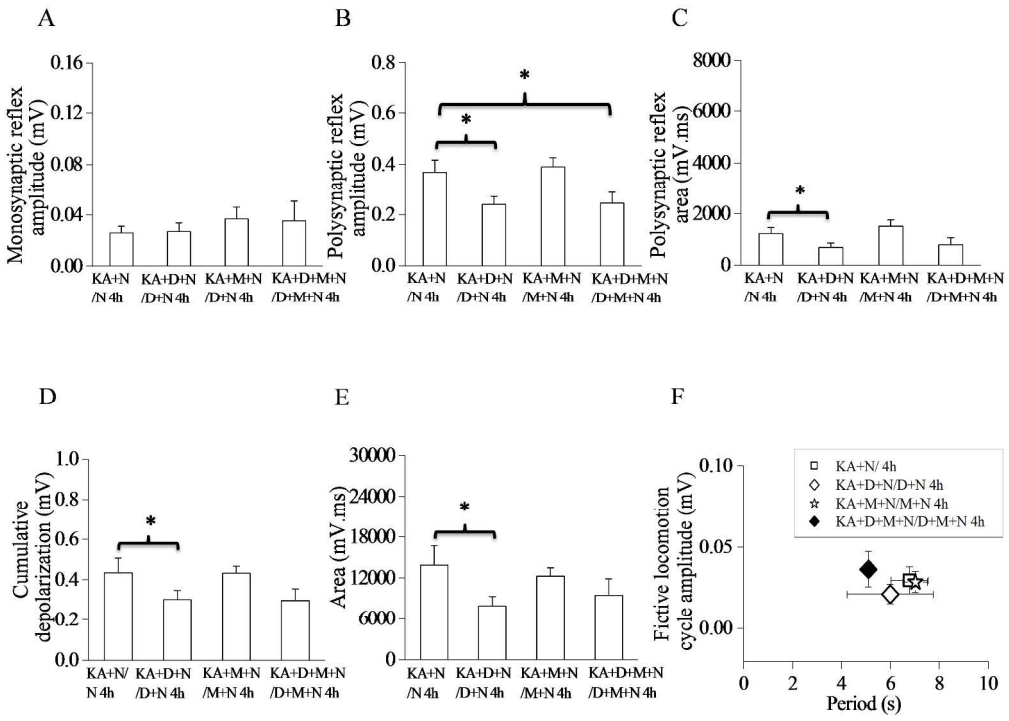

Figure 13

254x190mm (300 x 300 DPI)

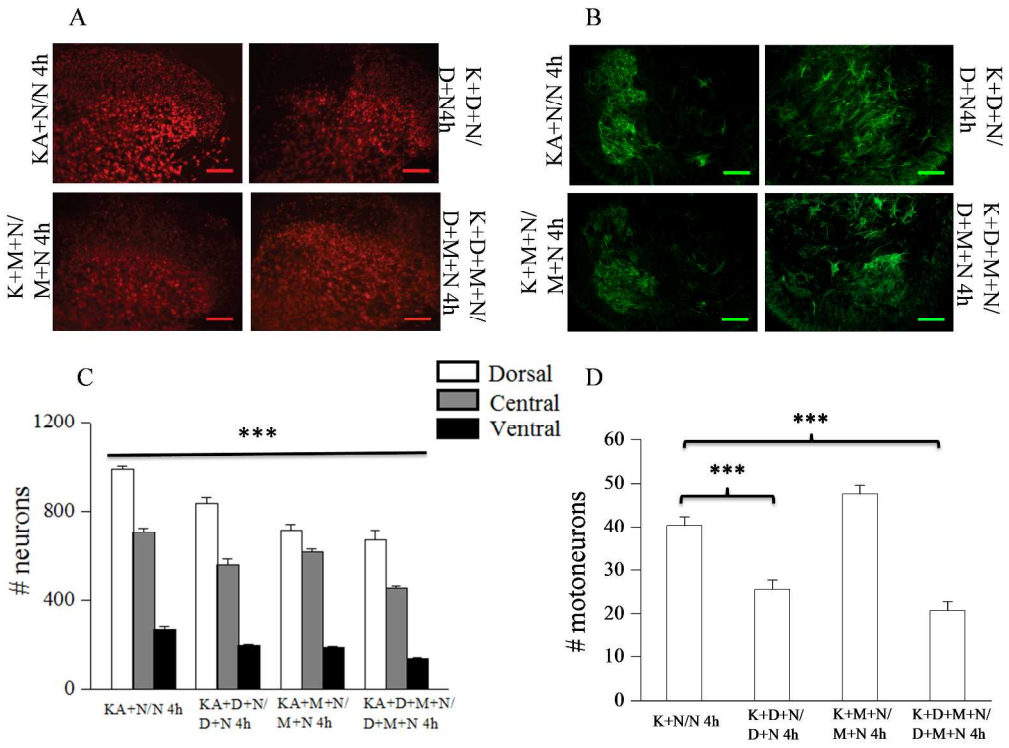

Figure 14

254x190mm (300 x 300 DPI)

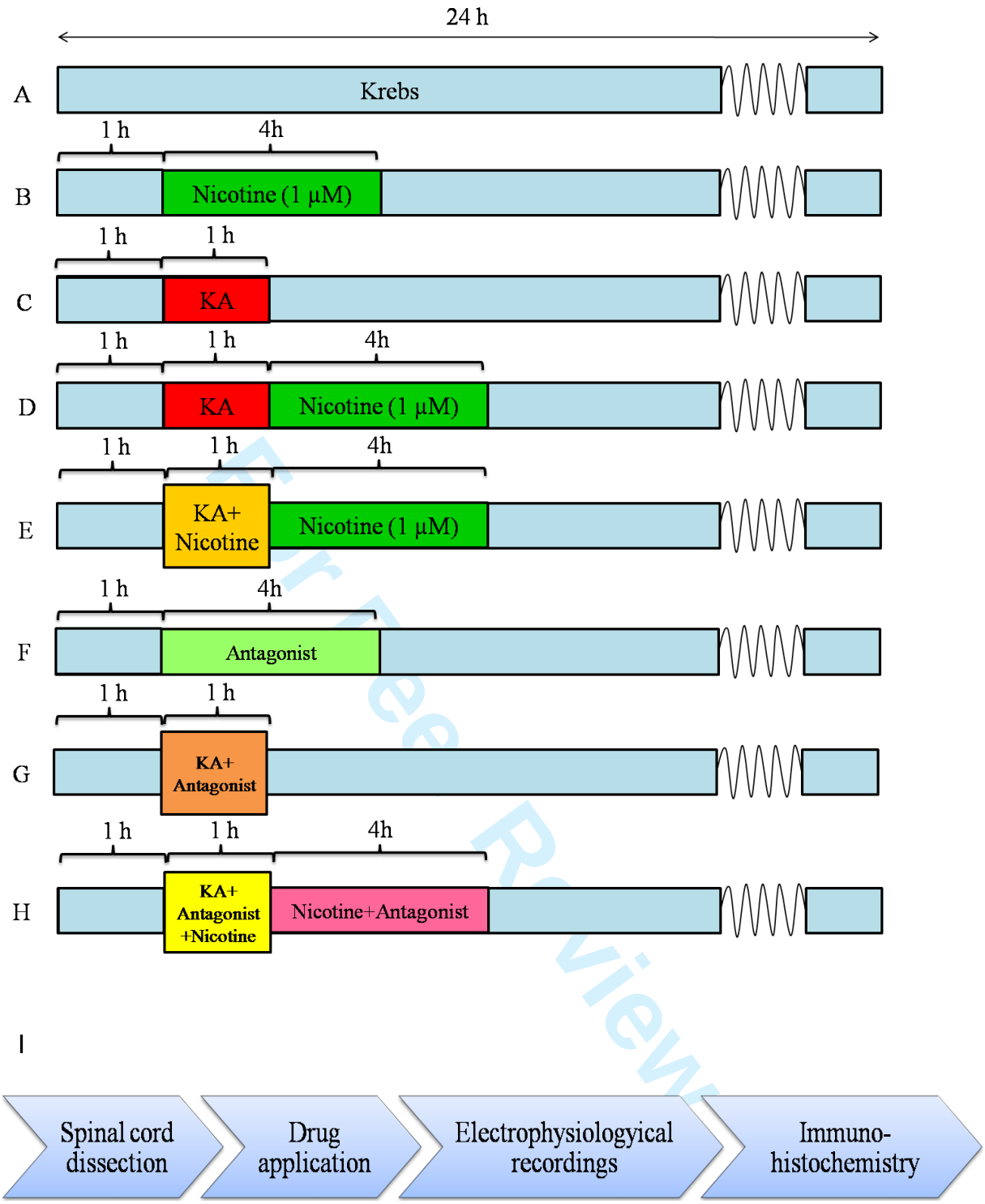

Supplemental Fig. 1. Schematic representation of experimental procedures used. (A-I) Diagram of different protocols used for drug administration where kainate (KA) was the excitotoxic stimulus and nicotine (1 µM) was applied for 4 h. Two nAChR antagonists, DHβE and MLA alone or in combination (DHβE+MLA) were used for 4 h.

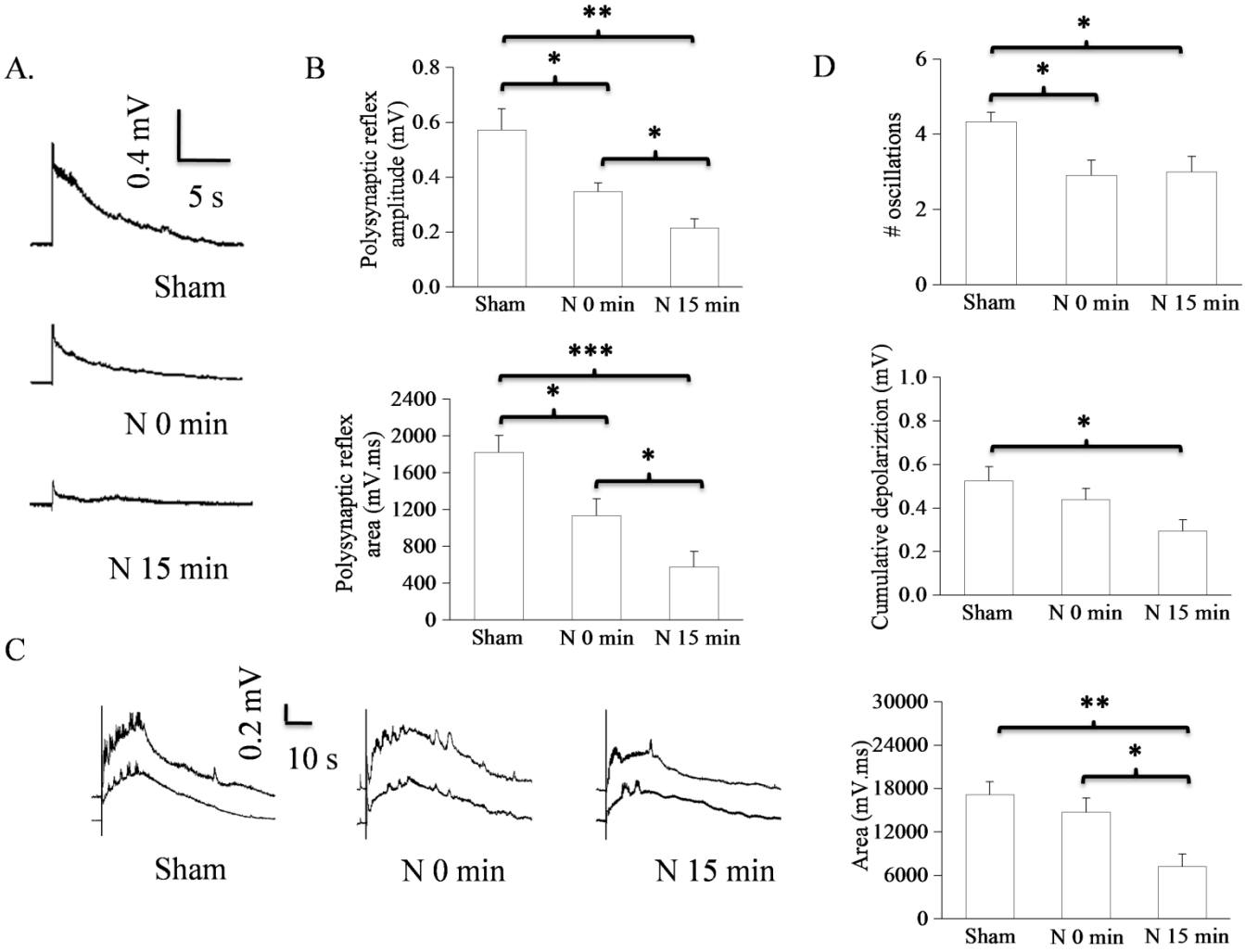

Supplemental Fig. 2. Changes in polysynaptic reflexes and electrically evoked fictive locomotion evoked by 1 µM nicotine reapplied on the second day in vitro after first application of nicotine (4 h) on the previous day. N0 indicates response immediately prior to second application of nicotine while sham indicates naïve preparations.(A, C) Sample records of changes in polysynaptic responses (A) and DR evoked fictive locomotion (C) by re-applying nicotine on day 2 for 15 min. (B) Bar graphs show further decrease in polysynaptic reflex amplitude and area by re-application of nicotine for 15 min (n = 4) in comparison to sham (n = 9) (**P = 0.002, U = 68; ***P = 0.001, t_{16} = 4.949, respectively ; sham vs N 15 min) and to nicotine 4 h treated spinal cords on day 1 (*P = 0.012, t_{14} = 2.877; P = 0.030, U = 59, respectively; N 0 min vs N 15 min). Fig. D shows depression in number of oscillations (P = 0.019, U = 42, sham vs N 15 min), cumulative depolarization amplitude (P = 0.041, t_{13} = 2.274, sham vs N 15 min) and area (P = 0.007, U = 36, sham vs N 15 min; P = 0.039, t_{11} = 2.345, N 0 min vs N 15 min) of DR evoked fictive locomotion.

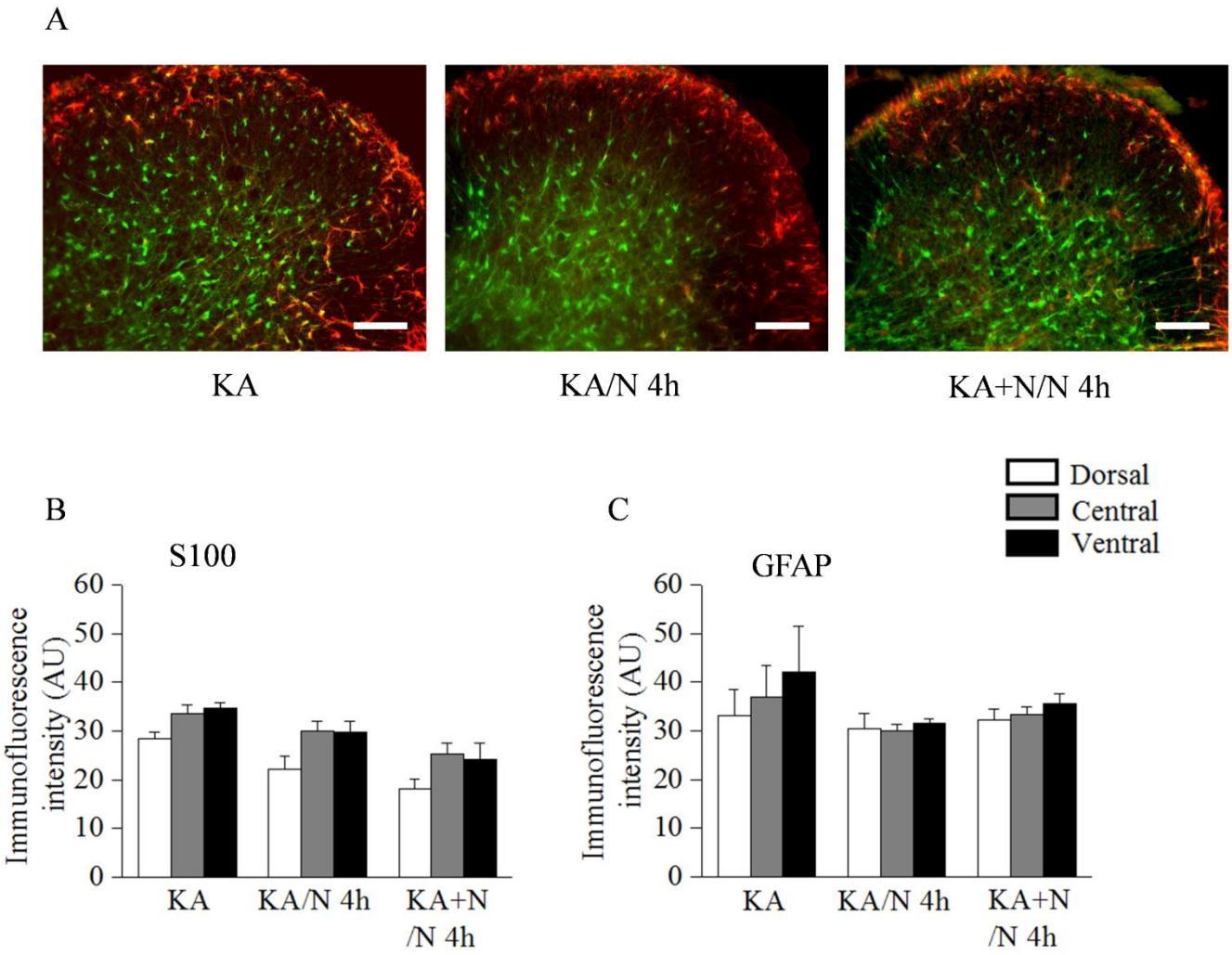

Supplemental Fig. 3. (A-C) No significant change in immunofluorescence intensity (AU) of astrocytes (green; S100 staining) and general glia (red; GFAP staining) by KA together with or followed by nicotine for 4 h (KA/N 4 h and KA+N/N 4 h, respectively). *n* = 3-6 spinal cords; 3-10 sections/preparation. Scale bar = 100 µm.

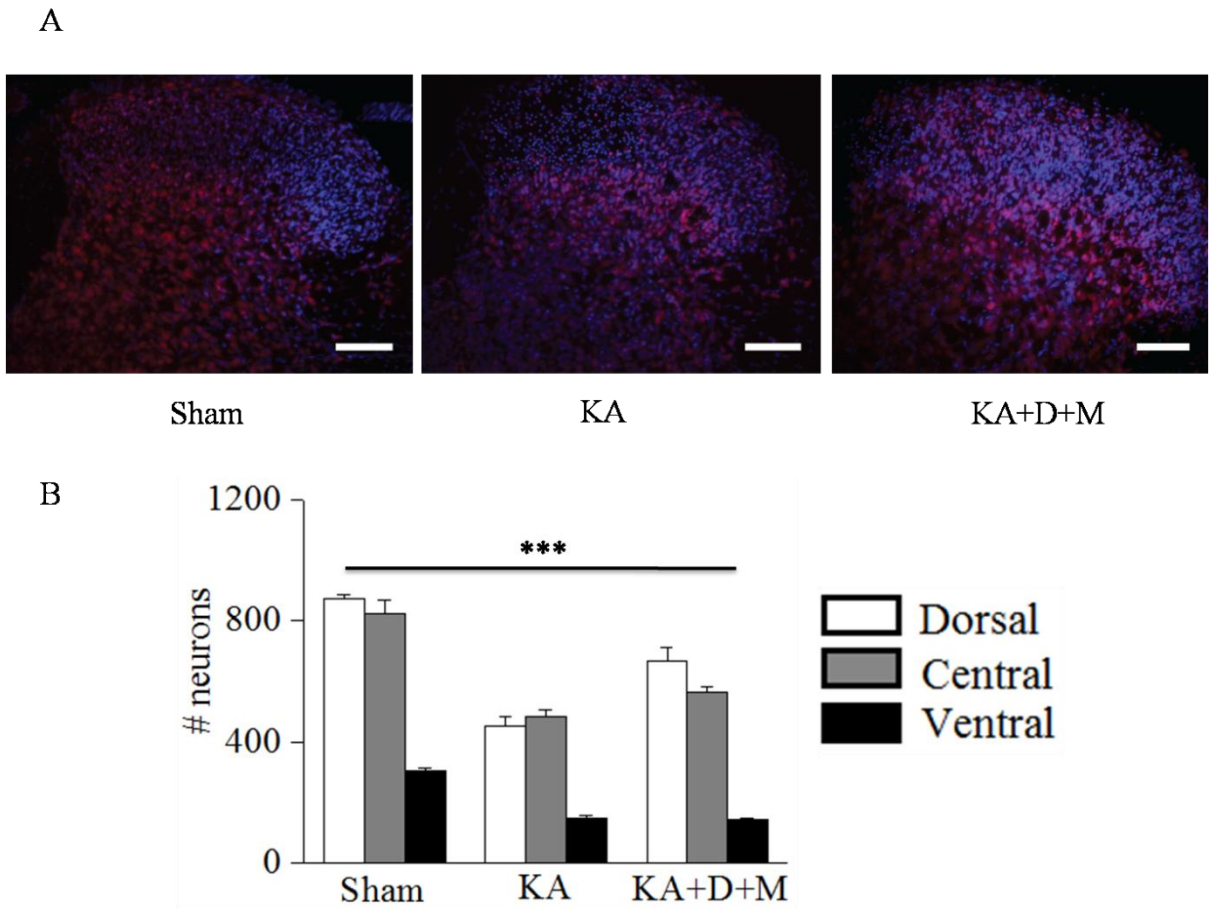

Supplemental Fig. 4. Example (A) of dorsal horns showing neurons (stained with NeuN, red) and cells (stained with DAPI, blue) 24 h after application of KA or KA plus nAChR antagonists. Histograms (B) show average neuronal numbers calculated after 24 h in vitro in sham condition (no treatment) or after 1 h application of kainate alone or with KA+DHβE+MLA (Dorsal: ***P = 0.001, t_{16} = 11.736; Central*:* P = 0.001, U = 0; Ventral: P = 0.001,t_{16} = 11.034,sham vs KA; Dorsal: P = 0.001, t_{18} = –3.927; Central: *P = 0.012, t16 = –2.828; Ventral; P = 0.429, t_{16} = 0.812, KA vs KA+D+M; Dorsal*:* P = 0.001, t_{18} = –4.044; Central: P = 0.001, U = 81; Ventral: P = 0.001, U = 0, sham vs KA+D+M). n = 3-5 spinal cords; 3-10 sections/preparation. Scale bar = 100 µm.

6 DISCUSSION

The principal findings of the present study reported in this thesis are summarized as:

- The neuroprotection produced by Methylprednisolone sodium succinate (MPSS; after 24 h in vitro SCI) was confined to white matter when damaged by providing dysmetabolic/hypoxic conditions with pathological medium (PM) applied for 1 h.

- MPSS could not reverse the excitotoxic damage evoked by kainate (100 µM) applied for 1 h.

- Histologically, delayed application of propofol has arrested neuronal and motoneuronal damage by kainate (50 µM).

- No good recovery in fictive locomotor patterns by propofol treatment, whereas disinhibited rhythmicity was improved.

- Nicotine (10 µM) was toxic.

- Nicotine (1 µM) administration has shown neuroprotective effects to spinal locomotor networks from excitotoxic damage induced by kainate (50 µM).

- Good histological recovery of motoneurons and neurons by nicotine (1 µM) after excitotoxic insult.

- Pre-treatment of celastrol has shown substantial neuroprotective effects against kainate-induced excitotoxicity.

1. In vitro spinal injury model

Current data were acquired by using an in vitro neonatal rat SCI model based on transient (1 h) application of kainate or pathological medium (PM). Although the in vitro preparations are immature, they possess a number of advantages such as giving an opportunity to study synaptic transmission, fictive locomotor oscillatory cycles recorded from lumbar ventral roots (Kiehn, 2006), intrinsic rhythmicity (Bracci et al., 1996a, b; Taccola & Nistri, 2007), and motoneuronal properties. Furthermore, these preparations provide an insight into pediatric SCI, show limited tissue damage which resembles actual new SCI cases (Jain et al., 2015), and allow studying delayed drug application with survival time up to 24 h (Shabbir et al., 2015; Nasrabady et al., 2012). In addition to in vivo animal models of SCI (Onifer et al., 2007), in vitro models provide useful data as they reduce the complexity of pathophysiology of in vivo SCI and help to identify particular injury processes without interference by general anaesthesia or blood pressure changes (Kuzhandaivel et al., 2011).

2. Excitotoxicity produces structural and functional deficits during spinal insult

In the past decades, excitotoxicity, a type of neurotoxicity produced by over-activation of glutamatergic system, has been at the centre stage of stroke research. Glutamate is the primary neurotransmitter in the adult CNS. Glutamate plays important roles in various physiological processes such as rapid synaptic transmission, neuronal growth and axon guidance, brain development and maturation etc. In order to investigate glutamate transport dysfunction as a primary excitotoxic event in neurodegenerative diseases, several models have been developed. It has previously been reported that blocking glutamate uptake is toxic to cortical and spinal motor neurons, through NMDA or non-NMDA receptor-dependent mechanisms respectively (Rothstein et al., 1993; Carriedo et al., 1996; Velasco et al., 1996).

Subsequent studies have demonstrated that kainate is a non-degradable analogue of glutamate and a potent neurotoxin (Vincent & Mulle, 2009). KA employs its neuro-excitotoxic and epileptogenic characteristics by acting on kainate receptors which ultimately lead to cell death (Wang et al., 2005). Kainate has extensively been used as an excitotoxic agent as it mimics the effect of glutamate in neurodegenerative disease models (Choi, 1992 a; Lipton & Rosenberg, 1994; Shaw, 1994; King et al., 2016). Kainate receptors mediate kainate-induced seizures and excitotoxic neuronal death, thereby serving as a model for neurodegeneration. In addition to kainate, other agents could be ibotenic acid (IBO) and NMDA, however, they are nonspecific in acting on different cell types and usually they do not cause seizures. In contrast, focal injection of KA leads to hippocampal damage (Jarrard, 2002). It has been reported that systematic administration of kainate results in a well-characterized seizure syndrome in rodents (Ben-Ari, 1985; Mulle et al., 1998). One h after kainate administration limbic motor seizures emerge and develop into status epilepticus lasting 1-2 h (Chuang et al., 2004). Electrophysiological recordings have suggested there is a critical threshold for excitotoxicity mediated by kainate which could fully suppress fictive locomotion. Ten μM kainate enables onset of locomotor patterns in the spinal cord although with smaller amplitude and slower periodicity than sham preparations. However, ≥ 50 μM is sufficient to evoke irreversible fictive locomotor damage and reflex suppression (Mazzone et al., 2010) 24 h after insult. Hence, we used 50 or 100 μM kainate application for 1 h to study its effect on spinal locomotor networks via electrophysiological recordings, histology (Taccola et al, 2008) as well as calcium imaging techniques.

With 50 or 100 μM kainate fictive locomotion disappeared and mono- and polysynaptic reflexes were highly depressed, while disinhibited bursts evoked by strychnine and bicuculline were still present despite increased periodicity and lower amplitude (Taccola et al., 2008; Margaryan et al., 2010). One possibility is that a primary targets for kainate are inhibitory interneurons important for fictive locomotion (Morin et al., 1998; Cossart et al., 2001). After kainate application, spinal networks retained their intrinsic rhythmicity supported via recurrent excitatory collaterals (Ballerini et al., 1999; Tscherter et al., 2001) because disinhibited bursting requires a circuitry simpler than fictive locomotion.

Histologically, neuronal numbers were highly reduced and pyknotic nuclei appeared in all three regions of gray matter (Taccola et al., 2008, Margaryan et al., 2009; Kuzhandaivel et al., 2010) observed 24 h after kainate application. Motoneurons were halved in the ventral horn of gray matter probably because they lack the calcium binding protein and remain very vulnerable to consequences of calcium overload evoked by kainate (Dekkers et al., 2004). Our data are in analogy with the previous reports (Bracci et al., 1996b; Taccola et al., 2008; Mazzone et al., 2013). Extensive production of poly-ADP-ribose (PAR) by hyperactivation of the poly (ADP-ribose) polymerase-1 (PARP-1) enzyme has recently been proposed as a novel programmed cell death, termed "parthanatos" (Andrabi et al., 2006, 2008) and applicable to excitotoxic death in the spinal cord.

3. Dysmetabolic perturbation induced spinal damage

Another protocol was based on dysmetabolic spinal lesion evoked by a toxic solution named as pathological medium (PM) that mimics the conditions (hypoxic/aglycemic) occurring shortly after acute SCI (Taccola et al., 2008). This kind of condition causes delayed cell death of oligodendrocytes by apoptosis (Shuman et al., 1997; Emery et al., 1998; Li et al., 1999; Springer et al., 1999) which is infrequent in SCI cases. Interestingly, in other models of neurodegeneration such as brain ischemia, Alzheimer's disease, etc, apoptotic cell death is not frequent and mainly involves glial cells (oligodendroglia, microglia and astrocytes; Jellinger & Stadelmann, 2000; Shibata et al., 2000; Narkilahti et al., 2003). Previous studies on neonatal spinal cord have shown that pyknosis occurs 24 h after the hypoxic conditions and it maximally damages the ventrolateral white matter of spinal cord (Kuzhandaivel et al., 2010). Similar results were observed in our case after treating the preparations with PM for 1 h (Sámano et al., 2016). This kind of apoptotic cell death was mediated by activation of caspase pathways (Kuzhandaivel et al., 2010). Despite white matter lesion occurred after 1 h application of PM, spinal locomotor networks retained their activity even though the oscillatory patterns were slower than those chemically evoked by NMDA+5HT (Taccola et al., 2008; Kuzhandaivel et al., 2010). However, dorsal root evoked locomotor patterns were absent (Taccola et al., 2008). Therefore, in this case, in spite of having intrinsic ability to induce locomotor

patterns, the sensory feedback, necessary to support locomotion, had been lost (Barbeau et al., 1999).

4. Neuroprotective effects of MPSS on histological and functional outcome

MPSS is a widely used GC for the treatment of neurological diseases (in a dose-dependent manner) due to its anti-inflammatory (Gold et al., 2001) and anti-oxidant properties. However, treatment with MPSS has become controversial because of modest neurological improvement and a number of serious side-effects (Bracken et al., 1984; Gerndt et al., 1997; Pointillart et al., 2000; Matsumoto et al., 2001) in patients with SCI. This drug is still in use for clinical trials (Nicholas et al., 2009; Bracken, 2012; Druschel et al., 2013; Miekisiak et al., 2014; Cheung et al., 2015) as the first approach to SCI. These observations raised the issue if distinct types of SCI might have more positive outcome than other cases. Therefore we tried two different toxic conditions, kainate (100 µM, completely abolished fictive locomotion) induced excitotoxicity or PM (applied for 1 h). Thereafter, we applied 6 or 10 µM MPSS (24 h application, Fehling et al., 2017) based on published clinical guidelines (Sauerland et al., 2000) and in vitro SCI models (Guzmán-Lenis et al., 2009; Sun et al., 2010). Histologically, neuroprotection induced by MPSS after PM application was restricted to ventrolateral white matter, as MPSS reversed the loss of astrocytes and to lesser extent oligodendrocytes. Functionally, the polysynaptic response area was increased after MPSS (10 µM) despite no changes in monosynaptic reflexes. Moreover, small improvements were observed in the area of cumulative depolarization and oscillations. A more positive outcome (slow alternating oscillations) was observed in chemically evoked fictive locomotion after PM followed by MPSS treatment. Basic network rhythmicity was also studied after pharmacological block of inhibition. Here MPSS was not able to change the period depression induced by kainate, however, it potentiated burst amplitude, which suggested little improvement in functional network connectivity. All these observations were in analogy to previous in vitro rat SCI reports which suggested MPSS had not efficiently protected neurons (Xu et al., 1998a; Liu et al., 1997; Lee et al., 2008).

5. Neuroprotection by propofol

As neurosurgery is performed under general anaesthesia, it seemed plausible that at least some positive contribution might come from the administration of general anaesthesia. Recently Shabbir et al. have reported in our lab that a volatile anaesthetic, methoxyflurane, could confer strong functional and histological neuroprotection in an in vitro rat SCI model (Shabbir et al., 2015). These results raised the issue whether a widely used i.v. anaesthetic such as propofol could also produce the same effects or it is an intrinsic property of gas anaesthetics only (which are less frequently used because of their toxic effects). It has been demonstrated that propofol has neuroprotective effects on various in vitro and in vivo models of brain injury (Velly et al., 2003; Kawaguchi et al., 2005; Rossaint et al., 2009; Vasileiou et al., 2009; Zhang et al., 2014; Fan et al., 2015). While propofol attenuates motoneuronal damage in spinal organotypic slice cultures (Bajrektarevic & Nistri, 2016), it is unknown what impact propofol poses on functional locomotor networks. Various studies have demonstrated that the clinically relevant concentration of propofol ranges from 0.5 to 10 µM (Gredell et al., 2004; Matute et al., 2004; Wakita et al., 2013; Eckle et al., 2015). As the drug has never been tested before for these spinal cord experiments, therefore we decided to use the mid value of 5 µM. The timing of propofol administration was chosen according to previous observations that maximum excitotoxic cell death pathways are activated within the first few hours of secondary insult (Kuzhandaivel et al., 2011). Also according to Bajrektarevic & Nistri (2016), propofol was administered for 8 h and good neuroprotection was achieved on spinal cultures. Thus, we applied propofol for 4 or 8 h after kainate (100 µM) and tested its effects the day after.

Propofol, when applied alone for 4 h, partially depressed network synaptic transmission (Jewett et al., 1992) and fictive locomotion. This depression was further exaggerated by propofol 8 h application. This phenomenon is in line with our observation that propofol potentiates $GABA_A$ (Adodra & Hales, 1995; Reynolds & Maitra, 1996) and depressed the NMDA mediated (Orser et al., 1995) receptor responses. Propofol (4 or 8 h) when applied after kainate structurally preserved neurons and motoneurons in all the regions (dorsal, central and ventral) of the spinal cord. Therefore, the simplest

interpretation might be that the drug has exerted its beneficial effects by suppressing the network excitability (Jewett et al., 1992). It could not attenuate the depression of synaptic transmission and cumulative depolarization caused by kainate; however, it arrested further damage by suppressing network excitability. In chemically induced fictive locomotion (recorded 24 h later), there was the emergence of some fictive locomotor cycles after 4 h propofol after kainate: this response was absent after 8 h propofol. This was not unexpected in line with the long-lasting depression evoked by the drug. In fact, disinhibited bursting that reflects the intrinsic rhythmicity of spinal networks (Streit, 1993; Bracci et al., 1996a) showed improved periodicity when 4-h propofol administration followed kainate washout. These results illustrate that when network output required activation of a limited circuitry (Bracci et al., 1996b), the protective action of propofol was manifested more efficiently than over a very wide locomotor network with complex connections (Kiehn, 2006, 2016). Anesthesiological studies demonstrate that full locomotor recovery in humans is incomplete for several h after propofol (Münte et al., 2001; Haavisto & Kauranen, 2002). The general advice is to be cautious against driving since dizziness and drowsiness may persist for 24 h (http://www.rxlist.com/diprivan-drug/patient-images-side-effects.htm). Thus, these observations are consistent with our depressed functional results which occur due to long-lasting network depression effect induced by this anaesthetic.

6. Effects of nicotine

Nicotine-mediated neuroprotection has been reported previously in several models such as in vitro (Garrido et al., 2003), in vivo (Xue et al., 2014) and in epidemiological studies (Quik et al., 2012), suggesting potential strategies to contrast neuronal death. Recently our lab has shown the neuroprotective effect of nicotine on brainstem motoneurons against excitotoxicity by activating nAChRs that triggered intracellular pathways to block reactive oxygen species (ROS) and regulated mitochondrial metabolism (Corsini et al., 2016; Tortora et al., 2017). These intriguing results motivated us to investigate the role of nicotine and nAChRs in neuroprotection against SCI. As Corsini et al. have achieved neuroprotective effects with 10 µM nicotine (Corsini et al., 2016), it seemed a good initial concentration to start the experiments. Unexpectedly, nicotine (10 µM) exerted minimal protection after excitotoxic damage by kainate (refer supplemental data, appendix I enclosed in the thesis). When tested histologically, the neuronal number was significantly

improved after kainate (50 µM) followed by nicotine or kainate+nicotine application (1 or 4 h) only in the dorsal horn with no change in the central and ventral horn of spinal cord. Similarly, the motoneuron numbers were not significantly increased with this concentration except in case where nicotine was applied for 1 h after kainate. These results indicated that nicotine (10 µM) might be toxic for spinal neurons and motoneurons. This assumption was confirmed by examining the effects by nicotine per se.

The next goal was to examine 0.5 or 1 or 2 µM nicotine (4 h) concentration and investigated its functional and structural effects alone and after or together with kainate (1 h). Electrophysiologically, nicotine 0.5 µM was not much effective to reverse the excitotoxic effect evoked by kainate, whereas 2 µM was suppressing the polysynaptic reflexes and fictive locomotion. Thus, I chose nicotine 1 µM to continue the project further. Nicotine 1 µM showed promising recovery in polysynaptic reflex, fictive locomotion, neuronal and motoneuron numbers in all the three ROIs. Since early treatment with nicotine could restore at least in part the amplitude and frequency of disinhibited bursts or Ca^{2+} transients (achieved by calcium imaging experiments with spinal organotypic cultures), these results indicate that certain elementary circuits relying on glutamatergic transmission for intrinsic rhythmicity (Bracci et al., 1996b) had been protected by nicotine and retained their connectivity because synchronicity was preserved even over a substantial distance. The only parameter not reversed by nicotine was monosynaptic reflexes. Hence, it seems likely that, despite near normalizing the motoneuron numbers by nicotine, their ability to respond to weak inputs had remained impaired after kainate application.

The subsequent step was to explore which nAChRs are important for spinal neuroprotection. Although various nAChR subunits have been identified in the rat spinal cord (Wada et al., 1989, 1990; Khan et al., 2003), α4β2 and α7 remain the prominent receptor assemblies (Hsu et al., 1997; Berg & Conroy, 2002). Furthermore, α4β2 and α7 receptors play a role in nAChR mediated neuroprotection against excitotoxicity in rat dissociated spinal cultures (Nakamizo et al., 2005; Shimohama, 2009). Thus, antagonists for α4β2 and α7 receptors, DHβE and MLA respectively, were used in the present excitotoxicity model. The experiments were performed by co-application of kainate+antagonists (+nicotine) to examine which receptors are involved in nicotine-

mediated neuroprotection. Antagonists' application with kainate did not modulate network depression evoked by kainate with only one exception namely, a partial preservation of chemically-induced fictive locomotion. We hypothesize that kainate-mediated excitation had led to release of endogenous ACh and that this phenomenon partly contributed to excitotoxicity at the level of the CPG network, though the exact locus of action remains unclear and needs future experiments. This suggestion is compatible with the modest protection by DHβE and it implies the possibility that at least part of the neuroprotection exerted by nicotine itself was caused by its dual action on nAChRs, namely rapid activation and desensitization.

7. Neuroprotective effect of celastrol

Several studies have investigated the effects of HSPs by over-expressing them or activating the heat shock response (HSR) in rodent models (Muchowski & Wacker, 2005; Neef et al., 2011; Leak, 2014; Duncan et al., 2015; Pratt et al., 2015; Bose & Cho, 2017; Calderwood & Murshid, 2017). Determining which HSR elements are effective in inhibiting protein aggregation and subsequent neurotoxicity is a crucial step in exemplifying targets for the development of therapeutics to combat neurodegenerative diseases. It has previously been reported that upregulation of HSR by treatment with drugs such as withaferin A, celastrol or arimoclomol resulted in increasing motoneuronal numbers and lifespan of mSOD1 expressing mice (Kieran et al., 2004; Kiaei et al., 2005; Lin et al., 2013; Patel et al., 2014). As celastrol is a potent HSP70 inducer and also possess anti-inflammatory and anti-oxidant properties (Westerheide et al., 2004), therefore in the present study of an in vitro SCI model, celastrol is used to investigate the neuroprotective effect of induced HSP70 by pre-treating the preparations with celastrol for 6 h followed by application of kainate for 1 h. Primarily the effective dose of celastrol, which is 0.75 µM was optimized by my colleague Priyadarshini Veeraraghavan. The further neuroprotective effect was studied by me by performing extracellular recordings (see supplemental data, appendix II). When celastrol was applied alone for 6 h on day 1 and recorded on a subsequent day showed depression of monosynaptic reflexes. However, the polysynaptic reflexes and DR evoked fictive locomotion were recovered back to normal. It is noteworthy that the amplitude of NMDA+5HT induced fictive locomotion was reduced to less than half and the periodicity was increased to double as

compared to sham preparations. Then kainate (50 µM) was applied after pre-treating the preparations with celastrol (6 h), which showed strong recovery in polysynaptic reflexes, electrically induced fictive locomotion and NMDA+5HT induced fictive locomotion even though with smaller amplitude and slower periodicity of oscillatory cycles. As this project is a part of collaboration with Antonela Petrović and Miranda Mladinić at the University of Rijeka, Department of Biotechnology, Croatia, therefore Petrović will continue the project by further performing molecular biology experiments.

7 CONCLUSIONS AND FUTURE PERSPECTIVES

The novel findings discussed in the present thesis are intriguing. Several attempts have been made earlier to examine the neuroprotective role of distinct pharmacological agents (Lee et al., 2003; Bagriyanik et al., 2008; Shabbir et al., 2015; Bajrektarevic & Nistri, 2017). Among glutamate release inhibitors, riluzole is the only present-day treatment for motoneuron disease with a rather limited lifespan of clinical efficacy (Wokke, 1996; Cheah et al., 2010). In our lab's experimental model, this drug cannot effectively contrast the excitotoxicity induced by kainate (Sámano et al., 2012) while it does act by decreasing glutamatergic transmission and voltage-activated Na^+ conductances (Cifra et al., 2013). MPSS has shown limited neuroprotection to spinal white matter against dysmetabolic/hypoxic conditions in our experimental model (Sámano et al., 2016). More promising neuroprotective results were obtained with propofol (Kaur et al., 2016), nicotine and celastrol against excitotoxic insult in our in vitro rat spinal cord model. These encouraging observations will require further experiments in vivo before considering their translational implications.

One limitation of our model is that the survival time of our preparation is 24 h: beyond this, it is not currently feasible to test whether any protection remains over longer times or emerges with an unexpected delay. Hence, in the future, further in vivo and clinical attempts are necessary to verify whether these drugs are effectively able to attenuate the excitotoxicity evoked after SCI. It is, however, important to reiterate that the present data offer proof of principle that pharmacological neuroprotection is indeed possible against experimental SCI.

8 REFERENCES

Abdin AA, & Hasby EA (2014) Modulatory effect of celastrol on Th1/Th2 cytokines profile, TLR2 and CD3C T-lymphocyte expression in a relapsingremitting model of multiple sclerosis in rats. Eur. J. Pharmacol. 742:102-112.

Alaynick WA, Jessell TM, Pfaff SL (2011) SnapShot: spinal cord development. Cell 146: 178-178.e1.

Albuquerque EX, Pereira EF, Alkondon M, Rogers SW. (2009) Mammalian nicotinic acetylcholine receptors: from structure to function. Physiol. Rev. 89:73-120.

Alexander JK, DeVries AC, Kigerl KA, Dahlman JM, Popovich PG (2009) Stress exacerbates neuropathic pain via glucocorticoid and NMDA receptor activation. Brain, Behavior and Immunity 23:851-860.

Allison AC, Cacabelos R, Lombardi VR, Alvarez XA, Vigo C (2001) Celastrol, a potent antioxidant and anti-inflammatory drug, as a possible treatment for Alzheimer's disease. Prog. Neuropsychopharmacol. Biol. Psychiatry 25:1341-1357.

Anderson DK, Hall ED (1989) Pathophysiology of spinal cord trauma. Ann. Emerg. Med. 22:987-992.

Anderson RE, Jakobsson JG (2004) Entropy of EEG during anaesthetic induction: a comparative study with propofol or nitrous oxide as sole agent. Br. J. Anaesth. 92:167-170.

Andrabi SA, Dawson TM, Dawson VL (2008) Mitochondrial and nuclear cross talk in cell death: parthanatos. Ann. N. Y. Acad. Sci. 1147:233-241.

Andrabi SA, Kim NS, Yu SW, Wang H, Koh DW, Sasaki M, Klaus JA, Otsuka T, Zhang Z, Koehler RC, Hurn PD, Poirier G G, Dawson VL, Dawson TM (2006) Poly(ADP-ribose) (PAR) polymer is a death signal. Proc. Natl. Acad. Sci. U.S.A. 103:18308-18313.

Aoki F, Wannier T, Grillner S (2001) Slow Dorsal-Ventral Rhythm Generator in the Lamprey Spinal Cord. Journal of Neurophysiology 85:211-218.

Aoki H, Mizobe T, Nozuchi S, Hiramatsu N (1998) In vivo and in vitro studies of the inhibitory effect of propofol on human platelet aggregation. Anesthesiology 88:362-370.
Bajrektarevic D, Nistri A (2016) Delayed application of the anesthetic propofol contrasts the neurotoxic effects of kainate on rat organotypic spinal slice cultures. Neurotoxicology 54:1-10.

Ballerini L, Galante M, Grandolfo M, Nistri A (1999) Generation of rhythmic patterns of activity by ventral interneurones in rat organotypic spinal slice culture. J. Physiol. 517:459-475.

Bannatyne BA, Edgley SA, Hammar I, Jankowska E, Maxwell DJ (2003) Networks of inhibitory and excitatory commissural interneurons mediating crossed reticulospinal actions. Eur. J. Neurosci. 18:2273-2284.

Bao FP, Zhang HG, Zhu SM (2017) Anesthetic considerations for patients with acute cervical spinal cord injury. Neural Regen. Res. 12:499-504.

Baranović S, Maldini B, Cengić T, Kolundzić R (2014) Anesthetic management of acute cervical spinal cord injury in pregnancy. Acta. Clin. Croat. 53:98-101.

Baraznenok IL, Jonsson E, Claesson A (2005) 3-(2,5-Dihydro-1H-pyrrol-2-ylmethoxy) pyridines: synthesis and analgesic activity. Bioorg. Med. Chem. Lett. 15:1637-16340.

Barbeau H, McCrea DA, O'Donovan MJ, Rossignol S, Grill WM, Lemay MA (1999) Tapping into spinal circuits to restore motor function. Brain Res. Brain Res. Rev. 30:27-51.

Barnard EA, Skolnick P, Olsen RW, et al (1998) International Union of Pharmacology. XV. Subtypes of γ-aminobutyric $acid_A$ receptors: classification on the basis of subunit structure and receptor function. Pharmacol. Rev. 50:291-313.

Barnes PJ (1998) Anti-inflammatory actions of glucocorticoids: molecular mechanisms. Clin. Sci. (Lond). 94:557-572.

Beato M, Nistri A (1999) Interaction between disinhibited bursting and fictive locomotor patterns in the rat isolated spinal cord. J. Neurophysiol. 82:2029-2038.

Becker DE (2013) Basic and clinical pharmacology of glucocorticosteroids. Anesth Prog. Spring 60:25-31.

Belelli D, Lambert JJ, Peters JA, et al (1997) The interaction of the general anesthetic etomidate with the gamma-aminobutyric acid type A receptor is influenced by a single amino acid. Proceedings of the National Academy of Sciences of the United States of America 94:11031-11036.

Bellardita C, Kiehn O (2015) Phenotypic characterization of speed-aasociated gait changes in mice reveals modular organization of locomotor networks. Curr. Biol. 25:1426-1436.

Ben-Ari Y (1985) Limbic seizure and brain damage produced by kainic acid: mechanisms and relevance to human temporal lobe epilepsy. Neuroscience 14:375-403.

Bohnen NI, Albin RL (2011) The cholinergic system and Parkinson disease. Behavioral Brain Research. 221:564-573.

Bonner TI (1989) The molecular basis of muscarinic receptor diversity. Trends Neurosci. 12: 148-151.

Bonner TI, Buckley NJ, Young AC, Brann MR (1987) Identification of a family of muscarinic acetylcholine receptor genes. Science 237:527-532.

Bonner TI, Young AC, Brann MR, Buckley NJ (1988) Cloning and expression of the human and rat m5 muscarinic acetylcholine receptor genes. Neuron 1:403-410.

Bose S & Cho J (2017) Targeting chaperones, heat shock factor-1, and unfolded protein response: promising therapeutic approaches for neurodegenerative disorders. Ageing Res. Rev. 35:155-175.

Bracci E, Ballerini L, Nistri (1996b) A Localization of rhythmogenic networks responsible for spontaneous bursts induced by strychnine and bicuculline in the rat isolated spinal cord. J. Neurosci. 16:7063-7076.

Bracken MB (2012) Steroids for acute spinal cord injury. Cochrane Database Syst. Rev. 18:1-51.

Bracken MB, Collins WF, Freeman DF et al (1984) Efficacy of methylprednisolone in acute spinal cord injury. JAMA 251:45-52.

Brown GT (1911) The intrinsic factors in the act of progresson in the mammal. Proc. R. Soc. Lond. 84:309-319.

Brown GT (1914) On the nature of the fundamental activity of the nervous centres; together with an analysis of the conditioning of rhythmic activity in progression, and a theory of the evolution of function in the nervous system. J. Physiol. 48:18-46.

Brown IR, Rush S, Ivy GO (1989) Induction of a heat shock gene at the site of tissue injury in the rat brain. Neuron 2:1559-1564.

Bunnelle WH, Dart MJ, Schrimpf MR (2004) Design of ligands for the nicotinic acetylcholine receptors: the quest for selectivity. Curr. Top. Med. Chem. 4:299-334.

Calderwood SK, Murshid A (2017) Molecular chaperone accumulation in cancer and decrease in Alzheimer's disease: the potential roles of HSF1. Front. Neurosci. 11:192.

Campagna JA, Miller KW, Forman SA. Mechanisms of Actions of Inhaled Anesthetics. New

Carmel JB, Kakinohana O, Mestril R, Young W, Marsala M, Hart RP (2004) Mediators of ischemic preconditioning identified by microarray analysis of rat spinal cord. Exp. Neurol. 185:81-96.

Carriedo SG, Yin HZ, Weiss JH (1996) Motor neurons are selectively vulnerable to AMPA/kainate receptor-mediated injury in vitro. J. Neurosci. 16:4069-4079.

Caulfield MP, Birdsall NJM (1998) International Union of Pharmacology. XVII. Classification of muscarinic acetylcholine receptors. Pharmacol. Rev. 50:279-290.

Cazalets JR, Sqalli-Houssaini Y, Clarac F (1992) Activation of the central pattern generators for locomotion by serotonin and excitatory amino acids in neonatal rat. J. Physiol. (Lond.) 455:187-204.

Changeux J, Edelstein SJ (2001) Allosteric mechanisms in normal and pathological nicotinic acetylcholine receptors. Curr. Opin. Neurobiol. 11:369-377.

Changeux JP, Edelstein SJ (1998) Allosteric receptors after 30 years. Neuron 21:959-980.

Cheung V, Hoshide R, Bansal V, Kasper E, Chen CC (2015) Methylprednisolone in the management of spinal cord injuries: Lessons from randomized, controlled trials. Surg. Neurol. Int. 6:142.

Choi D W (1992a) Bench to bedside: the glutamate connection. Science 258:241-243.

Christie DF, Michael AA, and Paul JK (2008) Subtypes of nicotinic acetylcholine receptors in nicotine reward, dependence, and withdrawal: Evidence from genetically modified mice. Behav. Pharmacol. 19:461-484.

Chuang YC, Chang AY, Lin JW, Hsu SP, Chan SH (2004) Mitochondrial dysfunction and ultrastructural damage in the hippocampus during kainic acid-induced status epilepticus in the rat. Epilepsia. 45:1202-1209.

Cizkova D, Carmel JB, Yamamoto K, Kakinohana O, Sun D, Hart RP, Marsala M (2004) Characterization of spinal HSP72 induction and development of ischemic tolerance after spinal ischemia in rats. Exp. Neurol. 185:97-108.

Clements JR, Grant S (1990) Glutamate-like immunoreactivity in neurons of the laterodorsal tegmental and pedunculopontine nuclei in the rat. Neurosci. Lett. 120:70-73.

Cleren C, Calingasan NY, Chen J, Beal MF (2005) Celastrol protects against MPTP- and 3-nitropropionic acid-induced neurotoxicity. Journal of Neurochemistry 94:995-1004.

Corringer PJ, Le Novere N, Changeux JP (2000) Nicotinic receptors at the amino acid level. Annu. Rev. Pharmacol. Toxicol. 40:431-458.

Cossart R, Dinocourt C, Hirsch JC, Merchan-Perez A, De Felipe J, Ben-Ari Y, Esclapez M, Bernard C (2001) Dendritic but not somatic GABAergic inhibition is decreased in experimental epilepsy. Nat. Neurosci. 4:52-62.

Cowley KC, Schmidt BJ (1995) Effects of inhibitory amino acid antagonists on reciprocal inhibitory interactions during rhythmic motor activity in the in vitro neonatal rat spinal cord. J. Neurophysiol. 74:1109-1117.

Crone S A, Zhong G, Harris-Warrick R, Sharma K (2009) In mice lacking V2a interneurons, gait depends on speed of locomotion. J. Neurosci. 29:7098-7109.

Crone SA, et al (2008) Genetic ablation of V2a ipsilateral interneurons disrupts left-right locomotor coordination in mammalian spinal cord. Neuron 60:70-83.

Dafny N (1999) Chapter 3: Anatomy of spinal cord, Section 2: Sensory Systems, Neuroscience Online. Website: http://neuroscience.uth.tmc.edu/s2/chapter03.html.

Dajas-Bailador FA et al (2000) The a7 nicotinic acetylcholine receptor subtype mediates nicotine protection against NMDA excitotoxicity in primary hippocampal cultures through a Ca2þ dependent mechanism. Neuropharmacology 39:2799-2807.

Dale HH (1914) The action of certain esters of choline and their relation to muscarine. J. Pharmacol. Exp. Ther. 6:147-190.

Dale HH, Dudley HW (1929) The presence of histamine and acetylcholine in the spleen of the ox and horse. J Physiol. 68:97-123.

Dani JA, Bertrand D (2007) Nicotinic acetylcholine receptors and nicotinic cholinergic mechanisms of the central nervous system. Annu. Rev. Pharmacol. Toxicol. 47:699-729.

Darwin C (1859) On the origin of species by natural selection, or the preservation of favoured races in the struggle for life. London, UK: John Murray

Datson NA, Morsink MC, Meijer OC, de Kloet ER (2008) Central corticosteroid actions: search for gene targets. European Journal of Pharmacology 583:272-289.

Delcomyn F (1980) Neural basis of rhythmic behaviour in animals. Science 210:492–498.

Donnelly DJ, Popovich PG (2008) Inflammation and its role in neuroprotection, axonal regeneration and functional recovery after spinal cord injury. Exp. Neurol. 209:378-388.

Donnelly-Roberts DL et al (1996) In vitro neuroprotective properties of the novel cholinergic channel activator (ChCA), ABT-418. Brain Res. 719:36–44

Dougherty KJ, et al (2013) Locomotor rhythm generation linked to the output of spinal Shox2 excitatory interneurons. Neuron 80:920-933.

Druschel C, Schaser KD, Schwab JM (2013) Current practice of methylprednisolone administration for acute spinal cord injury in Germany: a national survey. Spine 38:e669-e677.

Dubovsky AN, Arvikar S, Stern TA, Axelrod L (2012) The neuropsychiatric complications of glucocorticoid use: steroid psychosis revisited. Psychosomatics 53:103-115.

Duncan EJ, Cheetham ME, Chapple JP, van der Spuy J (2015) The role of Hsp70 and its co-chaperones in protein misfolding, aggregation and disease. Subcell. Biochem. 78:243-273.

Edgerton VR, Tillakaratne NJ, Bigbee AJ, de Leon RD, Roy RR (2004) Plasticity of the spinal neural circuitry after injury. Annu. Rev. Neurosci. 27:145-167.

Emery E, Aldana P, Bunge MB, Puckett W,Srinivasan A, Keane RW, Bethea J, Levi AD (1998). Apoptosis after traumatic human spinal cord injury. J. Neurosurg. 89:911-920.

Endo T, Kiehn O (2008) Asymmetric operation of the locomotor central pattern generator in the neonatal mouse spinal cord. J. Neurophysiol. 100:3043-3054.

Evaniew N, Belley-Côté EP, Fallah N, Noonan VK, Rivers CS, Dvorak MF (2016) Methylprednisolone for the Treatment of Patients with Acute Spinal Cord Injuries: A Systematic Review and Meta-Analysis. J. Neurotrauma. 33:468-481.

Fehlings MG, Wilson JR, Tetreault LA, Aarabi B, Anderson P, Arnold PM, Brodke DS, Burns AS, Chiba K, Dettori JR, Furlan JC, Hawryluk G, Holly LT, Howley S, Jeji T, Kalsi-Ryan S, Kotter M, Kurpad S, Kwon BK, Marino RJ, Martin AR, Massicotte E, Merli G, Middleton JW, Nakashima H, Nagoshi N, Palmieri K, Skelly AC, Singh A, Tsai EC, Vaccaro A, Yee A, Harrop JS (2017) A Clinical Practice Guideline for the Management of Patients With Acute Spinal Cord Injury: Recommendations on the Use of Methylprednisolone Sodium Succinate. Global Spine Journal 7:203S-211S.

Ferchmin PA et al (2003) Nicotinic receptors differentially regulate N-methyl-D-aspartate damage in acute hippocampal slices. J. Pharmacol. Exp. Ther. 305:1071-1078.

Forman SA, Chin VA (2008) General Anesthetics and Molecular Mechanisms of Unconsciousness. Int. Anesthesiol. Clin. 46:43-53.

Geisler FH, Dorsey FC, Coleman WP (1991) Recovery of motor function after spinal cord injury—a randomized, placebo-controlled trial with GM-1 ganglioside. N. Engl. J. Med. 324:1829-1838.

Gerndt SJ, Rodriguez JL, Pawlik JW et al (1997) Consequences of high-dose steroid therapy for acute spinal cord injury. J. Trauma. 42:279-284.

Ghosh M, Pearse DD (2014) The role of the serotonergic system in locomotor recovery after spinal cord injury. Front. Neural Circuits. 8:151.

Glen JB (1980) Animal studies of the anaesthetic activity of ICI 35 868. Br. J. Anaesth. 52: 731-742.

Glen JB, Hunter SC (1984) Pharmacology of an emulsion formulation of ICI 35 868. Br. J. Anaesth. 56:617-626.

Gold R, Buttgereit F, Toyka KV (2001) Mechanism of action of glucocorticosteroid hormones: possible implications for therapy of neuroimmunological disorders. J. Neuroimmunol. 117:1-8.

Gonzalez-Correa JA, Cruz-Andreotti E, Arrebola MM, Lopez-Villodres JA, Jodar M, De La Cruz JP (2008) Effects of propofol on the leukocyte nitric oxide pathway: in vitro and ex vivo studies in surgical patients. Naunyn-Schmiedeberg's Arch. Pharmacol. 376:331-339.

Goto T, Nakata Y, Saito H, et al (2000) Bispectral analysis of the electroencephalogram does not predict responsiveness to verbal command in patients emerging from xenon anaesthesia. Br. J. Anaesth. 85:359-363.

Gotti C, Clementi F (2004) Neuronal nicotinic receptors: from structure to pathology Progress in Neurobiology 74:363-396.

Goulding M (2009) Circuits controlling vertebrate locomotion: moving in a new direction. Nat. Rev. Neurosci. 10:507-518.

Grasshoff C, Rudolph U, Antkowiak B (2005) Molecular and systemic mechanisms of general anaesthesia: the 'multi-site and multiple mechanisms' concept. Current Opinion in Anaesthesiology 18:386-391.

Grillner S (1985) Neurobiological bases of rhythmic motor acts in vertebrates. Science 228: 143-149.

Grillner S (1986) Interaction between sensory signals and the central networks controlling locomotion in lamprey, dogfish and cat. In: Grillner S, Stein PSG, Stuart DG, Forssberg

F, Herman RM, editors. Neurobiology of vertebrate locomotion. Wenner Gren international symposium series. London: Macmillan. 45:505-512.

Grillner S (2003) The motor infrastructure: from ion channels to neuronal networks. Nat. Rev. Neurosci. 4:573-586.

Grillner S (2006) Biological Pattern Generation: The Cellular and Computational Logic of Networks in Motion. Neuron 52:751-766.

Grillner S, Hellgren J, Ménard A, Saitoh K, Wikström MA (2005) Mechanisms for selection of basic motor programs-roles for the striatum and pallidum. Trends Neurosci. 28:364-370.

Grillner S, Kozlov A, Kotaleski JH (2005c) Integrative neuroscience: linking levels of analyses. Curr. Opin. Neurobiol. 15:614-621.

Grouzmann E, Borgeat A, Fathi M, Gaillard RC, Ravussin P (2000) Plasma and cerebrospinal fluid concentration of neuropeptide Y, serotonin, and catecholamines in patients under propofol or isoflurane anaesthesia. Can. J. Physiol. Pharm. 78:100-107.

Grundmann U, Silomon M, Bach F, Becker S, Bauer M, Larsen B, Kleinschmidt S (2001) Recovery profile and side effects of remifentanil-based anaesthesia with desflurane or propofol for laparoscopic cholecystectomy. Acta. Anaesth. Scand. 45:320-326.

Guandalini L, Martini E, Gratteri P, Ghelardini C, Varani K, Romanelli MN (2006) Design, synthesis and binding affinity of new nicotinic ligands. Issue Italian-Swiss Medicinal Chemistry Meeting ARKIVOC VIII:50-65.

Guertin PA (2009) The mammalian central pattern generator for locomotion. Brain Research Reviews 62:45-56.

Guzma´ n-Lenis MS, Navarro X, Casas C (2009) Drug screening of neuroprotective agents on an organotypic-based model of spinal cord excitotoxic damage. Restor. Neurol. Neurosci. 27:335–349.

Ha KY, Carragee E, Cheng I, Kwon SE, Kim YH (2011) Pregabalin as a neuroprotector after spinal cord injury in rats: biochemical analysis and effect on glial cells. J. Korean Med. Sci. 26:404-411.

Ha KY, Kim YH, Rhyu KW, Kwon SE (2008) Pregabalin as a neuroprotector after spinal cord injury in rats. Eur. Spine J. 17:864-872.

Häggström M, Stannered, Hoffmeier, Settersr, Richfield D (2014) Diagram of the pathways of human steroidogenesis. WikiJournal of Medicine 1:5.

Ham AW, Cormack DH (1987) Histology, Edn. 8th , J.B. Lippincott company, Philadelphia and Torronto 485-517.

Heise C, Kayalioglu G (2009) Cytoarchitecture of the spinal cord. In: Watson C, Paxinos G, Kayalioglu G, editors. The spinal cord. A Christopher and Dana Reeve foundation text and atlas. San Diego: Elsevier Academic Press. 64-80.

Henneman E (1974) Spinal reflexes and the control of movement in Medical Physiology, 13th Edn, ed.V.B.Mount castle (StLouis: Mosby) 1:651-667.

Herman JP, Patel PD, Akil H, Watson SJ (1989) Localization and regulation of glucocorticoid and mineralocorticoid receptor messenger RNAs in the hippocampal formation of the rat. Molecular Endocrinology 3:1886-1894.

Hikosaka O, Nakamura K, Nakahara H (2006) Basal ganglia orient eyes to reward. J Neurophysiol. 95:567-584.

Hogg RC, Raggenbass M, Bertrand D (2003) Nicotinic acetylcholine receptors: from structure to brain function. Rev. Physiol. Biochem. Pharmacol. 147:1-46.

Hultborn H (1976) Transmission in the pathway of reciprocal Ia inhibition to motoneurones and its control during the tonic stretch reflex. Prog. Brain Res. 44:235-255.

Hurlbert RJ, Hadley MN, Walters BC, Aarabi B, Dhall SS, Gelb DE, Rozzelle CJ, Ryken TC, Theodore N (2013) Pharmacological Therapy for Acute Spinal Cord Injury. Neurosurgery 72:93-105.

Ishii H, Arai T, Segawa H, Morikawa S, Inubushi T, Fukuda K (2002) Effects of propofol on lactate accumulation and oedema formation in focal cerebral ischaemia in hyperglycaemic rats. Br. J. Anaesth. 88:412-417.

Ishikawa T, Suzuki H, Ishikawa K, Yasuda S, Matsui T, Yamamoto M, Kakeda T, Yamamoto S, Owada Y, Yaksh TL (2014) Spinal Cord Ischemia/Injury. Current Pharmaceutical Design 20:5738-5743.

Jarrard LE (2002) Use of excitotoxins to lesion the hippocampus: update. Hippocampus 12:405-414.

Jellinger KA, & Stadelmann CH (2000) The enigma of cell death in neurodegenerative disorders. J. NeuralTransm. Suppl. 60:21-36.

Jensen AA, Frølund B, Liljefors T, Krogsgaard-Larsen P (2005) Neuronal nicotinic acetylcholine receptors: structural revelations, target identifications, and therapeutic inspirations. J. Med. Chem. 48:4705-4745.

Jessell TM (2000) Neuronal specification in the spinal cord: inductive signals and transcriptional codes. Nat. Rev. Genet. 1:20-29.

Joyce DA, Steer JH, Abraham LJ (1997) Glucocorticoid modulation of human monocyte/macrophage function: control of TNF-alpha secretion. Inflammation Research: Official Journal of the European Histamine Research Society 46:447-451.

Kandel ER, Schwartz JH, Jessell TM (2000) Principles of neural science (4th ed.). New York: McGraw-Hill, Health Professions division.

Kannaiyan R, Shanmugam MK, Sethi G (2011) Molecular targets of celastrol derived from Thunder of God Vine: Potential role in the treatment of inflammatory disorders and cancer. Cancer Lett. 303:9-20.

Kaur J, Flores Gutiérrez J, Nistri A (2016) Neuroprotective effect of propofol against excitotoxic injury to locomotor networks of the rat spinal cord in vitro. Eur J Neurosci. 44:2418-2430.

Kiaei M, Kipiani K, Petri S, Chen J, Calingasan NY, Beal MF (2005) Celastrol blocks neuronal cell death and extends life in transgenic mouse model of amyotrophic lateral sclerosis. Neurodegener. Dis. 2:246-254.

Kiehn O (2006) Locomotor circuits in the mammalian spinal cord. Annu Rev Neurosci. 29:279-306.

Kiehn O (2016) Decoding the organization of spinal circuits that control locomotion. Nat. Rev. Neurosci. 17:224-238.

Kieran D, Kalmar B, Dick JR, Riddoch-Contreras J, Burnstock G, Greensmith L (2004) Treatment with arimoclomol, a coinducer of heat shock proteins, delays disease progression in ALS mice. Nat. Med. 10:402–405.

Kihara T, Shimohama S, Sawada H, Honda K, Naamizo T, Shibasaki H, Kume T, Akaike A, (2001) α7 nicotinic receptors transduces signals to phosphatidylinositol 3 kinase to block a β amyloid induced neurotoxicity. J. Biol. Chem. 276:13541-13546.

Kim YH, Ha KY, Kim SI (2017) Spinal Cord Injury and Related Clinical Trials. Clin. Orthop. Surg. 9:1-9.

King AE, Woodhouse A, Kirkcaldie MT, Vickers JC (2016) Excitotoxicity in ALS: Overstimulation, or overreaction? Experimental Neurology 275:162-171.

Kissin I (1997) A concept for assessing interactions of general anesthetics. Anesth.. Analg. 85:204-210.

Kremer E, Lev-Tov A (1997) Localization of the spinal network associated with generation of hindlimb locomotion in the neonatal rat and organization of its transverse coupling system. J. Neurophysiol. 77:1155-1170.

Kudo N, Yamad T (1987) N-methyl-D,L-aspartate–induced locomotor activity in a spinal cord– hindlimb muscles preparation of the newborn rat studied in vitro. Neurosci. Lett. 75: 43-48.

Kuizenga K, Wierda JM, Kalkman CJ (2001) Biphasic EEG changes in relation to loss of consciousness during induction with thiopental, propofol, etomidate, midazolam or sevoflurane. Br. J. Anaesth. 86:354-360.

Kurt M, Bilge SS, Kukula O, Celik S, Kesim Y (2003) Anxiolytic-like profile of propofol, a general anaesthetic, in the plus-maze test in mice. Pol. J. Pharmacol. 55: 973-977.

Kushida A, Inada T, Shingu K (2007) Enhancement of antitumor immunity after propofol treatment in mice. Immunopharmacol. Immunotoxicol. 29:477-486.

Kuzhandaivel A, Nistri A, Mazzone GL, Mladinic M (2011) Molecular mechanisms underlying cell death in spinal networks in relation to locomotor activity after acute injury in vitro. Front. Cell. Neurosci. 5:9.

Kuzhandaivel A, Margaryan G, Nistri A, Mladinic M (2010) Extensive glial apoptosis develops early after hypoxic-dysmetabolic insult to the neonatal rat spinal cord in vitro. Neuroscience 169:325-338.

Kwon BK, Tetzlaff W, Grauer JN, Beiner J, Vaccaro AR (2004) Pathophysiology and pharmacologic treatment of acute spinal cord injury. Spine J. 4:451-464.

L. Baraznenok, E. Jonsson, A. Claesson, Bioorg. Med. Chem. Lett. 2005, 15, 1637 – 1640.

Laitio RM, Kaskinoro K, Särkelä MOK, Kaisti KK, Salmi E, Maksimow A, Långsjö JW, Aantaa R, Kangas K, Jääskeläinen S, Scheinin H (2008) Bispectral Index, Entropy, and Quantitative Electroencephalogram during Single-agent Xenon Anesthesia. Anesthesiology 108:63-70.

Lapchak PA, Araujo DM, Song D, et al (2001) Neuroprotection by the selective cyclooxygenase-2 inhibitor SC-236 results in improvements in behavioral deficits induced by reversible spinal cord ischemia. Stroke 32:1220-1225.

Laviolette SR, van der Kooy D (2004) The neurobiology of nicotine addiction: bridging the gap from molecules to behaviour. Nat. Rev. Neurosci. 5:55-65.

Lavoie B, Parent A (1994) Pedunculopontine nucleus in the squirrel monkey: distribution of cholinergic and monoaminergic neurons in the mesopontine tegmentum with evidence for the presence of glutamate in cholinergic neurons. J Comp Neurol. 344:190-209.

Le Novere N, Changeux JP (1995) Molecular evolution of the nicotinic acetylcholine receptor: an example of multigene family in excitable cells. J. Mol. 40:155-172.

Le Ray D, Juvin L, Ryczko D, Dubuc R (2011) Chapter 4 - Supraspinal control of locomotion: the mesencephalic locomotor region. Progress in Brain Research. 188:51-70.

Leak RK (2014) Heat shock proteins in neurodegenerative disorders and aging. J. Cell Commun. Signal. 8:293-310.

Lee JM, Yan P, Xiao Q, Chen S, Lee KY, Hsu CY, Xu J (2008) Methylprednisolone protects oligodendrocytes but not neurons after spinal cord injury. J. Neurosci. 28:3141-3149.

Li GL, Farooque M, Holtz A, Olsson Y (1999) Apoptosis of oligodendrocytes occurs for long distances away from the primary injury after compression trauma to rat spinal cord. Acta. Neuropathol. 98, 473-480.

Li S, Mealing GA, Morley P, Stys PK (1999) Novel injury mechanism in anoxia and trauma of spinal cord white matter: glutamate release via reverse Na+-dependent glutamate transport. J. Neurosci. 19:RC16.

Li S, Stys PK (2000) Mechanisms of ionotropic glutamate receptormediated excitotoxicity in isolated spinal cord white matter. J. Neurosci. 20:1190-1198.

Lin P-Y, Simon SM, Koh WK, Folorunso O, Umbaugh CS, Pierce A (2013) Heat shock factor 1 over-expression protects against exposure of hydrophobic residues on mutant SOD1 and early mortality in a mouse model of amyotrophic lateral sclerosis. Mol. Neurodegener. 8:43.

Lindstrom J (2000) The structures of neuronal nicotinic receptors. In: Clementi F, Fornasari D, Gotti C (Eds.), Handbook of Experimental Pharmacology Vol. Neuronal Nicotinic Receptors. Springer, Berlin. 101-162.

Lipton SA & Rosenberg PA (1994) Excitatory amino acids as a final common pathway for neurologic disorders. N. Engl. J. Med. 330:613-622.

Liu D, Ahmet A, Ward L, Krishnamoorthy P, Mandelcorn ED, Leigh R, Brown JP, Cohen A, Kim H (2013) A practical guide to the monitoring and management of the complications of systemic corticosteroid therapy. Allergy Asthma Clin. Immunol. 9:30.

Liu XZ, Xu XM, Hu R, Du C, Zhang SX, McDonald JW, Dong HX, Wu YJ, Fan GS, Jacquin MF, Hsu CY, Choi DW (1997) Neuronal and glial apoptosis after traumatic spinal cord injury. J. Neurosci. 17:5395-5406.

Loewi O (1921) Uber humorale Ubertragbarkeit der Herznervenwirkung. Pflügers. 189:239-242.

Lu GB, Niu FW, Zhang YC, Du L, Liang ZY, Gao Y, Yan TZ, Nie ZK, Gao K (2016) Methylprednisolone promotes recovery of neurological function after spinal cord injury: association with Wnt/β-catenin signaling pathway activation. Neural Regen. Res. 11:1816-1823.

Maiarù M, Tochiki KK, Cox MB et al (2016) The stress regulator FKBP51 drives chronic pain by modulating spinal glucocorticoid signalling. Science Translational Medicine 8:1-11.

Malenka RC, Nestler EJ, Hyman SE (2009) Chapter 9: Autonomic Nervous System. In Sydor A, Brown RY. Molecular Neuropharmacology: A Foundation for Clinical Neuroscience (2nd ed.). New York: McGraw-Hill Medical. 234.

Margaryan G, Mattioli C, Mladinic M, Nistri A (2010) Neuroprotection of locomotor networks after experimental injury to the neonatal rat spinal cord in vitro. Neuroscience 165:996-1010.
Margaryan G, Mladinic M, Mattioli C, Nistri A (2009) Extracellular magnesium enhances the damage to locomotor networks produced by metabolic perturbation mimicking spinal injury in the neonatal rat spinal cord in vitro. Neuroscience 163:669-682.
Mashour GA, Forman SA, Campagna JA (2005) Mechanisms of general anesthesia: from molecules to mind. Best Pract. Res. Clin. Anaesthesiol. 19:349–364.

Matsumoto T, Tamaki T, Kawakami M, Yoshida M, Ando M, Yamada H (2001) Early complications of high-dose methylprednisolone sodium succinate treatment in the follow-up of acute cervical spinal cord injury. Spine (Phila Pa 1976) 26:426-430.

Matsusue Y, Horii-Hayashi N, Kirita T, Nishi M (2014) Distribution of corticosteroid receptors in mature oligodendrocytes and oligodendrocyte progenitors of the adult mouse brain. The Journal of Histochemistry and Cytochemistry 62:211-226.

Matthews PB (1972) Mammalian Muscle Receptors and their Central Actions. Baltimore: Williams and Wilkins. 1-95.

Matthews PB (1991) The human stretch reflex and the motor cortex. Trends Neurosci. 14:87-90.

Mazze RI (2006) Methoxyflurane Revisited: Tale of an Anesthetic from Cradle to Grave. Anesthesiology 105:843-846.

Mazzone GL, Margaryan G, Kuzhandaivel A, Nasrabady SE, Mladinic M, Nistri A (2010) Kainate-induced delayed onset of excitotoxicity with functional loss unrelated to the extent of neuronal damage in the in vitro spinal cord. Neuroscience 168:451-462.
Mazzone GL, Mladinic M, Nistri A (2013) Excitotoxic cell death induces delayed proliferation of endogenous neuroprogenitor cells in organotypic slice cultures of the rat spinal cord. Cell Death Dis. 4:e902.
McEwen BS, Weiss JM, Schwartz LS (1968) Selective retention of corticosterone by limbic structures in rat brain. Nature 220:911-912.

McKinley WO, Seel RT, Hardman JT (1999) Nontraumatic spinal cord injury: incidence, epidemiology, and functional outcome. Arch. Phys. Med. Rehabil. 80:619-623.

Mena-Segovia J, Winn P, Bolam JP (2008) Cholinergic modulation of midbrain dopaminergic systems. Brain Res. Rev. 58:265-271.

Mesulam MM, Geula C (1988) Nucleus basalis (Ch4) and cortical cholinergic innervation in the human brain: observations based on the distribution of acetylcholinesterase and choline acetyltransferase. J. Comp. Neurol. 275:216-240.

Mesulam MM, Geula C, Bothwell MA, Hersh LB (1989) Human reticular formation: cholinergic neurons of the pedunculopontine and laterodorsal tegmental nuclei and some cytochemical comparisons to forebrain cholinergic neurons. J. Comp. Neurol. 283:611-633.

Miekisiak G, Kloc W, Janusz W, Kaczmarczyk J, Latka D, Zarzycki D (2014) Current use of methylprednisolone for acute spinal cord injury in Poland: survey study. Eur. J. Orthop. Surg. Traumatol. 24:S269-273.

Mirski, M.A., Muffelman, B., Ulatowski, J.A. & Hanley, D.F. (1995) Sedation for the critically ill neurologic patient. Crit. Care Med., 23, 2038-2053.

Molander C, Xu Q, Grant G (1984) The cytoarchitectonic organization of the spinal cord in the rat. I. The lower thoracic and lumbosacral cord. J. Comp. Neurol. 230:133-141.

Molander C, Xu Q, Rivero-Melian C, Grant G (1989) Cytoarchitectonic organization of the spinal cord in the rat: II. The cervical and upper thoracic cord. J. Comp. Neurol. 289:375-385.

Morin F, Beaulieu C, Lacaille JC (1998) Selective loss of GABA neurons in area CA1 of the rat hippocampus after intraventricular kainate. Epilepsy Res. 32:363-369.

Muchowski PJ, Wacker JL (2005) Modulation of neurodegeneration by molecular chaperones. Nat. Rev. Neurosci. 6:11-22.

Mulle C, Sailer A, Pérez-Otaño I, Dickinson-Anson H, Castillo PE, Bureau I, Maron C, Gage FH, Mann JR, Bettler B, Heinemann SF (1998) Altered synaptic physiology and reduced susceptibility to kainate- induced secures in GluR6-deficient mice. Nature 392:601-605.

Nakamizo T, Kawamata J, Yamashita H, Kanki R, Kihara T, Sawada H, Akaike A, Shimohama S (2005) Stimulation of nicotinic acetylcholine receptors protects motoneurons . Biochemical and biophysical research communications 330:1285-1289.

Narkilahti S, Pirttilä TJ, Lukasiuk K, Tuunanen J, Pitkänen A (2003) Expression and activation of caspase 3 following status epilepticus in the rat. Eur. J. Neurosci. 18:1486-1496.

Nasrabady SE, Kuzhandaivel A, Akrami A, Bianchetti E, Milanese M, Bonanno G, Nistri A (2012) Unusual increase in lumbar network excitability of the rat spinal cord evoked by the PARP-1 inhibitor PJ-34 through inhibition of glutamate uptake. Neuropharmacology. 63:415-426.

National Spinal Cord Injury Statistical Center, Facts and Figures at a Glance (2014) Birmingham, AL: University of Alabama at Birmingham.

Neef DW, Jaeger AM, Thiele DJ (2011) Heat shock transcription factor 1 as a therapeutic target in neurodegenerative diseases. Nat. Rev. Drug Discov. 10:930-944.

Netter FH (2006) Atlas of Human anatomy. Philadelphia, PA: Saunders/Elsevier.

Newton R (2000) Molecular mechanisms of glucocorticoid action: what is important? Thorax 55:603-613.

Nicholas JS, Selassie AW, Lineberry LA, Pickelsimer EE, Haines SJ (2009) Use and determinants of the methylprednisolone protocol for traumatic spinal cord injury in South Carolina acute care hospitals. J. Trauma. 66:1446-1450.

Nicotinic acetylcholine receptors: Introduction (2014) IUPHAR Database. International Union of Basic and Clinical Pharmacology.

Nishiyama T, Matsukawa T, Hanaoka K (2004) Intrathecal propofol has analgesic effects on inflammation-induced pain in rats. Can. J. Anaesth. = Journal canadien d'anesthesie 51:899-904.

Nowak TS, Bond U, Schlesinger MJ (1990) Heat shock RNA levels in brain and other tissues after hyperthermia and trasient ischemia. J. Neurochem. 54:451-458.

Nuland SB (1988) Doctors: the biography of medicine. 1st ed. New York: Knopf.

Oakley RH, Cidlowski JA (2011) Cellular processing of the glucocorticoid receptor gene and protein: new mechanisms for generating tissue-specific actions of glucocorticoids. The Journal of Biological Chemistry 286:3177-3184.

Oakley RH, Cidlowski JA (2013) The biology of the glucocorticoid receptor: new signaling mechanisms in health and disease. The Journal of Allergy and Clinical Immunology 132: 1033-1044.

Onifer SM, Rabchevsky AG, Scheff SW (2007) Rat models of traumatic spinal cord injury to assess motor recovery. ILARJ 48:385-395.

Pain L, Oberling P, Launoy A, Di Scala G (1999) Effect of nonsedative doses of propofol on an innate anxiogenic situation in rats. Anesthesiology 90:191-196.

Pallavicini M, Moroni B, Bolchi C, Clementi F, Fumagalli L, Gotti C, Vailati S, Valoti E, Villa L (2004) Synthesis and alpha4beta2 nicotinic affinity of 2-pyrrolidinylmethoxyimines and prolinal oxime ethers. Bioorg. Med. Chem. Lett. 14:5827-5830.

Park E, Velumian AA, Fehlings MG (2004) The role of excitotoxicity in secondary mechanisms of spinal cord injury: a review with an emphasis on the implications for white matter degeneration. J. Neurotrauma. 21:754-774.

Patel P, Julien JP, Kriz J (2014) Early-stage treatment with withaferin A reduces levels of misfolded superoxide dismutase 1 and extends lifespan in a mouse model of amyotrophic lateral sclerosis. Neurotherapeutics. 12:217-233.

Peralta EG, Ashkenazi A, Winslow JW, Smith DH, Ramachandran J, Capon DJ (1987) Distinct primary structures, ligand binding properties and tissue-specific expression of four human muscarinic acetylcholine receptors. EMBO J. 6:3923-3929.

Pointillart V, Petitjean ME, Wiart L et al (2000) Pharmacological therapy of spinal cord injury during the acute phase. Spinal Cord 38:71-76.

Pratt WB, Gestwicki JE, Osawa Y, Lieberman AP (2015) Targeting Hsp90/Hsp70- based protein quality control for treatment of adult onset neurodegenerative diseases. Annu. Rev. Pharmacol. 55:353-371.

Prendergast MA et al (2001) Chronic nicotine exposure reduces N-methyl-D-aspartate receptor-mediated damage in the hippocampus without altering calcium accumulation or extrusion: evidence of calbindin-D28K overexpression. Neuroscience 102:75-85.

Quinlan KA, Kiehn O (2007) Segmental, synaptic actions of commissural interneurons in the mouse spinal cord. J. Neurosci. 27:6521-6530.

Rampil IJ, Kim JS, Lenhardt R, et al (1998) Bispectral EEG index during nitrous oxide administration. Anesthesiology 89:671-677.

Restrepo CE, et al (2009) Transmitter-phenotypes of commissural interneurons in the lumbar spinal cord of newborn mice. J. Comp. Neurol. 517:177-192.

Revollo JR, Cidlowski JA (2009) Mechanisms generating diversity in glucocorticoid receptor signaling," Annals of the New York Academy of Sciences 1179:167-178.

Rexed B (1952) The cytoarchitectonic organization of the spinal cord in the cat. J. Comp. Neurol. 96:414-495.

Rexed B (1954) A cytoarchitectonic atlas of the spinal cord in the cat. J. Comp. Neurol. 100: 297-379.

Roberts A, Roberts BL (1983) Neural origins of rhythmic movements. Cambridge, UK: Cambridge University Press.

Romanelli MN, Gratteri P, Guandalini L, Martini E, Bonaccini C, Gualtieri F (2007) Central Nicotinic Receptors: Structure, Function, Ligands, and Therapeutic Potential. 2:746-767.

Romanelli MN, Gualtieri F (2003) Cholinergic nicotinic receptors: competitive ligands, allosteric modulators, and their potential applications. Med. Res. Rev. 23:393-426.

Rossi MA, Chan CK, Christensen JD, DeGuzman EJ, Durieux ME (1996) Interactions between propofol and lipid mediator receptors: inhibition of lysophosphatidate signaling. Anesth. Analg. 83:1090-1096.

Rossignol S, Chau C, Brustein E, Giroux N, Bouyer L, Barbeau H, Reader TA (1998) Pharmacological activation and modulation of the central pattern generator for locomotion in the cat. Ann. N. Y. Acad. Sci. 860:346-359.

Rothstein JD, Jin L, Dykes-Hoberg M, Kuncl RW (1993) Chronic inhibition of glutamate uptake produces a model of slow neurotoxicity. Proc. Natl. Acad. Sci. U.S.A. 90:6591-6595.

Rowland JW, Hawryluk GW, Kwon B, Fehlings MG (2008) Current status of acute spinal cord injury pathophysiology and emerging therapies: promise on the horizon. Neurosurg. Focus. 25:E2.

Salminen A, Lehtonen M, Paimela T, Kaarniranta K (2010) Celastrol: molecular targets of thunder god vine. Biochem. Biophys. Res. Commun. 394:439-442.

Salzman SK, Lee WA, Sabato S, Mendez AA, Agresta CA, Kelly G (1993) Halothane anesthesia is neuroprotective in experimental spinal cord injury: early hemodynamic mechanisms of action. Res. Commun. Chem. Pathol. Pharmacol. 80:59-81.

Sámano C, Kaur J, Nistri A (2016) A study of methylprednisolone neuroprotection against acute injury to the rat spinal cord in vitro. Neuroscience 315:136-149.

Samuelson PN, Merin RG, Taves DR, Freeman RB, Calimlim JF, Kumazawa T (1976) Toxicity following methoxyflurane anaesthesia: IV. The role of obesity and the effect of low dose anaesthesia on fluoride metabolism and renal function. Canadian Anaesthetists' Society Journal 23:465-479.

Sanchez E (1990) Hsp56: a novel heat shock protein associated with untransformed steroid receptor complexes. The Journal of Biological Chemistry 265:22067-22070.

Sanchez-Conde P, Rodriguez-Lopez JM, Nicolas JL, Lozano FS, Garcia-Criado FJ, Cascajo C, Gonzalez-Sarmiento R, Muriel C (2008) The comparative abilities of propofol and sevoflurane to modulate inflammation and oxidative stress in the kidney after aortic cross-clamping. Anesth. Analg. 106:371-378.

Sapolsky RM, Romero LM, Munck AU (2000) How do glucocorticoids influence stress responses? Integrating permissive, suppressive, stimulatory, and preparative actions. Endocr. Rev. 21:55-89.

Sargent PB (1993) The diversity of neuronal nicotinic acetylcholine receptors. Annu. Rev. Neurosci. 16:403-443.

Sassa H, Kogure K, Takaishi Y, Terada H (1994) Structural basis of potent antiperoxidation activity of the triterpene celastrol in mitochondria: effect of negative membrane surface charge on lipid peroxidation. Free Radic. Biol. Med. 17:201-207.

Sassa H, Takaishi Y, Terada H (1990) The triterpene celastrol as a very potent inhibitor of lipid peroxidation in mitochondria. Biochem. Biophys. Res. Commun. 172:890-897.

Sauerland S, Nagelschmidt M, Mallmann P, Neugebauer EA (2000) Risks and benefits of preoperative high dose Methylprednisolone in surgical patients: A systematic review. Drug Saf. 23:449-461.

Scarr E (2012) Muscarinic Receptors: Their Roles in Disorders of the Central Nervous System and Potential as Therapeutic Targets. CNS Neurosci. Ther. 18:369-379.

Schanne FA, Kane AB, Young EE, Farber JL (1979) Calcium dependence of toxic cell death: a final common pathway. Science 206:700-702.

Schoenen J, Faull RLM (2004) Spinal cord: cyto- and chemoarchitecture. In: Paxinos G, Mai JK, editors. The human nervous system. 2nd ed. San Diego: Elsevier Academic Press. 190-232.

Sekhon LH & Fehlings MG (2001) Epidemiology, demo-graphics, and Pathophysiology of acute spinal cord injury. Spine 26:S2-S12.

Selverston AI (2005) A neural infrastructure for rhythmic motor patterns. Cell. Mol. Neurobiol. 25:223-244.

Shabbir A, Bianchetti E, Cargonja R, Petrovic A, Mladinic M, Pilipović K, Nistri A (2015) Role of HSP70 in motoneuron survival after excitotoxic stress in a rat spinal cord injury model in vitro. Eur J Neurosci 42:3054-3065.

Shabbir A, Bianchetti E, Nistri A (2015) The volatile anesthetic methoxyflurane protects motoneurons against excitotoxicity in an in vitro model of rat spinal cord injury. Neuroscience 285:269-280.

Shaqura M, Li X, Al-Khrasani M et al (2016) Membrane-bound glucocorticoid receptors on distinct nociceptive neurons as potential targets for pain control through rapid non-genomic effects. Neuropharmacology 111:1-13.

Shaqura M, Li X, Al-Madol MA et al (2016) Acute mechanical sensitization of peripheral nociceptors by aldosterone through non-genomic activation of membrane bound mineralocorticoid receptors in naive rats. Neuropharmacology 107:251-261.

Shaw PJ (1994) Excitotoxicity and motor neurone disease: a review of the evidence. J. Neurol. Sci. 124:6-13.

Shibata M, Hisahara S, Hara H, Yamawaki T, Fukuuchi Y, Yuan J, Okano H, Miura M (2000) Caspases determine the vulnerability of oligodendrocytes in the ischemic brain. J. Clin. Invest. 106:643-653.

Shuman SL, Bresnahan JC, Beattie MS (1997) Apoptosis of microglia and oligodendrocytes after spinal cord contusion in rats. J. Neurosci. Res. 50:798-808.

Sidman RL, Angevine JB Jr, Pierce ET (1971) Atlas of the mouse brain and spinal cord. Cambridge: Harvard University Press.

Sieghart W (1995) Structure and pharmacology of γ-aminobutyric $acid_A$ receptor subtypes. Pharmacol. Rev. 47:181-234.

Sierra A, Gottfried-Blackmore A, Milner TA, McEwen BS, Bulloch K (2008) Steroid hormone receptor expression and function in microglia. Glia 56:659-674.

Simon J, Wakimoto H, Fujita N, Lalande M, Barnard EA (2004) Analysis of the set of $GABA_A$ receptor genes in the human genome. J. Biol. Chem. 279: 41422-41435.

Sine SM, Engel AG (2006) Recent advances in Cys-loop receptor structure and function. Nature 440:448-455.

Skinner RD, Kinjo N, Henderson V, Garcia-Rill E (1990) Locomotor projections from the pedunculopontine nucleus to the spinal cord. Neurological Reports 1:183-186.

Smith C, McEwan AI, Jhaveri R, Wilkinson M, Goodman D, Smith LR, Canada AT, Glass PS (1994) The interaction of fentanyl on the Cp50 of propofol for loss of consciousness and skin incision. Anesthesiology 81:820-828.

Sonner JM, Antognini JF, Dutton RC, Flood P, Gray AT, Harris RA, Homanics GE, Kendig J, Orser B, Raines DE, Rampil IJ, Trudell J, Vissel B, Eger EI 2nd (2003) Inhaled

anesthetics and immobility: mechanisms, mysteries, and minimum alveolar anesthetic concentration. Anesth. Analg. 97:718-740.

Spencer RL, Young EA, Choo PH, McEwen B (1990) Adrenal steroid type I and type II receptor binding: estimates of in vivo receptor number, occupancy, and activation with varying level of steroid. Brain Research 514:37-48.

Springer JE, Azbill RD, Knapp PE (1999) Activation of the caspase-3 apoptotic cascade intraumatic spinal cord injury. Nat.Med. 5:943-946.

Stein RB, Capaday C (1988) The modulation of human reflexes during functional motor tasks. Trends Neurosci. 11:328-332.

Streit J (1996) Mechanisms of pattern generation in cocultures of embryonic spinal cord and skeletal muscle. Int. J. Dev. Neurosci. 14:137-148.

Sun YY, Wang CY, Hsu MF, Juan SH, Chang CY, Chou CM, Yang LY, Hung KS, Xu J, Lee YH, Hsu CY (2010) Glucocorticoid protection of oligodendrocytes against excitotoxin involving hypoxia-inducible factor-1a in a cell-type-specific manner. J. Neurosci. 30:9621-9630.

Taccola G, Margaryan G, Mladinic M, Nistri A (2008) Kainate and metabolic perturbation mimicking spinal injury differentially contribute to early damage of locomotor networks in the in vitro neonatal rat spinal cord. Neuroscience 155:538-555.

Taccola G, Mladinic M, Nistri A (2010) Dynamics of early locomotor network dysfunction following a focal lesion in an in vitro model of spinal injury. Eur J Neurosci. 31:60-78.

Taccola G, Nistri A (2007) Differential modulation by tetraethylammonium of the processes underlying network bursting in the neonatal rat spinal cord in vitro. Neuroscience 146:1906-1917.

Takakusaki K, Chiba R, Tsukasa N, Okumura T (2016) Brainstem control of locomotion and muscle tone with special reference to the role of the mesopontine tegmentum and medullary reticulospinal systems. Journal of Neural Transmission. 123:695-729.

Takakusaki K, Obara K, Nozu T, Okumura T (2011) Modulatory effects of the GABAergic basal ganglia neurons on the PPN and the muscle tone inhibitory system in cats. Archives Italiennes de Biologie 149:385-405.

Takakusaki K, Shiroyama T, Yamamoto T, Kitai ST (1996) Cholinergic and noncholinergic tegmental pedunculopontine projection neurons in rats revealed by intracellular labeling. J. Comp. Neurol. 371:345-361.

Talpalar AE, et al (2011) Identification of minimal neuronal networks involved in flexor-extensor alternation in the mammalian spinal cord. Neuron 71:1071-1084.

Talpalar AE, Bouvier J, Borgius L, Fortin G, Pierani A, Kiehn O (2013) Dual-mode operation of neuronal networks involved in left–right alternation. Nature 500:85-88.

Tinetti ME (2003) Clinical practice. Preventing falls in elderly persons. N. Engl. J. Med. 348:42-49.

Todd AJ, Sullivan AC (1990) Light microscope study of the coexistence of GABA-like and glycin-like immunoreactivity in the spinal cord of the rat. J. Comp. Neurol. 296:496-505.

Traub RD, Miles R, Jefferys JGR (1993) Synaptic and intrinsic conductances shape picrotoxin-induced synchronized after-discharges in the guinea-pig hippocampal slice. J. Physiol. (Lond) 461:525-547.

Tscherter A, Heuschkel MO, Renaud P, Streit J (2001) Spatiotemporal characterization of rhythmic activity in rat spinal cord slice cultures. Eur. J. Neurosci. 14:179-190.

van den Berg ME, Castellote JM, Mahillo-Fernandez I, de Pedro-Cuesta J (2010) Incidence of spinal cord injury worldwide: asystematic review. Neuroepidemiology 34:184-192.

Vasileiou I, Xanthos T, Koudouna E, Perrea D, Klonaris C, Katsargyris A, Papadimitriou L (2009) Propofol: A review of its non-anaesthetic effects. European Journal of Pharmacology 605:1–8.

Velasco I, Tapia R, Massieu L (1996) Inhibition of glutamate uptake induces progressive accumulation of extracellular glutamate and neuronal damage in rat cortical cultures. J. Neurosci. Res. 44:551-561.

Veselis RA, Pryor KO, Reinsel RA, Mehta M, Pan H, Johnson Jr, R (2008) Low dose propofol-induced amnesia is not due to a failure of encoding: left inferior prefrontal cortex is still active. Anesthesiology 109:213-224.

Veselis RA, Reinsel RA, Feshchenko VA, Johnson Jr, R, (2004) Information loss over time defines the memory defect of propofol: a comparative response with thiopental and dexmedetomidine. Anesthesiology 101:831-841.

Vielkind U, Walencewicz A, Levine JM, Bohn MC (1990) Type-II glucocorticoid receptors are expressed in oligodendrocytes and astrocytes. Journal of Neuroscience Research 27:360-373.

Vincent P & Mulle C (2009) Kainate receptors in epilepsy and excitotoxicity. Neuroscience 158:309-323.

von Euler M, Li-Li M, Whittemore S, Seiger A, Sundström E (1997) No protective effect of the NMDA antagonist memantine in experimental spinal cord injuries. J. Neurotrauma. 14:53-61.

Wang J, Yang X, Camporesi CV, Yang Z, Bosco G, Chen C, Camporesi EM (2002) Propofol reduces infarct size and striatal dopamine accumulation following transient middle cerebral artery occlusion: a microdialysis study. Eur. J. Pharmacol. 452:303-308.

Wang Q, Yu S, Simonyi A, Sun GY, Sun AY (2005) Kainic acid-mediated excitotoxicity as a model for neurodegeneration. Molecular Neurobiology 31:3-16.

Wang QS, Jiang YH, Wang TD, Xiao T, Wang JK (2013) Effects of betamethasone on neuropathic pain in a rat spare nerve injury model. Clin. Exp. Pharmacol. Physiol. 40:22-27.

Wang Y, Cao L, Xu LM, Cao FF, Peng B, Zhang X, Shen YF, Uzan G, Zhang DH (2015) Celastrol ameliorates EAE induction by suppressing pathogenic T cell responses in the peripheral and central nervous systems. J. Neuroimmune. Pharmacol. 10:506-516.

Warembourg M, Otten U, Schwab ME (1981) Labelling of schwann and satellite cells by [3H]dexamethasone in a rat sympathetic ganglion and sciatic nerve. Neuroscience 6:1139-1143.

Watson C, Paxinos G, Kayalioglu G, Heise C (2009) An atlas of the mouse spinal cord. In: Watson C, Paxinos G, Kayalioglu G, editors. The spinal cord. A Christopher and Dana Reeve foundation text and atlas. San Diego: Elsevier Academic Press. 308-379.

Weber I, Veress G, Szucs P, Antal M, Birinyi A (2007) Neurotransmitter systems of commissural interneurons in the lumbar spinal cord of neonatal rats. Brain Res. 1178:65-72.

Wei ZL, Xiao Y, Yuan H, Baydyuk M, Petukhov PA, Musachio JL, Kellar KJ, Kozikowski AP (2005) Novel pyridyl ring C5 substituted analogues of epibatidine and 3-(1-methyl-2(S)-pyrrolidinylmethoxy) pyridine (A-84543) as highly selective agents for neuronal nicotinic acetylcholine receptors containing beta2 subunits. J. Med. Chem. 48:1721-1724.

Wess J (1996) Molecular biology of muscarinic acetylcholine receptors. Crit. Rev. Neurobiol. 10:69-99.

Wessler I, Kirkpatrick CJ (2008) Acetylcholine beyond neurons: the non-neuronal cholinergic system in humans. Br. J. Pharmacol. 154:1558-1571.

Westerheide SD, Bosman JD, Mbadugha BN, Kawahara TL, Matsumoto G, Kim S, Gu W, Devlin JP, Silverman RB, Morimoto RI (2004) Celastrols as inducers of the heat shock response and cytoprotection. J. Biol. Chem. 279:56053-56060.

Wharton RS, Sievenpiper TS, Mazze RI (1980) Developmental toxicity of methoxyflurane in mice. Anesth. Analg. 59:421-425.

Whiting P, Lindstrom J (1986b) Pharmacological properties of immuno-isolated neuronal nicotinic receptors. J. Neurosci. 6:3061-3069.

Whiting P, Lindstrom J (1987) Purification and characterization of a nicotinic acetylcholine receptor from rat brain. Proc. Natl. Acad. Sci. U.S.A 84:595-599.

Whiting PJ, Lindstrom JM (1986a) Purification and characterization of a nicotinic acetylcholine receptor from chick brain. Biochemistry 25:2082–2093.

Wolman L (1965) The disturbances of circulation in traumatic paraplegia in acute and late stages: a pathological study. Paraplegia 2:213-226.

Wong KF, Yuan Y, Luk JM (2012) Tripterygium wilfordii bioactive compounds as anticancer and anti-inflammatory agents. Clin. Exp. Pharmacol. Physiol. 39:311-320.

Woodbridge PD (1957) Changing concepts concerning depth of anesthesia. Anesthesiology 18:536-550.

Woolf NJ (1991) Cholinergic systems in mammalian brain and spinal cord. Prog. Neurobiol. 37:475-524.

Wrathal JR, Teng YD, Marriott R (1997) Delayed antagonism of AMPA/kainate receptors reduces long-term functional deficits resulting from spinal cord trauma. Exp. Neurol. 145:565-573.

Xiong Y, Rabchevsky AG, Hall ED (2007) Role of peroxynitrite in secondary oxidative damage after spinal cord injury. J. Neurochem. 100:639-649.

Xu J, Fan G, Chen S, Wu Y, Xu XM, Hsu CY (1998a) Methylprednisolone inhibition of TNF-alpha expression and NF-kB activation after spinal cord injury in rats. Brain Res. Mol. Brain Res. 59:135-142.

Yamasaki T, Nakakimura K, Matsumoto M, Xiong L, Ishikawa T, Sakabe T (1999) Effects of graded suppression of the EEG with propofol on the neurological outcome following incomplete cerebral ischaemia in rats. Eur. J. Anaesthesiol. 16:320-329.

Young W (1993) Secondary injury mechanisms in acute spinal cord injury. J. Emerg. Med. 11:13-22.

Zacny JP, Coalson DW, Young CJ, Klafta JM, Lichtor JL, Rupani G, Thapar P, Apfelbaum JL (1996) Propofol at conscious sedation doses produces mild analgesia to cold pressor-induced pain in healthy volunteers. J. clin. anaesth. 8:469-474.

Zhang CX, Ge ZM, Cheng TM, Li RT (2006) Synthesis and analgesic activity of secondary amine analogues of pyridylmethylamine and positional isomeric analogues of ABT-594. Bioorg. Med. Chem. Lett. 16:2013-2016.

Zhang J, et al (2014) V1 and v2b interneurons secure the alternating flexor-extensor motor activity mice require for limbed locomotion. Neuron 82:138:150.

9 SUPPLEMENTARY DATA

9.1 Appendix I: Neurotoxicity of nicotine

1) We studied the structural and functional changes evoked by application 10 µM nicotine (for 1 or 4 h) after or during excitotoxicity induced by kainate (50 µM) in an in vitro SCI model. These experiments followed the same methods as previously explained in the result section.

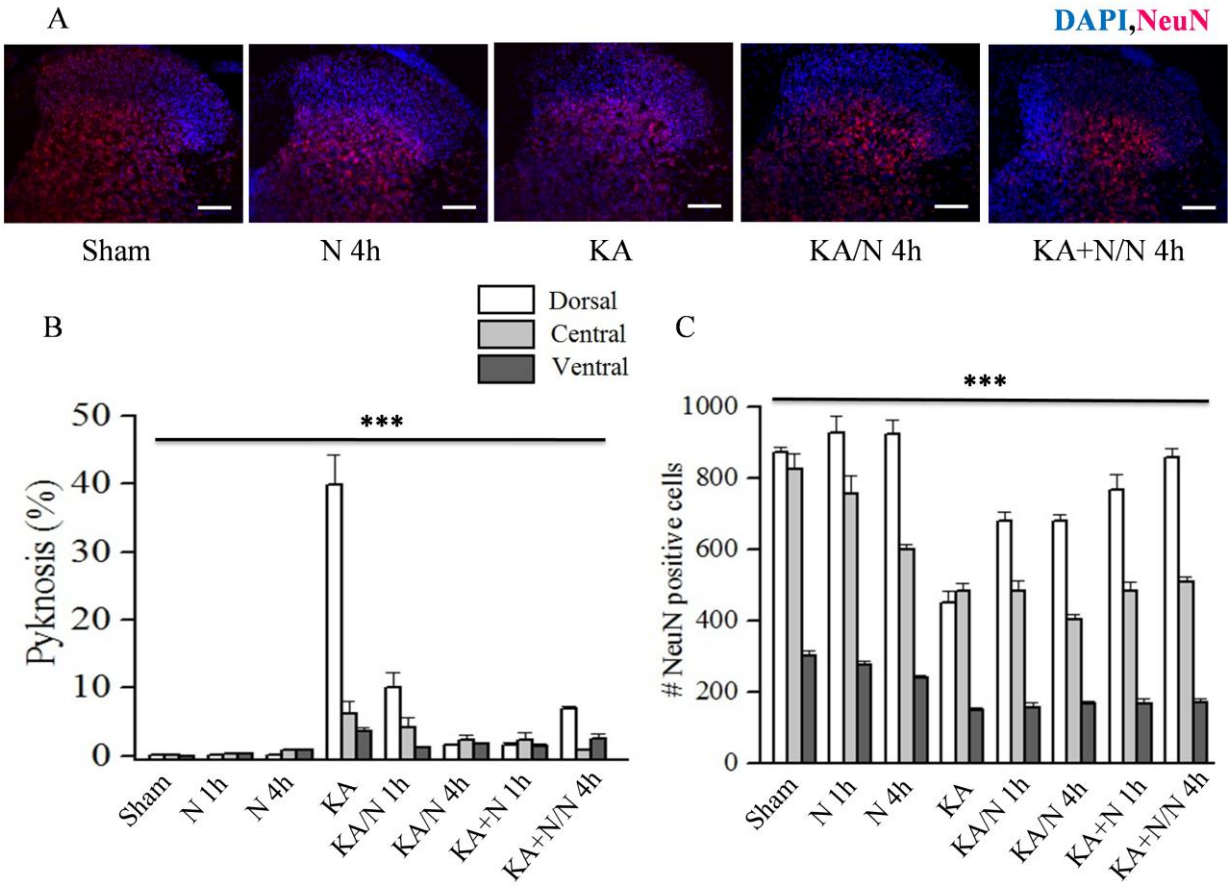

Fig. 1 Changes in percent pyknosis (stained with DAPI, blue) and neuronal (stained with NeuN, red) numbers by nicotine application alone (1 or 4 h) or after kainate (KA) and nicotine treatment (1 or 4 h) in all three ROI. (A, B) No damage induced by application of

nicotine alone. Kainate application induced significant percent pyknosis in all three ROI i.e., dorsal, central and ventral horn which is antagonized by nicotine treatment (***P = 0.001). (A, C) No change in the number of neurons in dorsal horn after nicotine alone application, however, the neuronal number was significantly reduced in central (P = 0.001) and ventral horn (P = 0.001) when nicotine was applied alone for 4 h. Kainate, when applied alone, has drastically reduced the number of neurons in all the ROI in comparison to sham or nicotine alone (P = 0.001). When nicotine was applied with or after kainate increased the neuronal number only in the dorsal ROI (P = 0.001) whereas no change observed in the central and ventral horn of spinal cord. Data are mean ±SEM. Scale bar = 100 µm. n = 3 to 6 where n is the number of spinal cords used and 3 to 5 sections/preparation were taken.

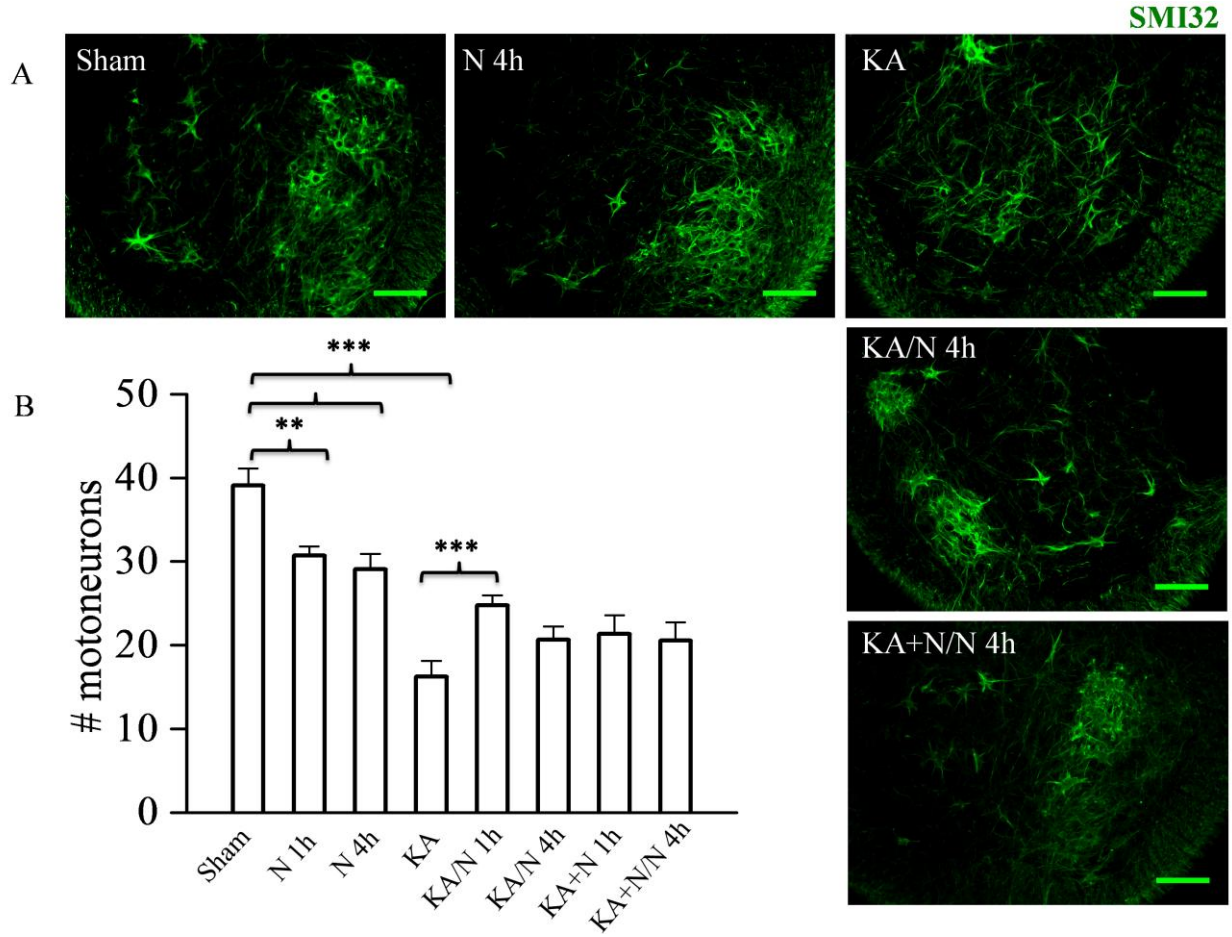

Fig. 2 Changes in motoneuronal number 24 h after excitotoxic injury by kainate alone or kainate and nicotine application. (A) Examples of motoneurons immuno-stained with SMI32, green. (B) Bar graph represents the significant reduction in motoneuronal number after nicotine alone application either for 1 h (**P = 0.002) or 4 h (***P = 0.001).

Kainate alone application has reduced the motoneuronal number to less than half in comparison to sham which was not significantly recovered by nicotine treatment with or after kainate except when nicotine was applied for 1 h after kainate (P = 0.001; KA vs KA/N 1h). Data are mean ±SEM. Scale bar = 100 µm. n = 3 to 7 where n is the number of spinal cords used and 4 to 7 sections/preparation were taken.

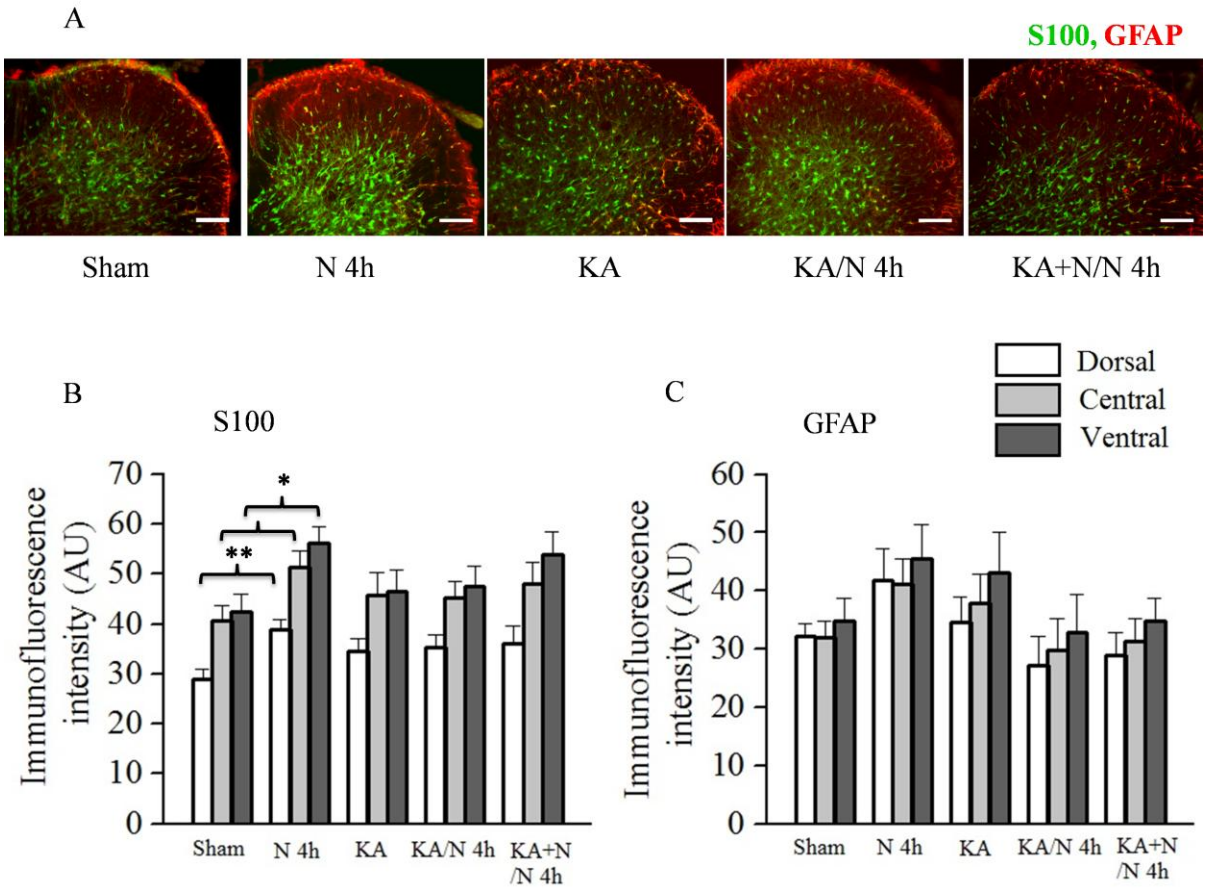

Fig. 3 Effect of nicotine and kainate on astroglia immunostained with S100 (green) and GFAP (red) 24 h later in vitro. (A) Examples of astroglia in sham, N 4h, KA, KA/N 4 h and KA+N/N 4 h treatments. (B, C) Histograms shows no alterations in immunofluorescence intensity of astroglia labelled with S100 and GFAP except in case of nicotine when applied alone in comparison to sham preparations in all the three ROI (dorsal: **P = 0.003; central: *P = 0.03; ventral: P = 0.013). Data are mean ±SEM. Scale bar = 100 µm. n = 7 to 10 where n is number of spinal cords used and 8 to 10 sections/preparation were taken.

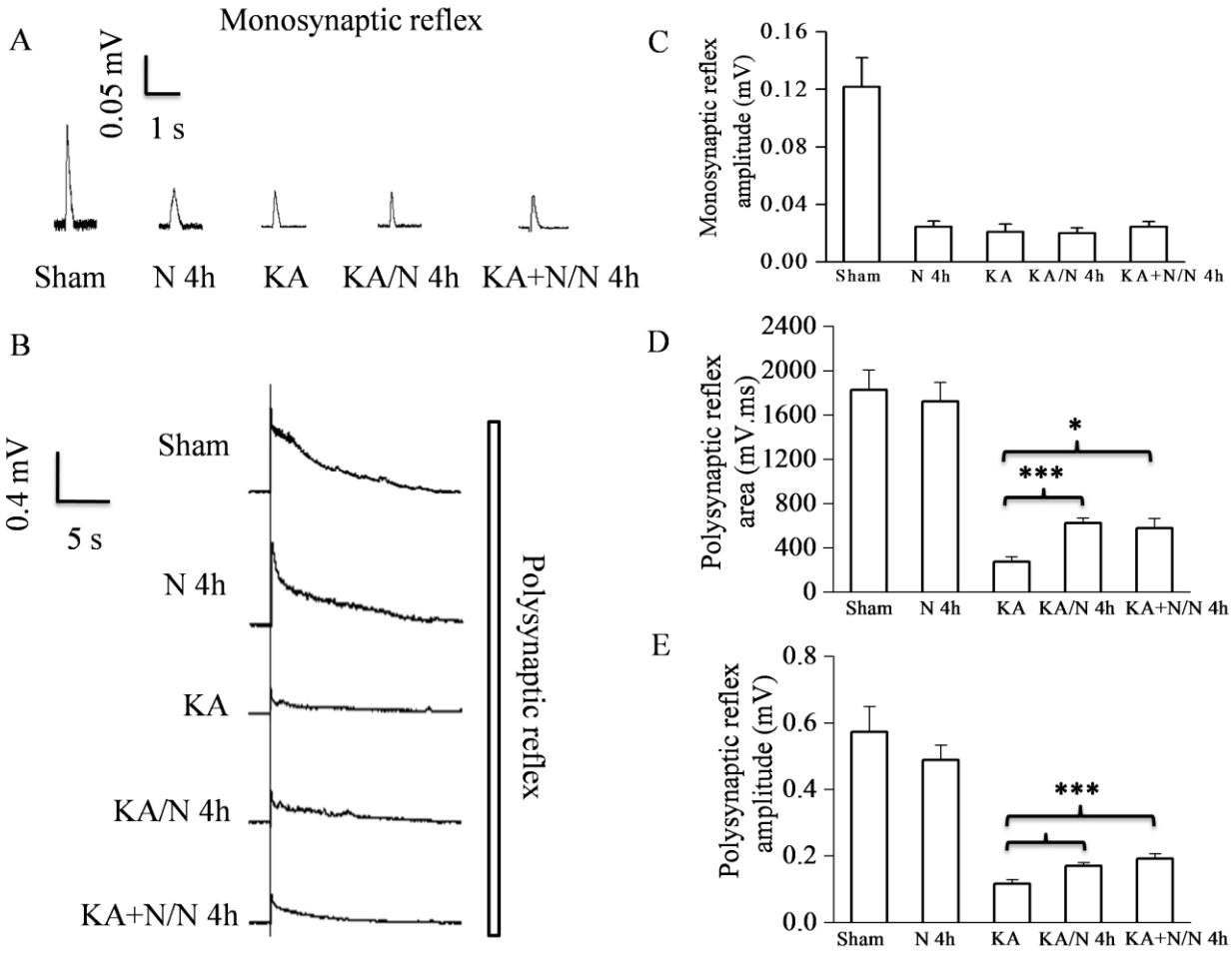

Fig. 4 Effect of nicotine (10 µM) and kainate (50 µM) on synaptic transmission recorded 24 h later. (A, B) Example recordings of monosynaptic and polysynaptic reflex responses in sham (n = 9), nicotine 4 h (N 4h; n = 5), kainate (KA; n = 8), kainate followed by nicotine 4 h (KA/N 4h; n = 7) and kainate co-applied with nicotine followed by nicotine for 4 h (KA+N/N 4h; n = 7) treatments. (D, E) Bar graphs show no change in polysynaptic reflexes (D, E) after nicotine alone application which were highly depressed by kainate when applied alone and a modest improvement observed by treatment with nicotine after or together with kainate (amplitude: ***P ≤ 0.001, *P ≤ 0.05; area: P ≤ 0.001; KA vs KA/N 4h, KA vs KA+N/N 4h, respectively). However, monosynaptic reflexes(C) were depressed in all cases in comparison to sham (P ≤ 0.001) as represented in the example records (A) and bar graph (C). Data are mean ±SEM. n denotes the number of spinal cords used.

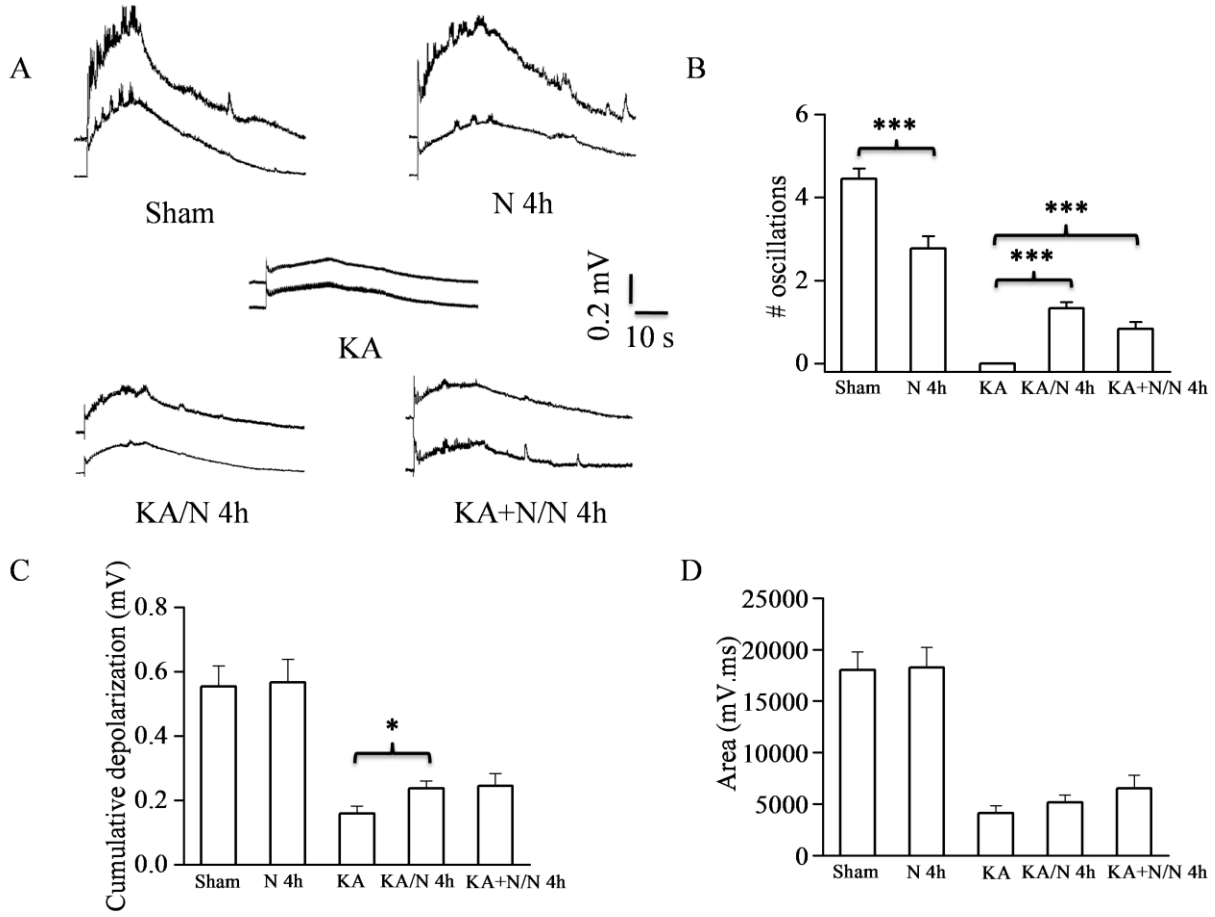

Fig. 5 Changes in DR train evoked VR responses after 24 h in vitro. (A) Examples of fictive locomotion induced by DR train in sham (n = 9), N 4h (n = 5), KA (n = 8), KA/N 4h (n = 7) and KA+N/N 4h (n = 7). (B-D) Histograms showing intense depression evoked by kainate alone application which was modestly improved after nicotine application (number of oscillations: ***P ≤ 0.001, KA vs KA/N 4h, KA vs KA+N/N 4h; cumulative depolarization: *P ≤ 0.05, KA vs KA/N 4h). Data are mean ±SEM. n denotes the number of spinal cords used.

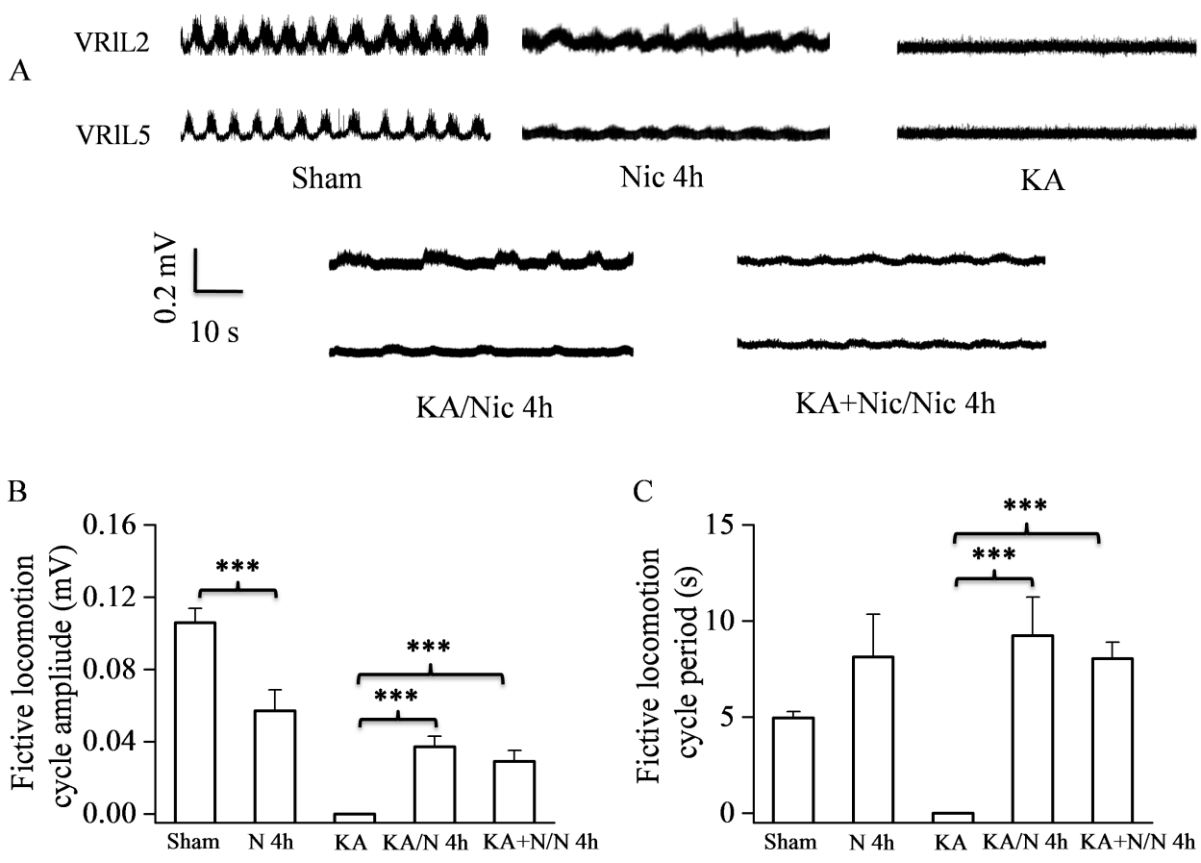

Fig. 6 Changes in chemically induced fictive locomotion recorded after 24 h in vitro. (A) Sample records of fictive locomotor patterns in sham (n = 9), N 4h (n = 5), KA (n = 8), KA/N 4h (n = 7) and KA+N/N 4h (n = 7). (B, C) The cycle amplitude has reduced and the periodicity has increased after application of nicotine alone. Kainate alone application has fully abolished the fictive locomotor patterns which were reversed by nicotine even though with smaller amplitude and longer periodicity (***P ≤ 0.001, KA vs KA/N 4h, KA vs KA+N/N 4h). Data are mean ±SEM. n denotes the number of spinal cords used.

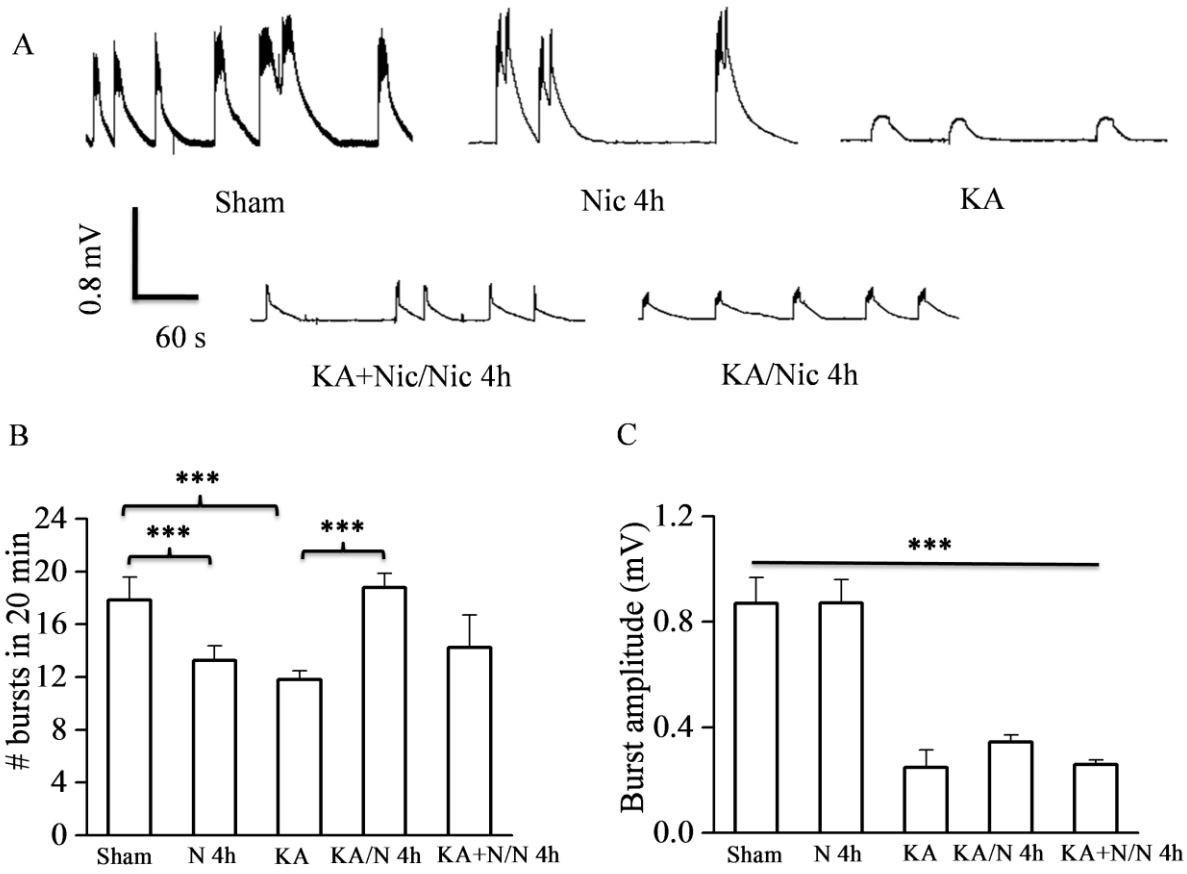

Fig. 7 Changes in intrinsic rhythmicity of spinal cords following kainate and nicotine treatment. (A) Example records of disinhibited bursts evoked by inhibiting GABAergic and glycinergic transmission with bicuculline and strychnine 24 h after in sham (n = 9), N 4h (n = 5), KA (n = 8), KA/N 4h (n = 7) and KA+N/N 4h (n = 7) preparations. (B, C) Bar graphs showing a significant decrease in number of bursts after nicotine alone application with no change in amplitude of the same in comparison to sham treated spinal cords. Kainate alone application has strongly depressed the number and amplitude of bursts. A significant recovery in number of bursts by nicotine applied after or together with kainate application with no further change in amplitude (***P ≤ 0.001). Data are mean ±SEM. n denotes the number of spinal cords used.

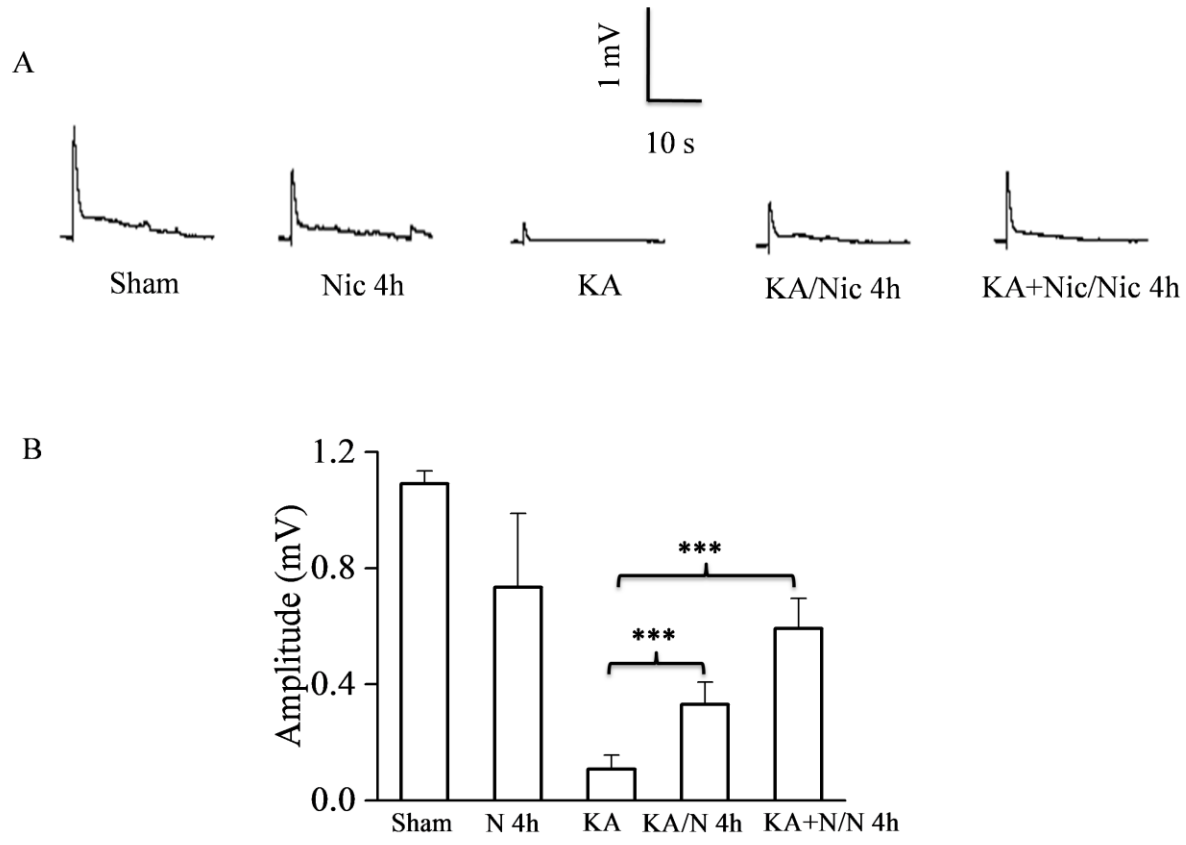

Fig. 8 Changes in DR-DR evoked responses recorded 24 h in vitro. (A) Representative traces of DR-DR evoked responses in sham (n = 4), N 4h (n = 3), KA (n = 4), KA/N 4h (n = 4) and KA+N/ 4 h (n = 5). (B) Histogram illustrates that kainate application has completely disrupted the amplitude of DR-DR responses which has significantly reversed by nicotine application (***$P \leq 0.001$).

9.2 Appendix II: Effects of celastrol

2) Changes in functional outcome were studied by pre-treating the spinal cords with celastrol for 6 h (0.75 µM) followed by excitotoxic injury (kainate, 1 h, 50 µM). These experiments followed the same methods as described in the enclosed papers in the result section.

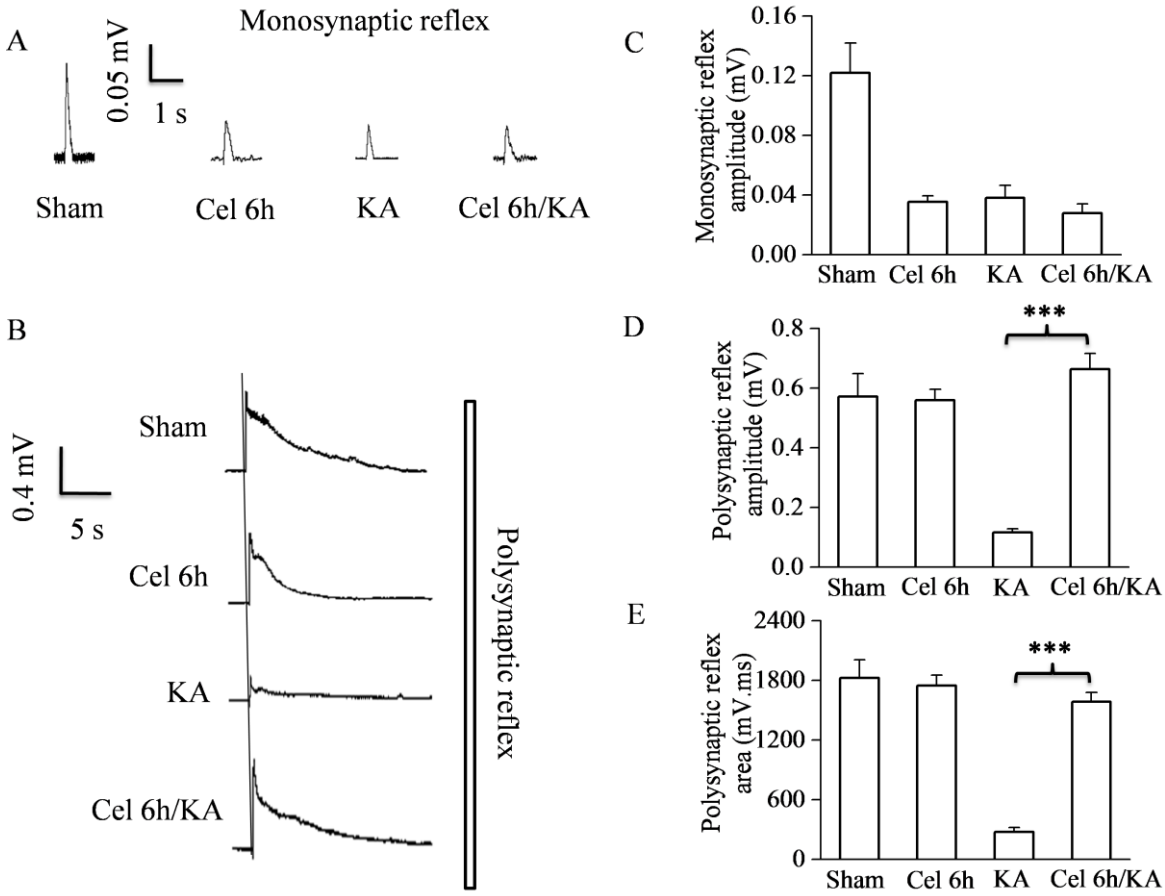

Fig. 1 Changes in reflex responses after celastrol and kainate application recorded from lumbar VRs 24 h after in vitro. (A, B) Sample records of mono- and polysynaptic reflex responses in sham, celastrol applied for 6 h (Cel 6 h), kainate application for 1 h (KA) and celastrol (6 h) for by kainate (CEL 6 h/ KA) treatments. (C) Histogram showing strong reduction in monosynaptic reflex responses in all the cases when compared to

sham preparations. (D, E) Bar graphs illustrating a good recovery in polysynaptic reflexes by pre-treating the preparations with celastrol followed by kainate in comparison to kainate alone (***P ≤ 0.001).

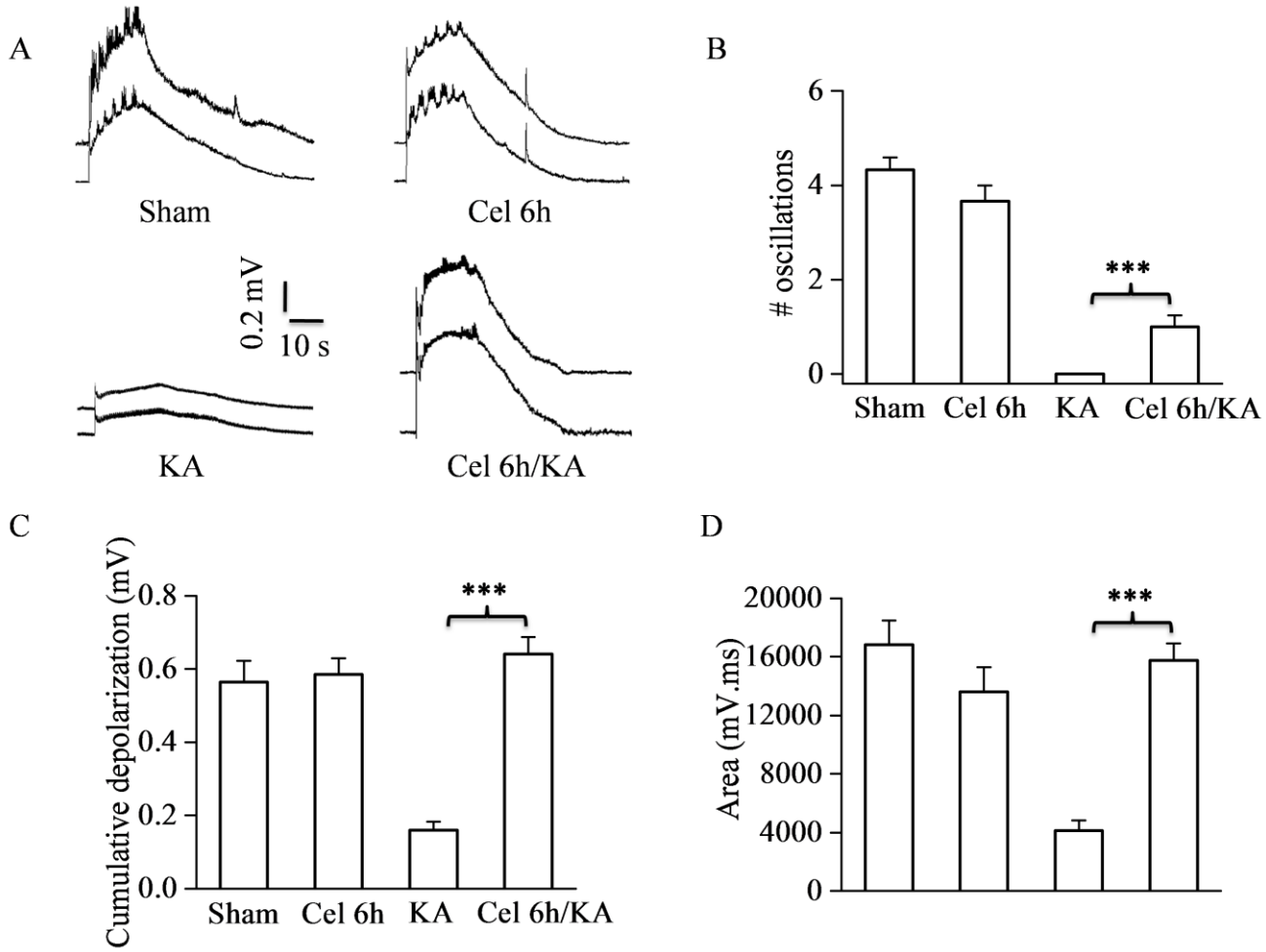

Fig. 2 Effect of celastrol pre-treatment followed by kainate on DR train evoked fictive locomotion. Note a strong recovery in electrically evoked fictive locomotion observed after celastrol followed by kainate application (P ≤ 0.001) as exemplified in sample records (A) and bar graphs (B-D).

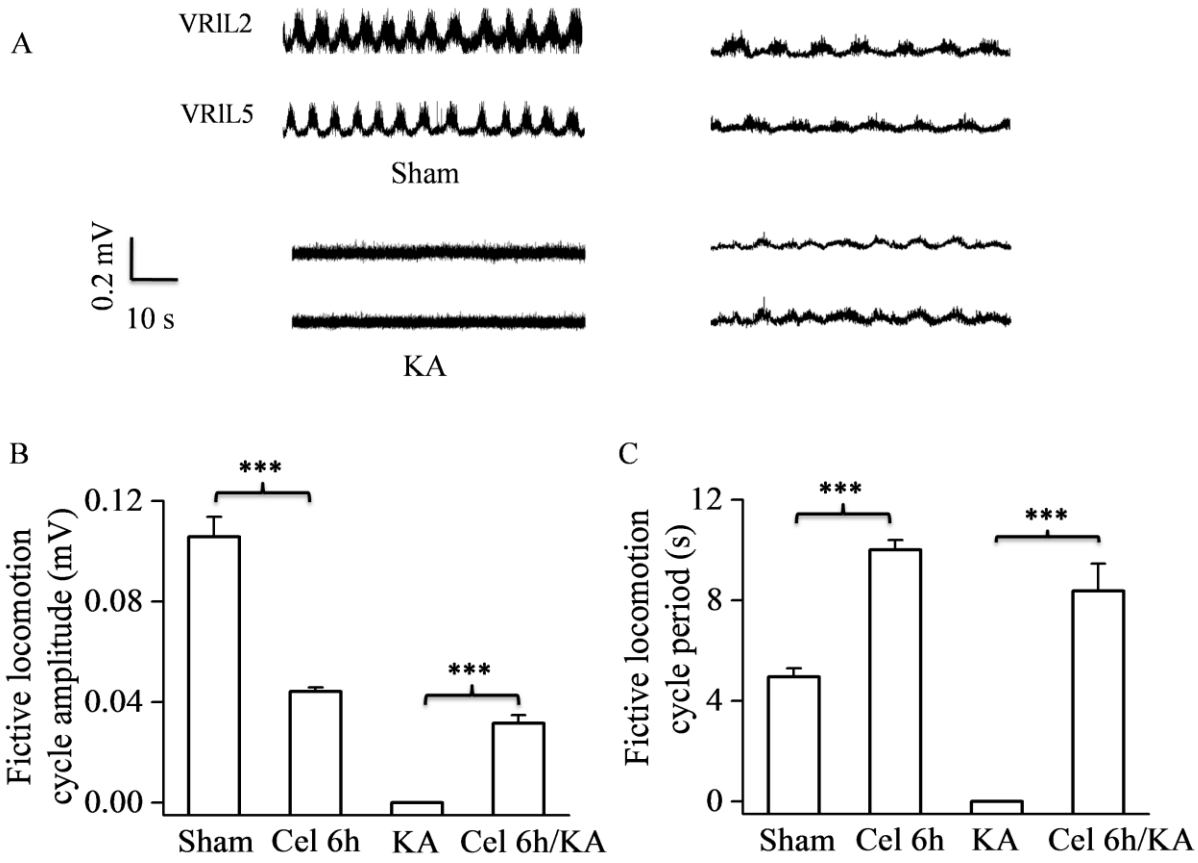

Fig. 3 Alternations in fictive locomotor patterns evoked by application of NMDA+5HT recorded 24 h in vitro. (A) Examples of chemically induced fictive locomotion in sham, Cel 6 h, KA and Cel 6 h/KA treatments. (B, C) Histograms represent a significant reduction of cycle amplitude and increased periodicity after celastrol alone application (6 h). Kainate alone application has completely abolished the fictive locomotion which was reversed by pre-treating the spinal cord with celastrol followed by kainate, although with less amplitude and longer periodicity (***$P \leq 0.001$).